

A MULTISCALE APPROACH TO UNDERSTAND
COMPLEX GROUNDWATER SYSTEMS AND SUSTAINABILITY

By

Zachary Kristopher Curtis

A DISSERTATION

Submitted to
Michigan State University
in partial fulfillment of the requirements
for the degree of

Environmental Engineering --- Doctor of Philosophy
Environmental Science and Policy --- Dual Major

2018

ABSTRACT

A MULTISCALE APPROACH TO UNDERSTAND COMPLEX GROUNDWATER SYSTEMS AND SUSTAINABILITY

By

Zachary Kristopher Curtis

Sustainable groundwater use is a growing and relatively ubiquitous concern. Yet, managing groundwater sustainably remains a significant societal challenge, largely because management must address a variety of issues across a multitude of scales. With rare exceptions, groundwater investigations have allocated limited resources to a narrow range of scales, in many cases ignoring important process interactions. Local-scale management is often done without proper understanding of the larger system controls, while system-based studies may not be sufficiently supplemented by subscale data collection and analysis, making it difficult to provide concrete, site-specific recommendations for management. This dissertation addresses a concrete example of a complex multiscale sustainability problem, namely, widespread salinization of shallow groundwater in southern Michigan, U.S.A, which appears to be due to natural basin-scale upwelling of deep brines, but is complicated by regional and local-scale human activities (e.g., pumping, road salting and land development). An integrated, end-to-end approach is developed and applied to investigate the complex interplay of upwelling brines, human activity, and climate variability at and across vastly disparate scales. Included are perspectives of basin-scale contamination, regional groundwater-surface water connections, local human-environment interactions, and well-scale analysis of water availability (quantity and quality). Data of different types, qualities, and resolutions/coverages (most of which are pre-existing and ‘big’) are integrated and critically evaluated with various modeling tools (data-driven, process-based and analytical solutions) to understand complex system dynamics and provide a basis for strategic regional planning, local operational management, and site-specific problem-solving. Data-driven approaches are used to characterize spatial patterns and temporal trends and provide diagnostic screening of different groundwater environments across multiple scales. Regional and local-scale process-based flow simulations are used to describe and quantify the relative importance of different processes controlling groundwater sustainability,

and to estimate future groundwater conditions by integrating detailed county-and township-level projections of water use and land use into model development. Through this integrated, multi-scale and multi-perspective analysis, several key scientific conclusions emerge: 1) slow, natural upwelling of brines is the dominant source of shallow saline groundwater in low-lying discharge areas across southern Michigan; 2) locally, impacts of brines are most severe where relatively continuous confining materials occur near or at the surface (precluding freshwater recharge as a freshwater flushing mechanism) and where groundwater levels are low; 3) cumulative impacts of gradual (multi-decadal) but significant increases in distributed water well networks have caused large declines (>15 m) in groundwater levels across broad subregions, which in turn is inducing movement of brine-influenced groundwater into areas historically less/not affected and worsening the severity and extent of shallow groundwater salinization; and 4) impacted aquifer systems will begin to stabilize as the rate of increase in pumping slows down, but local groundwater availability will still be limited by acceptable water quality of the user and/or required yield. The multi-scale, big data-enabled approach applied here provides a generalized framework for developing holistic understanding of groundwater systems important to sustainability, and for prioritizing limited resources needed for analysis in key areas to inform subregional and local-scale resource management.

This dissertation is dedicated to my parents, Kris and Nancy, two brothers, Ryal and Tyler, and dearly missed cousin, Shawn. Thank you for always being my source of inspiration.

ACKNOWLEDGEMENTS

I gratefully acknowledge the contributions of all those who made this research possible. My most profound gratitude goes to my Ph.D. advisor, Dr. Shu-Guang Li, Professor, Department of Civil and Environmental Engineering at Michigan State University (MSU), for his continuous guidance and encouragement throughout the course of my graduate studies. I would like to extend my very special thanks to my guidance committee - Dr. Jeffrey Andresen, Dr. David Long, Dr. Phanukumar Mantha and Dr. Yadu Pokhrel - for their willingness to serve and mentor, their patience and support, and for setting an excellent example of how researchers should conduct themselves

I thankfully acknowledge several collaborators that have been critical to aspects of the research presented here. Dr. Huasheng Liao, Senior Research Associate, Department of Civil and Environmental Engineering at MSU, was a key player in the flow modeling and calibration and processing of water quality data, and provided relentless efforts in developing new tools and making countless improvements in our groundwater modeling system Interactive Groundwater (IGW). Dr. Prasanna Sampath aided in much of the field sampling and statewide analysis of groundwater conditions. Dr. David Lusch helped establish project goals and provided correspondence with our project sponsors. I also wish to extend my thanks to the other members of our project team. They include: Jon Bartholic, Jeremiah Asher, Laura Young, Jason Piwarski, and James Duncan of the Institute of Water Research (IWR) at MSU; Paul Sachs, Matthew Chappuies of the Ottawa County, MI Planning and Performance Department; Pat Staskiewicz, Ottawa County, MI Public Utilities Director, and many other individuals from west-central southern Michigan that assisted with this research project. To all of my collaborators, I am grateful for your contributions and support which made all of this research possible.

I am thankful to the organizations that provided funding for my research, which include: Michigan Department of Rural and Agricultural Development; Ottawa County, Michigan Board of Commissioners;

Civil and Environmental Engineering Department at MSU; Environmental Science and Policy Program at MSU; the College of Engineering at MSU; and the Graduate School at MSU.

TABLE OF CONTENTS

| | |
|--|-----|
| LIST OF TABLES | x |
| LIST OF FIGURES | xii |
| OVERVIEW: MOTIVATION, APPROACH & KEY CONTRIBUTIONS | 1 |
| CHAPTER 1 Data-Driven Approach for Analyzing Hydrogeology and Groundwater Quality across Multiple Scales..... | 6 |
| 1.1 Executive Summary of Ch. 1 | 6 |
| 1.2 Ch. 1 Introduction | 6 |
| 1.2.1 Michigan Groundwater Salinity | 7 |
| 1.2.2 Objectives | 11 |
| 1.3 Ch. 1 Methods | 12 |
| 1.3.1 Data-driven Groundwater Modeling | 12 |
| 1.3.2 Spatial Interpolation of Massive Noise SWL Datasets | 16 |
| 1.3.3 Delineating Recharge and Discharge Areas..... | 22 |
| 1.3.4 Elevated Cl Overlays | 23 |
| 1.3.5 Field Sampling in the Michigan Lowlands | 24 |
| 1.3.6 Analytical Methods for Cl Measurement | 25 |
| 1.4 Ch. 1 Results | 25 |
| 1.4.1 Multiscale Hydraulic Head Distribution | 25 |
| 1.4.2 Multiscale Analysis of Elevated Cl Concentrations..... | 29 |
| 1.4.3 Three-Dimensional Cl Structure in the Michigan Lowlands | 33 |
| 1.5 Ch. 1 Discussion | 36 |
| 1.5.1 Cl-SWL Structure and Natural Brine Upwelling | 36 |
| 1.5.2 Potential Influence of Other Cl Sources..... | 38 |
| 1.5.3 Management Implications & Future Work | 40 |
| 1.6 Ch. 1 Conclusions | 41 |
| APPENDICES | 44 |
| APPENDIX A: Motivation for utilizing bedrock and drift wells for SWL delineation..... | 45 |
| APPENDIX B: Example of using different cutpoints..... | 48 |
| REFERENCES | 49 |
| CHAPTER 2 Groundwater modeling in a Spatially-rich World: Reassessing Data Needs, Availability, and Value | 56 |
| 2.1 Executive Summary of Ch. 2 | 56 |
| 2.2 Ch. 2 Introduction | 56 |
| 2.3 Modeling with Big Groundwater Data..... | 58 |
| 2.3.1 Opportunities & Questions..... | 59 |
| 2.3.2 Capturing the Aquifer Framework | 62 |
| 2.3.3 Characterizing Aquifer Properties..... | 63 |
| 2.3.4 Representing Surface Water Interactions..... | 64 |
| 2.3.5 Estimating Recharge | 68 |
| 2.3.6 Calibrating to Temporal Trends and Long-term Patterns | 69 |
| 2.4 Real World Illustrations | 71 |
| 2.4.1 Detailed Methodology..... | 71 |

| | |
|--|-----|
| 2.4.2 Results and Discussion..... | 81 |
| 2.4.3 Examples of Further Model Utilization | 94 |
| 2.5 Ch. 2 Conclusions | 99 |
| REFERENCES | 101 |
| | |
| CHAPTER 3 Simulation of Flow in a Complex Aquifer System Subjected to Long-term Well Network | |
| Growth | 107 |
| 3.1 Executive Summary of Ch. 3 | 107 |
| 3.2 Ch. 3 Introduction | 107 |
| 3.3 Modeling Challenges and Overview of Approach..... | 110 |
| 3.3.1 Conceptualization of a Complex Geologic Framework..... | 110 |
| 3.3.2 Conceptualization of Long-term, Distributed Stress Dynamics..... | 114 |
| 3.3.3 Characterization of System Dynamics | 117 |
| 3.4 Detailed Methodology and Model Development..... | 118 |
| 3.4.1 Stochastic-Deterministic Representation of Subsurface Geology | 120 |
| 3.4.2 Water Use Model | 125 |
| 3.4.3 Recharge Model | 126 |
| 3.4.4 Groundwater Flow Model..... | 128 |
| 3.4.5 Model Calibration | 131 |
| 3.5 Ch. 3 Results and Discussion..... | 133 |
| 3.5.1 Calibration Results..... | 133 |
| 3.5.2 Groundwater Head Dynamics | 141 |
| 3.5.3 Toward Sustainability: Next Steps..... | 145 |
| 3.6 Ch. 3 Conclusions | 147 |
| APPENDICES | 149 |
| APPENDIX A: Connection between the deep bedrock aquifer and the Grand River | 150 |
| APPENDIX B: Justification for using two separate layers to represent the bedrock aquifer | 151 |
| APPENDIX C: Accounting for switches to municipal water supply..... | 152 |
| APPENDIX D: Model well density vs. actual well density..... | 154 |
| REFERENCES | 156 |
| | |
| CHAPTER 4 A Multiscale Assessment of Shallow Groundwater Salinization in Southern Michigan | 162 |
| 4.1 Executive Summary of Ch. 4 | 162 |
| 4.2 Ch. 4 Introduction | 162 |
| 4.3 Overview of Ch. 4 Methods..... | 166 |
| 4.4 Statewide Data-Driven Characterization of Groundwater Conditions..... | 170 |
| 4.4.1 Screening-Level Evaluations of Local Conditions | 175 |
| 4.5 Detailed Subregional Modeling, Visualization, and Analysis | 182 |
| 4.5.1 3D Spatial Characteristics of Cl Concentrations..... | 183 |
| 4.5.2 Impacts of Pumping | 192 |
| 4.6 Ch. 4 Conclusions | 199 |
| REFERENCES | 201 |
| | |
| CHAPTER 5 Well-scale Predictions of Groundwater Sustainability that Account for Human-environment System Dynamics | 206 |
| 5.1 Executive Summary of Ch. 5 | 206 |
| 5.2 Ch. 5 Introduction | 206 |
| 5.3 Countywide Estimates of Future Groundwater Conditions | 207 |
| 5.3.1 Planning and Projections..... | 208 |
| 5.3.2 Estimates of Future Groundwater Flow Patterns | 214 |
| 5.4 Well-Scale Analysis of Future Groundwater Availability | 218 |

| | |
|---|-----|
| 5.4.1 Analytical Approach | 219 |
| 5.4.2 Illustrative Application to Several Key Areas | 222 |
| 5.5 Ch. 5 Conclusions | 225 |
| APPENDIX..... | 227 |
| REFERENCES | 229 |

LIST OF TABLES

| | |
|--|-----|
| Table 1.1: Details of the basin-scale SWL model (BW), the regional and local models developed for the Michigan Lowlands (ML-R and ML-L, respectively), and the regional and local models developed for the Saginaw Lowlands (SL-R and SL-L, respectively). Each model cell at a given scale was approximately square and of the same size..... | 17 |
| Table 1.2: Values of ρ_{wells} , L and N for all SWL models. See Table 1.1 for model abbreviation clarifications..... | 19 |
| Table 1.3: Information for the model variograms shown in Figure 1.6..... | 21 |
| Table 1.4: Statistics from the multiscale elevated CI-SWL analysis..... | 32 |
| Table 1.5: Statistics from the Michigan Lowlands regional elevated CI-SWL analysis using quartiles rather than tertiles as cutpoints for delineating recharge areas and discharge areas. Note that the percent ratios reported here are generally consistent with those reported in the Regional section of Table 1.3..... | 48 |
| Table 2.1: Example big datasets useful for modeling groundwater systems. *MWs = monitoring wells .. | 60 |
| Table 2.2: Michigan watersheds chosen for study. The ID numbers correspond to the number labels presented in Figure 2.2..... | 72 |
| Table 2.3: Summary of inputs for the two types of process-based models used in this study..... | 75 |
| Table 2.4: Grid properties of the models of the different watersheds, and the mean recharge (ϵ) and mean hydraulic conductivity (K)..... | 76 |
| Table 2.5 Parameters used for non-stationary kriging and spatial interpolation..... | 80 |
| Table 2.6: Model performance for Type I and Type II process-based simulations. Model ID indicates the watershed (by the beginning number) and model type (I or II following the dash). | 90 |
| Table 3.1: Number of cells and grid size of the geologic TP model, recharge (ϵ) model, and groundwater flow model..... | 120 |
| Table 3.2: Calibrated and mean observed pumping rates for domestic, public supply, irrigation and industrial/commercial water use sectors. | 136 |
| Table 3.3: Calibrated hydraulic conductivities (Kh_{TP}) of the aquifer material sets, including the ratio of horizontal conductivity to vertical conductivity (Kh_{TP}/Kz_{TP})..... | 138 |
| Table 3.4: Calibrated hydraulic conductivities (K_x) of the bedrock zones. | 140 |
| Table 4.1: Total number of CI scatter points available for countywide analysis and the number within cropland for each of the counties with notably elevated chloride concentrations in groundwater. | 172 |

| | |
|--|-----|
| Table 4.2: Compelling static water elevation declines observed within townships of the seventeen counties that were analyzed. | 181 |
| Table 5.1: Projected percent change in GDP and estimated groundwater pumping rates for large-use industrial/commercial wells in Ottawa County. Source: Ottawa County Planning and Performance Improvement Department (Ottawa County 2017). | 210 |
| Table 5.2: local transmissivity (T) and local effective specific capacity (Q/s) _{eff} utilized for well-scale analysis..... | 223 |
| Table 5.3: Results from the well-scale analysis. Sc.1 = Scenario 1, Sc.2 = Scenario 2, etc. Empty entries for Sc.3 and Sc.4 indicate that concentrations of Cl ⁻ were not measured at or above 100 mg/L or 250 mg/L during the analysis of subregional water quality..... | 224 |
| Table 5.4: Average local transmissivity (T) and local effective specific capacity (Q/s) _{eff} utilized for evaluation of management scenario 2..... | 228 |

LIST OF FIGURES

| | |
|---|----|
| Figure 1.1: Lower Peninsula of Michigan bedrock geology plan-view map, with a selected cross-section (A - B) of the shallow bedrock geology..... | 9 |
| Figure 1.2: Lower Peninsula of Michigan 10m Digital Elevation Model (NED, 2006) showing the location of the Saginaw and Michigan Lowlands..... | 10 |
| Figure 1.3: Spatial coverage of (a) Wellogig database and (b) WaterChem database. | 14 |
| Figure 1.4: Workflow diagram for integrated water quantity-quality data-driven modeling. | 16 |
| Figure 1.5: Schematic of a variogram (model and data) with annotations clarifying the nugget, partial sill and range terms of the model variogram. | 18 |
| Figure 1.6: Illustrative variograms at the (a) local scale (LV1, LV2, LV3); (b) regional scale (RV1, RV2, RV3) for the Michigan Lowlands analysis, and also at (c) basin-scale (BV1, BV2, BV3)..... | 21 |
| Figure 1.7: Long-term average SWL distributions delineated at the basin-scale. Third order and higher streams are included, as well as the delineated recharge and discharge zones. | 26 |
| Figure 1.8: Long-term average SWL distributions delineated at the regional scale for the (a) Michigan Lowlands and (b) Saginaw Lowlands, as well as at the local scale for the (c) Michigan Lowlands and (d) Saginaw Lowlands. Second order and higher streams are included for the regional scale graphics, while all order streams are included in the local scale graphics. | 28 |
| Figure 1.9: Occurrence of elevated Cl (>250, >500, >1000 mg/L) wells with respect to basin-scale SWL distributions..... | 29 |
| Figure 1.10: Occurrence of elevated Cl (>250, >500, >1000 mg/L) wells with respect to regional-scale SWL distributions for the (a) Michigan Lowlands and (b) the Saginaw Lowlands. | 30 |
| Figure 1.11: Occurrence of elevated Cl (>250, >500, >1000 mg/L) wells with respect to local-scale SWL distributions for the (a) Michigan Lowlands and (b) the Saginaw Lowlands. | 31 |
| Figure 1.12: Cl point measurements from Ottawa County, Michigan (central portion of the Michigan Lowlands) overlaid on a bedrock subcrop map. | 34 |
| Figure 1.13: Graphical relationship between well bottom elevation and chloride concentration from the field sampling dataset. | 35 |
| Figure 1.14: Three-dimensional view of Cl point measurements (a) from above, transparent land surface and bedrock surface shown; (b) from below, with bedrock surface shown; (c) from the west, with the DEM and bedrock surface shown. | 35 |
| Figure 1.15: Occurrence of elevated Cl (>250, >500, >1000 mg/L thresholds) wells and the Michigan highway network..... | 40 |
| Figure 1.16: Occurrence of elevated Cl (>250, >500, >1000 mg/L thresholds) and oil/gas wells. | 40 |

| | |
|--|----|
| Figure 1.17: Regional-scale groundwater elevations delineated using moving-window, non-stationary kriging of (a) bedrock wells; and (b) drift wells. The domain used for the local model is shown as a red rectangle..... | 46 |
| Figure 1.18: Regional-scale groundwater elevations delineated using moving-window, non-stationary kriging of (a) bedrock wells; and (b) drift wells. The domain used for the local model is shown as a red rectangle..... | 47 |
| Figure 2.1: Conceptual schematic of the key components of natural groundwater system. | 59 |
| Figure 2.2: Watershed chosen for study. Background image source: National Geographic Society, i-cubed (2013)..... | 72 |
| Figure 2.3: Example cross-sections to illustrate the two process-based modeling approaches used in this study. Arrows indicate groundwater velocity vectors. The red lines along the top and bottom of the models are the model boundaries..... | 75 |
| Figure 2.4: Comparison of the spatial occurrence of groundwater seep areas (top) and water balances (bottom) for the Au Sable watershed (ID=3). (a) Model utilizing two-way head dependent flux boundary conditions (BCs) for lakes and rivers/streams; and (b) one-way head-dependent flux for the entire land surface. Streams and lakes shown in (a) are from NHD USGS (2010). | 79 |
| Figure 2.5: Head distributions and calibration charts for the Escanaba watershed (ID=1)..... | 82 |
| Figure 2.6: Head distributions and calibration charts for the Tahquamenon watershed (ID=2)..... | 83 |
| Figure 2.7: Head distributions and calibration charts for the Au Sable watershed (ID=3)..... | 84 |
| Figure 2.8: Head distributions and calibration charts for the St. Clair watershed (ID=4). | 85 |
| Figure 2.9: Head distributions and calibration charts for the Huron watershed (ID=5). | 86 |
| Figure 2.10: Head distributions and calibration charts for the Kalamazoo watershed (ID=6). | 87 |
| Figure 2.11: Head distributions and calibration charts for the Grand River watershed (ID=7)..... | 88 |
| Figure 2.12: Head distributions and calibration charts for the Grand River watershed (ID=8)..... | 89 |
| Figure 2.13: Comparison of reverse particle tracking results and traditional Wellhead Protection Area (WHPA) delineations completed by the Michigan Department of Environmental Quality (MDEQ). | 92 |
| Figure 2.14: Calibration plot for the Au Sable watershed (ID: 3) utilizing arbitrary parameters: $K=100$ ft/day; $\epsilon=10$ in./yr.; Bottom elevation=Min. DEM – 200 ft..... | 95 |
| Figure 2.15: Location of significantly overestimated and underestimated simulated SWLs, St. Clair watershed (ID=). Red dots (left) are locations of overestimated points; blue dots (right) are locations of underestimated points; green dots are locations of all other points in the calibration plot (center)..... | 96 |
| Figure 2.16: Location of significantly underestimated simulated SWLs, Kalamazoo watershed (ID: 6).; blue dots (bottom) are locations of underestimated points; green dots are locations of all other points in the calibration plot (top)..... | 98 |

| | |
|--|-----|
| Figure 3.1: Study area in west-central Lower Peninsula of Michigan (nearly 3400 km ²). The 10m digital elevation model (DEM) was obtained from USGS NED (2006), and the surface water network is from USGS NHD (2010)..... | 109 |
| Figure 3.2: Large-scale geology underlying the study area: (a) glacial land systems (GWIM 2006) and (b) bedrock subcrop map (GWIM, 2006); and (c) representative cross-sections A-A', B-B', and C-C', with aquifer material types shown in the vertical borehole profiles. Wells and associated lithologic descriptions were extracted from Wellogig (MDEQ 2014) using the Michigan Groundwater Management Tool (MGMT) developed by Michigan State University (MSU, 2014)..... | 112 |
| Figure 3.3: Evolution of water wells within the study domain. Data were extracted from Wellogig (MDEQ 2014)..... | 115 |
| Figure 3.4: Workflow diagram of the models and data used for model input and calibration..... | 119 |
| Figure 3.5: Workflow for developing a three-dimensional hydraulic conductivity (K) field using the zone-based transition probability approach. The K-field shown here represents ln(K) variations..... | 122 |
| Figure 3.6: Cross-sections of the 3D glacial aquifer material model, overlaid with borehole lithologies from water wells. The approximate locations and horizontal/vertical extents of cross-sections A-A', B-B', and C-C' are shown in Figure 3.2..... | 124 |
| Figure 3.7: Conceptualization of the bedrock aquifer: (a) conceptual cross-section indicating the vertical extent of the different zones within the 1st (top-most) and 2nd bedrock layer; and (b) areal extent of the zones shown in (a) for the 1st and 2nd bedrock layer..... | 125 |
| Figure 3.8: Simulated recharge distributions for select time-steps..... | 128 |
| Figure 3.9: Comparison of simulated groundwater head with observation (SWL): (a) all glacial drift wells; and (b) all bedrock wells..... | 134 |
| Figure 3.10: Static Water Level (SWL) trend comparison (observations vs. simulated head) for the bedrock aquifer of four central townships in Ottawa County, MI..... | 135 |
| Figure 3.11: Calibrated water use curves and estimates of aggregated groundwater withdrawals for Ottawa County, Michigan from USGS (2005, and 2010) and MDARD/MDEQ (2012 and 2013). The red markers represents estimated water use, and the solid lines are simulated water use (IRRI = irrigation; HOSHLD=domestic; PUB = public supply; and INDUS = industry/commercial)..... | 136 |
| Figure 3.12: Simulated water use for 1995, 2005 and 2015, using the calibrated pumping rates presented in Table 2: (a) drift aquifer; and (b) bedrock aquifer..... | 137 |
| Figure 3.13: Hydraulic conductivity (K_x^{Model}) distribution in the six computational layers of the glacial aquifer..... | 139 |
| Figure 3.14: Three-dimensional head distribution for final time-step (2015). The magnified region is shown to highlight the significant depression in the central portion of the model domain due to significant increases in pumping..... | 142 |
| Figure 3.15: Simulated groundwater head distribution (bedrock aquifer) for representative time-steps.. | 143 |

| | |
|---|-----|
| Figure 3.16: Graphical representation of flux dynamics in the three central townships exhibiting significant drawdown from 1966-2015..... | 144 |
| Figure 3.17: Comparison of SWL trends for bands north and south of the Grand River, and along it. Data are from Wellogic (MDEQ, 2014)..... | 150 |
| Figure 3.18: Polygons use to represent areas where municipal water supply became available at different times since 1992. “GW-> SW” is a shortened form of “groundwater to municipal water supply.”..... | 153 |
| Figure 3.19: Comparison of well distribution in Blendon Township, Michigan (central portion of model domain): (a) from Wellogic only (834 wells); and (b) from Wellogic, Ottawa County Dept. of Environmental Health, and “visually added wells” (about 2500 wells). | 155 |
| Figure 4.1: Occurrence of wells with elevated Cl concentrations (>500 mg/L) and static water level (SWL) distributions at the (a) basin-scale; (b) regional scale (Michigan Lowlands); and (c) local scale (central Michigan Lowlands). Adapted from Curtis et al. (2018)..... | 165 |
| Figure 4.2: Multi-scale, data-driven modeling approach: datasets (cylinders), workflow (arrows), and resulting datasets/maps/analyses (rectangles). | 168 |
| Figure 4.3: Multi-scale, process-based modeling approach and integrated analyses and spatial overlays. | 169 |
| Figure 4.4: Chloride concentrations in groundwater, interpolated at the 3 km x 3 km cell size (center graphic) and at the 1 km x 1 km cell size (peripheral graphics). | 171 |
| Figure 4.5: Cropland (green) within the seventeen counties analyzed for water quality severity. Source: USDA, NASS Cropland Data Layer (2014). | 173 |
| Figure 4.6: Spatial mapping of Cl concentrations for the 95th percentiles, using only scatter points existing within cropland for each county. | 174 |
| Figure 4.7: Graphical depiction of Cl concentration percentiles computed using all Cl data points available in each county (50%, 75%, 95%) and using only scatter points existing within cropland for each county (50%-crops, 75%-crops, 95%-crops). | 175 |
| Figure 4.8: (from left to right) Screening-level mapping of chloride concentrations, SWL distributions and the stream network (gray-blue lines), glacial layer lithology, and bedrock formation subcrops: (a) Tuscola County (region 2 from Figure 4.4); (b) Lenawee County (region 3); (c) Ottawa County (region 1); and (d) St. Clair County (region 4). ‘AQ’ = aquifer, ‘MAQ’= marginal aquifer, ‘PCM’ = partially confining material, and ‘CM’ = confining material. | 178 |
| Figure 4.9: Static water level trends from selected townships in: (a) Tuscola County (b) Lenawee County; (c) Ottawa County; and (d) St. Clair County. The inset maps show the locations of wells extracted from Wellogic for the analysis. Green dots are glacial wells; blue dots are bedrock wells. | 180 |
| Figure 4.10: Key outputs from the modeling effort described in Liao et al. (in review) for the years 1970, 1980, 1990, 2000, 2010, and 2015. (a) Simulated drawdown in the bedrock aquifer and (b) simulated water use in the bedrock aquifer. | 183 |

Figure 4.11: Chloride (Cl) concentration point data for Ottawa County. (a) plan-view of Cl data collected in the field (adapted from Curtis et al. 2017); (b) plan-view of Cl mined from historical water quality records; (c) 3D visualization of Cl point data from the combined dataset, viewed from the west with the 10m DEM and bedrock surface (brown); and (d) 3D visualization of Cl point data viewed from the north, with the 10m DEM, bedrock surface, and the Coldwater Shale surface (green). 186

Figure 4.12: Graphical representation of Cl/Na molar ratio vs. Cl concentration for 248 locations yielding historical records of Na and Cl concentrations. 188

Figure 4.13: ‘Clay control cells’ used for 3D Cl interpolation. (a) 3D visualizations of the geologic material model characterizing the heterogeneity of the glacial deposits (from Liao et al., in review); (b) 3D depictions of control cell locations; and (c) Cl plume comparison. 190

Figure 4.14: Results from the 3D interpolation of Cl concentrations, shown as 2D distributions at various depths from the land surface. (a) 3D plume and representative cross-sections through the domain used for interpolation (b)-(d) 2D distributions of Cl in the glacial deposits (top layer, 3rd layer and bottom layer, respectively); and (d)-(f) 2D distributions from the bedrock aquifer (top layer, middle layer, and bottom layer, respectively). 191

Figure 4.15: Spatial relationship between Cl concentration and groundwater flow dynamics. (a) simulated drawdown (1966-2015) in the bedrock aquifer and all Cl point data collected from the bedrock aquifer (field sampling and data mining); and (b) 2015 head distribution in the bedrock aquifer and all Cl point data collected from the bedrock aquifer. 193

Figure 4.16: Graphical comparison of Cl concentrations vs. time. (a) dataset consisting of mined data from historical water well records; and (b) dataset from (a) shown with a reduced Cl concentration scale and linear regression trendlines. 194

Figure 4.17: Temporal analysis at wells with both historical and field-collected Cl concentration data. (a) comparison of Cl concentrations from field-collected data and historical water quality records at 248 locations (see inset map in Figure 4.11 for map of locations used in analysis); and (b) graphical comparison of Cl residual (field-collected mg/L – historical mg/L) as a function of well bottom elevation (amsl). 195

Figure 4.18: Results from 3D particle tracking. (a) initial particle positions and the position of high-capacity wells existing in 2015; and (b) particle flow paths after 20 years of steady-state simulation (2015 pumping and recharge simulated ad infinitum). 197

Figure 4.19: Cl plume modeling in Allendale Township (central Ottawa County) for three time periods: up to 1995 (left column), 1996-2005 (center column), and 2006-2015 (right column). (a) transverse data density across the three time periods; (b) 250 mg/L iso-surfaces for the three time periods; and (c) 400 mg/L iso-surfaces for the three time periods. 198

Figure 5.1: Work-flow of preparing projections provided by Ottawa County into future recharge and water use models needed for application of calibrated flow model. 208

Figure 5.2: Assigning new future wells to different vertical layers in the calibrated flow model. The ‘5th glacial layer’ is the deepest of the layers representing the unconsolidated glacial deposits. 213

Figure 5.3: Estimates of future groundwater levels based on application of the calibrated flow model:
 (top-right) countywide spatial mapping of additional groundwater decline expected over next 20 years;
 (bottom) detailed head dynamics in an area of concern..... 216

Figure 5.4: Groundwater level dynamics for 70 year of analysis (1966-2036): (top): Time-series of
 simulated heads at two different areas undergoing significant temporal change; (bottom): countywide
 spatial analysis of simulated groundwater level change for 1966-2015 (left) and 2016-2036 (right). 218

Figure 5.5: Work-flow for estimating available drawdown and maximum sustainable yield (pumping) at a
 specific location using results from the future simulations..... 221

Figure 5.6: Locations used for well-scale analysis (left) and an example conceptual schematic of available
 drawdown and maximum allowed pumping under different management scenarios (right)..... 223

OVERVIEW: MOTIVATION, APPROACH & KEY CONTRIBUTIONS

Sustainable groundwater use is a growing and relatively ubiquitous concern. Yet, managing groundwater sustainably remains a significant societal challenge, largely because management must address a variety of issues across a multitude of scales. With rare exceptions, groundwater investigations have allocated limited resources to a narrow range of scales, in many cases ignoring important process interactions. Local-scale management is often done without proper understanding of the larger system controls, while system-based studies may not be sufficiently supplemented by subscale data collection and analysis, making it difficult to provide concrete, site-specific recommendations for management.

The objective of this dissertation is to address a real-world groundwater sustainability problem that exhibits the above-mentioned characteristics. The specific issue is widespread salinization of shallow groundwater in southern Michigan, U.S.A, which appears to be due to natural basin-scale upwelling of deep brines, but is complicated by regional and local-scale human activities (e.g., pumping, road salting and land development). Specific research questions addressed are:

- How do different processes (natural and anthropogenic) interact to control the long-term sustainability of southern Michigan's shallow groundwater resources? How do interactions at local scales shape global system dynamics, and how do those macro-level dynamics determine long-term sustainability? To what extent are natural upwelling brines responsible? What is the relative importance of human activity?
- Is it even practical to try to characterize/model the entire system? How can we possibly find enough data to characterize groundwater conditions across large areas and different scales? How can we represent complex geology and dynamic stress frameworks in ways that do not over-parameterize groundwater flow models used to develop and test system understanding? How can we calibrate models of such systems in ways that allows evaluating long-term sustainability? How can we estimate location-specific groundwater availability (current or future) in ways that account for larger (and longer term) system dynamics?

An integrated, end-to-end approach is developed and applied to investigate the complex interplay of upwelling brines, human activity, and climate variability at and across vastly disparate scales. Included are perspectives of basin-scale contamination, regional groundwater-surface water connections, local human-environment interactions, and well-scale analysis of water availability (quantity and quality). Data of different types, qualities, and resolutions/coverages (most of which are pre-existing and ‘big’) are integrated and critically evaluated with various modeling tools (data-driven, process-based and analytical solutions) to understand complex system dynamics and provide a basis for strategic regional planning, local operational management, and site-specific problem-solving. Data-driven approaches are used to characterize spatial patterns and temporal trends and provide diagnostic screening of different groundwater environments across multiple scales. Regional and local-scale process-based flow simulations are used to describe and quantify the relative importance of different processes controlling groundwater sustainability, and to estimate future groundwater conditions by integrating detailed county- and township-level projections of water use and land use into model development

Chapter 1 describes a novel approach for data-driven modeling of high-density water well datasets – which are deemed by many too crude to be useful – that allows characterizing hidden patterns of groundwater quantity and quality across different spatial scales. A non-stationary kriging technique that automatically filters out errors and characterizes dominant spatial signals is applied at basin-, regional- and local-scales to identify prevailing spatial configurations of flow systems (i.e., occurrence of discharge zones and recharge zones) and areas of significantly (and statistically) elevated dissolved chloride (Cl) concentrations (as a proxy for salinity).

Chapter 2 investigates the integration and relative importance of data of different types, qualities, and resolutions for process-based modeling of groundwater systems. Generalized methods are applied to build a suite of process-based flow models of different sizes, types, and in different hydrologic regimes in Michigan, taking advantage of a comprehensive, preprocessed groundwater database. Performance is examined at different scales and model sensitivity is evaluated with respect to model parameters and

structure. Results show that, although groundwater is invisible and lots of data are required for simulation, those representing the land surface (topography, lakes, streams and surface seeps) are the most important for providing a system context to model perturbations across scales.

Chapter 3 presents innovative approaches for simulating complex aquifer systems in ways that avoid issues related to flow model over-parameterization. In particular, above-mentioned water well datasets were used to 1) implement a ‘zone-based’ Transition-Probability (TP) geostatistical approach to conceptualize complex three-dimensional spatial variability using a relatively small set of geologic material types; 2) model the intricate spatiotemporal evolution of water well withdrawals across several decades using a sector-based water use parameterization 3) capture long-term groundwater level declines in different parts of the aquifer system using a large amount of noisy groundwater level data.

Chapter 4 describes a holistic analysis of Cl dynamics in southern Michigan to understand and characterize links between water quality, groundwater pumping, and natural hydrogeologic controls. Multi-scale data-driven modeling of massive amounts of groundwater and geologic information is combined with detailed analysis of Cl patterns and results from process-based flow modeling at regional and local scales to not only explain water quantity-quality dynamics, but also perform diagnostic screenings and develop ‘groundwater severity’ rankings of at-risk counties across southern Michigan.

Chapter 5 presents the application of the calibrated groundwater flow model discussed in Chapter 3 to estimate future groundwater sustainability, informed by best estimates of projected land use/land cover (LULC) and future groundwater use developed by county-level planning and utilities departments in Ottawa County, Michigan. Likely long-term (2016-2036) simulated changes of groundwater levels due to human activity and climate change (recharge dynamics) are adjusted with well-scale analytical corrections to estimate sustainable yield (pumping rates) at different locations during “limiting situations” – when groundwater pumping will be at its largest and recharge is lowest. The framework enables calculation of available drawdown and sustainable groundwater yield (pumping) under different management criteria (water availability and acceptable water quality).

Through this integrated, multi-scale and multi-perspective analysis, several key scientific conclusions emerge:

- slow, natural upwelling of brines is the dominant source of shallow saline groundwater in low-lying discharge areas across southern Michigan, demonstrated by parallel, hierarchical spatial structures of water quality and water quantity across different scales (basin-, regional- and local-scale), namely, relatively frequent occurrence of elevated Cl concentrations in groundwater discharge zones and relatively infrequent occurrence of elevated Cl concentrations in recharge zones;
- in different counties in different regions of southern Michigan, the occurrence of brine-influenced groundwater coincides with declining groundwater levels and occurrence of clay lenses revealed through data-driven modeling, suggesting both natural and human controls are important at regional and local scales;
- process-based modeling of causal relationships between flow, geology and aquifer stress (pumping) in Ottawa County, Michigan shows that cumulative effects of decades of distributed small-scale pumping has drastically reduced groundwater levels across large subareas (so much so that a large ‘cone of depression’ continues to deepen and widen in the central part of Ottawa County) significantly altering flow system dynamics. In some areas, flow directions and groundwater-surface water interactions have actually reversed (e.g., stream stretches converting from gaining to losing), significantly changing subregional water balances;
- the current distribution of elevated Cl concentrations in Ottawa County coincides with areas where deep groundwater naturally discharges (matching the results from multi-scale analysis of prevailing spatial patterns of water quantity and quality), but also with the above-mentioned cone of depression, suggesting that pumping is making the problem worse;
- temporal analysis of Cl data augmented by flow model application (particle tracking of deep groundwater flow) confirms that Cl concentrations are increasing with time and salinization is becoming more widespread in some subareas in response to pumping; and

- based on best estimates of future groundwater use and land development, the calibrated flow model of the Ottawa County aquifer systems suggests that groundwater levels will begin to stabilize as the rate of increase in pumping slows down, but local groundwater availability will still be limited by acceptable water quality of the user and/or required yield (e.g., large-scale pumping used to support agriculture or industry may face challenges producing required yields without utilizing an unacceptable portion of the local saturated aquifer thickness).

The multi-scale, big data-enabled approach applied here provides a generalized framework for developing holistic understanding of groundwater systems important to sustainability, and for prioritizing limited resources needed for analysis in key areas to inform subregional and local-scale resource management.

Chapters 1-4 are written as research papers that are either currently published or in the peer-review process. As such, contributing authors are listed at the beginning of each Chapter (1-4). Chapter 1 is published in the Journal of Groundwater (Volume 56, Issue 3). Chapters 3 and 4 have been submitted to a 2nd round of peer-review and expected to be published soon (both in the Journal of Groundwater). Chapter 2 will soon be sent out for a first round of peer-review. Chapter 5 will soon be incorporated into a paper describing the integrated, end-to-end approach to understand complex groundwater systems and sustainability described here through application of addressing brine-influenced groundwater in southern Michigan. At this time, the contributing author list for Chapter 5 has not been fully determined.

CHAPTER 1

Data-Driven Approach for Analyzing Hydrogeology and Groundwater Quality across Multiple Scales

Contributing authors: Zachary Curtis, Shu-Guang Li, Hua-sheng Liao, David Lusch

1.1 Executive Summary of Ch. 1

Recent trends of assimilating water well records into statewide databases provide a new opportunity for evaluating spatial dynamics of groundwater quality and quantity. However, these datasets are scarcely rigorously analyzed to address larger scientific problems because they are of lower quality and massive. We develop an approach for utilizing well databases to analyze physical and geochemical aspects of groundwater systems, and apply it to a multiscale investigation of the sources and dynamics of chloride (Cl) in the near-surface groundwater of the Lower Peninsula of Michigan. Nearly 500,000 static water levels (SWLs) were critically evaluated, extracted, and analyzed to delineate long-term, average groundwater flow patterns using a non-stationary kriging technique at the basin-scale (i.e., across the entire peninsula). Two regions identified as major basin-scale discharge zones – the Michigan and Saginaw Lowlands – were further analyzed with regional- and local-scale SWL models. Groundwater valleys (‘discharge’ zones) and mounds (‘recharge’ zones) were identified for all models, and the proportions of wells with elevated Cl concentrations in each zone were calculated, visualized, and compared. Concentrations in discharge zones, where groundwater is expected to flow primarily upwards, are consistently and significantly higher than those in recharge zones. A synoptic sampling campaign in the Michigan Lowlands revealed concentrations generally increase with depth, a trend noted in previous studies of the Saginaw Lowlands. These strong, consistent SWL and Cl distribution patterns across multiple scales suggest that a deep source (i.e., Michigan brines) is the primary cause for the elevated chloride concentrations observed in discharge areas across the peninsula.

1.2 Ch. 1 Introduction

In recent years, a number of U.S. states have assembled statewide water well databases in an effort to improve the characterization and management of their groundwater resources. In some states, the process

of sorting, filtering, and merging data from various state and federal agency inventories is still on-going and the datasets are not yet ready for use (see, e.g., the Virginia Department of Environmental Quality well database), while in many states the databases are now being linked to GIS web-applications and data portals where data can easily be viewed and downloaded for further analysis (see, e.g., the Illinois State Geological Survey repository (ISGS 2015), Kansas' WIZARD water well levels database (KGS 2002), Michigan's Wellogic database (MDEQ 2014), and the Geosam Database for the State of Iowa (IGS 2015)). These datasets contain massive amounts of high-density physical groundwater data (water levels), and in some cases, water quality information. However, these datasets are scarcely rigorously analyzed to address larger scientific problems primarily because they are of lower quality and are massive in size. In this study, we develop an approach for utilizing these massive (but noisy) water well databases to better understand physical and geochemical aspects of groundwater systems, and apply it to an investigation of groundwater quality across multiple spatial scales in the Lower Peninsula of Michigan, namely, the sources and dynamics of chloride (Cl) in the near-surface groundwater.

1.2.1 Michigan Groundwater Salinity

In sedimentary basins across North America, groundwater exhibiting high salinities at great depths has been reported (e.g., Carpenter et al. 1974; Land and Prezbindowski 1981; Stueber and Walter 1991). The Michigan Basin (Figure 1.1) – an ovate, bowl-shaped accumulation of sedimentary rock with a maximum thickness of more than 5,300 m in the basin center (Lilienthal 1978) – is unique because, in addition to very high total dissolved solids concentrations (TDS > 450,000 mg/L) in the deep bedrock formations (Wilson and Long 1993a and 1993b), saline groundwater (TDS > 1000 mg/L) has been reported in shallower bedrock formations and glacial-drift aquifers in some areas of the basin. Several studies published as part of the U.S. Geological Survey (USGS) Regional Aquifer-System Analysis (RASA) program documented high dissolved-solids and dissolved-chloride (Cl) concentrations (TDS > 100,000 mg/L) within the Mississippian and Pennsylvanian bedrock formations (i.e., from the Marshall Sandstone unit up through the Saginaw Formation shown in Figure 1.1), with concentrations that increase toward the basin center

(e.g., Ging et al. 1996; Meissner et al. 1996; Westjohn and Weaver 1996b; Lampe 2009). Lane (1899) and Long et al. (1988) documented saline near-surface (<100 m) groundwater in east-central Lower Peninsula of Michigan – the Saginaw Lowlands (Figure 1.2). At discrete locations further inland, “salt springs” were reported (Albert 2001; Kost et al. 2007). More recently, analysis of drinking water wells in the west-central Lower Peninsula of Michigan – the Michigan Lowlands (see Figure 1.2) – revealed significant occurrence of Cl concentrations elevated above the US Environmental Protection Agency (EPA) secondary maximum contaminant level (SMCL) of 250 mg/L (IWR 2013; Long et al. 2015). Such elevated Cl concentrations make groundwater unfit for human consumption and for many agricultural uses, and are detrimental to the environment (Ayers and Westcott 1985).

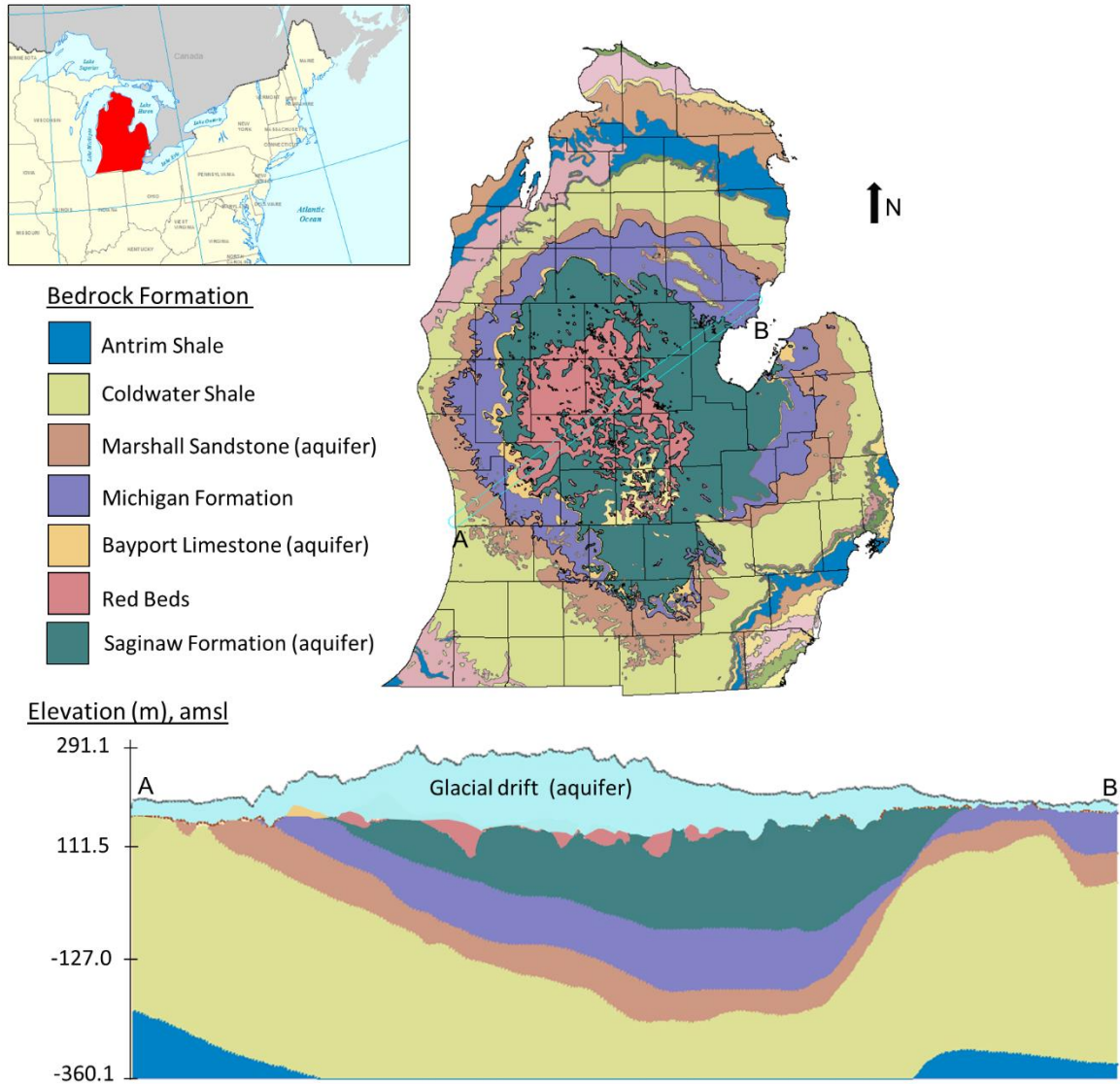


Figure 1.1: Lower Peninsula of Michigan bedrock geology plan-view map, with a selected cross-section (A - B) of the shallow bedrock geology.

Research probing the origin of the shallow saline groundwater has primarily involved site-specific geochemical approaches. Long et al. (1988) studied groundwater in the glacial and bedrock aquifers of the Saginaw Lowlands and found increasing Cl concentrations with increasing depth, as well as evidence of mixing between modern day, meteoric water and water that is much older. Analysis of pore water from the Saginaw Lowlands yielded strong vertical gradients in Cl concentrations and chloride:bromide ratios indicative of brine as the source for the chloride (Kolak et al. 1999). Steep gradients in Cl concentrations

with depth and evidence of brine-influenced groundwater were also observed along the basin margins in southwestern Ontario (Weaver et al. 1995) and in the formation waters of the Antrim Shale unit (McIntosh et al. 2004). Ma et al. (2005) used helium and major-ion data from bedrock aquifer samples in south-central Lower Michigan to demonstrate the influence of deeper brines on shallow bedrock aquifers in the study area. Although a careful geochemical study of the cause of chloride contamination in the groundwater of the Michigan Lowlands is lacking, a few studies suggest that mixing of brines and shallow fresh groundwater is responsible for saline groundwater in the area (Ging et al. 1996; Fitzpatrick et al. 2007; Long et al. 2015). Importantly, these separate geochemical studies in different areas of the Michigan Basin suggest upwelling brines are preferentially impacting some areas of Lower Michigan.

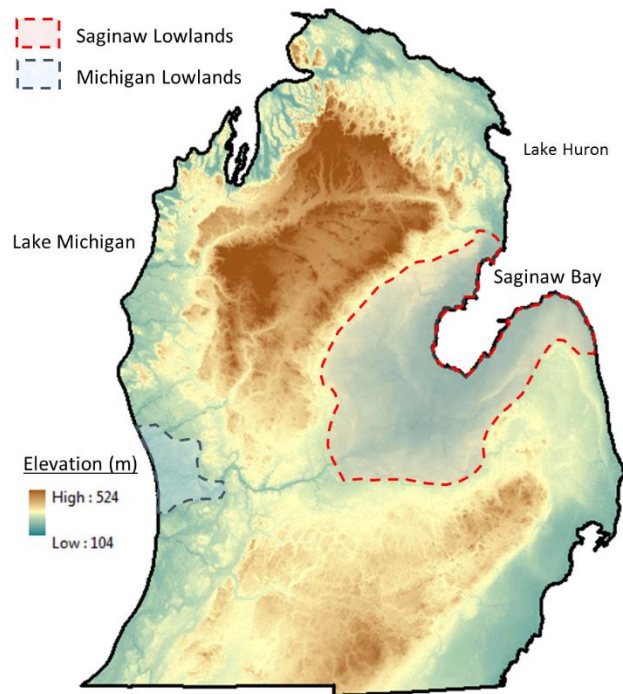


Figure 1.2: Lower Peninsula of Michigan 10m Digital Elevation Model (NED, 2006) showing the location of the Saginaw and Michigan Lowlands.

Natural brine upwelling and subsequent mixing with fresh groundwater as the source of saline near-surface groundwater in parts of the Michigan Basin requires vertical head gradients to drive advection of denser brines towards the land surface. Indeed, there has been some attempt to understand the groundwater hydrology of areas in which geochemical analyses inferred the upwelling of brine. Hoaglund et al. (2004)

used numerical models to show that, at present conditions, modern lake elevation in Saginaw Bay is exceeded by the head in the underlying Marshall aquifer by as much as 21 m, creating a significant potential for upward flow. Others studying the general basin-scale groundwater processes noted that the Michigan Lowlands and Saginaw Lowlands represent two major regional discharge zones, (e.g., Westjohn and Weaver 1996a; Westjohn et al. 1994; Hoaglund et al., 2002). The findings of the site-specific geochemical studies, coupled with knowledge of the basin-scale hydrogeology, suggest that the upwelling of brines systematically impacts the near-surface environment and its water resources in the Lower Michigan. However, it is still not clear to what extent the brines are responsible for elevated groundwater salinity across the peninsula, which has important implications for sustainable management of groundwater resources in this region. This is because a system-based understanding – one that addresses groundwater quality and quantity at different scales across the peninsula – is lacking.

1.2.2 Objectives

In this study, we develop and apply an approach for utilizing massive (but noisy) water well datasets to holistically evaluate hydrogeologic systems, examining correlations and patterns of groundwater quantity and quality at and across different spatial scales. In particular, we 1) map the two-dimensional (2D), vertically-integrated spatial distribution of groundwater levels in surficial aquifers; 2) identify groundwater mounds ('recharge zones') and valleys ('discharge zones'); 3) characterize the occurrence of elevated concentrations of Cl in shallow water wells (as a tracer of salinity); and 4) visualize, compare and analyze the groundwater and Cl dynamics. This process was applied at three different spatial scales: the basin scale (i.e., across the entire peninsula), regional scale, and local scale, with the two regions identified as major basin-scale discharge zones – the Michigan and Saginaw Lowlands – being further analyzed through the development of regional- and local-scale SWL models. Results from a field sampling campaign are presented to understand the three-dimensional (3D) Cl spatial structure within the Michigan Lowlands, which is then compared with results from previous studies in the Saginaw Lowlands where shallow, saline groundwater has been attributed to brine upwelling.

It is worth noting the necessity of a multi-scale approach in this study. The Lower Peninsula of Michigan is characterized by strong topographic variability and complex geology, which leads to the development of multi-scale groundwater flow systems (Toth 1963; Freeze and Witherspoon 1967; Meyboom 1967; Winter 1988, Sampath et al 2016). A particular flow system might be important at one scale in the study area, but may play no role at other scales. Different residence time distributions, source areas, and flow paths transmitted through different geologic materials may lead to high variability in the spatial distribution of groundwater quality (Toth, 2009; Huggenberger et al., 2013). Moreover, certain patterns may not be discernable when viewed at smaller scales, although their recognition at larger scales may spark new insights. In light of these considerations, this study evaluated the near-surface groundwater levels and Cl concentrations at the multiple spatial scales noted above.

1.3 Ch. 1 Methods

Recently assembled statewide groundwater databases were employed to delineate groundwater levels and Cl concentrations of the near-surface environment at different spatial scales. We apply an automated, continuously moving window statistical analysis to generate hydraulic head maps using Static Water Levels (SWLs) from drinking water well records. To evaluate Cl variability with respect to depth and bedrock geology within the Michigan Lowlands, 467 wells were sampled across Ottawa County, Michigan, which lies almost entirely within the Michigan lowlands.

1.3.1 Data-driven Groundwater Modeling

The traditional groundwater modeling approach typically implements process-based numerical models to simulate groundwater conditions, using a limited amount of data to verify the model at specific points in space and/or time. This is challenging because: 1) most natural systems are complex, and the development of multi-scale flow systems adds yet another layer of complexity; 2) data are expensive to collect; and 3) typically modelers have incomplete datasets to accurately characterize all of the parameters in the system. Even when sufficient data are available, significant time and effort is required for calibration. An opportunity is presented by considering that, when abundant data are available, reasonable estimation of

physical phenomena, including those related to hydrology, can be accomplished without developing a calibrated model (Cunge 2003; Garcia and Shigidi 2006). Although limited in nature (e.g., transient simulations and the estimations of water budgets and fluxes are not possible), data-driven groundwater models based on numerous head measurements across space and time and dependent on correlations between variables provide an efficient method for estimating the prevailing, long-term hydrogeological conditions. This affords the opportunity to concentrate more on understanding the natural processes rather than the issues related to numerical modeling of groundwater systems.

In this study, we apply a data-driven approach to generate statistical models of groundwater conditions in the Lower Peninsula of Michigan, capitalizing on substantial geospatial data integration completed by the Michigan Department of Environmental Quality (MDEQ) and Michigan State University that resulted in two extensive, high-resolution, statewide groundwater databases with records that go back several decades: (1) Wellogic, which includes information on static water levels (SWL) from over 550,000 water wells, including private domestic wells, public supply wells, and wells used for agriculture and industry (MDEQ 2014); and (2) WaterChem, which contains water quality information from over 1 million samples collected from water wells and analyzed at the State of Michigan's Drinking Water Analysis Laboratory (MDEQ 2010). Spatial coverage of the Wellogic (SWL) and WaterChem (Cl) wells (Figure 1.3) is very high throughout most of the peninsula, and especially for areas in and near the Michigan Lowlands (i.e., one location used for regional and local analysis). This provides an unprecedented amount of spatial information regarding groundwater across the study area. However, there are significant challenges that make using the datasets problematic, which are discussed next.

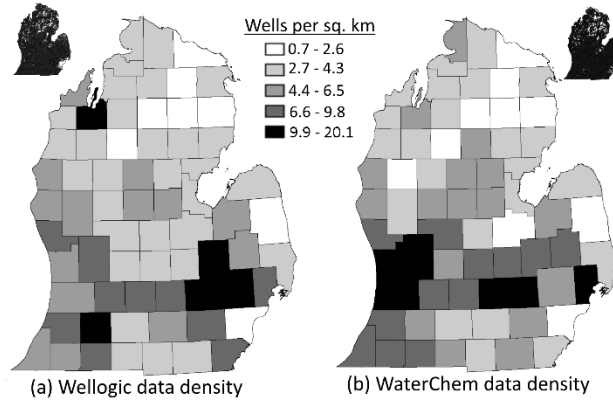


Figure 1.3: Spatial coverage of (a) Wellogic database and (b) WaterChem database.

1.3.1.1 Challenges Sources of Error

There are a number of sources of error and variability embedded in the SWL dataset that must be addressed during processing and analysis. First, there are sources of procedural error to address, including: ‘black and white’ errors, or data that are physically-impossible or so badly mislocated that they are many standard deviations outside of the local trend. These errors result from poor record keeping at the time of collection or transcription problems during data entry. There are also significant sources of uncertainty embedded in the SWL calculations. For example, each data point represents the SWL or Cl concentration at a single point in time, and therefore this study - which does not differentiate SWL or Cl data from different time periods, but rather uses all processed data from different times - presents long-term average groundwater level distributions and Cl spatial dynamics. Using SWL from different seasons, years or even decades, potentially results in relatively large SWL variability for locations in close proximity to one another, or between measurements taken at different times from a single well. Other sources of inaccuracy in SWL calculations include: 1) approximate well locations – most older well records lack GPS information required the use of geocoding or indirect information reported by the driller to estimate position; 2) the presence of vertical head gradients, which will impact the depth-to-water measurement depending on the depth of the well screen, resulting in SWL variability for adjacent wells, even if temporal trends are not present and especially when wells terminate in different aquifer units (note that Wellogic contains wells completed in both the glacial and bedrock aquifers of Lower Michigan, and in principle these aquifers could

be analyzed individually in areas of dense data coverage; however, in this study it was deemed appropriate to analyze glacial and bedrock wells together – see Appendix A at end of this chapter); 3) measurement uncertainty introduced by inconsistencies from driller to driller; and, 4) the use of 10m resolution DEM (the best available across all areas of study), which in areas of steep topographic gradients may result in the use of an inaccurate datum for calculation of the SWL.

These potential sources of inaccuracy in the SWL calculations raise a number of important questions related to using them to delineate groundwater levels. What is the cumulative impact of the sources of uncertainty in SWL calculations? How can we quantify and separate the noise from the SWL trend (or ‘signal’)? And how do we map the noise and signal at different spatial scales? Our systematic approach for addressing these important questions is presented next, which is the first step in the integrated workflow for utilizing the SWL and CI datasets to address the study objectives (see Figure 1.4). For analysis at a given scale, the major components of the workflow include: 1) pre-processing the SWL data to remove blatant errors and incomplete data; 2) assessing and modeling SWL spatial structure and local variability from locale to locale (cell-by-cell variogram development); 3) SWL interpolation and delineation of groundwater mounds and valleys (referred to as recharge zones and discharge zones, respectively); and graphical and statistical

analysis of Cl point data. The following subsections provide details for each component of the integrated water quantity-quality workflow.

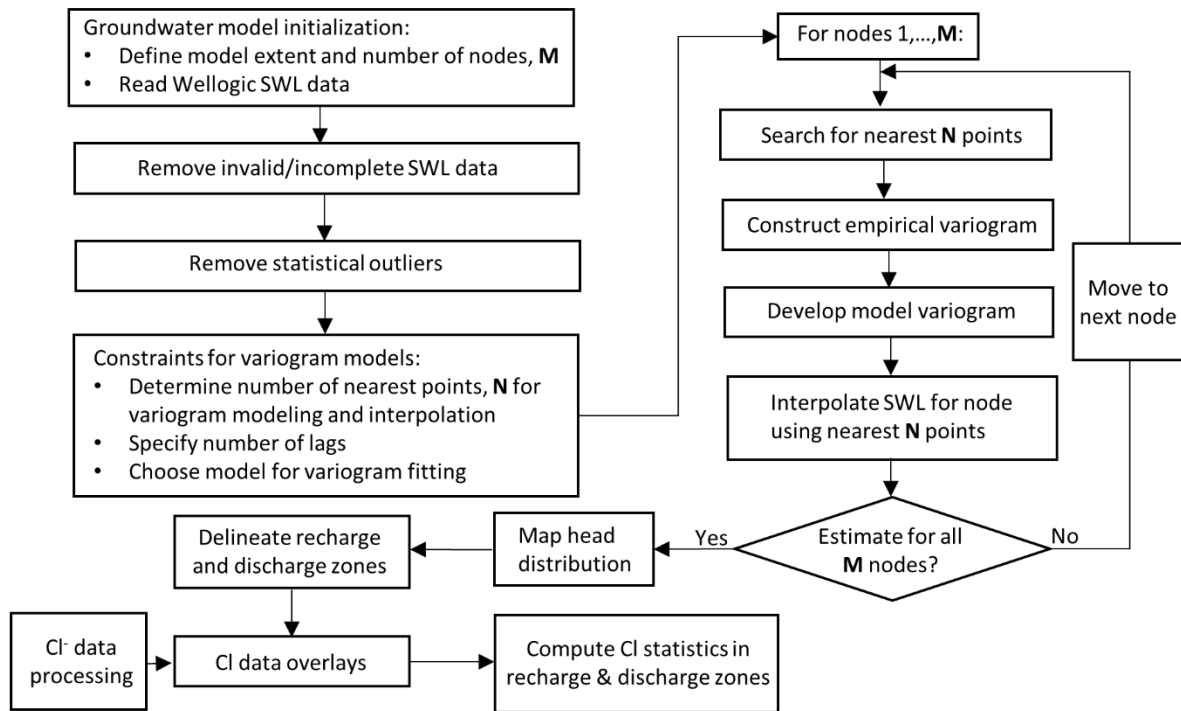


Figure 1.4: Workflow diagram for integrated water quantity-quality data-driven modeling.

1.3.2 Spatial Interpolation of Massive Noise SWL Datasets

Interactive Groundwater software – introduced by Li and Lui (2006), but being continuously updated (see, e.g., Li et al. 2006; Liao et al. 2015) – was used for the SWL spatial analysis.

1.3.2.1 Filtering Procedural Errors

The first step for delineating spatial SWL variations was to select a domain and model cell resolution, which determines the number of model nodes. After reading SWL data and subtracting the depth-to-water recorded in the well logs from the 10m DEM available in the National Elevation Dataset (NED USGS 20006), data that clearly wrong or incomplete were removed and a moving statistical analysis was used to identify and remove values that were more than three standard deviations from the local average, using the nearest 30 points to establish the local trend. Table 1.1 provides details of the basin-scale model and the

regional and local data-driven models developed for the Michigan Lowlands and Saginaw Lowlands. Note the large number of SWL data points involved for each model. The percentage of points removed at the basin-scale was 1.48%. For the Michigan Lowlands regional and local models, 1.89%, and 1.43% were removed, respectively. In the Saginaw Lowlands regional and local models, 1.38% and 1.41% were removed, respectively.

Table 1.1: Details of the basin-scale SWL model (BW), the regional and local models developed for the Michigan Lowlands (ML-R and ML-L, respectively), and the regional and local models developed for the Saginaw Lowlands (SL-R and SL-L, respectively). Each model cell at a given scale was approximately square and of the same size.

| Model | Area (km ²) | Grid size (m) | | SWL Data Points | |
|-------|----------------------------|---------------------|-----|-----------------------|---------|
| | | NX | NY | | |
| BW | 106751 | 4500 | 81 | 102 | 489,894 |
| ML-R | 17026 | 1480 | 80 | 112 | 110,760 |
| SL-R | 13,227 | 1490 | 88 | 79 | 44,803 |
| ML-L | 1108 | 250 | 150 | 130 | 6555 |
| SL-L | 1378 | 275 | 161 | 138 | 4374 |

1.3.2.2 Separating Noise from Signal

The general approach for quantifying and separating noise from SWL spatial trends is to assess the sub-cell variability and local (cell-to-cell) spatial structure for each estimation point of the SWL models, taking advantage of the high density SWL data available essentially ‘everywhere’ to quantify variations at very close distances (relative to the model size), and to use this critical information during spatial interpolation. This is sometimes generally referred to as nonstationary modeling or the automatic moving window approach, and has been used in recent geostatistical studies involving datasets of meteorological or environmental parameters distributed across space (see, e.g., Walter et al. 2001 Pardo-Iguzquiza et al. 2005; Lloyd 2010, Harris et al. 2010).

This approach implements kriging, an optimal interpolation method in geostatistics (Sun et al. 2009, Varouchakis and Hristopulos 2013) that provides estimates of values at any given point as a weighted sum of input values at surrounding points, with weights assigned based on spatial trends and correlations (Isaaks

and Srivastava 1989; Bossong et al. 1999). The weights are derived from fitting a model variogram to the empirical variogram, which are graphical depictions of separation distance, or lag, and semivariance (or dissimilarity) in values between pairs of input data (see Figure 1.5). For this study, the nugget represents the SWL variability (i.e., noise) across a single model grid cell (i.e., the impact of all sources of uncertainty in the SWL calculations for a given grid cell location); the partial sill is difference of the maximum modeled semivariance and the nugget, interpreted as the SWL signal, or the spatial trend across grid cells; and the range is the lag distance at which the variogram maximum modeled semivariance is (approximately) reached (i.e., semivariance no longer increases with separation distance).

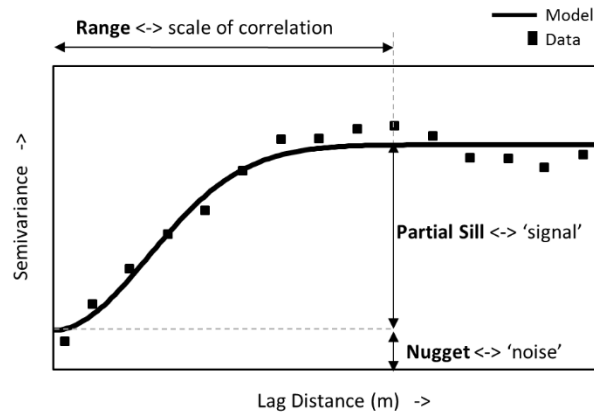


Figure 1.5: Schematic of a variogram (model and data) with annotations clarifying the nugget, partial sill and range terms of the model variogram.

When modeling an area with sparse data coverage, a single model variogram is typically developed using the global dataset. Traditionally, studies mapping groundwater elevations make use of many fewer high quality groundwater level measurements spread across relatively large distances because of the high costs associated with constructing monitoring wells to collect precise physical groundwater data. Thus, a single, global variogram is utilized for spatial interpolation. In some cases, data subsets in the vicinity of a cluster of estimation points are used to develop several local variograms rather than apply a single variogram derived from the global dataset, thereby improving interpolation results (see, e.g., Haas 1990 and 1995; Abedini et al. 2008). In this study, we capitalize on the very high data density of the SWL dataset to create a unique model variogram at each estimation point, using the nearest N points to develop the model

semivariogram and perform kriging estimation (see the process loop in Figure 1.4). The number of points, N , at each scale was determined by multiplying the average well density within the SWL model, ρ_{wells} , by the area to be used for kriging analysis, assumed to be a circular area with a diameter that is one-tenth the extent of the SWL model, L :

$$N = \rho_{wells} * \frac{\pi}{4} \left(\frac{1}{10} L \right)^2 \quad (2.1)$$

Values of ρ_{wells} , L and N for all SWL models are provide in Table 1.2. Although the selection of one-tenth of L as the ‘range of interest’ for variogram model development was chosen in a somewhat arbitrary manner, the general approach used here is a pragmatic way to ensure that the number of points is large enough to develop a model variogram that is statistically significant, but not so large as to overburden the computations, as $O(n^3)$ computations are required to solve the kriging equations involving n data (Cressie and Johannesson 2006).

Table 1.2: Values of ρ_{wells} , L and N for all SWL models. See Table 1.1 for model abbreviation clarifications.

| Model | ρ_{wells} (well per sq. km) | L (km) | N |
|-------|--|-------------|------|
| BW | 4.6 | 459 | 7594 |
| ML-R | 6.7 | 166 | 1440 |
| SL-R | 3.4 | 130 | 450 |
| ML-L | 5.9 | 37.5 | 66 |
| SL-L | 3.2 | 44 | 48 |

1.3.2.3 Example Variograms

Illustrative examples of the developed variograms from each spatial scale are shown in Figure 1.6, where the semivariance is plotted on the y-axes and lag distance is plotted on the x-axes. The data shown on each plot represent the average semivariance at each of the 15 lags. The Gaussian variogram model fitted to the data using least-square regression optimization is shown as a solid line. Table 1.3 provides information

on the nugget, range and partial sill of each example variogram model shown in Figure 1.6. Several important points can be made from these results: (1) for all variogram models, the nugget, or SWL variability (noise) at the grid cell location (node), was captured and was less than grid-to-grid SWL variability revealed by partial sill values; (2) the nuggets, partial sills, and ranges are not only different for the different variograms at a given scale, articulating the non-stationary spatial structure from grid cell to grid cell, but also are larger for larger models; 3) at each scale, the variograms are relatively well defined by the data, although for larger models the data best matches the model because of the larger number of data points available for assessing the spatial structure and the relative insensitivity of large area delineations to individual SWL points; and 4) the ranges at a given scale are approximately equal to the length of a few adjacent grid cells at that particular scale, which confirms that the approach captures the local spatial structure, where the relative size of ‘local’ depends on the scale of analysis. Note that the increase in nugget magnitude across scales is expected, since sub-grid variability increases as scales change from fine to coarse, reflecting a ‘scale-smoothing’ effect: smaller-scale variabilities are not represented in the variogram model structure, but are lumped in with the nugget.

Importantly, these examples from the non-stationary kriging approach demonstrate the relatively low impact of the sources of uncertainty embedded in the SWL calculations for the purposes of delineating the SWL spatial structure at a given modeling scale (i.e., the nugget magnitude is small compared to the total observed SWL variability). In addition, this technique fully utilizes the massive SWL dataset while remaining computationally feasible by solving many simplified problems rather than one set of kriging equations for the global dataset. Although this approach has been used in other geospatial studies (see above), the authors do not know of another groundwater mapping study that had sufficient data density available to implement the development of local variograms at each estimation point. Moreover, the previous geostatistical studies did not examine how variogram parameters differ across spatial scales as was shown here.

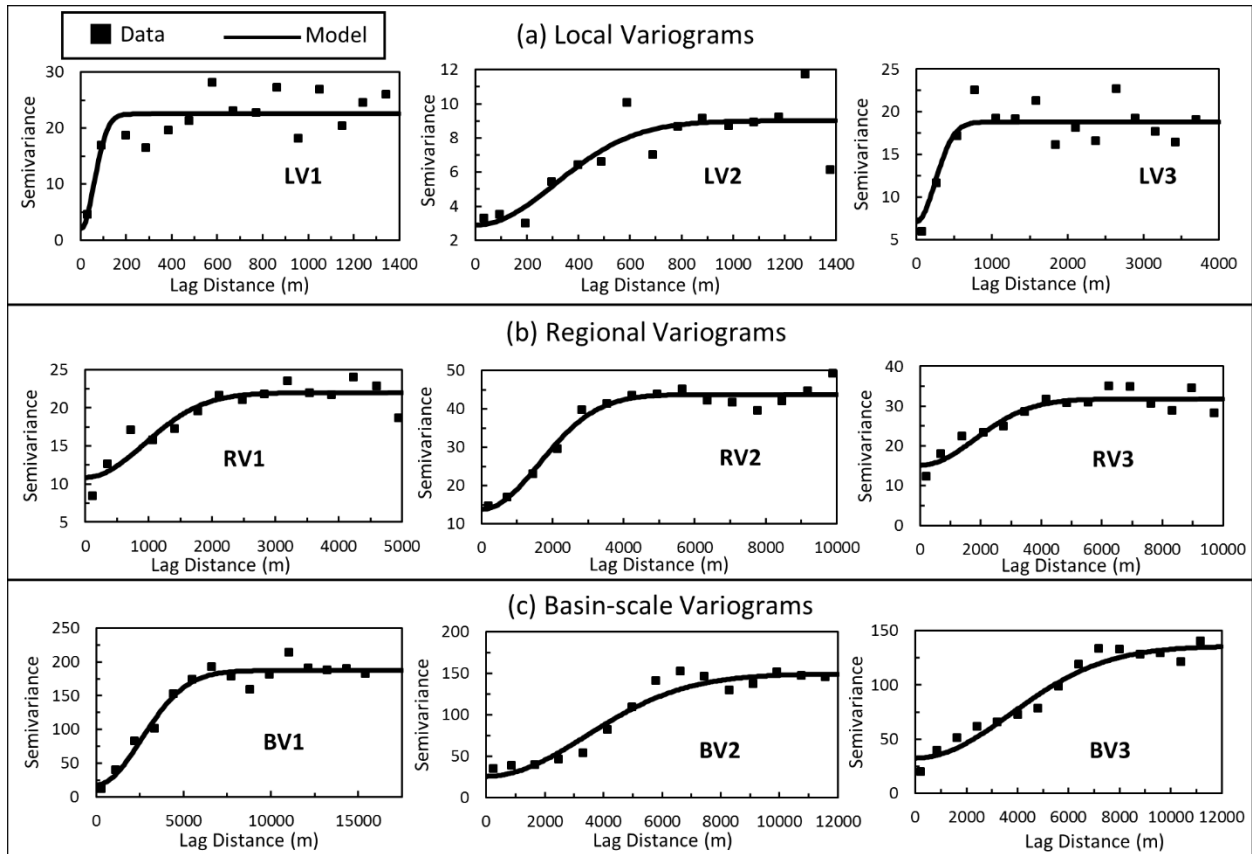


Figure 1.6: Illustrative variograms at the (a) local scale (LV1, LV2, LV3); (b) regional scale (RV1, RV2, RV3) for the Michigan Lowlands analysis, and also at (c) basin-scale (BV1, BV2, BV3).

Table 1.3: Information for the model variograms shown in Figure 1.6.

| Vario-gram Model | Node (i,j) | Nugget | Partial Sill | Range |
|------------------|------------|--------|--------------|-------|
| LV1 | 83,72 | 2 | 20.5 | 144 |
| LV2 | 142,99 | 2.9 | 6.1 | 756 |
| LV3 | 41,47 | 7.1 | 11.7 | 604 |
| RV1 | 58,27 | 10.9 | 11.1 | 2276 |
| RV2 | 69,54 | 13.8 | 30 | 3960 |
| RV3 | 30,51 | 15.1 | 16.7 | 4442 |
| BV1 | 55,73 | 29.1 | 190.8 | 12328 |
| BV2 | 28,49 | 26 | 123.6 | 8320 |
| BV3 | 35,30 | 32.5 | 103.2 | 9123 |

1.3.3 Delineating Recharge and Discharge Areas

The results from the 2D SWL interpolation were used to delineate groundwater mounds surrounded by lower groundwater elevations, as well as areas where the lowest groundwater elevations are found. In this study, these areas are referred to as recharge and discharge zones, respectively, although it should be noted that this definition is different from the theoretical definition concerning vertical head at the water table (Freeze and Cherry, 1979). Characterizing vertical gradients would require nested wells with precise knowledge of the land surface elevation – such data were not available in this study. Nonetheless, the practical approach of delineating groundwater mounds and valleys provides the necessary qualitative distinction between areas where groundwater is expected to have a relatively greater downward or upward flow component.

At each scale, head maps were displayed, and polygons were generated encircling continuous areas with head values above or below threshold values of the hydraulic head distribution considered to be associated with recharge areas or discharge areas, respectively. For discharge areas, the threshold value was the head that roughly separated the lower and middle tertiles of the head distribution; for recharge areas, the head that roughly separated the middle and upper tertiles was used as the threshold value. The exception is the local-scale analysis. Because fewer WaterChem data points were available within the local study area, the entire local model domain was classified as either within a zone of discharge or a zone of recharge in order to perform meaningful statistical analysis (see next subsection). The local-scale threshold value was the head that roughly separated the lower and middle tertiles of the head distribution. Effectively, this assumes that at local scales, lateral components of flow are dominated by vertical components. Note that the use of tertiles was a pragmatic approach and not necessarily founded in theory, although the authors experimented with different threshold values, e.g. based on quartiles, and the results from the integrated CI/SWL analysis did not change significantly (e.g., see Appendix B at the end of this chapter). The process was done using geospatial analysis tools in ArcMap version 10.1 (ESRI, 2011).

1.3.4 Elevated Cl Overlays

Point measurements of Cl concentrations from water well samples were overlaid on the head maps and a series of graphics using different thresholds to filter the Cl data were generated at each scale investigated. The thresholds used for graphical analysis were $[Cl] > 250$, $[Cl] > 500$, and $[Cl] > 1000$ mg/L, and hereafter, the term ‘elevated’ refers to Cl data points present after filtering with a given threshold. These thresholds were considered to be well above natural concentrations that are typically less than 15 mg/L for most shallow aquifers in the mid-continent region of North America (Hem 1985, Wahrer et al., 1996). After some experimentation, these thresholds were deemed to be the most appropriate to illustrate changes in spatial patterns at different concentrations. Of course, other potential sources might cause chloride concentrations to be elevated, e.g., halite from roadway deicing or infiltration of septic tank wastewater. In the Discussion section below, the impact of other Cl sources on the analysis is briefly explored.

When displayed in conjunction with the discharge and recharge zones delineated in the manner described above, this overlay analysis allows easy identification of Cl concentration clusters in hydrologically-distinct regions within the study domain. However, the number of wells completed in one zone as compared to the other is not always equal. At the basin-scale, there were 228,967 and 43,311 Cl data points available in discharge and recharge zones, respectively, but at the local scale (Saginaw Lowlands) 825 and 5222 points were available in discharge and recharge zones, respectively. To account for this, a quantitative analysis was implemented that considered the percentage of Cl data points above a given threshold relative to the total number of data points within the zone under analysis (discharge or recharge). The process was as follows: at all scales, quantify 1) the total number of Cl data points present in the discharge and recharge zones; 2) the number of data points present after filtering the Cl dataset for different thresholds; 3) the percentage of data points in the discharge and recharge zones that are above different thresholds by using the values obtained in steps 1 and 2; and 4) calculate the ratio of percentages (discharge:recharge). This also removes the potential bias related to multiple samples from a single well being used in the analysis. The thresholds used for these statistical analysis were $[Cl] > 100$, $[Cl] > 150$, $[Cl] > 200$, $[Cl] > 250$, $[Cl] > 500$, $[Cl] > 1000$, and $[Cl] > 1500$ mg/L.

1.3.5 Field Sampling in the Michigan Lowlands

Because the WaterChem dataset does not contain depth information, a synoptic countywide sampling campaign was conducted to gain an understanding of the present-day three-dimensional structure of the Cl concentrations in the near-surface environment of the Michigan Lowlands. Groundwater samples were collected from water wells at 468 locations in Ottawa County, Michigan. Wells completed in either the glacial deposits or the Marshall bedrock aquifer were used in the analysis, and well depths were obtained by cross-referencing information from the Wellogic driller logs and local water well records compiled by the Ottawa County Environmental Health Department (Ottawa County 2014). Well location (latitude, longitude) was measured at the wellhead when possible - otherwise it was measured at the sampling point - and was acquired using GPS-enabled smart-phones which delivered sub-10m accuracy. Samples were collected primarily during the fall months of 2014, although roughly one fourth of the samples were collected during the summer months of 2015. After the fall 2014 data were analyzed, they were used to guide the 2015 into critical areas: the fall 2014 data collection was relatively evenly dispersed across the aquifer system (both in lateral and vertical directions), and once analyzed, was used to identify locations where more data were needed (i.e., in areas where Cl concentrations were high and Cl gradients were large). Nonetheless, the slow advection and/or diffusion of solutes in groundwater justifies the assumption that sampling over roughly 9 months is considered a reasonable ‘temporal snap-shot’ of current water quality conditions across the county.

Samples were collected from outdoor spigots or indoor faucets into polypropylene, wide-mouth bottles that had been pre-rinsed with de-ionized water. Although the scientific standard for purging a well (flushing out stagnant water from the system) is to monitor the pumped water until the pH, electric conductivity, and temperature stabilize, we adopted a more practical standard of 5 minutes of flushing, since mineral salt content is not usually affected by residence time in the piping system (Harter, 2003). However, special care was made to sample from discharge points delivering untreated well water, i.e., groundwater that has not passed through a water softener, as periodic regeneration of such devices using brine solutions may artificially elevate chloride concentrations until the freshwater flushes through the system. In order to

minimize artificial Cl contamination of the samples, bottles remained capped until the very moment of sampling and were recapped immediately following sampling. During sampling, the bottles were always held at the bottom to avoid contamination from the technician's perspiration. Duplicate samples were taken at roughly 10% of the sampling locations, yielding an average error of -2.62 mg/L and a RSME (root-mean-square-error) of 12.1 mg/L. Field and lab blanks were utilized to ensure samples were not contaminated during the collection or analysis. All blanks yielded concentrations below 3 mg/L, with an average of 1.75 mg/L. Capped samples were stored in large plastic bags and transported back to Michigan State University for laboratory analysis, which was completed within 10 days of when the sample was obtained.

1.3.6 Analytical Methods for Cl Measurement

The measurement of Cl concentrations in the collected samples followed EPA Standard Method 9212 – Potentiometric determination of chloride in aqueous samples with ion-selective electrode (ISE). A chloride ISE (Cole-Parmer item number EW-27502-13) filled with 10% KNO₃ reference solution was used in conjunction with an electrode/benchtop meter to measure the mV response of the standards and collected samples. Although the samples were not stored in ice coolers during transportation, they were all were stored at room temperature for at least 24 hours with the stock solution (1000 ppm chloride, Cole-Parmer item number WU-27503-09) to ensure all solutions were at the same temperature during analysis ($\pm 1 \bullet C$). Standards and samples were mixed 50:1 with an ionic strength adjustment solution (5 molarity NaNO₃), and calibration was performed by analyzing a series of standards and plotting mV vs. chloride concentration on semi-log plots. Sample chloride concentrations were determined from the calibration curve.

1.4 Ch. 1 Results

1.4.1 Multiscale Hydraulic Head Distribution

The results of the SWL spatial interpolation across multiple scales is shown in Figures Figure 1.7 and Figure 1.8. Recharge and discharge zones are also delineated, although at the local scale the unshaded area is considered all discharge, as mentioned previously. Clearly the SWL patterns exhibit a hierarchical structure:

basin-scale recharge areas in the northern and southern highlands of Lower Michigan clearly contrast with the basin-scale discharge areas in the Saginaw Lowlands, Michigan Lowlands and along the coastal zone (Figure 1.7), consistent with the findings of previous studies (see Barton et al. (1996), Hoaglund et al. (2002) and Feinstein et al. 2010)). Regional SWL distributions developed for the Michigan Lowlands and the Saginaw Lowlands (Figure 1.8a and Figure 1.8b) exhibit strong SWL variability with clear recharge zones in regional highlands and discharge zones in the lowlands and along the coasts. The local models developed within the regional discharge zones again showed significant SWL variability characterized by local recharge and discharge areas not discernible at the regional or peninsula-wide scale (Figure 1.8c and Figure 1.8d).

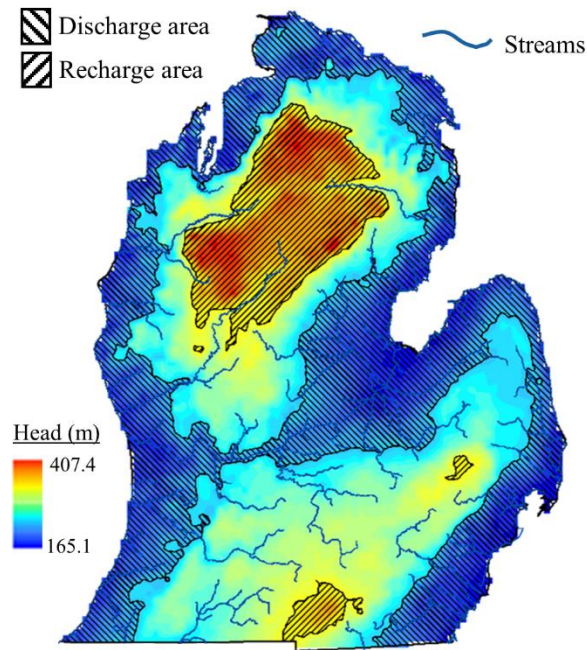


Figure 1.7: Long-term average SWL distributions delineated at the basin-scale. Third order and higher streams are included, as well as the delineated recharge and discharge zones.

In the Michigan Lowlands, the influence of streams is more pronounced than at the basin-scale, as many stream corridors coincide with relative depressions in the SWL surface, and clearly the larger streams are a dominant sink of groundwater in the region (Figure 1.8a). Similar to the regional analysis, the influence

of streams at the local scale is significant, with almost all 2nd-order stream valleys or higher representing local discharge areas and most 2nd-order interfluves primarily representing local recharge areas (Figure 1.8c). Note that the results from the Michigan Lowlands regional and local groundwater mapping are consistent with the simulation results of pre-development heads in the glacial aquifer system completed by Feinstein et al. (2010), which involved numerical simulation of a 20-layer model characterizing interactions between surface water bodies, glacial deposits and the underlying bedrock of the Lake Michigan watershed. It is encouraging that the relatively simple 2D, long-term average delineations of regional and local groundwater levels presented here agree with the results from a complex, process-based approach that considered the deeper aspects of the groundwater system.

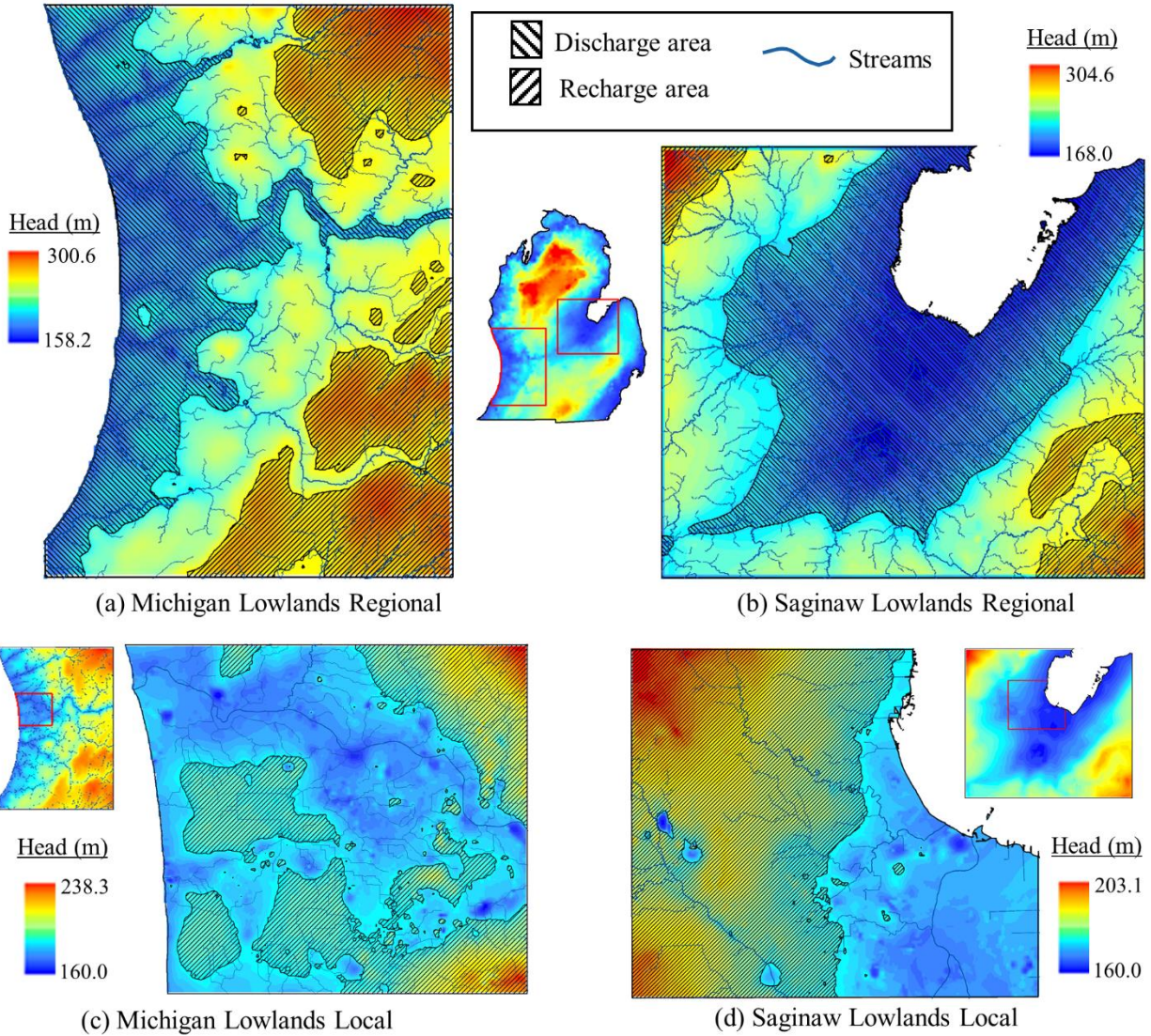


Figure 1.8: Long-term average SWL distributions delineated at the regional scale for the (a) Michigan Lowlands and (b) Saginaw Lowlands, as well as at the local scale for the (c) Michigan Lowlands and (d) Saginaw Lowlands. Second order and higher streams are included for the regional scale graphics, while all order streams are included in the local scale graphics.

The regional and local discharge zones of the Saginaw Lowlands are more expansive than those seen in the Michigan Lowlands (Figure 1.8b and Figure 1.8d). Moreover, the range of SWL variability (especially for the local scale) is less than that of the SWL models of the Michigan Lowlands. This indicates relatively low regional and local recharge to the Saginaw Lowlands shallow aquifer system, which was inferred also from geochemical analyses complete by Long et al (1988). The glacial sediments

underlying the Saginaw Lowlands are notably fine-textured and strongly contribute to the paucity of shallow recharge.

1.4.2 Multiscale Analysis of Elevated Cl Concentrations

The multiscale graphical analysis of elevated chloride concentrations is presented in Figure 1.9, Figure 1.10 and Figure 1.11, where the occurrence of wells yielding Cl concentrations above prescribed thresholds are overlaid on the hydraulic head maps described in the previous subsection. For each threshold and at each scale, a pattern emerges: the occurrence of elevated Cl concentrations is spatially associated with the discharge zones. At the basin scale (Figure 1.9), elevated concentrations occur predominately occur in the Saginaw Lowlands, Michigan Lowlands, and in clusters along the coastline (e.g., along Lake Huron in southeast Michigan), while in the northern basin-scale recharge zone, and to a lesser degree in southern counterpart, there are significantly fewer elevated Cl data points, especially at the >500 and >1000 mg/L thresholds. There is also a significant clustering of elevated Cl concentrations near the groundwater recharge mound in southeast Michigan, an exception to the pattern of significant clustering in discharge zones relative to recharge zones. This area is further examined below.

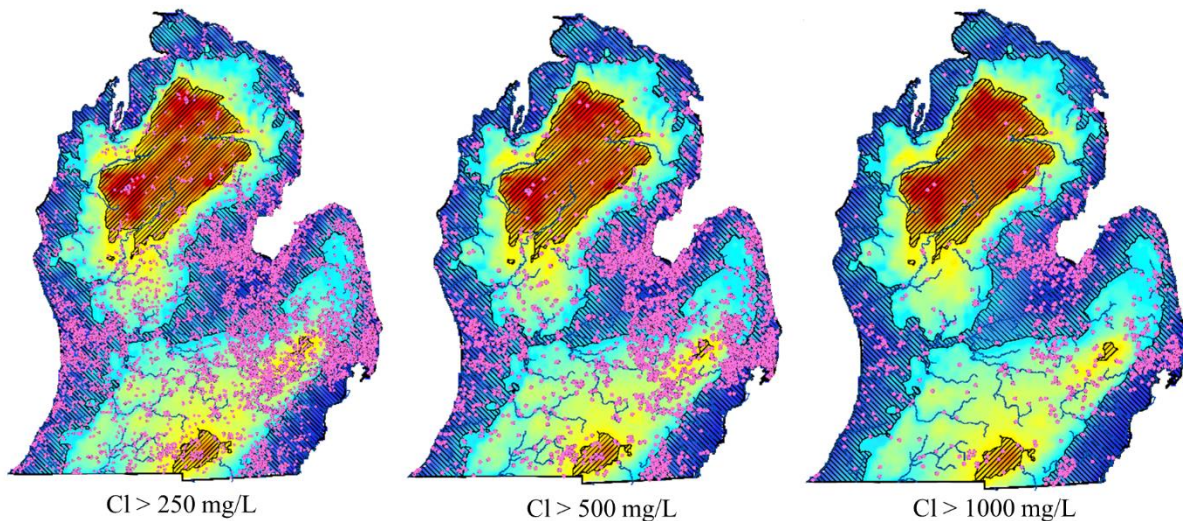


Figure 1.9: Occurrence of elevated Cl (>250, >500, >1000 mg/L) wells with respect to basin-scale SWL distributions.

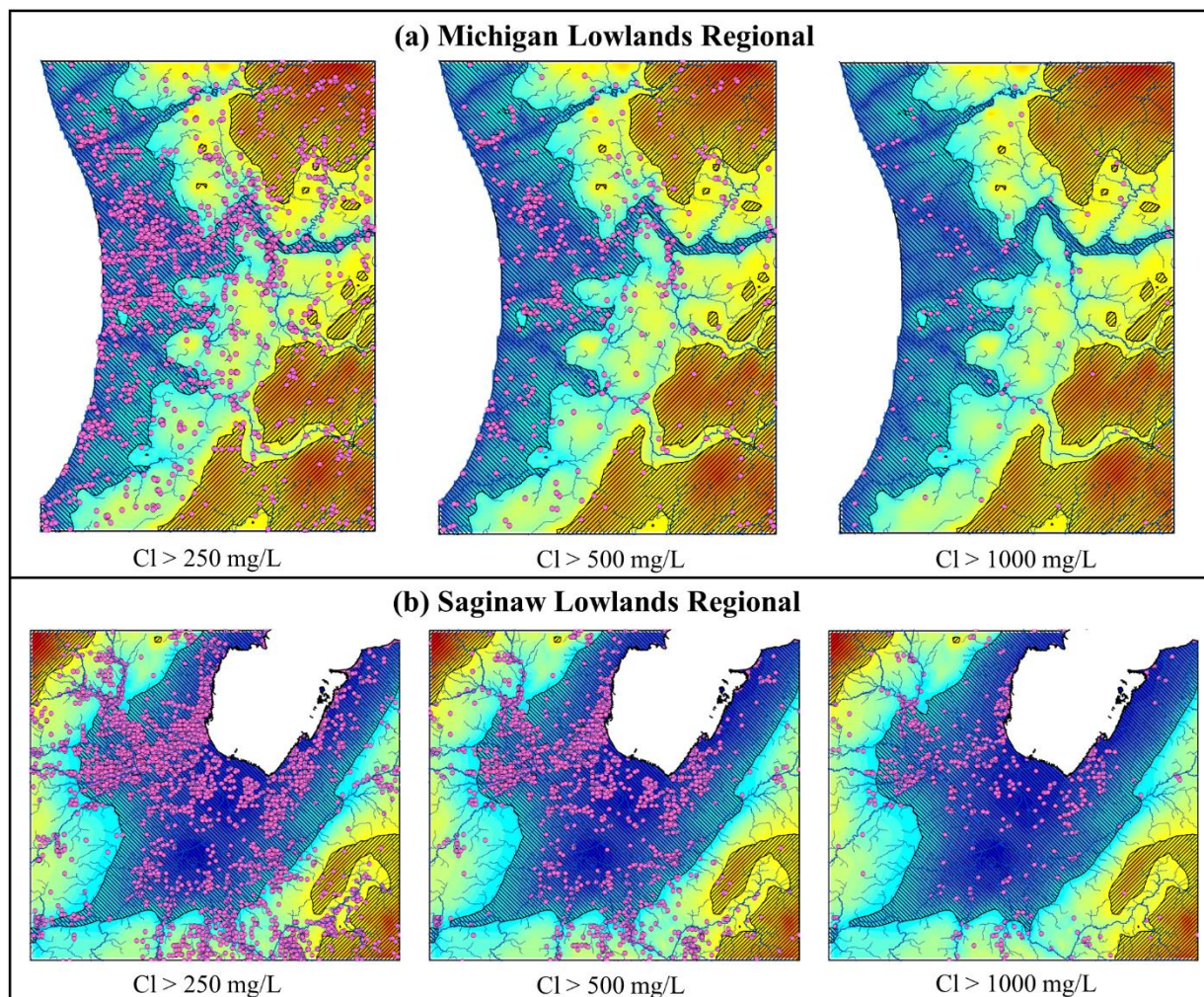


Figure 1.10: Occurrence of elevated Cl (>250, >500, >1000 mg/L) wells with respect to regional-scale SWL distributions for the (a) Michigan Lowlands and (b) the Saginaw Lowlands.

At the regional scale (Figure 1.10), the occurrence of elevated Cl concentrations for the >250 mg/L threshold is clustered in the regional discharge zones along the coast and in stream valleys, some of which cut through or near recharge zones. However, for the >500 mg/L threshold and especially for the >1000 mg/L threshold, the recharge zones and the interfluvies between major streams are mostly devoid of elevated Cl concentrations. The Michigan Lowlands local-scale analysis (Figure 1.11a) demonstrates again, for each threshold, clusters of elevated Cl concentrations primarily occur within local discharge zones. The most prominent clustering appears in the central and northwest regions where the SWLs are lowest. Similar to the regional analysis, few elevated Cl concentrations are seen in recharge areas or in between stream corridors for the >500 and >1000 mg/L thresholds. For the Saginaw Lowlands local analysis (Figure 1.11b),

elevated Cl concentrations for all thresholds are seen in both local recharge and discharge areas, which could be due to a sampling bias (e.g. many fewer Cl points in the local discharge zone, as noted above), and/or because the paucity of shallow recharge in this area noted above (i.e., essentially all groundwater is discharging within the area chosen for local analysis).

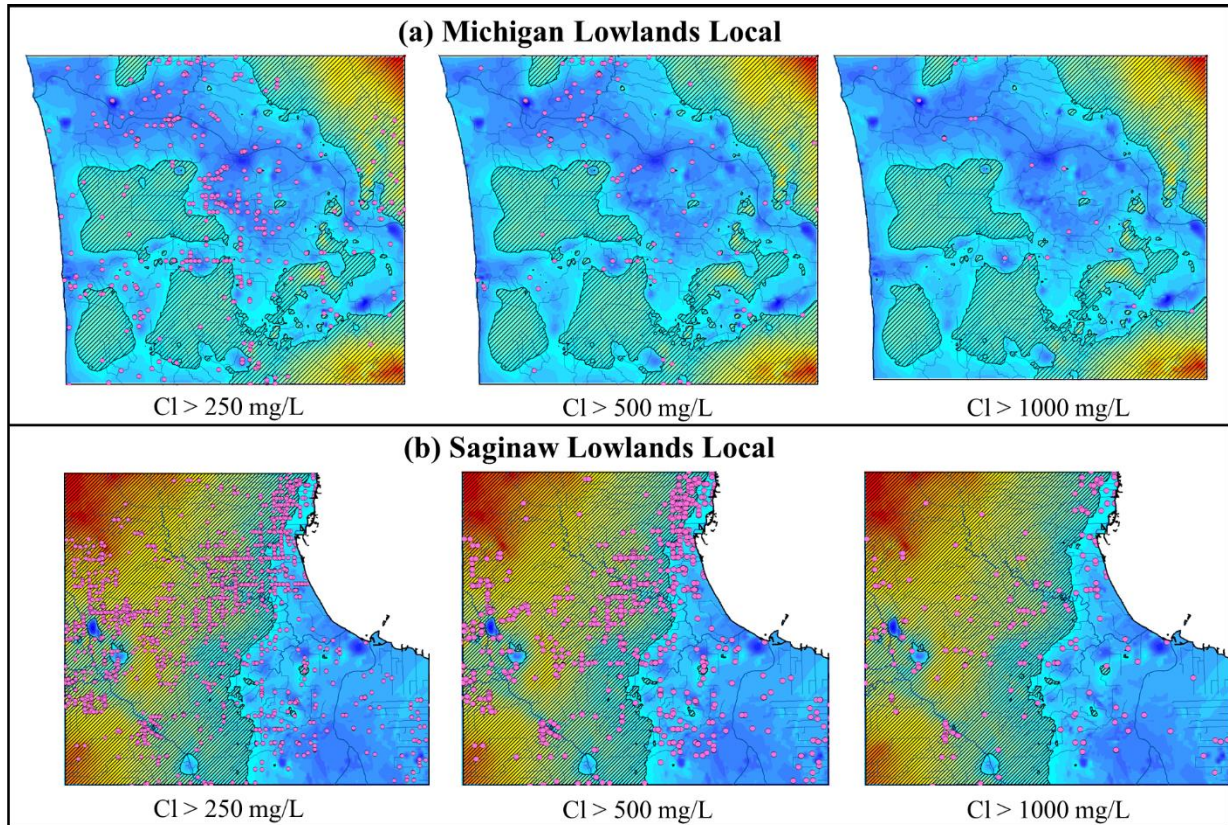


Figure 1.11: Occurrence of elevated Cl (>250, >500, >1000 mg/L) wells with respect to local-scale SWL distributions for the (a) Michigan Lowlands and (b) the Saginaw Lowlands.

The results of the basin-scale, regional and local quantitative analyses of elevated Cl concentrations and their occurrence in discharge and recharge zones are presented in Table 1.4. The percentage of wells with elevated Cl concentrations in the discharge and recharge zones is given, as well as the ratio of these percentages (discharge to recharge). In general, the results are consistent with the graphical analyses: at each scale and for all models, there are a consistently a higher percentage of wells with elevated Cl concentrations in discharge zones than in recharge zones (as indicated by the ratios greater than one). Furthermore, as the threshold value increases, i.e., smaller concentrations are removed from the analysis, the ratio of percentages increases, e.g., from 3.22 at the >100 threshold to 18.56 at the >1500 threshold for

the basin-scale analysis; 1.94 to 5.14 for the Michigan Lowlands regional scale analysis, etc. All ratios for the >500, >1000, and >1500 mg/L thresholds are at least 3 or larger, demonstrating a particularly strong statistical relationship between relatively low SWL elevations and the frequent occurrence of high Cl concentrations (i.e., above 500 mg/L). Note that the ratios are all greater than one for even the Saginaw Lowlands local model, which confirms that the graphical analysis (Figure 1.11b) was probably skewed by many more wells being sampled in what was designated as the local recharge area, and hence the need for evaluating percentages of wells with elevated Cl rather than just the absolute number of wells within discharge and recharge zones.

Table 1.4: Statistics from the multiscale elevated Cl-SWL analysis.

| Cl dataset | Wells with elevated Cl, discharge zones | Wells with elevated Cl, recharge zones | % of wells with elevated Cl, discharge zones | % of wells with elevated Cl, recharge zones | % ratio (discharge: recharge) |
|---|---|--|--|---|-------------------------------|
| Peninsula-wide | | | | | |
| >100 | 35693 | 2032 | 15.59 | 4.69 | 3.32 |
| >150 | 25282 | 1013 | 11.04 | 2.34 | 4.72 |
| >200 | 19448 | 628 | 8.49 | 1.45 | 5.86 |
| >250 | 15321 | 405 | 6.69 | 0.94 | 7.16 |
| >500 | 6504 | 81 | 2.84 | 0.19 | 15.19 |
| >1000 | 1612 | 14 | 0.70 | 0.03 | 21.78 |
| >1500 | 785 | 8 | 0.34 | 0.02 | 18.56 |
| Michigan Lowlands - Regional Scale | | | | | |
| >100 | 6685 | 1912 | 11.96 | 6.15 | 1.94 |
| >150 | 4098 | 991 | 7.33 | 3.19 | 2.30 |
| >200 | 2691 | 582 | 4.82 | 1.87 | 2.57 |
| >250 | 1806 | 392 | 3.23 | 1.26 | 2.56 |
| >500 | 463 | 84 | 0.83 | 0.27 | 3.06 |
| >1000 | 79 | 12 | 0.14 | 0.04 | 3.66 |
| >1500 | 37 | 4 | 0.07 | 0.01 | 5.14 |
| Saginaw Lowlands - Regional Scale | | | | | |
| >100 | 8692 | 638 | 23.91 | 4.71 | 5.07 |
| >150 | 7403 | 360 | 20.36 | 2.66 | 7.66 |
| >200 | 6229 | 248 | 17.13 | 1.83 | 9.35 |
| >250 | 5323 | 179 | 14.64 | 1.32 | 11.08 |
| >500 | 2707 | 31 | 7.45 | 0.23 | 32.52 |
| >1000 | 730 | 9 | 2.01 | 0.07 | 30.21 |

Table 1.4 (cont'd)

| | | | | | |
|---------------------------------|------|------|-------|-------|--------------|
| >1500 | 341 | 7 | 0.94 | 0.05 | 18.14 |
| Michigan Lowlands - Local Scale | | | | | |
| >100 | 1576 | 583 | 16.33 | 9.67 | 1.69 |
| >150 | 1055 | 309 | 10.93 | 5.12 | 2.13 |
| >200 | 695 | 191 | 7.20 | 3.17 | 2.27 |
| >250 | 454 | 113 | 4.70 | 1.87 | 2.51 |
| >500 | 123 | 14 | 1.27 | 0.23 | 5.49 |
| >1000 | 20 | 2 | 0.21 | 0.03 | 6.25 |
| >1500 | 7 | 1 | 0.07 | 0.02 | 4.37 |
| Saginaw Lowlands - Local Scale | | | | | |
| >100 | 510 | 2789 | 61.82 | 53.41 | 1.16 |
| >150 | 486 | 2386 | 58.91 | 45.69 | 1.29 |
| >200 | 465 | 1997 | 56.36 | 38.24 | 1.47 |
| >250 | 447 | 1649 | 54.18 | 31.58 | 1.72 |
| >500 | 322 | 763 | 39.03 | 14.61 | 2.67 |
| >1000 | 81 | 162 | 9.82 | 3.10 | 3.16 |
| >1500 | 30 | 63 | 3.64 | 1.21 | 3.01 |

1.4.3 Three-Dimensional Cl Structure in the Michigan Lowlands

The results from the synoptic field sampling are presented in Figure 1.12, Figure 1.13 and Figure 1.14. A plan view overlay of the Cl point measurements, major streams and a bedrock subcrop map of the area is presented in Figure 1.12. The distribution of Cl concentrations is generally consistent with that derived from the analysis of the WaterChem data, with clustering of elevated (>250 mg/L) Cl concentrations in the central region of the Michigan Lowlands. Note that almost all samples with [Cl] > 100 mg/L occur within the Marshall Formation subcrop, including all samples with [Cl] > 250 mg/L. However, a number of wells yielded water with low (<100 mg/L) Cl concentrations in close proximity to wells with high Cl concentrations, suggesting a strong vertical structure is present.

Indeed, a vertical analysis of measured Cl concentrations demonstrated that Cl concentration generally increased with decreasing elevation of the well bottom, i.e., with increasing depth (Figure 1.13). This trend was observed in geochemical studies of upwelling brines in the Saginaw Lowlands (Long et al.,1988), and helps to explain the presence of strong lateral Cl gradients seen in Figure 1.12, i.e., neighboring wells that

are completed at different depths can have significantly different concentrations of Cl. To further test this interpretation, three-dimensional visualizations of the Cl concentrations and the bedrock top elevation surface were utilized (Figure 1.14). The bedrock top was delineated using lithologic information from the Wellogic records of wells located in Ottawa County (MDEQ 2014), and the 10m DEM was generated from the NED dataset (NED USGS 2010). Clearly, elevated Cl concentrations are concentrated in the Marshall bedrock aquifer, and all but a few of the glacial wells with elevated Cl concentrations are screened at or near the bedrock surface. In principle, this deeper groundwater has a longer residence time than shallow groundwater in the aquifer system, and therefore dissolved Cl concentrations are expected to be somewhat higher in the bedrock aquifer. However, the very high Cl concentrations observed in the field-collected and WaterChem datasets suggests this mechanism is relatively weak compared to the source of hypersaline groundwater down-dip from the subcropping units beneath the Michigan Lowlands.

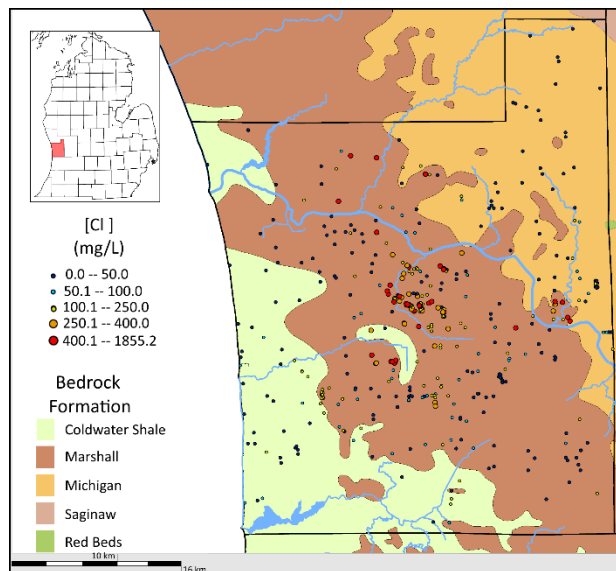


Figure 1.12: Cl point measurements from Ottawa County, Michigan (central portion of the Michigan Lowlands) overlaid on a bedrock subcrop map.

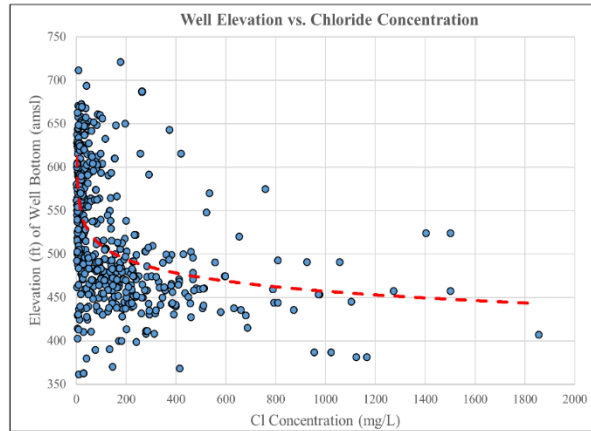


Figure 1.13: Graphical relationship between well bottom elevation and chloride concentration from the field sampling dataset.

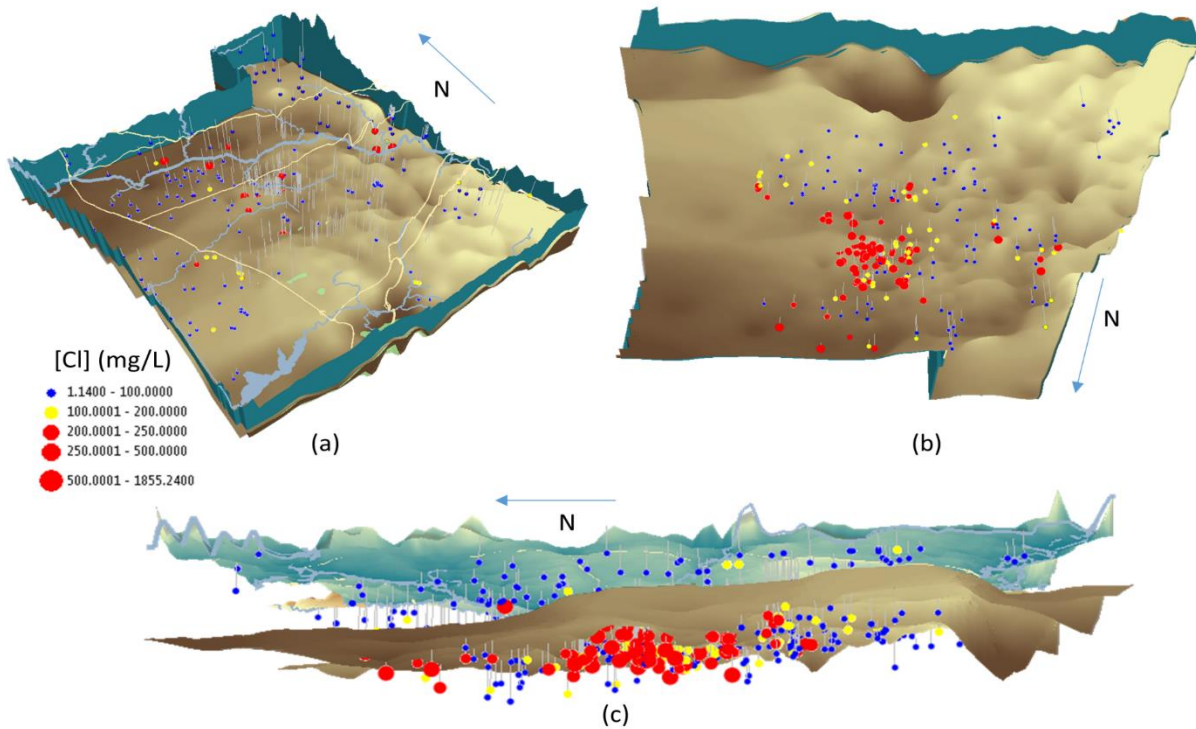


Figure 1.14: Three-dimensional view of Cl point measurements (a) from above, transparent land surface and bedrock surface shown; (b) from below, with bedrock surface shown; (c) from the west, with the DEM and bedrock surface shown.

1.5 Ch. 1 Discussion

1.5.1 Cl-SWL Structure and Natural Brine Upwelling

The multi-scale analysis of SWL distributions and occurrence of elevated Cl concentrations in water wells revealed a significant spatial relationship coupling the hydrology and near-surface groundwater salinity distribution. In particular, there is a multi-scale, hierarchical spatial structure of relatively frequent occurrence of elevated Cl concentrations in ‘discharge zones’ (including along stream corridors), and relatively infrequent occurrence of elevated Cl concentrations in ‘recharge zones’ and in interfluves. Moreover, this nested relationship becomes stronger as higher chloride concentration thresholds were considered.

In discharge areas, a component of the groundwater flow is moving upwards, whereas in recharge areas a component of the groundwater flow is moving downward (Freeze and Cherry, 1979). Thus, the results of the multi-scale Cl-SWL analyses are interpreted as follows: deep flow patterns naturally deliver brackish water towards the statewide shallow groundwater discharge areas; undulations in the regional topography and the major stream networks form regional flow patterns that act as ‘natural pumps’ of the brine-influenced groundwater, concentrating the Cl contamination along large stream corridors; and locally, both large and small streams largely control the distribution of chloride. More succinctly, the natural process of upwelling brine is controlled by the peninsula-wide, multi-scale flow system, which in turn controls the nested, multi-scale structure of the elevated Cl concentrations. This interpretation is consistent with Heath’s (1984) overview of the hydrogeology of the glaciated central region of the U.S., which included the entire Lower Peninsula of Michigan: “... the depth to saline water is less under valleys than under uplands, both because of lower altitudes and because of the upward movement of saline water to discharge.” This study, however, provides greater spatial details for the Lower Peninsula of Michigan, new statistical evidence for this interpretation, and new insight into the multi-scale nature of the groundwater dynamics of the region obtained through the use of data-driven modeling.

The results from the field sampling are consistent with the brine upwelling hypothesis for the elevated groundwater salinity in the Michigan Lowlands, notably that Cl⁻ concentrations increase with depth (consistent with a deep source), and that almost all samples yielding high Cl⁻ concentrations, i.e., above 250 mg/L, came from wells completed in the Marshall bedrock aquifer (which is known to contain brines down-dip of the subcrop area in the Michigan Lowlands – see Ging et al., 1996). This pattern is consistent with that observed in the Saginaw Lowlands, where geochemical analyses implied upwelling brine as the source of elevated Cl⁻. This comparison, along with the similar Cl⁻–SWL structures seen in the regional- and local- scale analyses, confirms the premise that brines are systematically impacting both of these major peninsula-wide discharge areas.

1.5.1.1 Anomaly of Southeast Michigan

It is worth noting that the basin-scale analysis revealed that, with the exception of a major cluster near the recharge area in southeast Michigan, significant clusters of elevated Cl⁻ are focused within statewide discharge areas. However, consideration of the regional hydrogeology provides a reasonable explanation of the apparent anomaly in the basin-scale Cl⁻–SWL spatial structure. The eroded crests of two anticlines (Freedom Anticline and Howell Anticline) underlie this area, abruptly pinching out the bedrock formations overlying the Coldwater Shale aquitard unit. Several formations form the regional bedrock surface, including those that make up the Saginaw Aquifer, Parma-Bayport Aquifer, and Marshall Aquifers, all of which are known to yield saline water (Apple and Reeves, 2007). In Shiawassee County – which sits at the core of this cluster – approximately 59 percent of the wells are completed in the bedrock units, and thus, completion of a relatively large number of bedrock wells in this area may contribute to the clustering of elevated Cl⁻ wells in this area as seen in the peninsula-wide analysis. There also appears to be a significant potential for vertical flow connections between bedrock and the large number of streams in the area. The glacial geology in the area is characterized by strong three-dimensional heterogeneity that resulted from a complex depositional history (Westjohn et al. 1994), and it is therefore possible that saline bedrock water is upwelling through preferential flow paths primarily in the vicinity of gaining streams. Thus, although the

region was not classified as a statewide discharge area, knowledge of the regional hydrogeology suggests that brines are likely the dominant source of the elevated Cl, at least for Cl concentrations near or greater than 1000 mg/L.

1.5.2 Potential Influence of Other Cl Sources

Note that the basin-scale database analysis did yield some exceptions (e.g., wells with elevated Cl concentrations were present in recharge zones for all thresholds, albeit to a lesser degree than in discharge zones) and that spatial patterns connecting near-surface groundwater hydrology to the elevated Cl concentrations were not as easily discernable at lower Cl thresholds. While a small portion of these may be considered “bad” Cl data with erroneous spatial locations as a result of poor record keeping, patterns of elevated Cl around population centers in Figure 1.9 suggests an anthropogenic surface source for some of the lower Cl (i.e., 250 mg/L and less) contamination and potentially some of the local points or clusters of higher levels of contamination. Roughly 15 million metric tons of halite are used for roadway deicing each year in the U.S., a majority of which is applied in northern states, including Michigan (USGS 2012). Most studies quantifying Cl concentrations due to road salt application have focused on surface water bodies (e.g., Kaushal et al. 2005; Kelly et al. 2007, Corsi et al., 2010), but those including groundwater have reported mean groundwater concentrations ranging from roughly 100 mg/L (Huling and Hollocher 1972; Williams et al. 2000) to 275 mg/L (Perera et al. 2010) and up to 476 mg/L (Howard and Haynes, 1993) and 640 mg/L (Foos 2003), although higher concentrations were generally localized to specific areas along major roads. Michigan also has approximately 1.2 million septic systems (Sacks and Falardeau 2004), that can raise Cl concentrations above natural conditions. Harman et al. (1996) measured a Cl concentration of 207 mg/L in septic tank effluent, higher than the 53 mg/L reported by Viraraghavan and Warnok (1975). A comprehensive analysis by Katz et al. (2011) reported concentrations ranging from 20 to 100 mg/L in an analysis of 1848 samples from domestic wells from 19 aquifers that were in the vicinity of a septic system. Finally, agricultural sources may contribute Cl to the groundwater system, e.g., from livestock excretion or

fertilizer application (KCl), but the expected concentrations are typically below 30 mg/L (Kelly et al., 2012).

In light of these findings, we performed a simple geospatial analysis of the potential impact of anthropogenic sources on this study by overlying elevated Cl⁻ concentrations (>250, >500, and >1000 mg/L) over a map of the Lower Michigan highway network (Figure 1.15). The clustering around population centers for the >250 mg/L threshold, e.g., the suburbs of Detroit (southeast Lower Michigan) and the Greater Lansing area (south-central Lower Michigan), and the slight association for the >500 mg/L threshold, when considered with the expected concentrations found in the aforementioned literature, suggests that anthropogenic sources are at least partially responsible for the clustering of elevated Cl⁻ concentrations at these thresholds, although the CISWL analysis shown earlier suggests brines are a major (if not the dominant) source. For the >1000 mg/L threshold, elevated Cl⁻ concentrations are not associated with areas of dense road and highway networks, suggesting brines are responsible for the very high Cl⁻ concentrations. In other words, the ‘signal’ from brines is most obvious at higher concentrations, which is consistent with the large ratios shown in Table 1.4 at the >500 L threshold and higher.

Another source of Cl⁻ potentially impacting the analyses are leaky/fractured natural gas and oil wells. Figure 1.16 presents overlays of elevated Cl⁻ concentrations and oil and gas wells across the Lower Michigan. Although there are instances where elevated Cl⁻ concentrations are near oil/gas wells - even for the >1000 mg/L threshold - there are large clusters of oil/gas wells that are not associated any significant clustering of elevated Cl⁻. Thus, there may be localized instances where leaky oil/gas wells are impacting the near-surface environment, e.g., in southeast Michigan along the coastline as shown in Figure 1.16, but there does not seem to be a significant peninsula-wide spatial correlation between oil/ gas wells and elevated Cl⁻ concentrations for the thresholds considered.

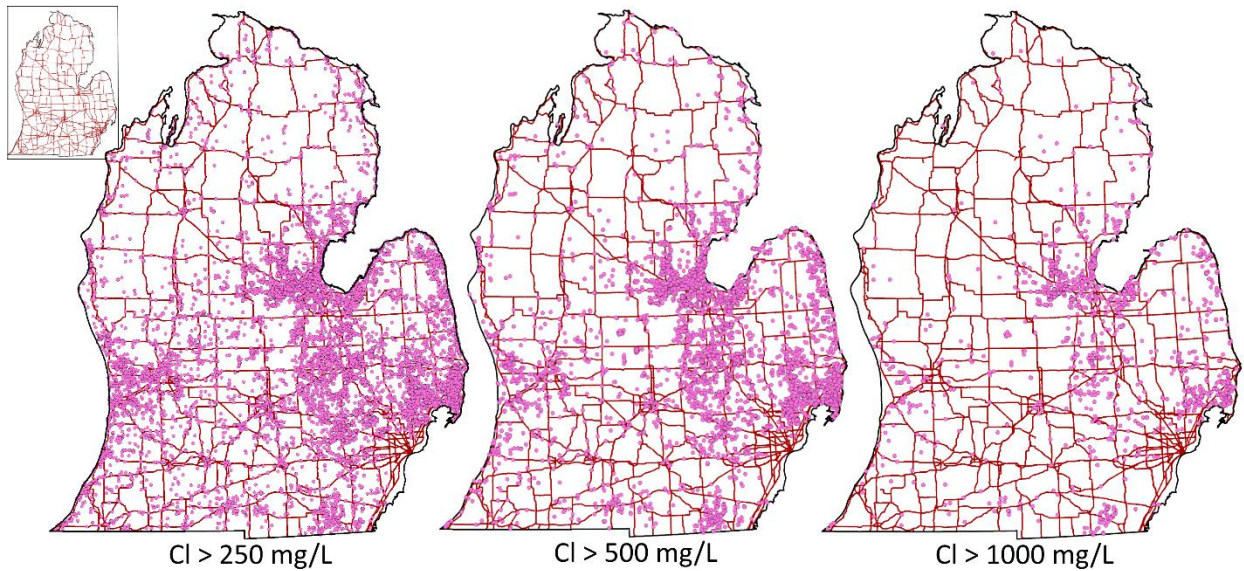


Figure 1.15: Occurrence of elevated Cl (>250, >500, >1000 mg/L thresholds) wells and the Michigan highway network.

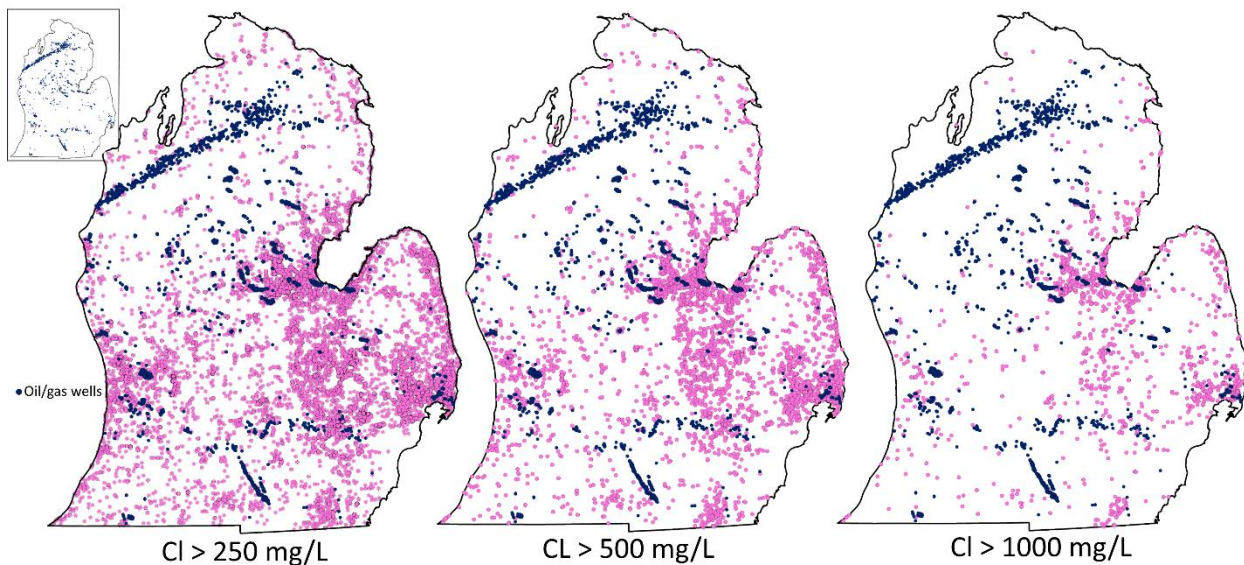


Figure 1.16: Occurrence of elevated Cl (>250, >500, >1000 mg/L thresholds) and oil/gas wells.

1.5.3 Management Implications & Future Work

The data-driven, integrated water quantity-quality approach applied here confirms that the underlying process controlling the occurrence of elevated Cl concentrations in the shallow groundwater across the Lower Peninsula of Michigan is the mixing of deep brines and shallow freshwater, particularly in areas where groundwater elevations are low. This system-based understanding of brine-influenced shallow

groundwater in Lower Michigan has important implications for groundwater resource development in a state that currently uses roughly 700 million gallons of groundwater per day (NGWA 2016). Determining if and where wells might be at risk to elevated Cl concentrations can be aided by an understanding of the local and regional hydrology, and in particular, the locations of recharge and discharge zones. Considering the spatial and statistical structures of different Cl concentration thresholds can help communities identify the source(s) of contamination of the near-surface groundwater (e.g., road deicing versus brine-influenced groundwater).

Of course, a limitation of the multiscale analysis is that it considers long-term, average conditions of the near-surface environment, and, therefore, does not consider temporal trends in hydrology or water quality. Similarly, the synoptic field sampling in the Michigan Lowlands provided an understanding of only the current conditions. A few questions that naturally emerge from this study include: Has the brine upwelling become worse in recent decades? Is it subject to influence from external system stresses, e.g., human activity such as groundwater pumping or climate change? The answers to these questions would be scientifically important and of practical use to groundwater resource managers, but require more sophisticated analyses, including the use of time-series datasets and the use of process-based models to better understand system response under different scenarios. In forthcoming work, we consider further aspects of brine-influenced groundwater in Michigan by using detailed regional and local scale datasets and process-based numerical approaches.

1.6 Ch. 1 Conclusions

We investigated the extent and severity of brine-influenced shallow groundwater across the Lower Peninsula of Michigan by capitalizing on massive, recently assembled statewide water well databases that include information on groundwater levels and groundwater quality. We developed a generalized approach for filtering, processing and analyzing the water well datasets, and applied it at multiple scales (peninsula-wide, regionally, and locally) for two major peninsula-wide discharge zones – the Michigan and Saginaw Lowlands - to characterize the long-term average static water level (SWL) distributions and their

relationship to the occurrence of elevated concentrations of dissolved-chloride (Cl). An automated, non-stationary kriging approach was used to perform spatial interpolations of SWLs, and areas of groundwater lows and highs (interpreted as discharge and recharge zones, respectively) were delineated at each scale and used to evaluate and compare the proportion of elevated Cl wells (>100, >150, >200, >250, >500, >1000 and >1500 mg/L) in the different zones. A synoptic field sampling campaign was conducted to better understand the three-dimensional structure of Cl in one of the major peninsula-wide discharge zones – the Michigan Lowlands. Anthropogenic sources were briefly considered to better understand their potential impact on the analyses done in this study.

The results show that, at each scale, the Cl concentrations in the discharge areas, where groundwater flows primarily upwards, are consistently and significantly higher than those in the recharge areas. An exception to this pattern was noted in southeast Lower Michigan; however, careful consideration of the regional and local hydrogeology suggests brines are preferentially impacting discharge areas in this region of the state as well. Analysis of field samples collected from the central portion of the Michigan Lowlands showed that Cl concentrations in groundwater increase with depth and that almost all samples yielding concentrations above 250 mg/L were drawn from wells completed in the Marshall bedrock aquifer, consistent with patterns observed in the Saginaw Lowlands where upwelling brines are the source of saline or near-saline shallow groundwater. This strong, consistent Cl distribution patterns across multiple scales suggests that brine upwelling from the deep bedrock formations is a dominant source of chloride contamination observed in the near-surface environment of Lower Michigan.

The multiscale, integrated water quantity-quality analysis done here was previously difficult to conduct because of the costs of traditional hydrogeological field investigations which require invasive data collection and extensive water quality sampling. However, it was demonstrated here that massive (but noisy) statewide groundwater databases can yield important hydrogeological insights if the data are processed and modeled appropriately. Therefore, in addition to providing practical knowledge useful to resource managers in the Lower Peninsula of Michigan, this study is an important example of how to take

advantage of emerging GIS-enabled, statewide water well databases in a way that enables system-based understanding of complex, multi-scale groundwater problems.

APPENDICES

APPENDIX A: Motivation for utilizing bedrock and drift wells for SWL delineation

The choice to use wells terminated in both glacial aquifers and near-surface bedrock aquifers (rather than analyze them individually) was motivated, in part, by the fact that a large portion Lower Michigan does not contain bedrock wells, e.g., in southwest and southeast Lower Michigan where the underlying bedrock formations are of very low transmissivity or in north-central where the glacial deposits are hundreds of meters thick. However, ignoring bedrock wells altogether would remove a significant amount of useful data, especially in areas where the glacial drift is absent or very thin (e.g., in northeast Lower Michigan). Thus, using data from both aquifers provides a more complete dataset for the basin-scale interpolation and, as shown does not inflate the sub-grid variability to problematic levels. Additionally, in our experience this approach does not significantly impact the delineated SWL spatial patterns (see Figure 1.17 and Figure 1.18 for an example), i.e., the SWL variability from aquifer to aquifer is small relative to the range of SWLs observed across the model domain. Moreover, CI data extracted from WaterChem does not differentiate between aquifers, the CI and SWL datasets are ‘similar’ in that they capture overall dynamics of the shallow groundwater.

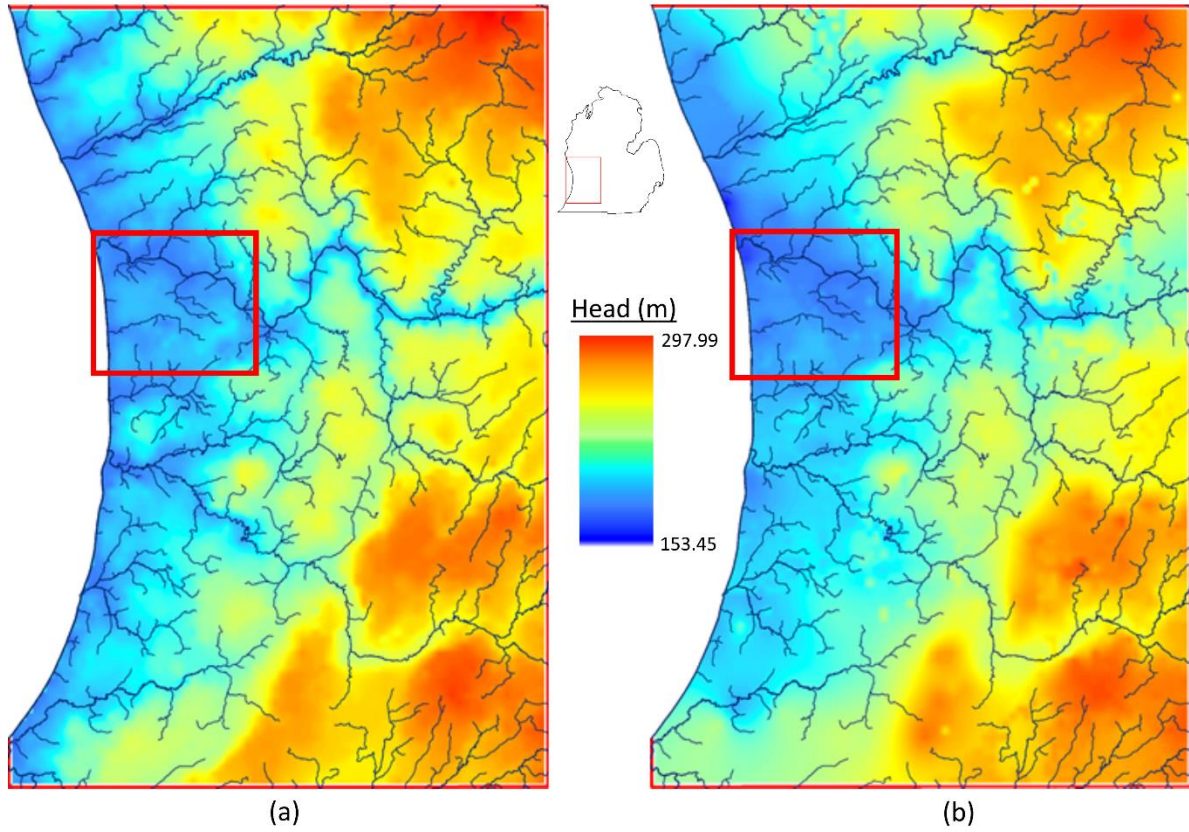


Figure 1.17: Regional-scale groundwater elevations delineated using moving-window, non-stationary kriging of (a) bedrock wells; and (b) drift wells. The domain used for the local model is shown as a red rectangle.

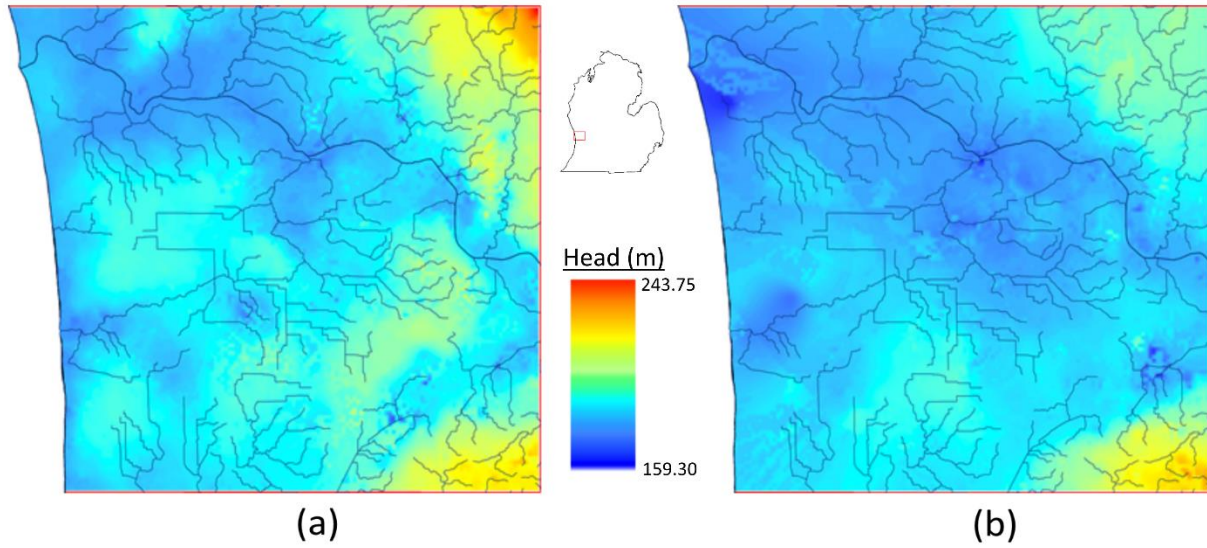


Figure 1.18: Regional-scale groundwater elevations delineated using moving-window, non-stationary kriging of (a) bedrock wells; and (b) drift wells. The domain used for the local model is shown as a red rectangle.

APPENDIX B: Example of using different cutpoints

Table 1.5: Statistics from the Michigan Lowlands regional elevated Cl-SWL analysis using quartiles rather than tertiles as cutpoints for delineating recharge areas and discharge areas. Note that the percent ratios reported here are generally consistent with those reported in the Regional section of Table 1.3.

| Cl dataset | % of wells with elevated Cl, discharge zones | % of wells with elevated Cl, recharge zones | % ratio (discharge: recharge) |
|------------|--|---|-------------------------------|
| >100 | 11.71 | 5.87 | 1.99 |
| >150 | 7.20 | 2.95 | 2.44 |
| >200 | 4.73 | 1.74 | 2.71 |
| >250 | 3.11 | 1.16 | 2.68 |
| >500 | 0.81 | 0.29 | 2.85 |
| >1000 | 0.15 | 0.03 | 4.58 |
| >1500 | 0.07 | 0.02 | 3.03 |

REFERENCES

REFERENCES

- Abedini, M. J., Nasserli, M., & Ansari, A. 2008. Cluster-based ordinary kriging of piezometric head in West Texas/New Mexico—Testing of hypothesis. *Journal of Hydrology*, 351(3), 360-367.
- Albert, D. A. 2001. Natural community abstract for Inland salt marsh Michigan Natural Features Inventory (pp. 4). Lansing, Michigan.
- Apple, B. A. and Reeves, H.W. 2007. Summary of Hydrogeologic Conditions by County for the State of Michigan—U.S. Geological Survey Open-File Report 2007-1236, 87 pp.
- Ayers, R.S., Westcot, D.W. 1985. Water quality for agriculture (Vol. 29). Rome: Food and Agriculture Organization of the United Nations.
- Barton, G. J., Mandle, R. J., & Baltusis, M. A. 1996. Predevelopment freshwater heads in the glaciofluvial, Saginaw, and Marshall aquifers in the Michigan Basin (No. 95-319). US Geological Survey; Branch of Information Services [distributor].
- Bossong, C. R., Karlinger, M. R., Troutman, B. M., & Vecchia, A. V. 1999. Overview and technical and practical aspects for use of geostatistics in hazardous-, toxic-, and radioactive-waste-site investigations (No. PB--99-165326/XAB; USGS/WRI--98-4145). Geological Survey, Water Resources Div., Denver, CO (United States); Corps of Engineers, Washington, DC (United States).
- Carpenter, A. B., Trout, M. L., & Pickett, E. E. 1974. Preliminary report on the origin and chemical evolution of lead-and zinc-rich oil field brines in central Mississippi. *Economic Geology*, 69(8), 1191-1206.
- Corsi, S.R., Graczyk, D.J., Geis, S.W., Booth, N.L. and Richards, K.D. 2010. A fresh look at road salt: aquatic toxicity and water-quality impacts on local, regional, and national scales. *Environmental Science & Technology*, 44(19), pp.7376-7382.
- Cressie, N., & Johannesson, G. 2006, April. Spatial prediction for massive data sets. In *Australian Academy of Science Elizabeth and Frederick White Conference* (pp. 1-11). Australian Academy of Science Canberra, Australia.
- Cunge, J. 2003. “Of data and models.” *Journal of Hydroinformatics*, 5, 75-98.
- ESRI. 2011. ArcGIS Desktop: Release 10. Redlands, CA: Environmental Systems Research Institute.
- Foos, A. 2003. Spatial distribution of road salt contamination of natural springs and seeps, Cuyahoga Falls, Ohio, USA. *Environmental Geology*, 44(1), pp.14-19.
- Feinstein, D.T., Hunt, R.J. and Reeves, H.W. 2010. Regional groundwater-flow model of the Lake Michigan Basin in support of Great Lakes Basin water availability and use studies. U. S. Geological Survey Scientific Investigations Report 2010-5109.
- Fitzpatrick ML, Long DT, Pijanowski BC. 2007. Exploring the effects of urban and agricultural land use on surface water chemistry, across a regional watershed, using multivariate statistics. *Applied Geochemistry* 22: 1825–1840.

- Freeze, R. A., & Cherry, J. 1974. A. 1979. Groundwater. Prentice—Hall, Inc Englewood cliffs, New Jersey. 604, pg. 194.
- Freeze, R. A., & Witherspoon, P. A. 1967. Theoretical analysis of regional groundwater flow: 2. Effect of water-table configuration and subsurface permeability variation. *Water Resources Research*, 3(2), 623-634.
- Garcia, L. A., and Shigidi, A. 2006. "Using neural networks for parameter estimation in ground water." *Journal of Hydrology*, 318, 215-231.
- Ging, P. B., Long, D. T., & Lee, R. W. 1996. Selected Geochemical Characteristics of Ground Water from the Marshall Aquifer in the Central Lower Peninsula of Michigan U.S. Geological Survey Water-Resources Investigations Report 94-4220.
- Haas, T. C. 1990. Lognormal and moving window methods of estimating acid deposition. *Journal of the American Statistical Association*, 85(412), 950-963.
- Haas, T. C. 1995. Local prediction of a spatio-temporal process with an application to wet sulfate deposition. *Journal of the American Statistical Association*, 90(432), 1189-1199.
- Harman, J., Robertson, W.D., Cherry, J.A. and Zanini, L. 1996. Impacts on a sand aquifer from an old septic system: nitrate and phosphate. *Groundwater*, 34(6), pp.1105-1114.
- Harris, P., Charlton, M. and Fotheringham, A.S. 2010. Moving window kriging with geographically weighted variograms. *Stochastic Environmental Research and Risk Assessment*, 24(8), pp.1193-1209.
- Harter, T. 2003. Groundwater sampling and monitoring. UCANR Publications.
- Heath, R. C. 1984. Ground-water regions of the United States (p. 45). Geological Survey Water-Supply Paper 2242 .Washington, DC: US Government Printing Office.
- Hem, J.D. 1985. Study and Interpretation of the Chemical Characteristics of Natural Water, 2nd Ed. Geological Survey Water-Supply Paper 2254.
- Hoaglund, J.R., Huffman, G. C., and Nor. G. Grannemann. 2002. Michigan Basin Regional Ground Water Flow Discharge to Three Great Lakes. *Ground Water* 40, no. 4 (July 2002): 390–406.
- Hoaglund, J. R., Kolak, J. J., Long, D. T., & Larson, G. J. 2004. Analysis of modern and Pleistocene hydrologic exchange between Saginaw Bay (Lake Huron) and the Saginaw Lowlands area. *Geological Society of America Bulletin*, 116(1-2), 3-15.
- Howard, K.W. and Haynes, J. 1993. Groundwater contamination due to road de-icing chemicals—salt balance implications. *Geoscience Canada*, 20(1).
- Huggenberger, P., Epting, J., & Scheidler, S. 2013. Concepts for the sustainable management of multi-scale flow systems: the groundwater system within the Laufen Basin, Switzerland. *Environmental earth sciences*, 69(2), 645-661.
- Huling, Edwin E., and Thomas C. Hollocher. "Groundwater contamination by road salt: Steady-state concentrations in East Central Massachusetts." *Science* 176, no. 4032 (1972): 288-290.

- Institute of Water Research (IWR), Dept. of Civil & Environmental Engineering. 2013. Ottawa County Water Resource Study Final Report, Michigan State University.
- ISGS. 2015. Illinois State Geological Survey. *ILWATER*, Repository for records of wells drilled in the State of Illinois (periodically updated). Available at: <http://www.isgs.illinois.edu/ilwater>
- IGS. 2016. Iowa Geological Survey, based at IIHR – Hydrosceience & Engineering, University of Iowa. Available at: <https://www.iihr.uiowa.edu/igs/geosam/home>
- Isaaks, E. H., Srivastava, R. M. 1989. Applied geostatistics: Oxford University Press. New York, 561.
- Katz, B.G., Eberts, S.M. and Kauffman, L.J. 2011. Using Cl/Br ratios and other indicators to assess potential impacts on groundwater quality from septic systems: a review and examples from principal aquifers in the United States. *Journal of Hydrology*, 397(3), pp.151-166.
- Kaushal, S.S., Groffman, P.M., Likens, G.E., Belt, K.T., Stack, W.P., Kelly, V.R., Band, L.E. and Fisher, G.T. 2005. Increased salinization of fresh water in the northeastern United States. *Proceedings of the National Academy of Sciences of the United States of America*, 102(38), pp.13517-13520.
- Kelly, V.R., Lovett, G.M., Weathers, K.C., Findlay, S.E., Strayer, D.L., Burns, D.J. and Likens, G.E., 2007. Long-term sodium chloride retention in a rural watershed: legacy effects of road salt on streamwater concentration. *Environmental science & technology*, 42(2), pp.410-415.
- Kelly, W.R., Panno, S.V. and Hackley, K. 2012. The sources, distribution, and trends of chloride in the waters of Illinois. Illinois State Water Survey Bulletin 74.
- KGS. 2002. Kansas Geological Survey. *WIZARD*, water well levels database (periodically updated). Available at: <http://www.kgs.ku.edu/Magellan/WaterLevels/index.html>
- Kolak, J. J., Long, D. T., Matty, J. M., Larson, G. J., Sibley, D. F., & Councell, T. B. 1999. Groundwater, large-lake interactions in Saginaw Bay, Lake Huron: A geochemical and isotopic approach. *Geological Society of America Bulletin*, 111(2), 177-188.
- Kost, M. A., Albert, D. A., Cohen, J. G., Slaughter, B. S., Shillo, R. K., Weber, C. R., & Chapman, K. A. 2007. Natural Communities of Michigan; Classification and Description. Michigan Natural Features Inventory Report Number 20007-21 (pp. 314). Lansing, MI.
- Lampe, D. C. 2009. Hydrogeologic framework of bedrock units and initial salinity distribution for a simulation of groundwater flow for the Lake Michigan basin (No. 2009-5060). US Geological Survey.
- Land, L. S., & Prezbindowski, D. R. 1981. The origin and evolution of saline formation water, Lower Cretaceous carbonates, south-central Texas, USA. *Journal of Hydrology*, 54(1), 51-74.
- Lane, A.C. 1899. Lower Michigan mineral waters U.S. *Geological Survey Water Supply Paper* 30.
- Li, S.G., and Q. Liu. 2006. Interactive Ground Water (IGW). *Environmental Modelling & Software*, 21, no. 3: 417–18. doi:10.1016/j.envsoft.2005.05.010.

- Li, S.G., Q. Liu, and S. Afshari. 2006. An Object-Oriented Hierarchical Patch Dynamics Paradigm (HPDP) for Modeling Complex Groundwater Systems Across Multiple Scales. *Environmental Modeling and Software*. Vol. 21, Issue 5.
- Liao, H.S., P.V. Sampath, Z.K. Curtis; S.G. Li. 2015. Hierarchical modeling and parameter estimation for a coupled groundwater-lake system. *Journal of Hydrologic Engineering*, 20(11).
- Lloyd, C.D. 2010. Nonstationary models for exploring and mapping monthly precipitation in the United Kingdom. *International Journal of Climatology*, 30(3), pp.390-405.
- Long, D. T., Voice, T. C., Chen, A., Xing, F., & Li, S. G. 2015. Temporal and spatial patterns of Cl⁻ and Na⁺ concentrations and Cl/Na ratios in salted urban watersheds. *Elementa: Science of the Anthropocene*, 3(1), 000049.
- Long, D. T., Wilson, T. P., Takacs, M. J., & Rezaee, D. H. 1988. Stable-isotope geochemistry of saline near-surface ground water; east-central Michigan Basin. *Geological Society of America Bulletin*, 100(10), 1568-1577.
- Li, S.G. and Liu, Q. 2006. Interactive Ground Water (IGW). *Environmental Modeling and Software*, 21(3), 417-418.
- Lilienthal, R. T. 1978. Stratigraphic cross-sections of the Michigan Basin. Geological Survey Division Michigan Department of Natural Resources.
- Ma, L., Castro, M. C., Hall, C. M., and L.M. Walter. 2005. Cross-Formational Flow and Salinity Sources Inferred from a Combined Study of Helium Concentrations, Isotopic Ratios, and Major Elements in the Marshall Aquifer, Southern Michigan: AQUIFER FLOW AND SALINITY SOURCES.” *Geochemistry, Geophysics, Geosystems* 6, no. 10.
- McIntosh, J. C., L. M. Walter, and A. M. Martini. 2004. Extensive microbial modification of formation water geochemistry: Case study from a midcontinent sedimentary basin, United States, *Geol. Soc. Am. Bull.*, 116(5–6),743–759.
- Meyboom, P. 1967. Mass-transfer studies to determine the groundwater regime of permanent lakes in hummocky moraine of western Canada. *Journal of Hydrology*, 5, 117-142.
- MDEQ. 2014. Michigan Department of Environmental Quality. Wellogic System (periodically updated). Available at <https://secure1.state.mi.us/wellogic/>.
- MDEQ. 2010. Michigan Department of Environmental Quality. WaterChem, Statewide Water Quality Database (periodically updated).
- Meissner, B. D., Long, D. T., & Lee, R. W. 1996. Selected Geochemical Characteristics of Ground Water from the Sagnia Aquifer in the Central Lower Peninsula of Michigan U.S. Geological Survey Water-Resources Investigations Report 93-4200.
- MSU. 2014. Michigan Groundwater Management Tool. East Lansing, Michigan: Department of Environmental Engineering, Michigan State University.
- NGWA. 2016. National Ground Water Association. *Groundwater Use in Michigan* [Fact sheet]. Retrieved from: <http://www.ngwa.org/Documents/States/Use/mi.pdf>

- NED USGS. 2006. National Elevation Dataset. US Department of Interior: United States Geological Survey, <http://ned.usgs.gov/Ned/about.asp>.
- NHD USGS. 2010. USGS: National Hydrography Dataset. US Department of Interior: United States Geological Survey, <http://nhd.usgs.gov/index.html>.
- Ottawa County, Michigan. Environmental Health – Scanned Well & Water Quality files (continuously updated). Accessed 2014-2015.
- Pardo-Igúzquiza, E., Dowd, P.A. and Grimes, D.I., 2005. An automatic moving window approach for mapping meteorological data. *International journal of climatology*, 25(5), pp.665-678.
- Perera, N., Gharabaghi, B., Noehammer, P. and Kilgour, B. 2010. Road Salt Application in Highland Creek Watershed, Toronto, Ontario--Chloride Mass Balance. *Water Quality Research Journal of Canada* (Canadian Association on Water Quality), 45(4).
- Sacks, R. and Falardeau, R. MDEQ. (Michigan Department of Environmental Quality). *Whitepaper on the Statewide Code for On-site Wastewater Treatment*. Lansing, MI, October 19, 2004.
- Sampath, P. V., Liao, H. S., Curtis, Z. K., Herbert, M. E., Doran, P. J., May, C. A., Landis, D.A., and Li, S. G. 2016. Understanding fen hydrology across multiple scales. *Hydrological Processes*, 30(19), pp. 3390-2407.
- Stueber, A. M., & Walter, L. M. 1991. Origin and chemical evolution of formation waters from Silurian-Devonian strata in the Illinois basin, USA. *Geochimica et Cosmochimica Acta*, 55(1), 309-325.
- Sun, Y., Kang, S., Li, F., & Zhang, L. 2009. Comparison of interpolation methods for depth to groundwater and its temporal and spatial variations in the Minqin oasis of northwest China. *Environmental Modelling & Software*, 24(10), 1163-1170.
- Toth, J. 1963. A theoretical analysis of groundwater flow in small drainage basins. *Journal of geophysical research*, 68(16), 4795-4812.
- Toth, J. 2009. Gravitational systems of groundwater flow: theory, evaluation, utilization. Cambridge University Press.
- U.S. Geological Survey (USGS). 2012. Mineral Commodities Summaries 2102 – Salt [Online]. Accessed December 12, 2014. Available at: <http://minerals.usgs.gov/minerals/pubs/commodity/salt/mcs-2014-salt.pdf>
- USGS (U.S. Geological Survey). 2012. National Water Information System data available on the World Wide Web (USGS Water Data for the Nation), accessed [June 10, 2012], at URL [<http://waterdata.usgs.gov/nwis/>].
- Varouchakis, E. A., & Hristopulos, D. T. 2013. Comparison of stochastic and deterministic methods for mapping groundwater level spatial variability in sparsely monitored basins. *Environmental monitoring and assessment*, 185(1), 1-19.
- Viraraghavan, T. and Warnock, R.G. 1976. Groundwater pollution from a septic tile field. *Water, Air, & Soil Pollution*, 5(3), pp.281-287.

- Wahrer, M. A., D. T. Long, and R. W. Lee. Selected geochemical characteristics of ground water from the Glaciofluvial aquifer in the central Lower Peninsula of Michigan. No. 94-4017.
- Walter, C., McBratney, A.B., Douaoui, A. and Minasny, B., 2001. Spatial prediction of topsoil salinity in the Chelif Valley, Algeria, using local ordinary kriging with local variograms versus whole-area variogram. *Soil Research*, 39(2), pp.259-272.
- Weaver, T.R., S.K. Frappe, and J.A. Cherry 1995. Recent cross-formational fluid flow and mixing in the shallow Michigan Basin, *Geological Society of America Bulletin*, 107(6), 697-707.
- Westjohn, D. B., Weaver, T. L., & Zacharias, K. F. 1994. Hydrogeology of Pleistocene glacial deposits and Jurassic red beds in the central lower peninsula of Michigan. *Water-resources investigations report (USA)*.
- Westjohn, D. B., & Weaver, T. L. 1996a. Hydrogeologic framework of Mississippian rocks in the central Lower Peninsula of Michigan U.S. Geological Survey Water-Resources Investigations Report 94-4246.
- Westjohn, D. B., & Weaver, T. L. 1996b. Configuration of Freshwater/Saline-Water Interface and Geologic Controls on Distribution of freshwater in a regional aquifer system, central Lower Peninsula of Michigan U.S. Geological Survey Water-Resources Investigations Report 94-4242.
- Wilson, T. P., & Long, D. T. 1993a. Geochemistry and isotope chemistry of Ca Na Cl brines in Silurian strata, Michigan Basin, USA. *Applied geochemistry*, 8(5), 507-524.
- Wilson, T. P., & Long, D. T. 1993b. Geochemistry and isotope chemistry of Michigan Basin brines: Devonian formations. *Applied Geochemistry*, 8(1), 81-100.
- Williams, D. D, Williams, N.E., and Y. Cao. Road salt contamination of groundwater in a major metropolitan area and development of a biological index to monitor its impact. *Water Research* 34, no. 1 (2000): 127-138.
- Winter, T. C. 1988. A conceptual framework for assessing cumulative impacts on the hydrology of nontidal wetlands. *Environmental Management*, 12(5), 605-620.

CHAPTER 2

Groundwater modeling in a Spatially-rich World: Reassessing Data Needs, Availability, and Value

Contributing authors: Zachary Curtis, Shu-Guang Li, Hua-Sheng Liao

2.1 Executive Summary of Ch. 2

Lack of data has long been a source difficulty in groundwater modeling. Ongoing advancements in geospatial data collection – such as remote sensing, in situ sensor networks, and digitization of traditional information – has drastically increased data availability. However, these data are underutilized because they are: of variable quality, coverage and resolution; scattered across different databases; and massive, making them time-consuming to process. This study focuses on applying big data for groundwater modeling and understanding groundwater systems across scales. We define big data in the context of groundwater modeling and discuss ways they can be used to model different systems. We apply generalized methods to build a suite of process-based flow models of different sizes, types, and in different hydrologic regimes in Michigan, U.S.A, taking advantage of a comprehensive, preprocessed groundwater database to eliminate or significantly relax data management and processing bottlenecks. We examine their performance at different scales and evaluate model sensitivity with respect to model parameters and structure. Results show existing data alone enable effective modeling of prevailing conditions of regional and subregional groundwater systems. Of all the existing datasets, those representing topography, lakes, streams and surface seeps are the most important. Digital Elevation Models (DEMs) are especially useful for mapping surface drainage features. In fact, DEM-based treatment of groundwater surface seepage may be the most robust approach for initial modeling of a large groundwater systems, which can then be used as a: 1) starting point for system-based management; 2) context to study local perturbations; and 3) guide for local data collection.

2.2 Ch. 2 Introduction

Managing environmental sustainability requires understanding the underlying systems that connect the integrated components of the environment and human society (NRC 2002; Miller et al. 2008; Pahl-Wostl 2005; Liu et al. 2007a, 2007b; Bhaduri et al. 2016). In the context of sustainable groundwater management,

it is therefore necessary to study the larger groundwater systems that underlie and influence our site-specific groundwater resources. Developing a holistic characterization of groundwater systems is, however, a challenging task. One long-standing difficulty is the lack of data, needed both for the analysis or characterization of the system and for conceptualizing, building, calibrating and validating numerical models used to probe, test, and further develop system understanding. This is especially the case when a system exhibits complex heterogeneity and multi-scale behavior. For many years, hydrogeological field investigations simply lacked resources to collect enough data across space and time to properly characterize groundwater systems.

Recently, however, a global movement of spatial data integration has drastically increased the amount of environmental data that are available. Much of this information is useful for investigating groundwater systems - both for the analysis or characterization of the system and for building and calibrating numerical models. Yet, the implementation of 'big groundwater data' is not widespread, especially in groundwater management and practice. This is in part because of data management and processing bottlenecks: the massive size of big data renders them difficult to maneuver (e.g., download, store and access), process and assemble all information needed to conceptualize and characterize groundwater systems. On the other hand, inconsistencies and variabilities between different datasets (e.g., different spatial coverages and resolutions, different levels of completeness, etc.) makes application to modeling groundwater systems a challenging task, especially given the lack of research systematically addressing this particular issue.

In this study, we address challenges associated with groundwater modeling applications of big data, reserving considerations of data management and processing issues for separate studies. We investigate how big data-enabled groundwater modeling can be used for understanding groundwater systems across scales, and for systematically guiding subscale analysis, monitoring network design, data collection, and model refinement. We build a suite process-based flow models of different sizes, types, and in different hydrologic regimes, taking advantage of a recently assembled, comprehensive database of pre-processed, 'ready-to-go' groundwater information. (In this way, processing and data management/processing

bottlenecks are relaxed/eliminated so that present focus may remain on aspects of data implementation.). We compare these diverse models with data, examine their performance at different scales, and perform systematic sensitivity analysis with respect to model parameters and model structure. We use these comparisons and analyses to explore the power and limitations of existing data, and to understand the importance of different data components.

The rest of this chapter is organized as follows: we first define what big data are in the context of groundwater modeling, raising key research questions related to how these data can be used to model groundwater systems. We discuss generalized big data groundwater modeling approaches, and illustrate them by generating a diverse set of groundwater models for 8 large watersheds ('test beds') in different parts of Michigan, U.S.A. The results are presented to evaluate data worth and modeling implications. We finish with a brief discussion of how these models can be modified, extended, improved, and further customized based on study objectives and other available (local) data, as well as user experience and expertise.

2.3 Modeling with Big Groundwater Data

Process-based numerical simulations are a primary means for investigating groundwater systems, as they allow: probing of important processes that control system dynamics; evaluating the relative strength of interactions in the system and their uncertainties; and testing the impact of potential perturbations. Essentially, groundwater modeling consists of estimating where (and how much) water is entering and leaving the aquifer system, and describing (qualitatively and quantitatively) how water moves through subsurface material. The aquifer framework (i.e., top surface and bottom surface geometry, lateral boundaries) and sources and sinks of water (recharge, evapotranspiration, surface water exchange, or even pumping) control where (and how much) water is entering and leaving the aquifer system (Figure 2.1), and aquifer properties (hydraulic conductivity, storage) and their spatial variabilities control flow directions and groundwater fluxes through the subsurface.

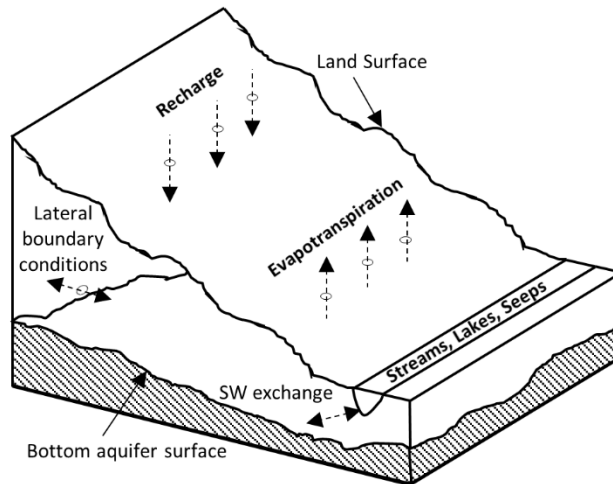


Figure 2.1: Conceptual schematic of the key components of natural groundwater system.

2.3.1 Opportunities & Questions

Ongoing advancements in geospatial data collection has drastically increased the amount of groundwater-centric data available for characterizing above-mentioned aspects of groundwater system. Parallel development of Geographic Information Systems (GIS) and web-based data acquisition from big data repositories provides modelers with an unprecedented opportunity to integrate data collected from various sources (e.g., traditional hydrogeological field studies, remote sensing products, etc.) within a common spatial framework. Table 2.1 presents examples of various types of big datasets related to groundwater modeling, including: Digital Elevation Models (DEMs); climate forcing data (e.g., precipitation or air temperature); hydrography (lakes, streams, watersheds), and groundwater level and lithology records from massive water well datasets. Table 2.1 is not meant to be an exhaustive list of big datasets useful for groundwater modeling, but rather an illustrative summary of the rich amount of information that is available. Details are referenced throughout the following subsections, but for now, note the different variety of data types, qualities, resolutions and coverages (spatial and/or temporal coverage). Generally speaking, the various big groundwater datasets can be categorized as 1) remote sensing products (e.g., DEMs, hydrography, land use/land cover, or even GRACE land water storage and MODIS evapotranspiration estimates), which tend to provide seamless spatial information with excellent spatial coverage but varying degrees of quality; 2) in-situ sensors and field instrumentation (monitoring wells,

stream gages, etc.), which provide accurate historical and present-day observations needed for modeling and analysis but are scattered across distinct locations; and 3) high-density compilations of point-base subsurface information from water wells, oil and gas wells, etc. (static water levels, lithology, soil type, etc.), which often provide excellent spatial coverage but are noisy (i.e., they have significant sources of error and uncertainty that should be addressed); and 5) data layers of aquifer characteristics (e.g., permeability maps, long-term mean recharge maps, etc.) derived from various sources of traditional or site-specific local information, which offer statewide/provincial, national or even global spatial coverage, but may be of provide little information for local groundwater studies because of low quality/resolution or incompleteness (spatial ‘gaps’ or clearly wrong estimates based on limited input data for deriving aquifer characteristics). Thus, while this wealth of spatially-rich information provides much needed data for groundwater modeling, the variety and inconsistencies between datasets presents a new set of challenges.

Table 2.1: Example big datasets useful for modeling groundwater systems. *MWs = monitoring wells

| Parameter / Data Type | Example Dataset, Source | Spatial Coverage | Resolution / Sizes / # of Samples | Modeling Usage |
|-----------------------------------|--|-------------------------|---|--------------------------------|
| <i>Digital Elevation Models</i> | National Elevation Dataset, NED USGS (2006) | National (U.S.A) | 30, 10 m | Input |
| | LiDAR-based (various sources- see Summary and Conclusions) | Statewide / Local | 3, 1, <1 m | |
| | ASTER Global DEM, NASA LP DAAC (2015) | Global | 90 m | |
| <i>Lakes / Wetlands</i> | National Hydrography Dataset NHD USGS (2010) | National (U.S.A) | Size 1 (< 3,000 m ²) - Size 5 (> 500,000 m ²) | Input / Analysis / Calibration |
| | HydroLAKES, Messenger et al. (2016) | Global | >10,000 m ² | |
| <i>Streams / Rivers</i> | NHD USGS (2010) | National (U.S.A) | Order 1 (small) – Order 10 (large) | Input / Analysis / Calibration |
| <i>Watersheds</i> | NHD USGS (2010) | National (U.S.A) | 2 digit (large) - 12 digit (small) | Input |
| | HydoBASINS, Lehner (2013) | Global | > 100 km ² | |
| <i>Static Water Levels (SWLs)</i> | Wellogic (MDEQ) WIZARD (KGS 2002) Geosam (IGS) | Statewide | ~600,000 wells | Input/Analysis/ Calibration |

Table 2.1 (cont'd)

| | | | | |
|--|---|------------------|---|---------------------------|
| <i>Surficial geology, depths, aquifers</i> | ORNL DAAC Soil Collections archive, Pelletier et al. (2016) | Global | 1 km | Input / Analysis |
| | Shangguan et al. (2016) | Global | 250 m (depth only) | |
| <i>Lithology</i> | GLiM, Hartmann and Moosdorf (2012) | Global | > 1.2 million polygons | Input / Analysis |
| | GWIM, State of Michigan (2006) | Michigan | ≈500 million data points | |
| <i>Bedrock geology, depths, aquifers</i> | GWIM, State of Michigan (2006) | Michigan | 500 m | Input / Analysis |
| <i>Permeability / Conductivity</i> | GLJYMPS, Huscroft et al. (2018) and Gleeson et al. (2011) | Global | 10 km (sediment layers) | Model Input |
| <i>Climate Data</i> | PRISM Climate Group, PRISM (2004) | National (U.S.A) | 8000 m (Daily/Monthly), 400 m (35-year Normal) | Input (recharge modeling) |
| <i>Land Use / Land cover</i> | USGS LULC Dataset (Fry et al. 2011) | National (U.S.A) | 30 m | Input (recharge modeling) |
| | WaterBase | Global | 800 and 400 m | |
| <i>Soil Type / Root Zone Depth</i> | USDA SSURGO, SSS NRCS (2016) | National (U.S.A) | 60 m | Input (recharge modeling) |
| | Harmonized World Soil Database, Fischer et al. (2008) | Global | 1 km | |
| <i>Recharge</i> | NHDPlus USGS (2002) Reitz et al. (2017) | National (U.S.A) | 1 km Mean Annual ϵ 800 m Mean Annual ϵ | Input / Calibration |
| <i>ET</i> | MODIS, ORNL DAAC (2018) | Global | 1 km ² at 8-day, monthly, annual intervals | Input / Calibration |
| <i>Groundwater storage</i> | GRACE, Swenson (2012) | Global | 100 km, monthly | Analysis / Calibration |
| Sensor Data (MWs and SW*) | USGS Water Data, USGS (2016). | National (U.S.A) | Variable spatial density and temporal coverage | Calibration |

Research Questions. The foregoing discussion raises several important questions that have yet to be systematically addressed:

- How can the various types of big data be used for modeling groundwater systems?
- Can big data alone be used to model groundwater systems and assess model accuracy? If so, at what scales?

- What is the impact of combining big data of different qualities, resolutions, and different levels of completeness? Which ones are most important for proper representation of prevailing groundwater system conditions?
- What does big-data enabled modeling mean for site-specific data collection, modeling and analysis?

In the following subsections, we discuss generalized approaches for using big data to model groundwater systems, focusing primarily on modeling of surficial (unconfined) aquifers critical to water resourced and sustaining of groundwater-dependent ecosystems. We also present ways in which big data enable evaluation of groundwater model performance and model calibration (fine-tuning of parameters and model structure). This is followed by real-world applications and evaluations.

2.3.2 Capturing the Aquifer Framework

Aquifer Top Surface. The top boundary of surficial/unconfined aquifers follow the land surface, which can now be represented with detailed Digital Elevation Models (DEMs). DEMs are grid-formatted, continuous datasets with high spatial resolution (90m, 30m, or 10 m) and (typically) seamless coverage. Even 1m or sub-meter LiDAR- (Light Detection and Ranging) based DEM products are in development or already available across large areas. For instance, the U.S. States of Delaware, Indiana, Iowa, Minnesota, Ohio, and Pennsylvania have completed statewide DEMs using LiDAR (see, e.g., OSPC 2007, IOLEP 2011, IDNR 2017), and a number of others are in various stages of development. There are also several national movements in progress, e.g., see Finland's National DEM (NLS Finland 2015), Switzerland's swissSURFACE3D (FOT Switzerland 2015), or England's National LIDAR database (EA UK 2018). Accurate, detailed representation of the land surface improves model structure and calculations related to aquifer top surface (e.g., aquifer thickness, groundwater level elevation computed as land surface minus measured distance to water level in a monitoring well, etc.). As we discuss below, high-resolution delineation of a surficial aquifer's top surface is also useful for estimating the spatial occurrence and magnitude of groundwater discharge to streams, lakes, and wetlands/seeps (see Representing Sources and Sinks below).

Aquifer Bottom Surface. The bottom surface of near surficial/unconfined aquifers is commonly represented as a data layer that follows the interface between unconsolidated sediments and consolidated rock material (usually assumed to be a ‘no-flow’ boundary condition when the yield of rock is expected to be low relative to that of the overlying sediments). This interface has traditionally been estimated site-by-site using available geologic information, geophysical methods (e.g., electric resistivity mapping, borehole seismic profiles, etc.) and limited intrusive subsurface data (cores and lithologic descriptions from deep boreholes). Large-scale maps of surficial aquifer thickness (which implicitly contain aquifer bottom surface information) have recently been generated by integrating different subsurface data (see examples in Table 2.1: Shangguan, 2017, Pelletier et al. 2016), although quality varies spatially depending on local data availability, in some cases rendering the estimates inaccurate (or even useless). With the digitization of historical water well information, increasingly dense datasets of borehole data (and lithologic descriptions) allow for direct spatial interpolation of the surface representing the interface between surficial sediments and underlying bedrock. This data-intensive approach is applied for delineating aquifer bottom boundaries in real-world examples (see Real-world Illustrations).

Lateral Boundaries. Datasets of distributed zones (polygons) containing geologic, lithologic, and hydrogeologic descriptions of surficial geology are useful for delineating groundwater lateral aquifer extents. In some places, direct data layers of aquifer extents are available, e.g., shallowest principal aquifers in the conterminous United State (USGS 2003). Watershed and sub-catchment boundaries available in hydrography datasets (e.g., USGS NHD 2010) may also be useful for choosing a groundwater model domain (see Real-World Illustrations below).

2.3.3 Characterizing Aquifer Properties

Permeability. The permeability of the subsurface is parameterized with hydraulic conductivity (K) model inputs that typically vary in space and may typically require fine-tuning through model calibration. Big data products consisting of distributed zones of lithologic descriptions of surficial geology are useful for estimating variabilities in K, but recently big data layers with direct estimates of K have become available at statewide, national, or even global scales (see, e.g., State of Michigan, 2006; Gleeson et al. (2011).

However, like global data sets of aquifer bottom surface, quality of broad coverage K layers depends on local data availability, and resolutions are typically relatively coarse for the purpose of modeling subregional groundwater systems. For detailed characterization of intra-aquifer geologic variability that influences K distributions, spatial interpolation methods such as kriging and transition probability (Markov chain) geostatistics have been increasingly popular as more borehole data are generated and compiled into databases (see, e.g., Weissmann and Fogg 1999; Traum et al. 2014 He et al. 2014 Sampath et al 2015; 2016). Detailed representations of aquifer heterogeneity are necessary for common management practices such of site-scale plume modeling and groundwater remediation, which depends critically on small-scale subsurface heterogeneities not captured by large-scale data layers (Heinz et al. 2003, Zheng and Gorelick 2003, Ronayne et al. 2010)

Storage. For transient simulations of groundwater systems, characterization of aquifer storage (specific yield or storativity) is needed. The GLobal HYdrogeology MaPS (GLHYMPS) database provides 10 km resolution data layers of porosity, and GRACE satellite data (Swenson 2010) provides gridded data layers (100 km resolution) of monthly land water mass. Each of these datasets can used to estimate aquifer storage anywhere on earth, although 10 km (and especially 100 km) resolution is problematic for many site-specific studies of groundwater systems. (Another utility of GRACE data is the analysis of large-scale temporal trends – see Calibrating to Temporal Trends and Long-term Patterns).

2.3.4 Representing Surface Water Interactions

There are two general approaches for representing groundwater interactions with surface water bodies (lakes, streams, wetlands, and springs/seeps): i) integrated surface water-groundwater modeling; and ii) assigning boundary conditions. In both approaches, implementation of big datasets enables generalized modeling of groundwater-surface water interactions, although there are modeling trade-offs worth considering.

Integrated Modeling. Groundwater-surface water exchange can be simulated with integrated surface water-groundwater modeling approaches that computes surface water dynamics (stage and flows) as part of the

solution process. In this approach, the surface water continuity equation is coupled to the groundwater system via a groundwater source/sink term. The surface water continuity equation is:

$$\frac{\partial V}{\partial t} = SW_{in} - SW_{out} - GW \quad (2.1)$$

$$\frac{\partial V}{\partial t} = A \frac{\partial s}{\partial t} + s \frac{\partial A}{\partial t} \quad (2.2)$$

where V is the volume of the surface water body, t is time, SW_{in} and SW_{out} are the surface water inputs and outputs, respectively, GW is the incoming ($GW < 0$) or outgoing ($GW > 0$) flux of groundwater computed using Eq. (4) (see below), A is the surface area of the surface water body, and s is the stage. Big data products provide key surface water inputs - including surface water inflows (from stream gage networks), precipitation (from climate forcing datasets), surface run-off (estimated based on land use/type or as output from an integrated watershed model) – and outputs – including surface water outflows (sensor networks) and evaporation (e.g., MODIS satellite ET products).

Coupling of surface water-groundwater interactions may be included as part of an integrated, distributed-parameter watershed model that simulates – in addition to as surface water flows – land runoff, recharge, groundwater and vadose zone dynamics by solving the near-surface water balance (see, e.g., Tuppad et al. 2011, He et al. 2014, Davison et al. 2015). Governing equations for different physical processes (saturated flow, unsaturated flow, evapotranspiration) are coupled and solved simultaneously. Detailed big data representations of watershed characteristics (land use and land cover, soil type, root zone depth, lithology, topography – see Table 2.1) and climate forcing data (precipitation, air temperatures, irradiance, etc.) provide necessary inputs to the governing equations, and time-series streamflow measurements from distributed sensor networks help to improve model details and to constrain simulated fluxes. However, because coupled process-based models are data-intensive and require time-steps on the order of minutes (or even seconds) to resolve the numerous surface processes impacting watershed interactions, computational costs associated with this approach may be impractical for the purposes of long-term modeling of

groundwater systems important to water resources (where flows are characterized by residence times of months, years and decades).

Assigning Boundary Conditions. An alternative approach for representing groundwater-surface water interactions is through representing lakes, stream, etc. as conceptual features in the groundwater model (or as ‘internal’ boundary conditions). Surface water stages are provided as input for calculations of groundwater head or flux in/out of the model in the appropriate model cells. Prescribed head conditions are expressed as:

$$h_{i,j}(t) = s_{i,j}(t) \quad (2.3)$$

where $h_{i,j}$ is the head in the i,j^{th} (x,y) model cell at time-step t , and $s_{i,j}(t)$ is the stage for the corresponding cell and time-step. Although in general stage may vary in space or time, big hydrography datasets (e.g., NHD 2010 or Messenger et al. 2016 - see Table 1), typically provide long-term average stages (or single measurements assumed to be representative of long-term conditions), or spatially-variable stage information (particularly in the case of streams) that may be used in Eq. (3). Time-varying stages are typically available in sensor records (e.g., USGS time-series stream gages), but obviously these are for discrete locations. Adopting these considerations, head-dependent flux conditions are expressed as:

$$q_{SW} = L_{SW}(h - s) \quad (2.4)$$

where q_{SW} [LT^{-1}] is the flux per unit area infiltrating ($+q_{SW}$) or exfiltrating ($-q_{SW}$) the aquifer through the surface water-groundwater interface, h [L] is the head in the aquifer cell, s is the surface water stage, and L_{SW} the leakance of the streambed/lakebed/etc. (hydraulic conductivity per unit thickness). Leakance is typically fine-tuned during calibration or estimated from other properties (e.g., stream order or lake size, gradient, etc.).

A few limitations to these approaches are worth noting. First, caution should be used when applying prescribed head conditions, as they are unresponsive to stresses in the groundwater system. For example, if a constant-head boundary is used for a lake that is near a pumping well, it will continue to supply water and maintain a constant head, even though the continued pumping would eventually result in a cone of

depression that would expand and lower the head where the lake is located (i.e., the lake becomes an ‘infinite’ supply of groundwater). Second, while Eq. (4) allows flux to vary in response to changes in head, slight errors in leakance can lead to large errors in flux calculations, especially in the case of infiltration (see Real-World Illustrations).

Land Surface as a Seep Surface. To avoid problems associated with artificially supplying water through excess infiltration, Eq. (4) may be altered so that water is restricted from leaving the surface water body and entering the aquifer (‘one-way’ head-dependent flux):

$$q_{sw} = \begin{cases} L_{sw}(h - s) & \text{if } h > s \\ 0 & \text{otherwise} \end{cases} \quad (2.5)$$

By extension, the entire land surface may be treated as a one-way head dependent boundary condition (seepage) that allows groundwater to discharge to the surface where the groundwater level intercepts the land surface:

$$q_{seep} = \begin{cases} L(h - z) & \text{if } h > z \\ 0 & \text{otherwise} \end{cases} \quad (2.6)$$

where q_{seep} [LT⁻¹] is the flux per unit area leaving the aquifer through the land surface, z is the land elevation, and L is the leakance (hydraulic conductivity per unit thickness) of the land surface. Given the high-resolution DEMs currently available for representing the land surface, z can be assigned with a high degree of accuracy and the spatially-constant leakance term can be calibrated, e.g., if the leakance is too low, the flooded area will be large, and vice versa. Essentially, this approach predicts where the water table intersects the land surface as part of the solution process, rather than assume complete knowledge of where this condition is satisfied. In other words, it is able to account for seeps not identified in hydrography datasets, while also ‘automatically’ capturing discharge to surface water bodies (whose long-term, average stage levels are reflected in high-resolution DEMs). Of course, some actual infiltration will not be captured with this approach, thereby introducing error into the water balance. However, as we show later, this error is expected to be small in areas where surface water bodies are predominantly gaining (e.g., regional discharge

areas). In fact, the ‘one way’ treatment may be the most robust approach for modeling extensive surface water networks of large watersheds (see example in Detailed Methodology in subsection below).

2.3.5 Estimating Recharge

Net infiltration of precipitation, or aquifer recharge, is represented as input to cells in topmost groundwater model layers. Depending on the modeling application, recharge may be constant, spatially-variably, and/or time-varying. We briefly review the links between big data and the range of choices for estimating recharge.

Empirical approaches. Historically, aquifer recharge has been estimated by relating observations of precipitation to net infiltration via mathematical models with relatively few model parameters that can be adjusted (see Yu et al. 1999). As more hydrologic data have become available, other have applied statistical regression techniques involving observed stream flow hydrographs, water tables fluctuations, etc. and information related to land use, soil conditions, and watershed characteristics (see Risser et al. 2008, or Holtschlag 1997). Although local improvements are typically needed, the emergence of national or global datasets of land/watershed characteristics and hydrological observables (see Table 2.1) means that empirical approaches can be applied for many different places to provide reliable first-order estimates of recharge.

Semi-empirical approaches. Another approach is to solve the vadose zone water balance by considering precipitation, snowmelt and sublimation, accumulation/surface storage, surface water run-on, evapotranspiration, redistribution within the vadose zone, and net infiltration (recharge). The water balance parameters can be derived empirically from precipitation and temperature data, topography, soil type/lithology, and land use/land cover datasets. These semi-empirical approaches allow modeling both spatially-varying and time-varying recharge, but the large number of parameters used to compute the water balance terms can make their implementation tedious and the model insensitive to adjustments. An example of this type of model is the INFIL 3.0 – a grid-based, distributed-parameter watershed model by USGS (USGS, 2008). Also see Reitz et al. (2017)

Process-based simulations. Similar to semi-empirical approaches, process-based approaches solve the near-surface water balance, providing estimates of recharge as a simulation output. However, rather than derive

water balance terms from empirical relationships, coupling of governing physical equations is used to calculate water balance terms. Process-based models are capable of producing detailed estimates of recharge in time and space and are useful for probing potential impacts of climate change or abstracting of water, but may be computationally impractical when for the purposes of long-term modeling of groundwater systems important to water resources (see more details above in Representing Surface Water Interactions).

2.3.6 Calibrating to Temporal Trends and Long-term Patterns

Sensor Data. Spatially-distributed sensor networks linked to web-based data repositories provide crucial information needed for characterizing temporal trends and calibrating groundwater models, namely: historic and present-day groundwater levels; surface water stages; and stream/reservoir flows. For the steady-state groundwater modeling, typically groundwater levels collected at different times (but across large areas) are compared to simulated head and model parameters (conductivity, recharge, etc.) are adjusted to improve overall model performance. In many long-term studies of aquifer systems (e.g., regional investigations by USGS), monitoring well networks are established and operated for several/many years so that long-term groundwater level data are available for transient model calibration, among other uses (see Taylor and Alley 2001). When available, stream flows and surface water stage are useful for constraining fluxes (especially baseflow and recharge). However, for many areas with a growing (or emerging) dependence on groundwater, monitoring wells and/or surface water sensors are not available (or do not span the appropriate times and/or locations).

Water Well Data. Another, more universal source of physical groundwater data (water levels) are Static Water Level (SWL) measurements, which are water levels measured in wells at the time of installation (prior to pumping). Massive SWL datasets are becoming increasingly available in different U.S. States and elsewhere (see, e.g., Illinois State Geological Survey repository (ISGS, 2015), Kansas' WIZARD water well levels database (KGS, 2002), and the GeoSam Database for the State of Iowa (IGS, 2016)), and although there are a number of sources of error and variability embedded in them (e.g., approximate well

locations, measurement uncertainty due to QA/QC variabilities from well driller to well driller, and physically impossible data due to procedural error), recent research shows systematic processing and critical evaluation of SWLs yields important insights into groundwater systems. We briefly discuss these next.

Spatial Interpolation of SWLs. Using Static Water Levels (SWLs) as input data, an automated, continuously moving window statistical analysis can be used to delineate large-scale, prevailing flow patterns. The approach follows a nonstationary kriging technique described in Curtis et al. (2018), in which many noisy water level measurements taken across space and time are used to generate maps of long-term mean head distributions. This approach assesses sub-grid variability and local spatial structure for each estimation point; this information is then used to assign weights to the input values used for spatial interpolation. Although SWL data are noisy and temporal variations are assimilated into the spatial analysis (introducing SWL variability at location), the nonstationary kriging technique has been shown to be effective for the purposes of delineating long-term, prevailing SWL spatial structures (Curtis et al. 2018), and has also been used in geostatistical studies involving meteorological datasets or environmental parameters (see, e.g., Walter et al. 2001, Lloyd 2010, Harris 2010). This approach is demonstrated below as part of Real-World Illustrations.

Temporal Analysis of SWLs. Because each SWL represents one measurement made at one time, time-series analysis at a single point is not possible with SWL datasets. However, by spatially aggregating SWLs, it is possible to detect long-term temporal trends that are larger than the SWL variability caused by spatial aggregation and noise in the measurements themselves. Examples of this applying this approach for detecting multi-decadal trends in a complex aquifer subjected to increase in distributed groundwater withdrawals are presented in Chapter 3 and Chapter 4.

We next illustrate and evaluate some of the generalized big data modeling approaches described in preceding subsections through application to a series of real-world test beds

2.4 Real World Illustrations

The modeling objective of the real-world illustrations is to simulate natural groundwater conditions in near-surface aquifers (i.e., the unconfined, water table aquifer) critical to water resources and sustaining of groundwater-dependent ecosystems. Through this application we explore relative importance of different data components and discuss implications of incomplete datasets, inconsistent data qualities, and scale of analysis.

2.4.1 Detailed Methodology

Database and Test Beds. The State of Michigan was chosen as the study area because of the unique opportunity to utilize large volumes of pre-processed, ready-to-go GIS and hydrologic data layers available across the state. Over the past 15 or so years, significant efforts to assemble, digitize, and properly process massive amounts of data by Michigan's Department of Environmental Quality (MDEQ), the U.S. Geological Society, and Michigan State University resulted in several statewide groundwater databases (State of Michigan 2006, MDEQ 2010, 2014; MNFI 2010). These databases allow for modeling groundwater flow in almost any part of the state using pre-processed data layers, e.g., statewide maps of aquifer elevations and spatially-explicit hydraulic conductivity and recharge estimates.

Figure 2.2 shows the locations and extents of the watersheds used for real-world illustrations, and Table 2.2 provides additional details (formal name and area). The watershed boundaries are derived from the 2-digit watershed boundaries available in the National Hydrography Dataset (NHD) (NHD 2010). The watersheds vary in size (from 2147 to 5238 km²) and shape (e.g., long and thin or short and wide). Six watersheds have surface water outlets into one of the North American Great Lakes (Lake Superior, Lake Huron, Lake Michigan or Lake Erie), while one of the watersheds (Pine, watershed ID=8 from Table 2.2) is 'land-locked' (i.e., its outlet is an inlet for a downstream 2-digit NHD watershed). All watersheds are drained by strong surface water networks and contain unconsolidated glacial deposits, in many places characterized by strong heterogeneity and three-dimensional (3D) structure due to their chaotic depositional history (Westjohn et al. 1994) (e.g., the Huron and Lower Grand watersheds). The surficial sediments are

underlain by interbedded sequences of bedrock, some of some of which act as productive aquifer units and others that are considered aquitards. At least some portion of the surficial sediments are underlain by bedrock aquifers in each of the studied watersheds, but especially for the Kalamazoo (ID=6), Au Sable (ID=3) and Lower Grand (ID=7) watersheds (State of Michigan 2006). Types of land cover includes developed or other human use (e.g., throughout the Huron watershed, or in parts of the Kalamazoo and Lower Grand watersheds), but most of the combined study area is covered in agricultural vegetation or forest and woodland (USGS 2011).

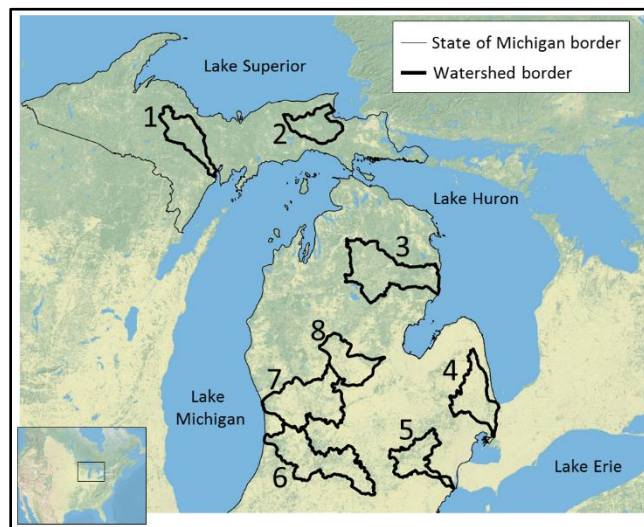


Figure 2.2: Watershed chosen for study. Background image source: National Geographic Society, i-cubed (2013).

Table 2.2: Michigan watersheds chosen for study. The ID numbers correspond to the number labels presented in Figure 2.2.

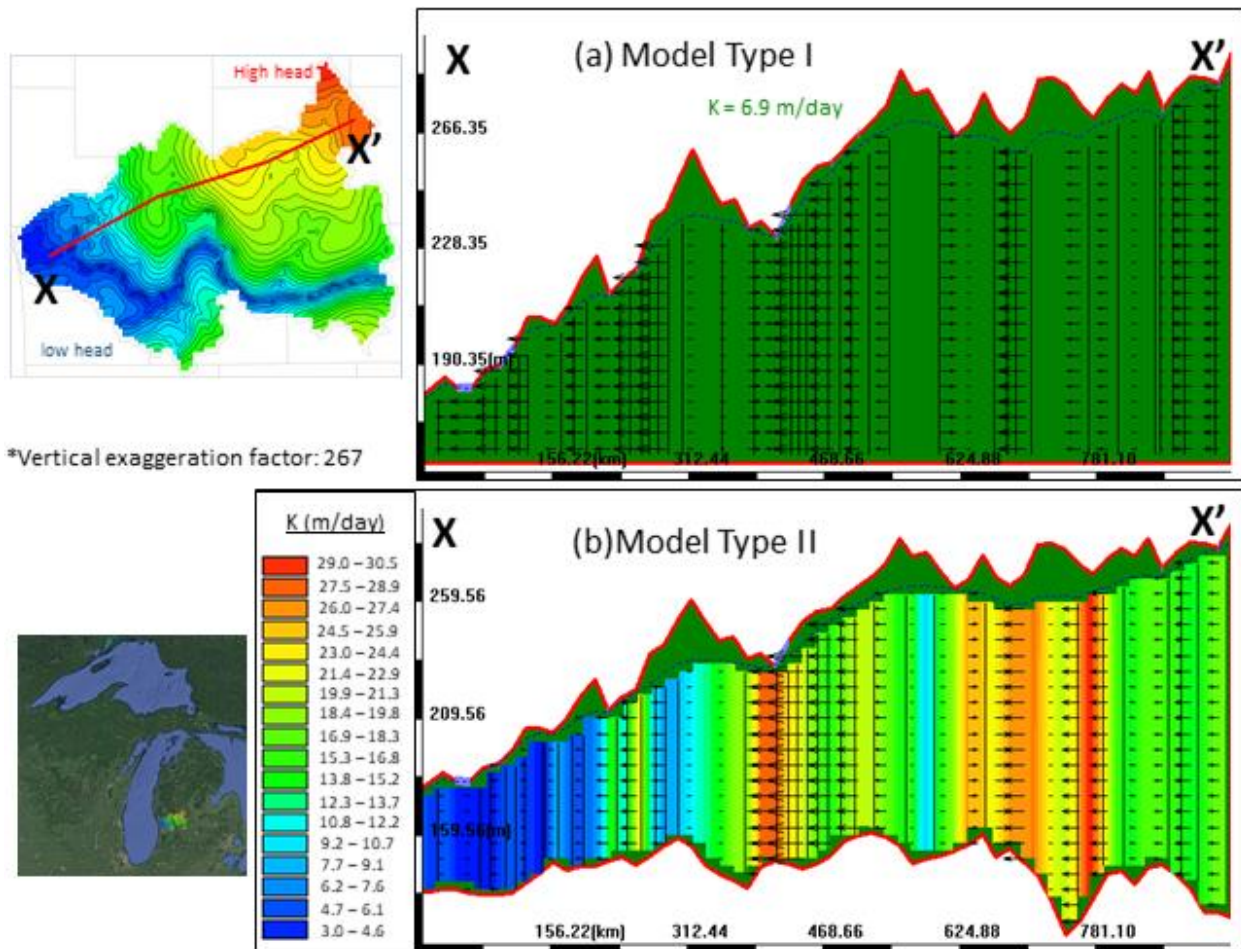
| ID | Name | Area (sq. km.) |
|----|-------------|----------------|
| 1 | Escanaba | 2392 |
| 2 | Tahquamenon | 2147 |
| 3 | Au Sable | 5328 |
| 4 | St. Claire | 3098 |
| 5 | Huron | 2358 |
| 6 | Kalamazoo | 5257 |
| 7 | Lower Grand | 5216 |
| 8 | Pine | 2687 |

The following subsections provide details on the development of the process-based groundwater flow models and the methods for comparing simulated head outputs to water level measurements taken across space and time.

Software and Data. The flow models were created with an integrated, GIS-enabled groundwater modeling system, *Interactive Groundwater* (Li and Liu 2006; Li et al. 2009; Liao et al. 2015a;b), which uses the finite difference approximation of the governing partial differential equation to solve confined and unconfined flow conditions. The modeling environment is live-linked to a database containing terabytes of raw and derived information on groundwater systems, with several sources of statewide information useful for the purposes of this real-world illustration: 1) high-resolution (10 m) resolution DEM (NED USGS 2006) for mapping topographic variations and simulating groundwater surface seeps; 2) water well records from *Wellogic* (MDEQ 2015), which contain valuable physical groundwater data (static water level measurements and borehole lithologies) collected during past decades from over 530,000 locations, useful for evaluating model performance and delineating the spatially-variable bottom boundary of the unconsolidated sediments (i.e., the bedrock top surface); 3) a spatially-variable, two-dimensional (2D) raster of horizontal hydraulic conductivity (K); and 4) a spatially-variable raster of natural (long-term average) groundwater recharge (ϵ), (State of Michigan 2006). The bedrock top elevation raster (500 m resolution) was interpolated from *Wellogic* borehole records. The conductivity raster (540 m resolution) was generated by interpolating estimates of K from records in the *Wellogic* database, MDEQ public water supply and U.S. Geological Society aquifer-tests, and aquifer properties reported in literature (State of Michigan 2006). The recharge raster (1609 m resolution) was generated following empirical methods presented in Holtschlag (1997) involving observed stream flow hydrographs and information related to land use, soil conditions, and watershed characteristics.

Model Types. The statewide datasets were used to create 1-layer, 2D steady groundwater flow models of the unconfined aquifer layer for the eight selected watersheds in Michigan. For each watershed, two types of models were created: Model Type II, informed by the statewide big data products; and Model Type I,

informed by accurate land surface representation, but no other big groundwater data. More specifically, while both models utilize the 10 m DEM, Model Types II apply the spatially-explicit bottom aquifer elevation, conductivity, and recharge inputs, whereas Model Types I models utilize a single, effective value for conductivity and recharge for all cells in the model and a constant bottom aquifer elevation, computed as the minimum DEM elevation minus a user-prescribed length, Z . (Note that, after some trial and error, 28.3m = 60 ft. was chosen as Z , however, this value could be determined during model calibration – see Examples of Further Model Utilization.) Figure 2.3 provides example cross-sections for each type of model for the Lower Grand watershed (ID=7) to help illustrate the key conceptual differences between model types. A summary of the two types of groundwater flow models generated for each watershed is provided in Table 2.3.



*Vertical exaggeration factor: 267

Figure 2.3: Example cross-sections to illustrate the two process-based modeling approaches used in this study. Arrows indicate groundwater velocity vectors. The red lines along the top and bottom of the models are the model boundaries.

Table 2.3: Summary of inputs for the two types of process-based models used in this study.

| Parameter or Feature | Model Type I | Model Type II |
|-------------------------|------------------|--------------------|
| Top elevation | 10m DEM | 10m DEM |
| Bottom elevation | Min. DEM minus Z | Bedrock top raster |
| Conductivity (K) | Mean K | K raster |
| Recharge (ϵ) | Mean ϵ | ϵ raster |

The primary purpose of developing these two types of models for each watershed was to evaluate the

relative importance of capturing additional details of the system framework beyond the topographic variability, namely spatially-explicit recharge, conductivity and aquifer bottom elevation.

Grid Properties. The two types of models utilize the same 2D grid configuration, i.e., the number of cells in the x-direction, NX, and the number of cells in the y-direction, NY, is the same for both types of models for a given watershed. Grid cells are approximately square (DX, the cell length in the x-direction, is approximately equal to DY, the cell length in the y-direction). Table 2.4 provides grid properties of the process-based models created for each watershed. The mean recharge and mean conductivity values, computed from the raster cell values within each model domain, are also provided. These values were applied as the single effective K and ϵ values for the Type I models, although these two parameters could be fine-tuned during calibration (see Examples of Further Model Utilization subsection below).

Table 2.4: Grid properties of the models of the different watersheds, and the mean recharge (ϵ) and mean hydraulic conductivity (K).

| ID | NX | NY | DX (m) | Mean ϵ (in./yr.) | Mean K (ft./day) |
|----|-----|-----|-----------|------------------------------|---------------------|
| 1 | 80 | 100 | 947 | 10.7 | 11.7 |
| 2 | 100 | 66 | 796 | 13.4 | 11.5 |
| 3 | 100 | 69 | 1260 | 10.2 | 29.2 |
| 4 | 56 | 99 | 1184 | 5.7 | 8.7 |
| 5 | 100 | 92 | 865 | 8.3 | 26.3 |
| 6 | 100 | 65 | 1478 | 11.6 | 26.1 |
| 7 | 100 | 83 | 1102 | 10.4 | 22.8 |
| 8 | 100 | 81 | 874 | 8.6 | 22.8 |

Lateral and Bottom Boundary Conditions. The lateral boundaries and bottom for all models were assigned as no-flow boundary conditions (i.e., groundwater flux across them is zero), under the assumption that significant groundwater does not flow across watershed divides or from the underlying bedrock. Of course, this may not reflect actual groundwater conditions; some watersheds overlie productive bedrock units with significant flux transfer between the unconsolidated sediments and bedrock, and groundwater divides do not necessarily coincide with watershed boundaries (especially when pumping is present). As a result, the models may provide poor estimates of head near the model boundaries. However, rather than focusing on acquiring accurate boundary conditions through data collection, nested flow modeling, etc., the lateral boundary conditions used here offer a quick starting point for building a model and evaluating its performance. Boundary location/type can then be updated in areas where the model is clearly under- or overestimating head (again, see Examples of Further Model Utilization subsection).

Representing Groundwater Discharge at the Surface. In the previous section, a number of ways for representing groundwater-surface water interactions were presented. The ‘one-way’ head-dependent flux approach (i.e., treating land surface as a seepage surface – see Eq. 6) was selected for the real-world modeling applications - which, as we show next, may be the most robust approach for modeling extensive surface water networks of large watersheds.

As a comparative example, water balance results for two Type II process-based models representing the Au Sable watershed (ID=3) were generated, with one model representing surface water features using the ‘one-way’ approach described above, and the other utilizing two-way head dependent boundary conditions (see Eq. 4). For this example, different leakances, L_{SW} , were assigned to stream segments (or lake feature) based on stream order (or lake size), i.e., smaller lakes and lower order stream segments utilize smaller L_{SW} values compared to the larger lakes and higher order stream segments. A comparison of the simulated aquifer water balances of the different models is shown in Figure 2.4. Consider that the annual average precipitation spread across the watershed is about 28 in./yr., or 10,400,000 m³/day (PRISM 2004), and the 28-year average annual discharge at the Au Sable river mouth (i.e., where it discharges to Lake Huron) is about

3,700,000 m³/day (USGS 2016), the following can be said about the results from two-way representation of surface water bodies: a groundwater outflow to rivers (or baseflow) of 6,900,000 m³/day, which is over 70% of total average river outflow, seems unreasonably high and (2) a river inflow (source term) of 4,200,000 m³/day across the watershed, or about 40% of the total precipitation, is not likely for water-abundant places such as Michigan with water tables close to (or at) the land surface (and thus most streams are gaining). This, together with the fact that the simulated seepage areas (Figure 4b) generally coincide the spatial configuration of the stream network (Figure 4b), suggests that the two-way treatment of surface water bodies requires careful implementation and additional data for constraining the water balance as compared to one-way seep treatment. Of course, further testing is needed for rigorous comparison of these two (and other) techniques for representing surface water bodies when modeling larger groundwater systems, which we explore in forthcoming work (Curtis et al., in prep.).

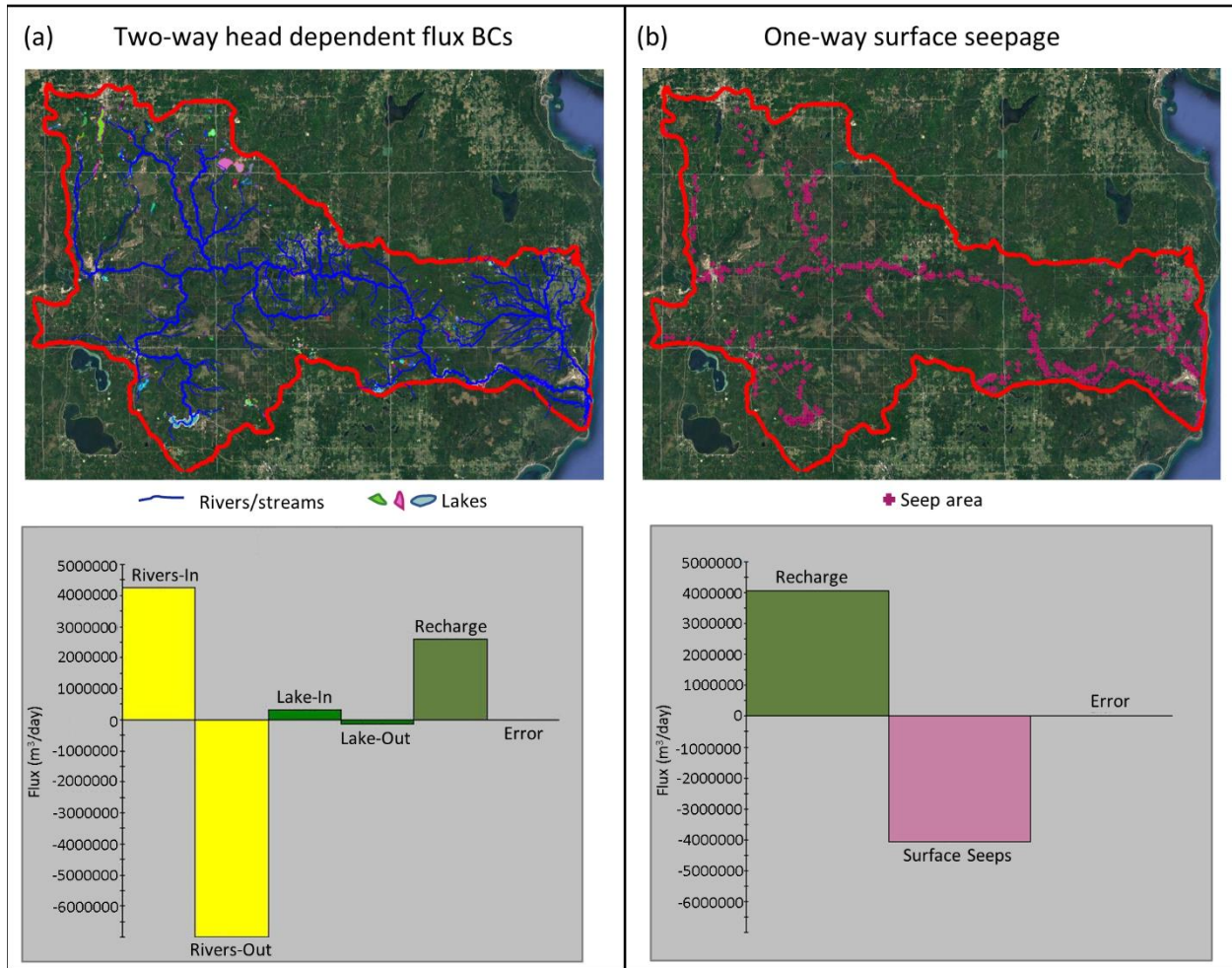


Figure 2.4: Comparison of the spatial occurrence of groundwater seep areas (top) and water balances (bottom) for the Au Sable watershed (ID=3). (a) Model utilizing two-way head dependent flux boundary conditions (BCs) for lakes and rivers/streams; and (b) one-way head-dependent flux for the entire land surface. Streams and lakes shown in (a) are from NHD USGS (2010).

(No) pumping stresses. None of the models included pumping used to support human activities. Obviously, this is an oversimplification of reality, as groundwater is withdrawn from all of the watersheds examined in this study, albeit mostly for small-use, domestic water wells. Later in the Results and Discussion, we discuss how comparisons of these ‘pre-development’ steady-state simulations with water level data collected across space and time can be used to guide model refinement and data collection (e.g., in areas of the model where prediction accuracy is clearly suffering from neglecting pumping).

Evaluating Model Performances. The performance of each model was evaluated by mapping water levels measurements for each watershed using the non-stationary kriging approach described above, and comparing the data-driven flow patterns (in the form of head contour maps) with the flow patterns output from the process-based models. Each data-driven flow representation utilizes the same grid (NX and NY) as the process-based models for a given watershed (see Table 2.4: Grid properties of the models of the different watersheds, and the mean recharge (ϵ) and mean hydraulic conductivity (K).). Following Curtis et al. (2018), the number of nearest points, M, used for assessing spatial structure and performing kriging estimation was computed as:

$$M = \rho_{\text{wells}} * \frac{\pi}{4} \left(\frac{1}{10} L \right)^2 \quad (2.7)$$

where ρ_{wells} is the well density (per sq. km) and L is the model extent. Values of ρ_{wells} , L, and M for all watersheds are provided in Table 2.5 Parameters used for non-stationary kriging and spatial interpolation., in addition to the total number of points available for kriging and the number of outliers removed during analysis. The total number of points includes SWL outside of the model domain (as ignoring these points may result in biased estimated values near the boundary) and the outliers were identified and removed using a moving window statistical analysis, i.e., data values that were more than 3 standard deviations from the local average (computed using the nearest 30 points) were removed before kriging

Table 2.5 Parameters used for non-stationary kriging and spatial interpolation.

| <i>ID</i> | <i>well density (per sq. km)</i> | <i>L (km)</i> | <i>M (NS krig)</i> | <i>Total Points</i> | <i>Outliers removed</i> |
|-----------|--------------------------------------|---------------|------------------------|-------------------------|-----------------------------|
| 1 | 0.47 | 114.3 | 48 | 1711 | 26 (1.52%) |
| 2 | 0.61 | 81.2 | 32 | 1878 | 35 (1.90%) |
| 3 | 1.79 | 139.5 | 274 | 14013 | 313 (2.28%) |
| 4 | 1.65 | 118.7 | 183 | 10598 | 131 (1.45%) |
| 5 | 143.23 | 78.8 | 6985 | 45483 | 683 (1.56%) |
| 6 | 4.79 | 160.0 | 962 | 33071 | 504 (1.55%) |
| 7 | 5.28 | 108.6 | 489 | 37678 | 515 (1.39%) |
| 8 | 3.62 | 78.6 | 176 | 13135 | 190 (1.45%) |

Each SWL measurement available in each watershed was compared to the simulated head at that location to graphically and statistically evaluate the goodness of fit between the process-based models and observed Static Water Levels. The simulated head was computed from a weighted average (traditional bi-linear interpolation) of values at surrounding nodes. Statistical indicators - namely, the root-mean-square error (RMSE), mean error, and Nash-Sutcliffe coefficient (E) were computed to assess the predictive abilities of the process-based flow models. Mean error and RMSE error are common indicators in regression statistics, and E is typically used for comparing simulated discharge to observed discharge. For the purposes of this study, E was computed as:

$$E = 1 - \frac{\sum_{s=1}^S (h_{sim}^s - h_o^s)^2}{\sum_{s=1}^S (h_o^s - \bar{h}_o)^2} \quad (2.8)$$

where h_{sim}^s and h_o^s is the simulated head and observed head (SWL), respectively, of the s^{th} pair ($s=1,2,\dots,S$, where S the total number of data pair), and \bar{h}_o is the mean of the head observations.

2.4.2 Results and Discussion

The results for each watershed are presented in Figure 2.5 – Figure 2.12, beginning with the Escanaba watershed (ID=1) and proceeding in order through the Pine watershed (ID=8) (see Table 2.2 for watershed IDs). Each figure contains head maps (upper section) generated from (a) the Type I model; (b) the Type II model; and (c) non-stationary kriging. All head maps for a given watershed share the same color scheme and legend for easy comparisons. Also included in Figures 2.5 – 2.12 are (d) calibration plots (lower section) comparing the results of the Type I models with SWLs (left-side chart) and similarly for the Type II models (right-side chart). Confidence intervals of 2 standard deviations and moving window averages (‘band mean’) were computed and added to assist with graphical analysis of the sets of data pairs for each watershed. Table 2.6 contains the statistical indicators used to evaluate model performance and will be referred to during the following discussion.

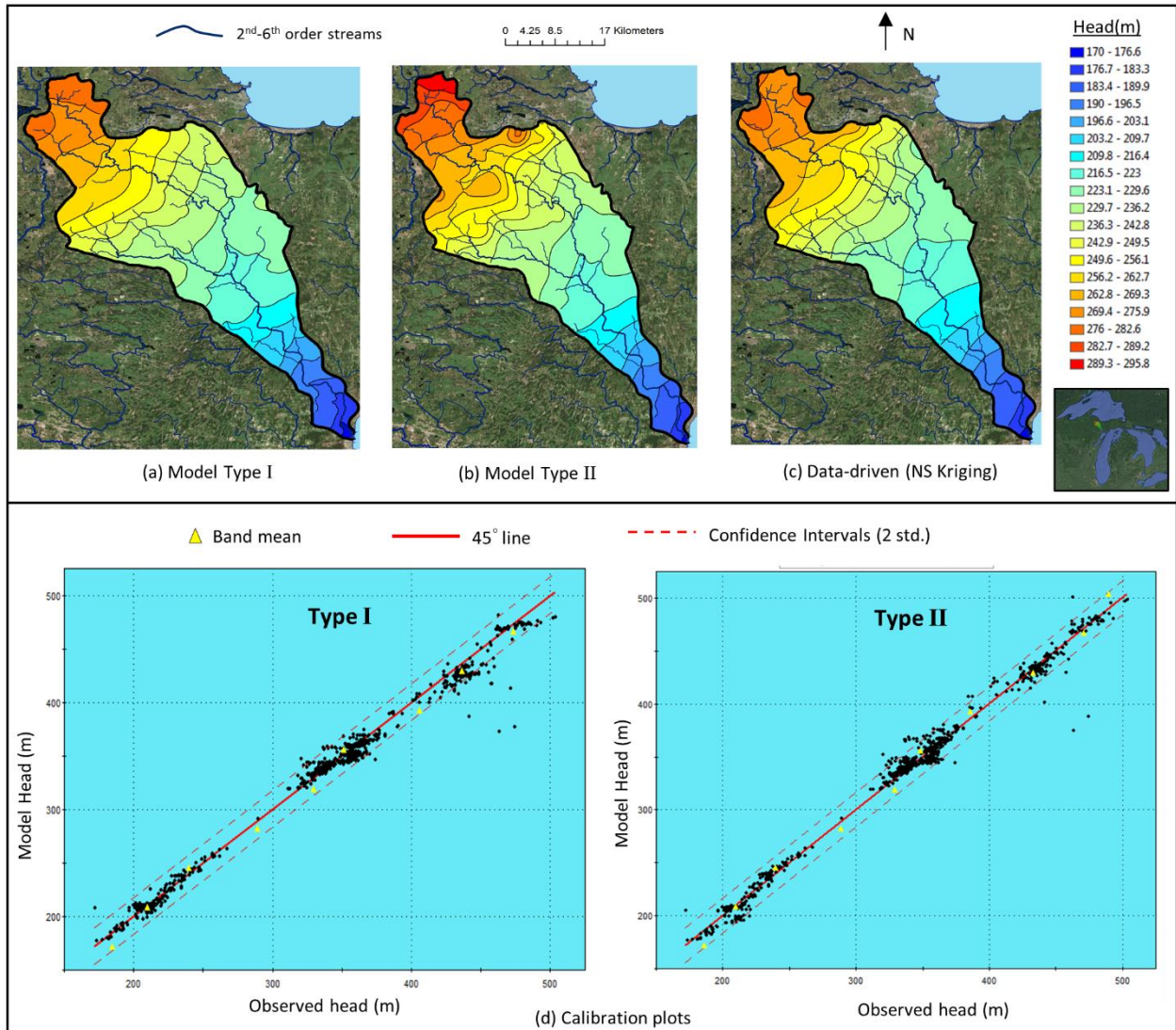


Figure 2.5: Head distributions and calibration charts for the Escanaba watershed (ID=1).

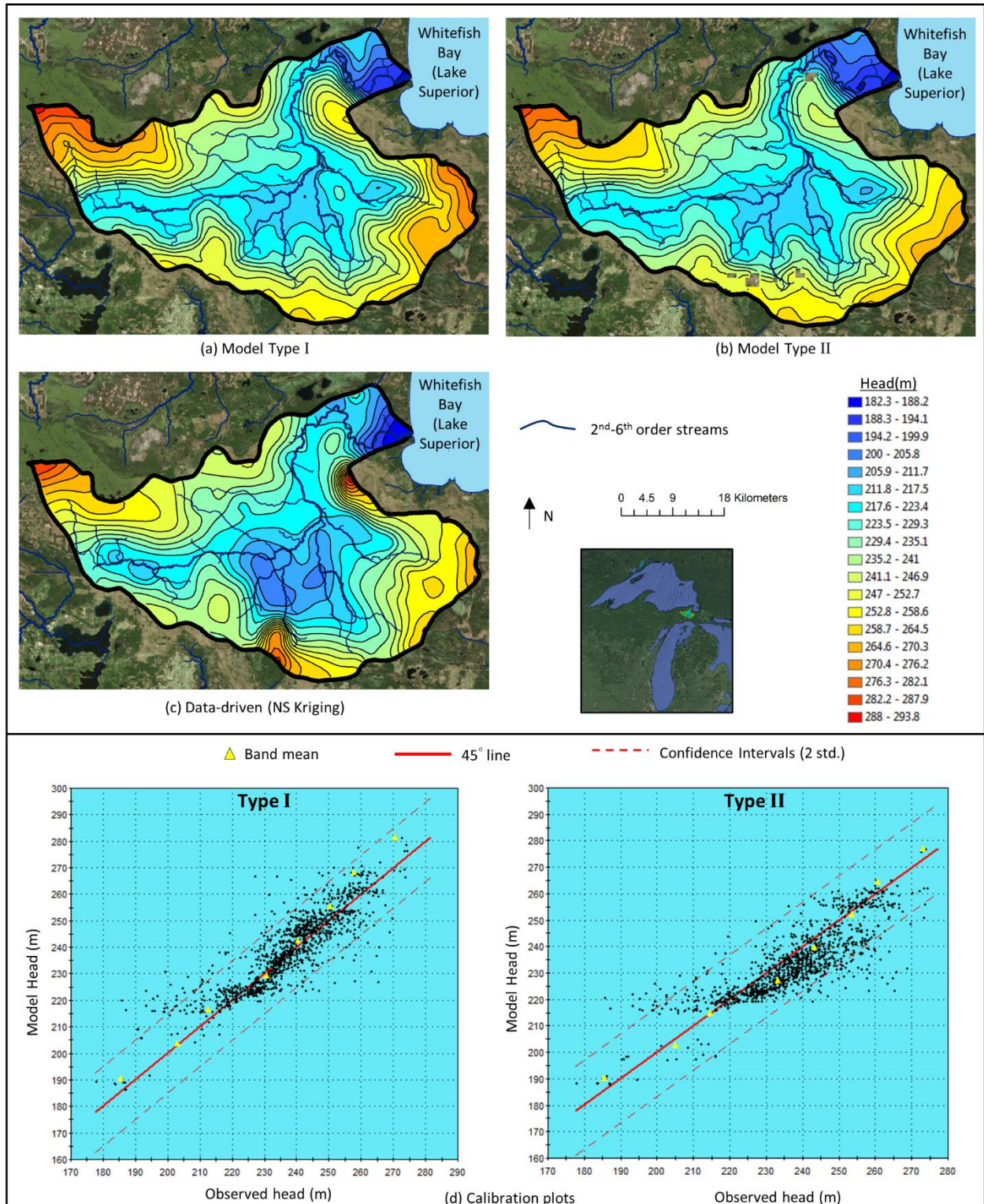


Figure 2.6: Head distributions and calibration charts for the Tahquamenon watershed (ID=2).

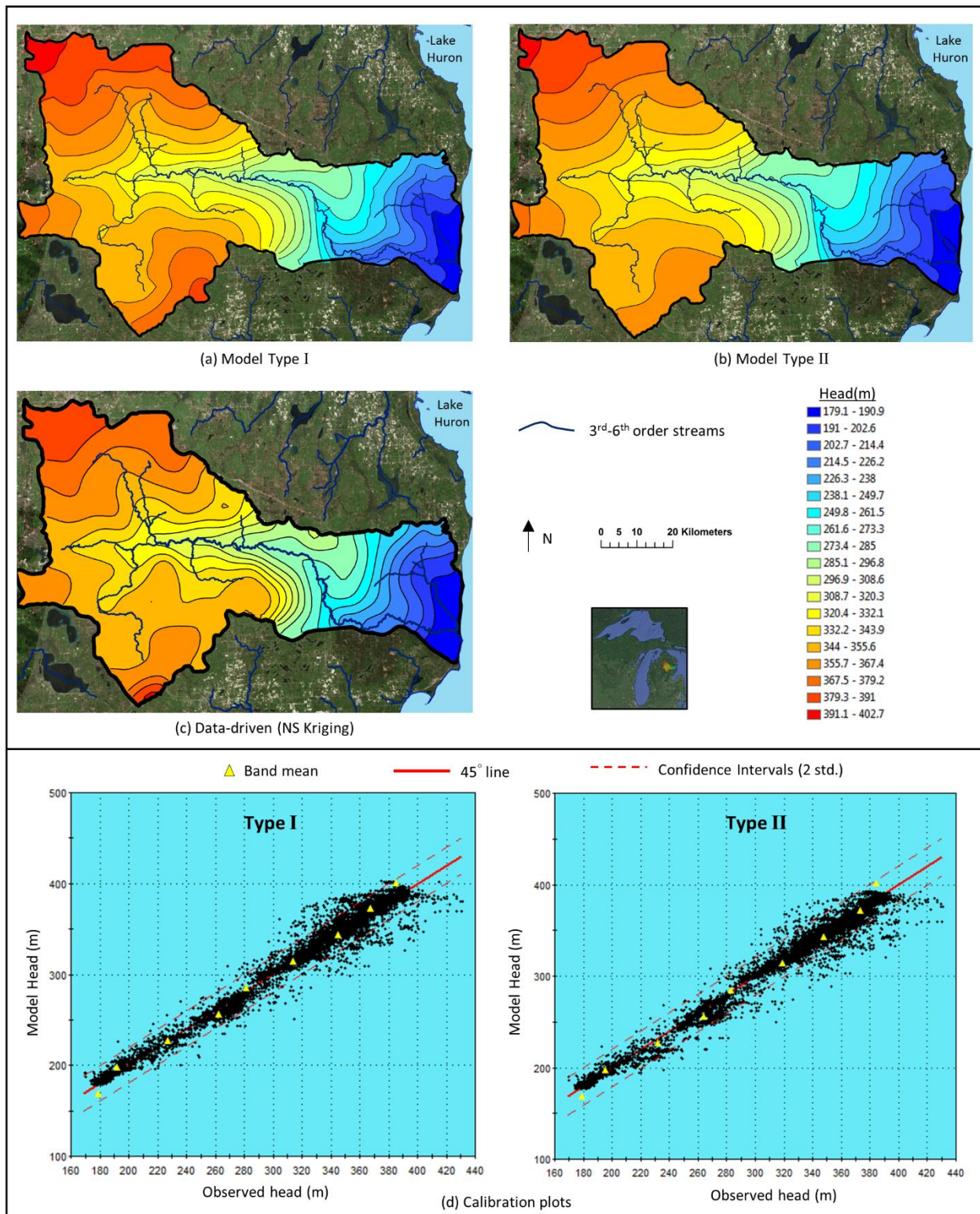


Figure 2.7: Head distributions and calibration charts for the Au Sable watershed (ID=3).

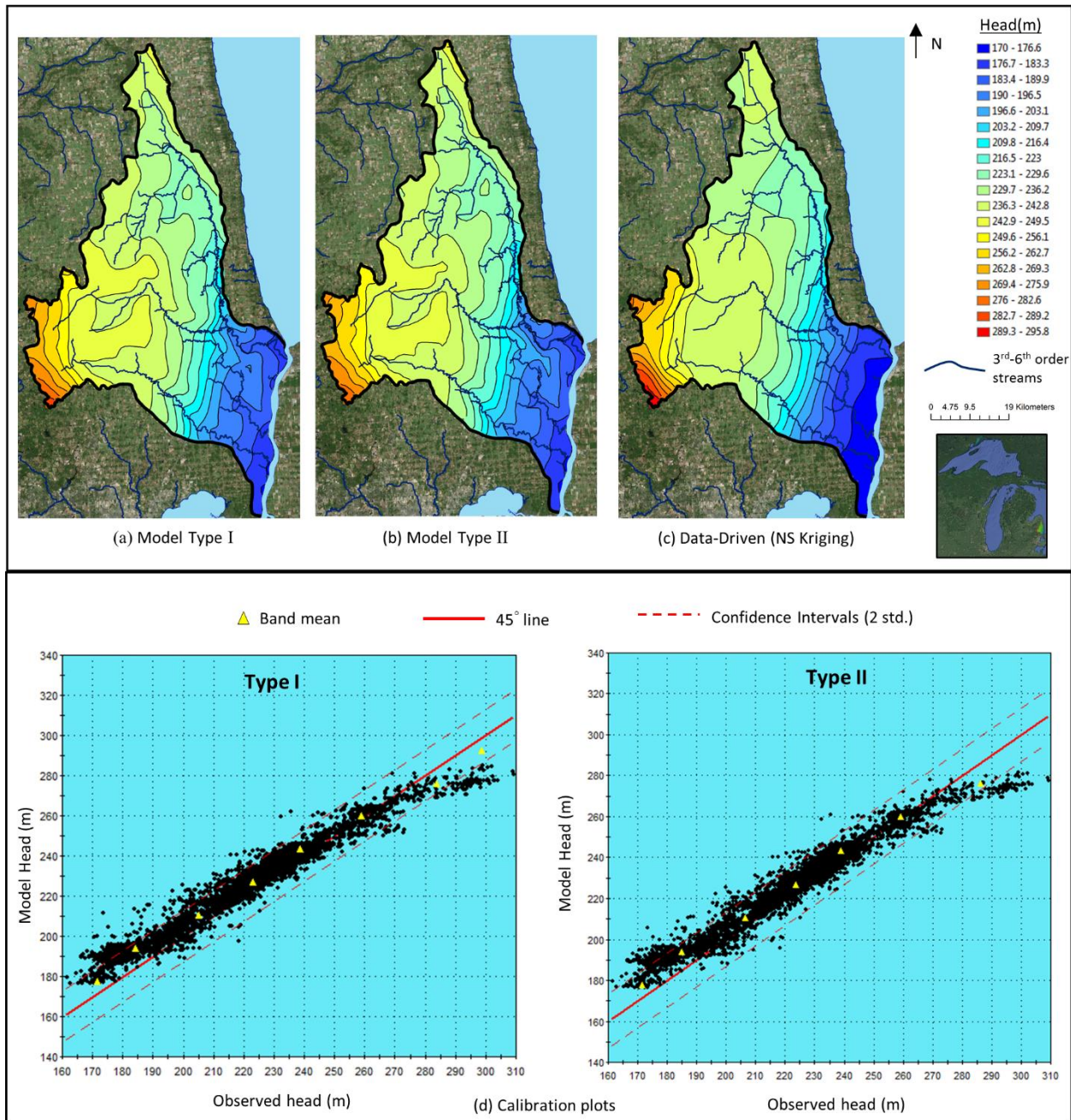


Figure 2.8: Head distributions and calibration charts for the St. Clair watershed (ID=4).

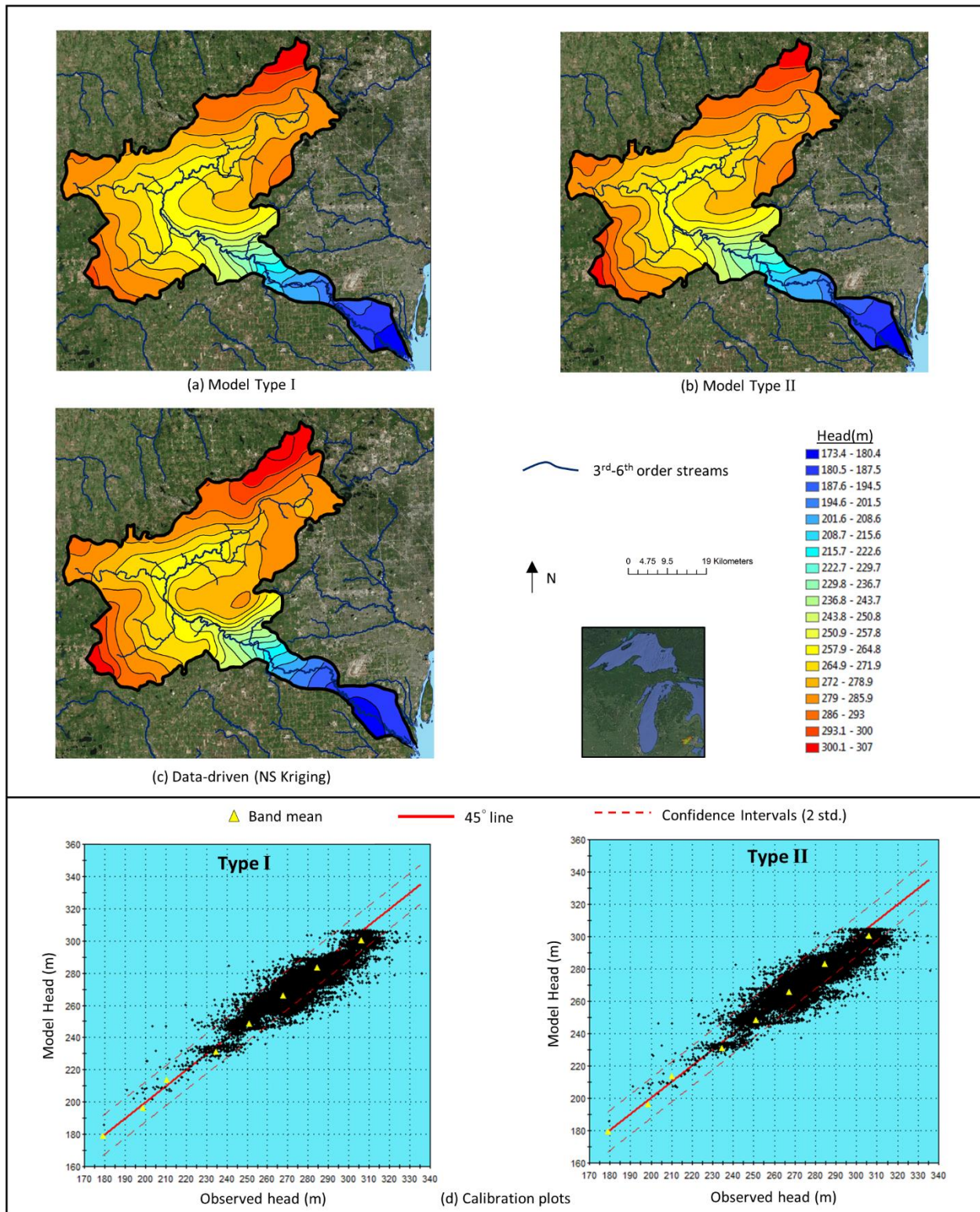


Figure 2.9: Head distributions and calibration charts for the Huron watershed (ID=5).

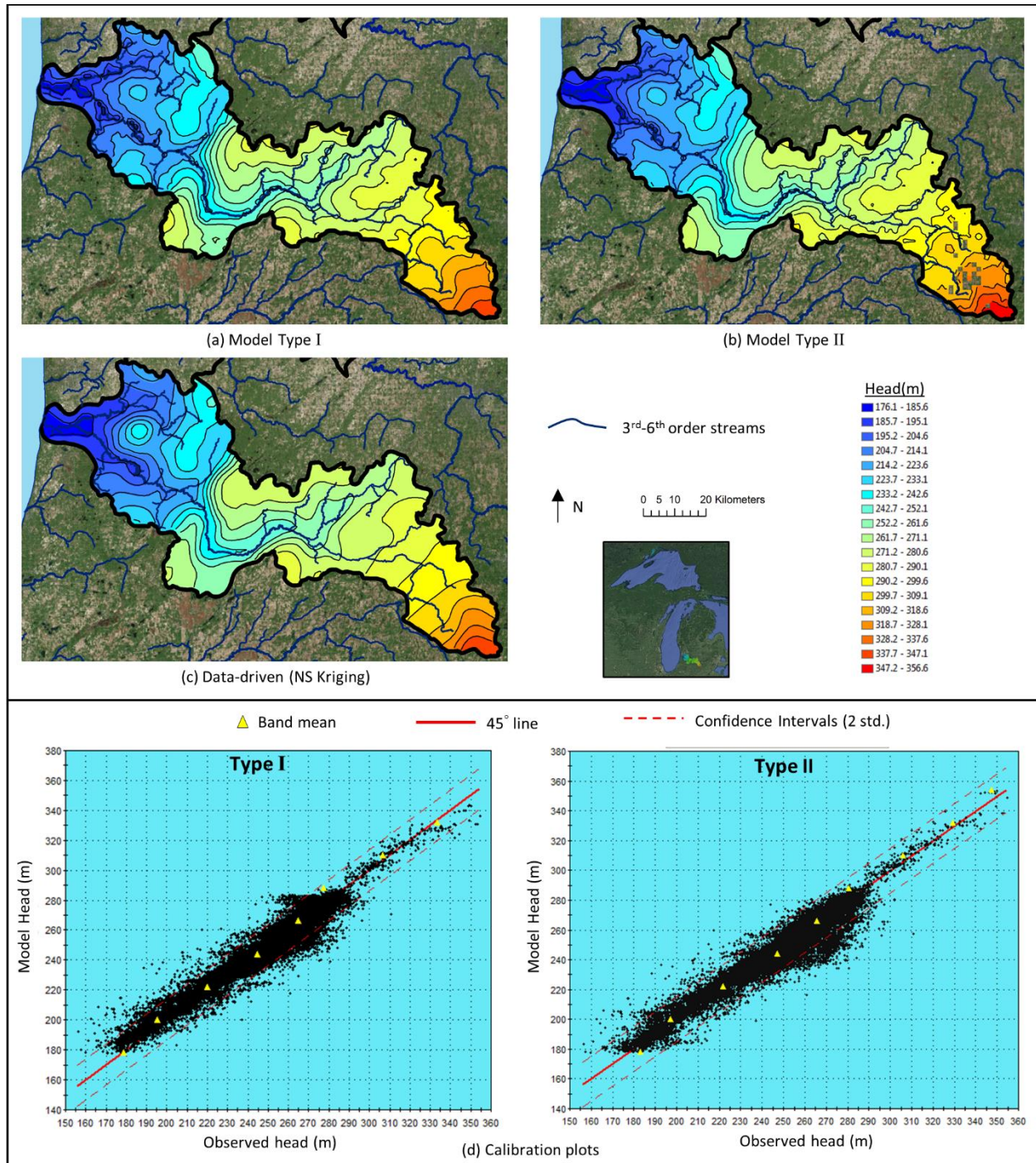


Figure 2.10: Head distributions and calibration charts for the Kalamazoo watershed (ID=6).

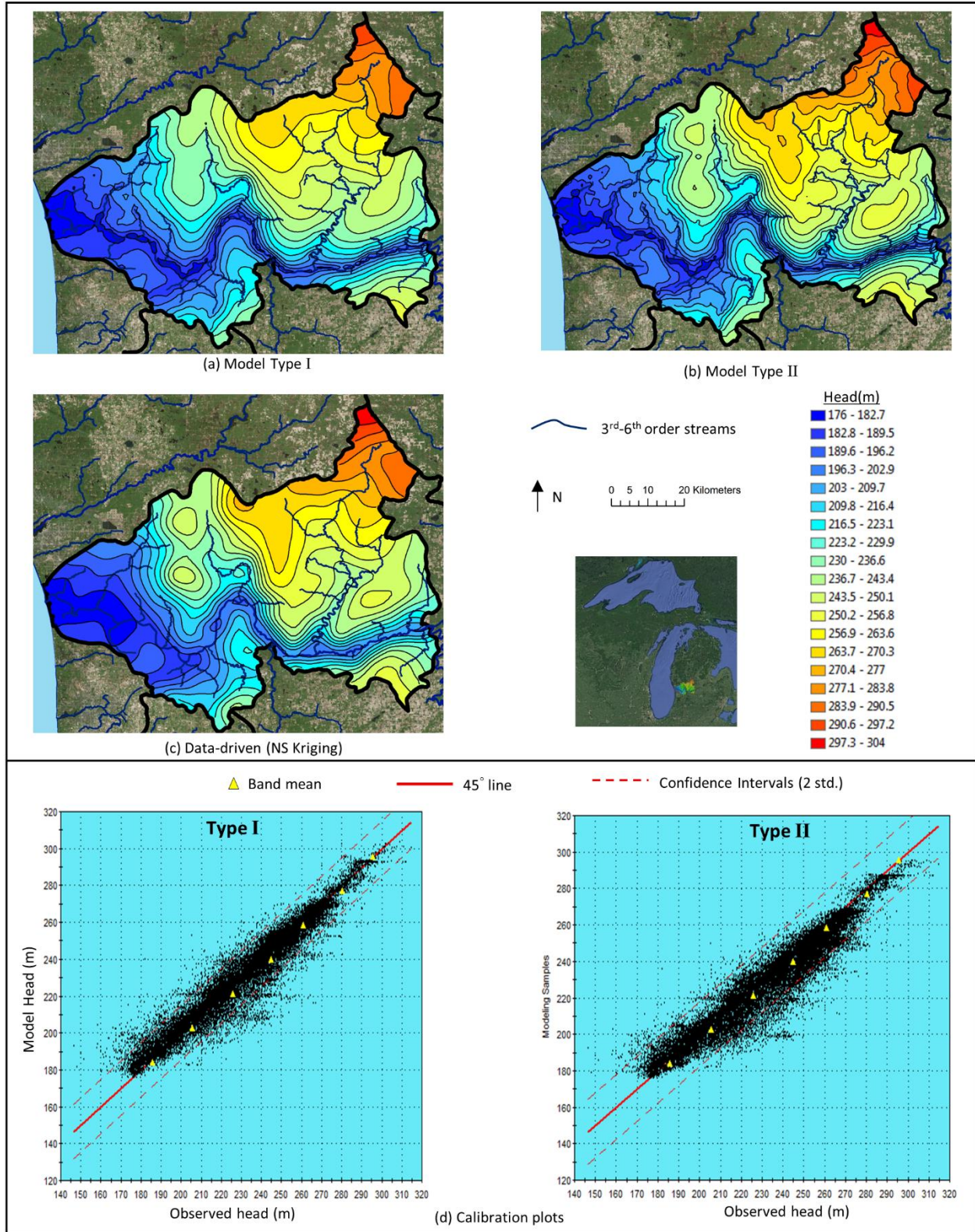


Figure 2.11: Head distributions and calibration charts for the Grand River watershed (ID=7)..

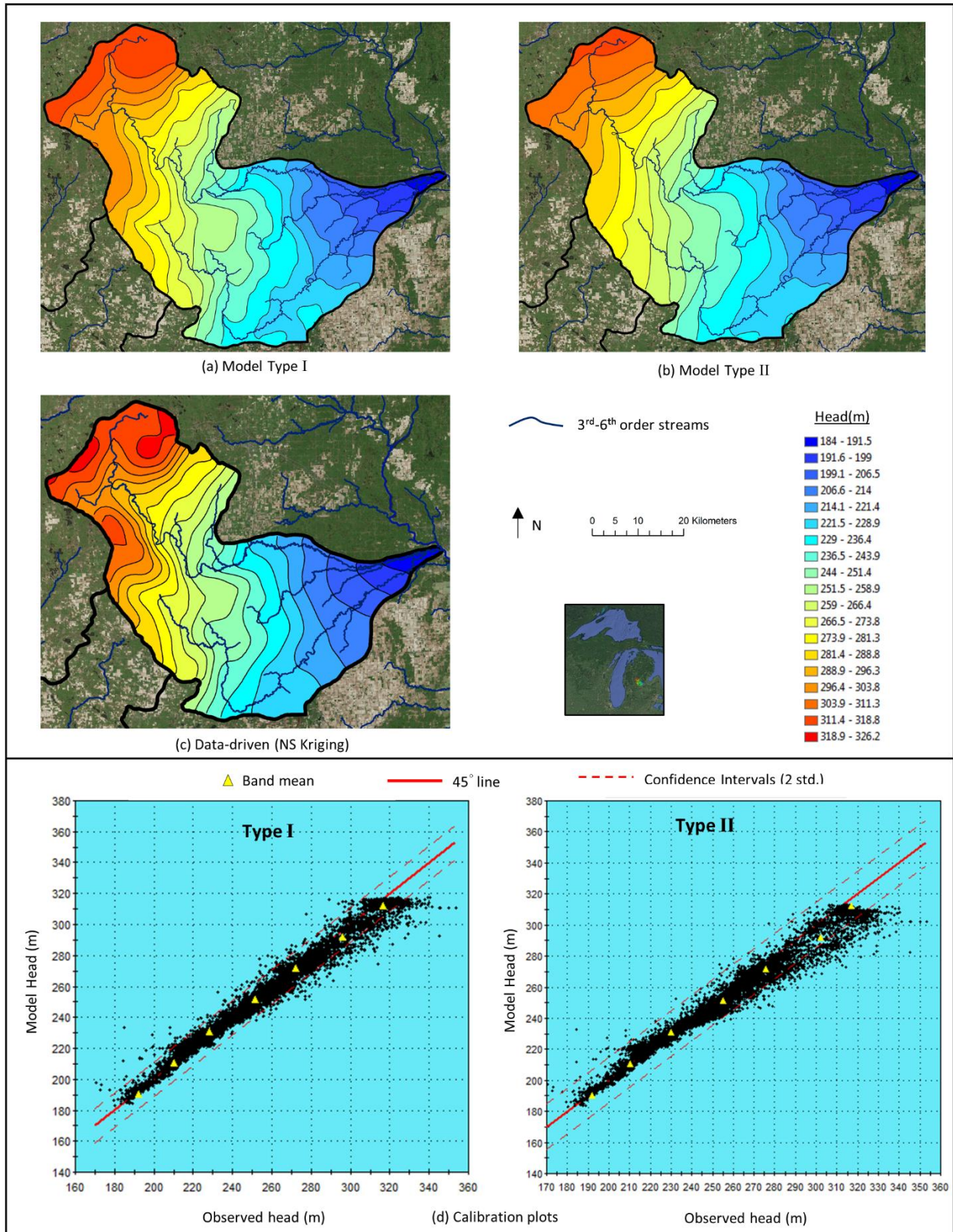


Figure 2.12: Head distributions and calibration charts for the Grand River watershed (ID=8).

Table 2.6: Model performance for Type I and Type II process-based simulations. Model ID indicates the watershed (by the beginning number) and model type (I or II following the dash).

| Model ID | Calib. Pts. | RMSE (m) | Mean Error (m) | Nash-Sutcliffe |
|----------|-------------|----------|----------------|----------------|
| 1-I | 1042 | 8.54 | -1.37 | 0.99 |
| 1-II | | 8.17 | -0.80 | 0.99 |
| 2-I | 1286 | 7.48 | -2.07 | 0.72 |
| 2-II | | 8.41 | 3.35 | 0.62 |
| 3-I | 9435 | 9.86 | -1.97 | 0.97 |
| 3-II | | 10.14 | 2.20 | 0.97 |
| 4-I | 4982 | 6.35 | -4.76 | 0.91 |
| 4-II | | 6.58 | -4.10 | 0.92 |
| 5-I | 33049 | 6.09 | 2.44 | 0.82 |
| 5-II | | 6.19 | 2.36 | 0.82 |
| 6-I | 24831 | 6.83 | -1.51 | 0.94 |
| 6-II | | 7.50 | 0.17 | 0.92 |
| 7-I | 27262 | 7.46 | -0.60 | 0.93 |
| 7-II | | 8.85 | 3.64 | 0.88 |
| 8-I | 9392 | 5.71 | 0.26 | 0.98 |
| 8-II | | 7.34 | 2.99 | 0.95 |

Flow Patterns. In general, flow patterns are consistent between both the Type I and Type II models as well as the process-based models and the results from non-stationary kriging, e.g., the highest heads and lowest heads are found in similar areas of the different flow representations, and head contours converge to major streams and rivers or coastlines. The most noticeable differences between flow representations are concerned with local areas of a given watershed, see, e.g., the northwest portion of the Escanaba watershed (Figure 2.5), the south-central portion of the Tahquamenon watershed (Figure 2.6), and the eastern portion of the Kalamazoo watershed (Figure 2.10).

Some watersheds have remarkably similar patterns between the Type I and Type II process-based models, namely, Tahquamenon (Figure 2.6), Au Sable (Figure 2.7), St. Claire (Figure 2.8), Huron (Figure 2.9), and Pine (Figure 2.12). In some cases, the Type I model yielded flow patterns more similar to those from non-stationary kriging than compared to the Type II process-based model: Escanaba watershed (ID=1),

Kalamazoo watershed (ID=6), and the Lower Grand watershed (ID=7). In these cases, the Type II process-based model yielded small-scale variability not seen in the data-driven modeling. This is likely related to the more spatially-detailed inputs of aquifer thickness, conductivity, and/or recharge in the Type II models, which may cause more abrupt changes in head. The Type II process-based model even yielded some dry cells (whereas the Type I models did not, e.g., see Tahquamenon watershed (ID=2), Kalamazoo (ID=6)). This may be related to modeling issues created by unreasonable or inconsistent values of aquifer thickness, recharge, and/or conductivity assigned to a cell (or set of cells) from big data input.

To further test the accuracy of the spatial flow patterns from the Type I models, Wellhead Protection Areas (WHPAs) delineated by the MDEQ (State of Michigan, 2006) were compared to results from reverse particle tracking applications in the watersheds. Examples from the Lower Grand watershed (ID=7) are shown in Figure 2.13. The Traditional WHPAs were delineated using a network of monitoring wells installed by MDEQ. Particles were placed at the location of wellhead locations, and allowed to advect backwards along the flow field using the velocity vectors output from the Type I simulation. The collections of particle pathlines, shown as purple zones in Figure 2.13, match well with the traditional WHPAs, which was found elsewhere in the State (not shown here). This demonstrates that a simple surface framework model provides a robust initial characterization of flow patterns for a large groundwater system, even when considering relatively local (or subregional) application.

Importantly, the Type I models – despite the lack of detailed spatial inputs (K , ϵ , and aquifer bottom elevation) – were able to reproduce the overall flow patterns exhibited by the observation data and from the more detailed Type II models. This important conclusion is consistent with theoretical and empirical studies indicating that water tables generally mimic variations in the of land surface (Toth 1963, Witherspoon 1967, Winter 1988, Haitjema and Mitchell-Bruker 2005).

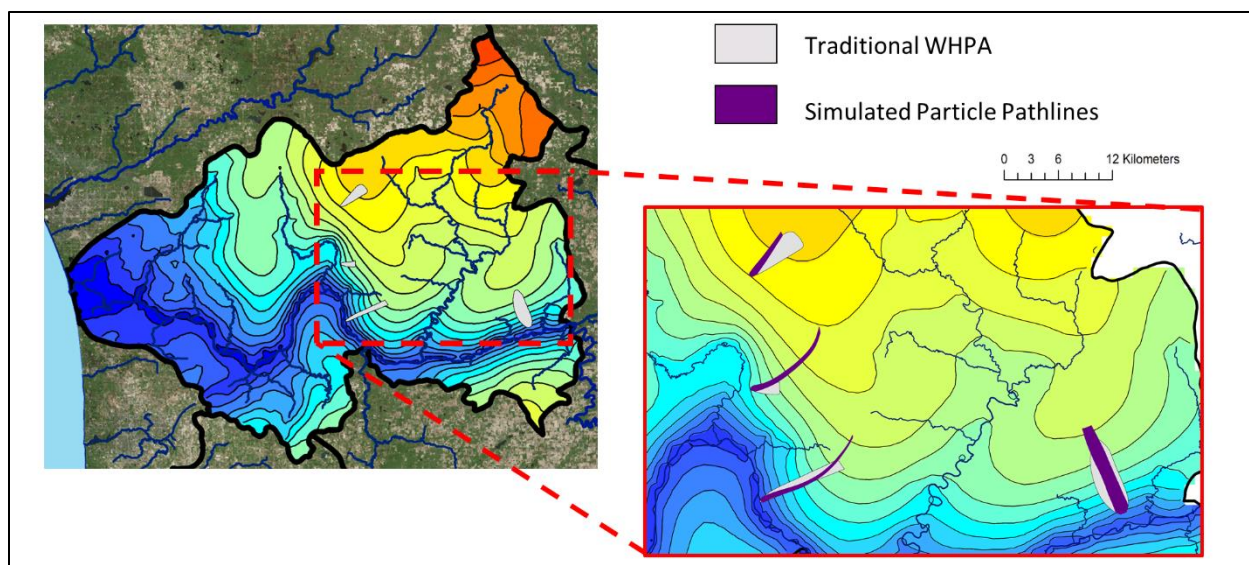


Figure 2.13: Comparison of reverse particle tracking results and traditional Wellhead Protection Area (WHPA) delineations completed by the Michigan Department of Environmental Quality (MDEQ).

Statistical Indicators & Calibration Plots. In almost all of the watersheds, both the Type I and Type II process-based models performed reasonably well, as indicated by the strong Nash-Sutcliffe coefficients (E) of >0.90 for 11 of the 16 flow representations (see Table 2.6) and $E > 0.8$ for all flow representations of all watershed except for the Tahquamenon watershed (Model IDs 2-I and 2-II in Table 2.6). The Tahquamenon watershed has relatively flat terrain, and thus, the driving potential for unsaturated flow is low. The result is that the range of head variability relative to SWL noise is small for this watershed as compared to the others.

The general agreement between both the Type I and Type II models and data can also be seen visually, as a majority of the many thousands of data points used for evaluation fall within 2 standard deviation, and the band mean (moving average) data markers generally fall on or close to the 45° lines of ‘perfect agreement’ (all points on this line have the same simulated and observed heads). In a few watersheds – such as the Au Sable, (Figure 2.7), St Clair (Figure 2.8), and Pine (Figure 2.12), calibration plots both the Type I and Type II have at least one band mean data marker that suggests over- or underestimation of head by the model for a localized region of the watershed. This suggests a key system feature (structural component or flow process) that is not represented by the model is needed to reproduce real-world

conditions (see more details in next subsection). Similarly, although there is a large spread in the “data clouds”, the spread is generally centered about the line of perfect agreement. This is supported by the absolute mean error of < 2.5 m for 11 of the 16 process-based flow representations. Models 4-I and 4-II (St. Clair watershed) yielded the only absolute mean errors of 4-5 m. For 5 of the 8 watersheds, the Type II model yielded a smaller absolute mean error, although the values are largely similar for each watershed.

The large spread in the data clouds is reflected both visually and in the RSME values ranging from 5.71 to 10.14 m (see Table 2.6). These large RSME values partially reflect the significant noise embedded in the SWL dataset described in the previous section (see Curtis et al. 2018 for more details). The large spread in plots and large RSME values are also related to the inability of the model to resolve sub-grid variabilities or system structures that are reflected in the observational data. For example, the watersheds with the largest RSME values – the Escanaba (1-I and 1-II), Au Sable (3-I and 3-II), and Lower Grand (7-I and 7-II) – overlie productive sub-cropping bedrock units that may lead to vertical head gradients not captured by the models. Also, as stated earlier, many of the glacial deposits in Michigan exhibit strong heterogeneity and three-dimensional (3D) structure (Westjohn et al. 1994), which would also contribute to significant variability not captured by the models used here. Similarly, neglecting transient processes (e.g., pumping, dynamic recharge, etc.) may lead to considerable spread in the data cloud seen in the calibration plots of Figures 2.5 – 2.12. Nonetheless, although the RSME values are relatively large when compared to precise measurements collected for scientific purposes (e.g., from a monitoring well), they generally represent less than 10% of the head variability across an entire model. The graphical comparison of the many head measurements across space and time is therefore a useful reasonable approach for understanding the overall system dynamics (long-term mean head for different places across a large area). Moreover, it is an effective way to analyze the level of model complexity needed to capture real-world variabilities, e.g., more spread in the calibration chart usually indicates more significant spatial and/or temporal variabilities exist than what is currently being modeled. This is discussed in more detail next.

2.4.3 Examples of Further Model Utilization

The following examples help to illustrate how the models and SWL datasets can be used to improve system understanding and guide subscale data collection and model development.

Issues with Systematic Bias. Recall that, for each watershed, mean K and mean ϵ values were computed from the spatially-explicit rasters, and then used as the effective K and ϵ values for the all cells in the Type I models. This pragmatic approach may not be available in all cases (e.g., for watersheds with little subsurface data available for estimating mean K), forcing modelers to use educated guesses for the effective K and ϵ values. In addition, after some trial and error, the Z parameter for computing the aquifer bottom elevation, was chosen as 60 ft., but again, this may be difficult or time-consuming to estimate. As an example, an arbitrary set of parameters was chosen for a Type I simulation of the Au Sable watershed (ID=3): $K=100$ ft/day; $\epsilon=10$ in./yr., and $Z=200$ ft. The calibration results are presented in Figure 2.14. Clearly, the model is biased towards underpredicting head, as evidenced by the majority of band mean data markers falling below the 45° line and the large mean error value of 8.70 m. Additionally, the RMSE error has increased to 12.88 m (compare to 9.86 m of model DEM-3). As before, the measurements of head distributed across space and time can be used to guide model refinement to reduce the RMSE and remove systematic model bias. In this case, the process of ‘system-wide’ calibration (adjusting K , ϵ , and Z to the values used in model DEM-3) improves the model’s ability to capture overall system dynamics.

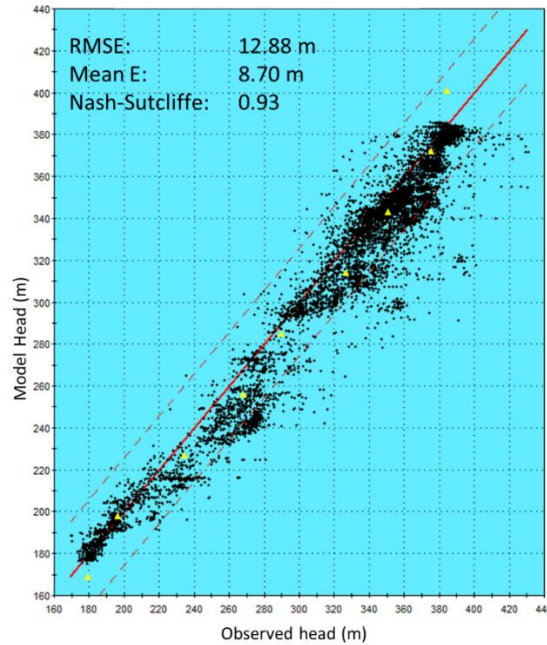


Figure 2.14: Calibration plot for the Au Sable watershed (ID: 3) utilizing arbitrary parameters: $K=100$ ft/day; $\epsilon=10$ in./yr.; Bottom elevation=Min. DEM – 200 ft.

Issues Near Model Boundaries. In the calibration plots for the St. Clair watershed (Figure 2.8), there were many data points at high heads for which the simulated head was significantly less than the observed head. There were also many data points at low heads for which the simulated head was significantly more than the observed head. Figure 2.15 provides the spatial locations of the underestimated points (simulated head less than observed) and overestimated points within the St. Clair watershed. All of the underestimated points occur near the southwest model boundary, which was consistently predicted as the ‘recharge area’, i.e., the area of highest head within the watershed (see Figure 2.8). This suggests that the choice of no-flow boundaries along this portion of the model domain is artificially blocking groundwater flux that would otherwise raise heads to the values reflected in the observation data. This problem can be alleviated by 1) expanding boundaries to ensure the actual groundwater divide is captured; or 2) assign new boundary conditions (e.g., prescribed head or prescribed flux), although, as mentioned earlier, the latter should be done with caution to prevent unreasonable sources of water along this boundary.

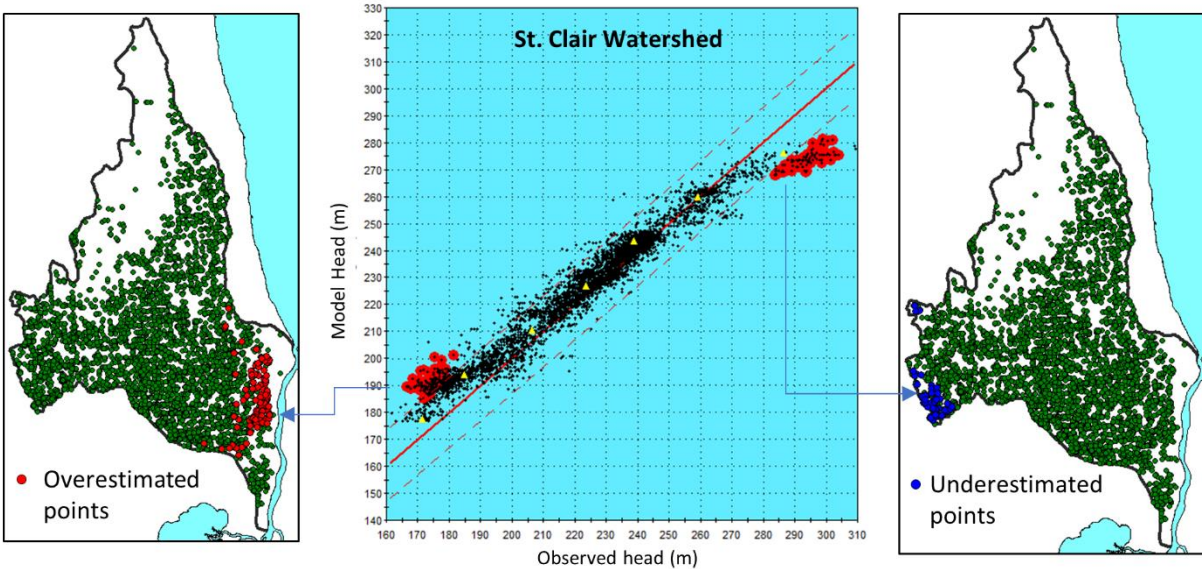


Figure 2.15: Location of significantly overestimated and underestimated simulated SWLs, St. Clair watershed (ID=). Red dots (left) are locations of overestimated points; blue dots (right) are locations of underestimated points; green dots are locations of all other points in the calibration plot (center).

Within the St. Clair watershed the cloud of overestimated points occurs near the southeast model boundary along the St. Clair River (Figure 2.15). This suggests that the model is missing important system variabilities/processes that act to lower actual heads in the aquifer, which could include: groundwater pumping; lower stages of the St. Clair River, which sets the baseline groundwater levels within the watershed, or lateral outflows through the eastern boundary of the model (which are assumed to be zero by the simulation). Further data collection or review of available information on historical river stages, groundwater withdrawals, or groundwater heads east of the east-northeast watershed boundary could then guide the model refinement process.

Issues with Local Structure. Another example of probing and improving a model with big data is illustrated by considering the calibration plot (Type II model) for the Kalamazoo watershed (Figure 2.10, ID=6). For heads between ≈ 240 and ≈ 290 m, simulated head was significantly less than the observed head. Figure 2.16 shows that watershed the cloud of underestimated points occurs within the central region of the model domain. It may be that the values in the K and ϵ rasters used in the Type II model have unreasonable values for this part of the model, namely, K is too high and/or ϵ is too low. Or, it may be related to the treatment of the underlying bedrock. In this area, the glacial deposits are thin overlies two bedrock units – the

Coldwater Shale (confining unit) and Marshall Formation (very transmissive aquifer unit) – occur along a NW-SE striking direction. It is possible that significant amounts of groundwater moves through the bedrock into the glacial layer along margins of the interface between bedrock units, thereby raising actual heads reflected in the observation data. This suggests that modeling the transmissive Marshall formation is an important part of reproducing real-world groundwater conditions in the Kalamazoo watershed. Note that the Type I model performs better than the Full model for this part of the watershed, probably because of the larger thickness being applied that more effectively captured the actual transmissivity of the aquifer system. In any case, the ability to locate the systematically underestimated simulated heads provides a means for prioritizing further investigation and research.

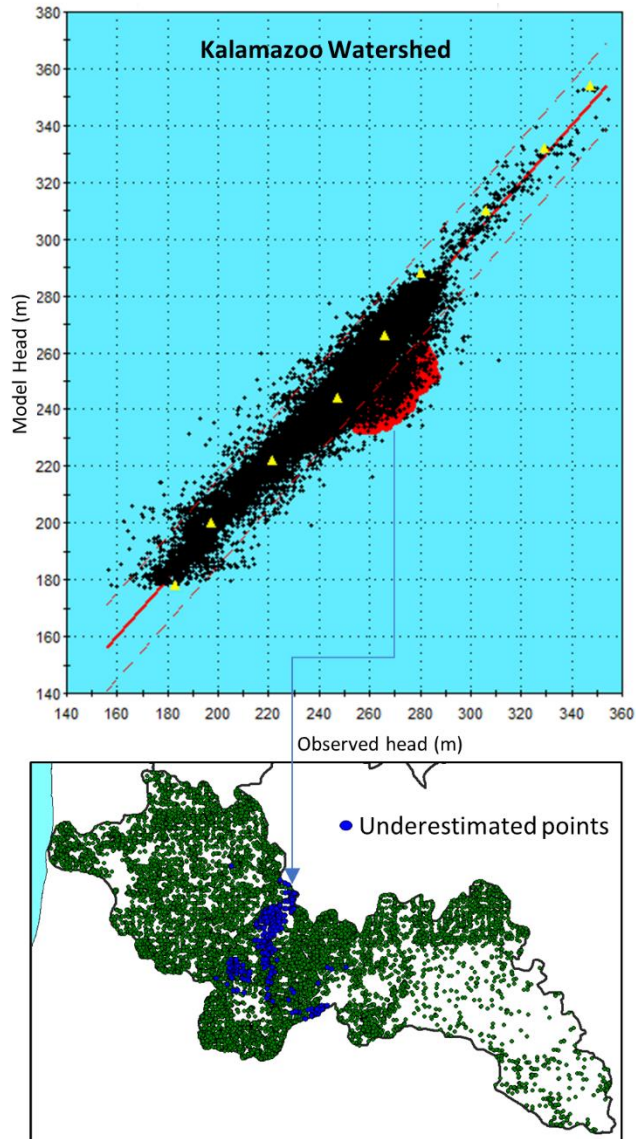


Figure 2.16: Location of significantly underestimated simulated SWLs, Kalamazoo watershed (ID: 6); blue dots (bottom) are locations of underestimated points; green dots are locations of all other points in the calibration plot (top).

Importantly, for these examples and others, once the overall system dynamics are consistent with observations (e.g., the clouds of data fall along the 45° line and within 2 standard deviations), more detailed analyses such as nested, local-scale modeling can be made based on the system-wide flow patterns as appropriate boundary conditions.

2.5 Ch. 2 Conclusions

In this study, we defined what big data are in the context of groundwater modeling, and discussed how these data can be used to model groundwater systems. We capitalized on a statewide, comprehensive groundwater database – created through years of effort and collaboration – to generate a diverse set of groundwater models for 8 large watersheds (‘test beds’) in different parts of Michigan for the purposes of exploring different ways of using big groundwater data for systems modeling. Through spatial and statistical comparisons of model outputs (head) and data (observed water levels), the relative importance of the different inputs were assessed.

The analyses provided here demonstrate that existing data alone enables modeling of overall system dynamics, i.e., the prevailing spatial distribution of regional or subregional groundwater flow patterns, upon which local (short-term) and cumulative long-term changes occur. And while groundwater modeling requires a significant amount of data, those representing topography, lakes, streams and other surface seeps are the most important. In other words, at regional scales, detailed system framework inputs, namely spatially-explicit recharge, conductivity, and bottom aquifer thickness are less important, although in localized subregions representing these variabilities (or other structures/processes not captured by the simulation) is necessary for accurate reproduction of observations. This study also demonstrates the usefulness of Digital Elevation Models (DEMs) for representing critical surface drainage effects. In fact, DEM-based treatment of groundwater seepage may be the most robust approach for modeling large groundwater systems, although this was not rigorously tested here but will be investigated in forthcoming work.

The implication of these findings is that a model that can properly represent the surface drainage effects provides an initial solution that can be used as: 1) a starting point for system-based management; 2) a context to study local perturbations (e.g., geological & stress variability); and 3) a guide for local data collection. This approach allows modelers to incrementally add details and perform testing to improve the model and better represent real-world complexities when/where the initial model is inconsistent with other

knowledge (observations, antidotal evidence, perspectives from other disciplines, e.g., ecology, geology, etc.). This affords greater opportunity for model testing and re-conceptualizing – a vital part of model development – than is possible with fully assembling a complicated groundwater model that, in the end, may be narrowly applicable. Importantly, of all the big datasets related to groundwater, those representing the land surface geometry (DEMs and hydrography) are typically of the highest resolution and accuracy, widely available, and relatively easy to use.

One limitation of this study was the relatively large spread in the observation data used to evaluate model performance, which in turn required larger models to permit meaningful comparisons, i.e., it was not possible to develop local-scale models and evaluate their performance because the observational noise would be of similar (or perhaps larger) magnitude to the range of head variability at that scale. Therefore, it was not necessary to utilize a high-resolution DEM (e.g., 10m or 3m) given the relatively large cell sizes. However, high-resolution (10m or better) DEM products are becoming increasingly available across the globe; even 1m or sub-meter LiDAR- (Light Detection and Ranging) based DEM products are in development or already available across large areas across the globe. These high-resolution DEMs will be powerful tools for efficiently developing system-based models of groundwater systems and guiding data collection across different scales – from regional, to subregional (as was done here), or even at site-scale.

REFERENCES

REFERENCES

- Bhaduri, A., Bogardi, J., Siddiqi, A., Voigt, H., Vörösmarty, C., Pahl-Wostl, C., Bunn, S.E., Shrivastava, P., Lawford, R., Foster, S. and Kremer, H., 2016. Achieving Sustainable Development Goals from a Water Perspective. *Frontiers in Environmental Science*, 4, p.64.
- Curtis, Z.K., Li, S.G., Liao, H.S. and Lusch, D., 2018. Data-Driven Approach for Analyzing Hydrogeology and Groundwater Quality Across Multiple Scales. *Groundwater*, 56(3), pp.377-398.
- EA UK (2018). Environment Agency (EA) United Kingdom (UK). LIDAR Composite Digital Surface Model – 2 m, 1m, 15 cm (updated annually). Available at: <https://data.gov.uk/dataset/80c522cc-e0bf-4466-8409-57a04c456197/lidar-composite-dsm-1m>.
- FOT Switzerland. 2015. Federal Office of Topography (FOT), Switzerland. swissSURFACE3D, classified point cloud of Switzerland (on-going development until 2013). Available at: https://shop.swisstopo.admin.ch/en/products/height_models/surface3d
- Feinstein, D.T., Fienen, M.N., Reeves, H.W. and Langevin, C.D., (2016). A Semi-Structured MODFLOW-USG Model to Evaluate Local Water Sources to Wells for Decision Support. *Groundwater*, 54(4), pp.532-544.
- Fischer, G., F. Nachtergaele, S. Prieler, H.T. van Velthuisen, L. Verelst, D. Wiberg, 2008. Global Agro-ecological Zones Assessment for Agriculture (GAEZ 2008). IIASA, Laxenburg, Austria and FAO, Rome, Italy.
- Fry, J., Xian, G., Jin, S., Dewitz, J., Homer, C., Yang, L., Barnes, C., Herold, N., and Wickham, J. 2011. Completion of the 2006 National Land Cover Database for the Conterminous United States, PE&RS, Vol. 77(9):858-864.
- Gleeson, T., Smith, L., Moosdorf, N., Hartmann, J., Dürr, H., Manning, A. H., van Beek, L.P.H, Jellinek, A. M. 2011. Mapping permeability over the surface of the Earth. *Geophysical Research Letters*, 38 (2) DOI: 10.1029/2010GL045565.
- Haitjema, H.M. and Mitchell-Bruker, S. (2005). Are water tables a subdued replica of the topography?. *Groundwater*, 43(6), pp.781-786.
- Harris, P., M. Charlton, and A.S. Fotheringham. (2010). Moving window kriging with geographically weighted variograms. *Stochastic Environmental Research and Risk Assessment* 24, no. 8: 1193–1209.
- Hartmann, J. and Moosdorf, N. (2012). The new global lithological map database GLiM: A representation of rock properties at the Earth surface. *Geochemistry, Geophysics, Geosystems*, 13(12).
- Heinz, J., Kleineidam, S., Teutsch, G., & Aigner, T. (2003). Heterogeneity patterns of Quaternary glaciofluvial gravel bodies (SW-Germany): application to hydrogeology. *Sedimentary geology*, 158(1), 1-23.
- Holtschlag, D.J. (1997). A generalized estimate of ground-water-recharge rates in the Lower Peninsula of Michigan (No. 2437). US Geological Survey; Information Services [distributor],.

- Huscroft, J., Gleeson, T., Hartmann, J. and Börker, J. (2018). Compiling and Mapping Global Permeability of the Unconsolidated and Consolidated Earth: GLobal HYdrogeology MaPS 2.0 (GLHYMPS 2.0), *Geophysical Research Letters*, 45, 4, (1897-1904).
- IDNR (2017). Iowa Department of Natural Resources (IDNR), State of Iowa. Elevation data from Iowa LiDAR Project 2007-2010 (last updated Aug. 2017). Available at Iowa GEODATA: <https://geodata.iowa.gov/dataset/iowa-lidar-project-2007-2010>
- IGS (2016). Iowa Geological Survey, based at IIHR – Hydrosceience & Engineering, University of Iowa. Available at: <https://www.iihr.uiowa.edu/igs/geosam/home>
- ISGS (2015). Illinois State Geological Survey. ILWATER, Repository for records of wells drilled in the State of Illinois (periodically updated). Available at: <http://www.isgs.illinois.edu/ilwater>
- IOLEP (2011). Indiana Orthophotography, LiDAR, & Elevation Program (IOLEP), Indiana University (updated annually). Available at the Indiana Spatial Data Portal: http://gis.iu.edu/datasetInfo/statewide/in_2011.php
- KGS (2002). Kansas Geological Survey. WIZARD, water well levels database (periodically updated). Available at: <http://www.kgs.ku.edu/Magellan/WaterLevels/index.html>
- Lehner, B., Grill G. (2013): Global river hydrography and network routing: baseline data and new approaches to study the world’s large river systems. *Hydrological Processes*, 27(15): 2171–2186. Data is available at www.hydrosheds.org.
- Li, S.G., and Q. Liu. (2006). A Real-Time, Interactive Steering Environment for Integrated Ground Water Modeling.” *Ground Water* 44(5), pg. 758-763.
- Li, S. G., Liao, H., Afshari, S., Oztan, M., Abbas, H., and Mandle, R.(2009). “A GIS-enabled hierarchical patch dynamics paradigm for modelling complex groundwater systems across multiple spatial scales.” *Modelling of pollutants in complex environmental systems*, Vol. 1, ILM, Hertfordshire, U.K., 177.
- Liao, H.S. Sampath, P.V., Curtis, Z.K., Li, S.G. (2015a). Hierarchical modeling and parameter estimation for a coupled groundwater lake system. *Journal of Hydrologic Engineering*, 20(11), pg. 04015027. DOI: 10.1061/(ASCE)HE.1943-5584.0001219.
- Liao, H.S., Sampath, P.V., Curtis, Z.K. and Li, S.G. (2015b). Hierarchical modeling of a groundwater remediation capture system. *Journal of Hydrology*, 527, pp.196-211.
- Liu J, Dietz T, Carpenter SR, Alberti M, Folke C, Moran E, Pell AN, Deadman P, Kratz T, Lubchenco J, Ostrom E. 2007a. Complexity of coupled human and natural systems. *Science*, 317(5844), 1513-1516.
- Liu, J., Dietz, T., Carpenter, S.R., Folke, C., Alberti, M., Redman, C.L., Schneider, S.H., Ostrom, E., Pell, A.N., Lubchenco, J. and Taylor, W.W. 2007b. Coupled human and natural systems. *AMBIO: a journal of the human environment*, 36(8), 639-649.
- Lloyd, C.D. 2010. Nonstationary models for exploring and mapping monthly precipitation in the United Kingdom. *International Journal of Climatology* 30, no. 3:390–405.
- MDEQ (2010) Michigan Department of Environmental Quality. WaterChem, Statewide Water Quality Database (periodically updated).

- MDEQ (2014). Michigan Department of Environmental Quality. Wellogic System (periodically updated). Available at <https://secure1.state.mi.us/wellogic/>
- Messenger, M.L., Lehner, B., Grill, G., Nedeva, I., Schmitt, O. (2016): Estimating the volume and age of water stored in global lakes using a geo-statistical approach. *Nature Communications*: 13603. doi: 10.1038/ncomms13603. Data is available at www.hydrosheds.org.
- Miller, C., D. Sarewitz, A. Light. 2008. *Science, Technology, and Sustainability: Building a Research Agenda*, National Science Foundation Workshop, Sept. 8-9
- MNFI. (2010). GIS Data for Michigan's Prairie Fens and 2010 Survey of Mitchell's satyr Butterfly sites. Michigan Natural Features Inventory.
- National Research Council (NRC). 2002. *Our Common Journey: A Transition Toward Sustainability*. Washington, DC: National Academy Press.
- NASA LP DAAC (2015), ASTER Level 1 Precision Terrain Corrected Registered At-Sensor Radiance. Version 3. NASA EOSDIS Land Processes DAAC, USGS Earth Resources Observation and Science (EROS) Center, Sioux Falls, South Dakota (<https://lpdaac.usgs.gov>), accessed January 1, 2016, at http://dx.doi.org/10.5067/ASTER/AST_L1T.003.
- NED USGS. (2006). National Elevation Dataset. US Department of Interior: United States Geological Survey, <http://ned.usgs.gov/Ned/about.asp>.
- NHD USGS. (2010). USGS: National Hydrography Dataset. US Department of Interior: United States Geological Survey, <http://nhd.usgs.gov/index.html>.
- NLS Finland (2015). National Land Survey of Finland. Elevation model 10 m and Elevation model 2 m (periodically updated). Accessible at: <https://www.maanmittauslaitos.fi/en/e-services/open-data-file-download-service>
- OSPC (2007). Delaware Office of State Planning Coordination, Delaware Elevation Contours, produced from 2007 LiDAR data. Available at: http://opendata.firstmap.delaware.gov/datasets?group_ids=a71a054cfcb949dab46c719e0a99e3bb
- ORNL DAAC. (2018). MODIS and VIIRS Land Products Global Subsetting and Visualization Tool. ORNL DAAC, Oak Ridge, Tennessee, USA. <https://doi.org/10.3334/ORNLDAAC/1379>
- Pahl-Wostl, C. (2007). The implications of complexity for integrated resources management. *Environmental Modelling & Software*, 22(5), 561-569.
- Pelletier, J.D., P.D. Broxton, P. Hazenberg, X. Zeng, P.A. Troch, G. Niu, Z.C. Williams, M.A. Brunke, and D. Gochis. (2016). Global 1-km Gridded Thickness of Soil, Regolith, and Sedimentary Deposit Layers. ORNL DAAC, Oak Ridge, Tennessee, USA. <http://dx.doi.org/10.3334/ORNLDAAC/1304>
- PRISM Climate Group, Oregon State University, <http://prism.oregonstate.edu>, created 4 Feb 2004.
- Reitz, M., Sanford, W.E., Senay, G.B. and Cazenias, J., 2017. Annual Estimates of Recharge, Quick-Flow Runoff, and Evapotranspiration for the Contiguous US Using Empirical Regression Equations. *JAWRA Journal of the American Water Resources Association*, 53(4), pp.961-983.

- Risser, D.W., Thompson, R.E. and Stuckey, M.H., 2008. Regression method for estimating long-term mean annual ground-water recharge rates from base flow in Pennsylvania (No. 2008-5185). US Geological Survey.
- Ronayne, M. J., Gorelick, S. M., & Zheng, C. (2010). Geological modeling of submeter scale heterogeneity and its influence on tracer transport in a fluvial aquifer. *Water Resources Research*, 46(10).
- Sampath, P.V., Liao, H.S., Curtis, Z.K., Doran, P.J., Herbert, M.E., May, C.A. and Li, S.G. (2015). Understanding the groundwater hydrology of a geographically-isolated prairie fen: implications for conservation. *PloS one*, 10(10), p.e0140430.
- Sampath, P.V., H.S. Liao, Z.K. Curtis, M.E. Herbert, P.J. Doran, C.A. May, D.A. Landis, and S.G. Li. (2016). Understanding fen hydrology across multiple scales. *Hydrological Processes* 30, no. 19: 3390–2407.
- Scheibe, T., & Yabusaki, S. (1998). Scaling of flow and transport behavior in heterogeneous groundwater systems. *Advances in Water Resources*, 22(3), 223-238.
- Shangguan, W., Hengl, T., de Jesus, J.M., Yuan, H. and Dai, Y., 2017. Mapping the global depth to bedrock for land surface modeling. *Journal of Advances in Modeling Earth Systems*, 9(1), pp.65-88.
- Soil Survey Staff (SSS), Natural Resources Conservation Service (NRCS), United States Department of Agriculture. Soil Survey Geographic (SSURGO) Database for west-central southern Michigan. Available online at <https://gdg.sc.egov.usda.gov/>. Accessed October 10, 2016.
- State of Michigan. (2006). Public Act 148—Groundwater inventory and map project (GWIM), executive summary, Michigan State Univ., East Lansing, MI.
- S.C. Swenson. (2012). GRACE monthly land water mass grids NETCDF RELEASE 5.0. Ver. 5.0. PO.DAAC, CA, USA. Dataset accessed [YYYY-MM-DD] at <http://dx.doi.org/10.5067/TELND-NC005>.
- Taylor, C.J. and Alley, W.M. (2001). Ground-water-level monitoring and the importance of long-term water-level data (Vol. 1217). Geological Survey (USGS).
- Toth, J. 1963. A theoretical analysis of groundwater flow in small drainage basins. *Journal of Geophysical Research* 68, no. 16: 4795–4812.
- Tuppad, P., Douglas-Mankin, K.R., Lee, T., Srinivasan, R. and Arnold, J.G., 2011. Soil and Water Assessment Tool (SWAT) hydrologic/water quality model: Extended capability and wider adoption. *Transactions of the ASABE*, 54(5), pp.1677-1684.
- US Geological Survey, 2003. Principal aquifers of the 48 conterminous United States, Hawaii, Puerto Rico, and the US Virgin islands.
- USGS (2011). U.S. Geological Survey Gap Analysis Program, 20160513, GAP/LANDFIRE National Terrestrial Ecosystems 2011: U.S. Geological Survey, <https://doi.org/10.5066/F7ZS2TM0>.
- USGS (2016). U.S. Geological Survey National Water Information System data available on the World Wide Web (USGS Water Data for the Nation), accessed [September 11, 2018], at https://nwis.waterdata.usgs.gov/nwis/inventory/?site_no=04137500&agency_cd=USGS.

- Walter, C., A.B. McBratney, A. Douaoui, and B. Minasny. 2001. Spatial prediction of topsoil salinity in the Chelif Valley, Algeria, using local ordinary kriging with local variograms versus whole-area variogram. *Soil Research* 39, no. 2: 259–272.
- Winter, T.C. 1988. A conceptual framework for assessing cumulative impacts on the hydrology of nontidal wetlands. *Environmental Management* 12, no. 5: 605–620.
- Westjohn, D. B., Weaver, T. L., & Zacharias, K. F. (1994). Hydrogeology of Pleistocene glacial deposits and Jurassic red beds in the central lower peninsula of Michigan. Water-resources investigations report (USA).
- Yu, B., 1999. A comparison of the Green-Ampt and a spatially variable infiltration model for natural storm events. *Transactions of the ASAE*, 42(1), p.89.
- Zhou, H., Gómez-Hernández, J. J., & Li, L. (2014). Inverse methods in hydrogeology: Evolution and recent trends. *Advances in Water Resources*, 63, 22-37.

CHAPTER 3

Simulation of Flow in a Complex Aquifer System Subjected to Long-term Well Network Growth

Contributing Authors: Zachary Curtis, Hua-sheng Liao, Prasanna Sampath, Shu-Guang Li

3.1 Executive Summary of Ch. 3

In west-central Lower Peninsula of Michigan, population growth and expanded agricultural activities have resulted in significant increases in distributed groundwater withdrawals. The well network growth and anecdotes of water shortages (dry wells) have raised concerns over the groundwater sustainability of the region. We developed an unsteady, three-dimensional (3D) groundwater flow model to describe system dynamics over the last 50 years and evaluate long-term impacts of groundwater use. Simulating this large aquifer system was challenging; the geologic framework is strongly heterogeneous and 3D, making it difficult to avoid over-parameterization using traditional approaches for conceptualizing and calibrating a flow model. Moreover, pumping and water level data were lacking and prohibitively expensive (or impossible) to collect given the large-scale and long-term nature of this study. An approach was developed to develop and calibrate the flow model through innovative use of high-density (yet severely underutilized) water well datasets, which allowed 1) implementation of a ‘zone-based’, non-stationary stochastic approach to conceptualize complex 3D spatial variability using a small set of geologic material types; and 2) modeling the spatiotemporal evolution of many water well withdrawals across several decades using sector-based parameterization. The model’s ability to reproduce long-term trends of groundwater decline suggests that these new approaches offer a significant improvement for capturing complex spatial structure of subsurface geology and well network growth that controls overall aquifer system response to distributed pumping. High-density water well datasets are becoming increasingly available in different U.S. States and elsewhere, and thus, methods presented here have general applicability elsewhere.

3.2 Ch. 3 Introduction

The State of Michigan, USA – although surrounded by four North American Great Lakes – relies heavily on groundwater. Over 700 million gallons are withdrawn each day (NGWA, 2016) to support agricultural

and industrial activities and provide drinking water supplies to roughly half of all Michigan citizens (MDEQ, 2018). In the Michigan Lowlands of west-central Lower Peninsula (LP) of Michigan, the fastest growing area in the State, increases in groundwater withdrawals have helped meet mounting water supply demands. Ottawa County, which sits squarely within the Michigan Lowlands, has experienced a 7.0 % population increase from 2010 to 2016 and recent expansion of agricultural activities (US Census Bureau 2017; IWR 2013). To support increases in water supply demands, it is estimated that aggregated groundwater use in Ottawa County nearly doubled in recent decades - from 8 million gallons per day (MGD) in 1985 to about 15 MGD in 2010 (USGS 2012).

Historically, this region is not perceived as water stressed because of an abundance of surface water and regional discharge of groundwater in the surficial aquifers and the deeper bedrock formations of Michigan's Lower Peninsula (e.g., Westjohn et al. 1994; Curtis et al. 2017). The area is bordered to the west by Lake Michigan, and the land surface contains a number of streams (including Grand River, a large 6th-order stream) and several inland lakes ranging from 7.2 km² to less than 0.02 km² (see Figure 3.1). However, a screening-level analysis of Static Water Levels (SWLs) obtained from the water wells showed modest to significant decline in parts of the aquifer system in recent years (IWR 2013), raising serious concerns over the long-term sustainability of the groundwater resources of the region. In particular, local and state officials want to know: what is the timescale of the aquifer system sustainability (i.e., how quickly is the aquifer being depleted due to systematic increases in groundwater withdrawals across space and time)? and how can we proactively manage to promote long-term sustainability of groundwater in the region?

This study addresses a crucial first step in the problem-solving process of managing long-term sustainability of groundwater resources in this region: characterizing overall groundwater system dynamics – or how groundwater flow patterns emerge over space and time in response to the geologic setting and system stresses (e.g., groundwater pumping network growth). Specifically, we seek to identify and reproduce, via process-based numerical simulation, multi-decadal temporal trends of groundwater level for all subregions of the study area shown in Figure 3.1. This system-based characterization will serve as the basis for more detailed analysis of sustainability, including: subscale data collection, modeling and analysis in key areas

of concern (i.e., where groundwater levels have declined significantly); scenario testing to evaluate impacts of potential perturbations or different management scenarios; and probing relationships between flow and groundwater quality dynamics. Other published and forthcoming work (Curtis et al., 2018 and Curtis et al. in review) addresses these additional aspects of sustainability analysis in west-central Michigan, and more broadly, the Lower Peninsula of Michigan so that present focus may remain on technical challenges of investigating this natural groundwater system over the past 50 years of groundwater development (1966-2015).

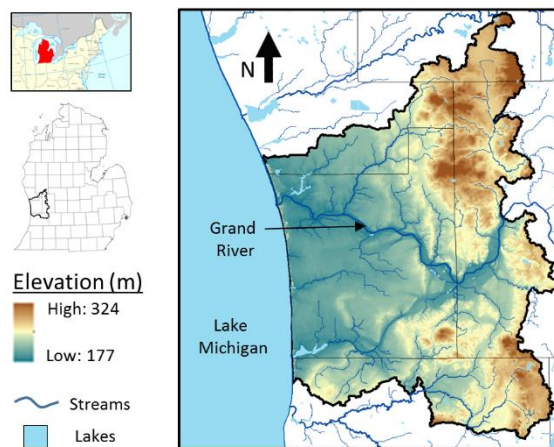


Figure 3.1: Study area in west-central Lower Peninsula of Michigan (nearly 3400 km²). The 10m digital elevation model (DEM) was obtained from USGS NED (2006), and the surface water network is from USGS NHD (2010).

The technical challenges of simulating the long-term aquifer system dynamics arise from the fact that: (1) the geologic framework exhibits strong three-dimensional (3D) variability and comprises both stochastic and deterministic geologic structures that impact groundwater flow; (2) data related to pumping are limited to recent times or are available at insufficient spatial scales needed for understanding spatial dynamics; and (3) there is no established monitoring well network for calibration of model parameters through comparison of simulated outputs with real-world observations, nor was it practical (or even possible) to establish a monitoring network for the purposes of this study. These data-limited conditions made it difficult to use traditional modeling approaches – such as deterministic, layer-based zonation of aquifer variability or assigning well-specific pumping rates as model inputs – without requiring fine-tuning of many model

parameters with inverse approaches. As such, over-parameterization and its related issues (numerical instability, impractical computational costs, ill-posed groundwater problems, and non-unique calibration – see Carrera et al. 2005; Zhou et al. 2014 for detailed reviews of this topic) plagued model development despite significant effort to test and apply different conceptual models.

This struggle to apply traditional approaches with limited data prompted a deeper look at existing data and creative ways to use them for model development. We explored approaches for utilizing information embedded in thousands of water well records, such as lithologic descriptions, well auxiliary data (times of construction, water use sectors, etc.) and physical groundwater level measurements (Static Water Levels, or SWLs), to capture critical aspects of aquifer system structure and responses to disturbed stress. Transient model calibration was performed using noisy but plentiful SWL datasets to determine the potential usefulness of proposed approaches for modeling long-term groundwater system dynamics.

The rest of this chapter is organized as follows: details of technical challenges and proposed approaches associated with the aquifer system conceptualization and parametrization are provided next; a discussion of flow model development follows; and results of model calibration flow simulations and next steps for using the model as a tool for reaching long-term sustainability are discussed.

3.3 Modeling Challenges and Overview of Approach

In the following subsections, further details are provided for above-mentioned aspects that makes modeling this system difficult using traditional approaches, followed by an overview of the proposed methods for addressing these challenges. Details of implementing approaches for model development are discussed in the next section.

3.3.1 Conceptualization of a Complex Geologic Framework

The study area is underlain by a shallow aquifer of unconsolidated glacial deposits and a deeper aquifer consisting of fractured bedrock. Along the coast, many wells are screened in thick, sandy eolian and lacustrine sediments (Figure 3.2a and Figure 3.2c). Throughout central and east-central portions of the study area – where thin, coarse-grained lacustrine deposits occur above the thick, relatively continuous

layer of fine-grained sediments (e.g., clay, silt, etc.) – most wells are completed in the fractured bedrock aquifer. The unconsolidated deposits in the eastern portion exhibit strong lateral and vertical heterogeneity that resulted from a complex depositional history, a phenomena seen throughout many parts of Michigan (Westjohn et al. 1994). The bedrock formations strike NW – SE (see Figure 3.2b and Figure 3.2c) and generally pinch out along their western subcrop extents, increasing in thickness in the WNW direction. Most of the wells that terminate in the bedrock do so in the Marshall Formation, as the other units of relevant thickness within the study area (Coldwater Shale and Michigan Formation) are composed primarily of shales and siltstones and are therefore unproductive.

The brief review of the study area geology highlights some two important aspects to consider during model conceptualization: 1) bedrock geology is more or less deterministic; 2) glacial geology is more chaotic, non-stationary, and strongly heterogeneous, especially in eastern portion of the study domain. However, there is important large-scale structure controlling groundwater flow in the glacial aquifer as well (e.g., the thick sand deposits along the shoreline and the relatively continuous clay and silt deposits in the central part of Ottawa County). Simulating flow in the bedrock aquifer therefore requires a proper delineation of the large-scale geometry of the bedrock units, whereas simulation of flow in the glacial aquifer requires understanding both small- and large-scale details, as well as complex transition between the regions dominated by different scales of heterogeneity.

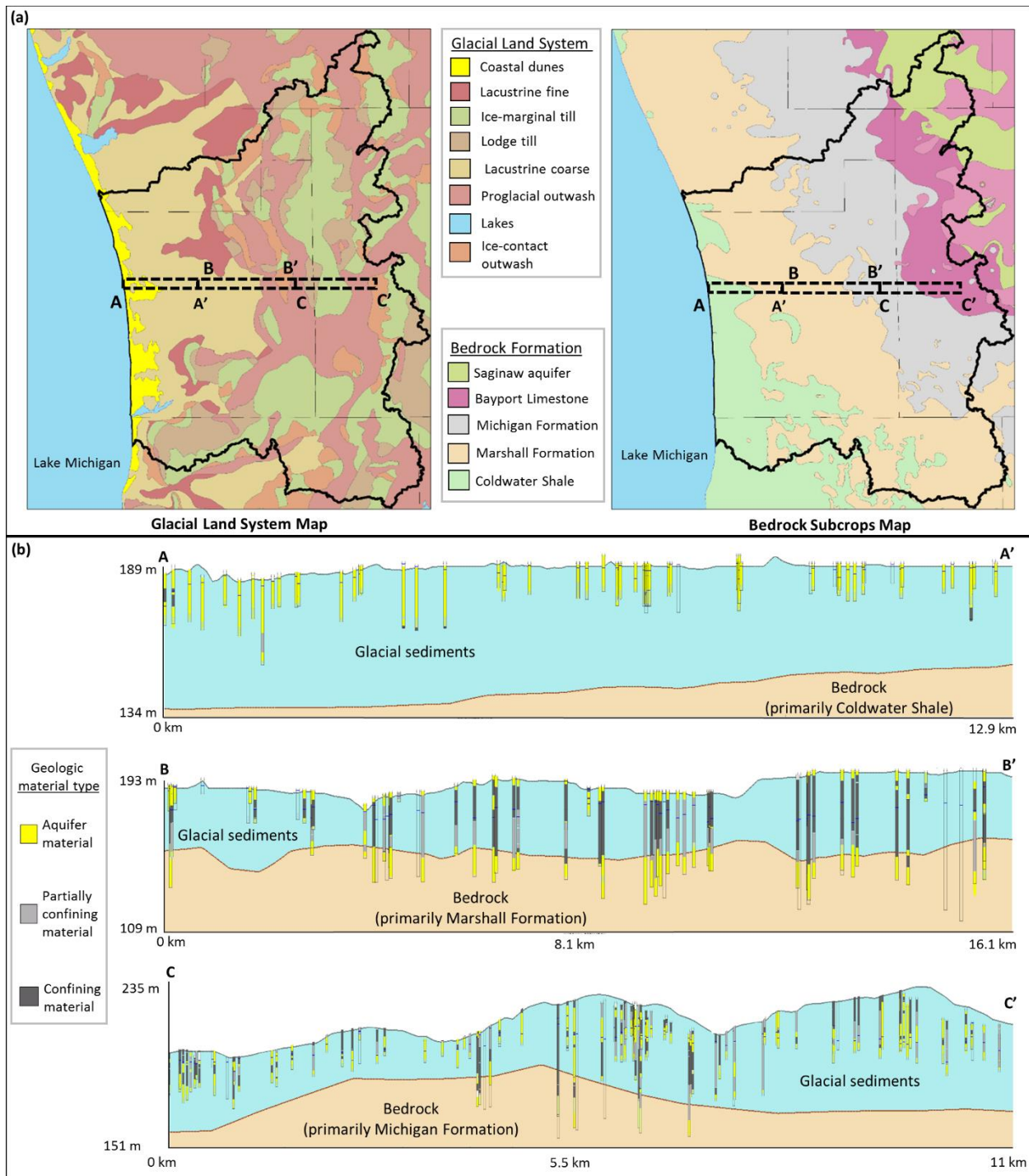


Figure 3.2: Large-scale geology underlying the study area: (a) glacial land systems (GWIM 2006) and (b) bedrock subcrop map (GWIM, 2006); and (c) representative cross-sections A-A', B-B', and C-C', with aquifer material types shown in the vertical borehole profiles. Wells and associated lithologic descriptions were extracted from Wellogig (MDEQ 2014) using the Michigan Groundwater Management Tool (MGMT) developed by Michigan State University (MSU, 2014).

Previous Deterministic Approaches. Historically, the most common approach to representing geologic variability is deterministic zonation, which consists of explicitly subdividing the model into several areas (zones) based on available geological and geophysical information. Typically, a single, homogenous effective parameter value is assigned each zone, such that all model nodes within the same zone share the same parameter value and changes in parameter values occur between zones (Anderson et al. 2015). In this approach, smaller-scale heterogeneities and variabilities are implicitly ignored, which may have important impacts on flow and, especially, solute transport (Zheng and Gorelick 2003;). If the modeler attempts to capture more variabilities, e.g., by adding more layers and/or zones, more parameters must be estimated, and above-mentioned issues related to over-parameterization may arise. Although advanced inverse modeling techniques or multistage and multiscale calibration approaches have been put forth to handle large number of parameters used to describe complex aquifer structure (see, e.g., Zhu and Yeh 2006; Liu and Kitanidis 2011), ultimately the delineation of zones is subjective and data rarely (or perhaps never) suffice for unequivocal definition of the ‘correct’ zonation. Moreover, it has been shown that incongruous delineation of zones can lead to misleading results in model applications (Sun et al 1998). Nonetheless, zonation remains the preferred approach amongst practitioners and for large (regional or basin-scale) groundwater studies (e.g., Best and Lowry 2014).

Previous Stochastic Approaches. Others have explored stochastic approaches that utilize randomly varying fields described by probabilistic distributions to incorporate the effects of small-scale heterogeneity during inverse modeling. The properties of the hydraulic conductivity (K) values are estimated from prior estimates of K using geostatistics and/or available head or concentration measurements. Stochastic approaches recognize the impossibility of fully and precisely describing the spatial characterization of hydraulic parameters and enables the quantification of uncertainty that is not available in a deterministic approach. However, contrary to deterministic methods, the stochastic approach has had relatively limited application in large scale problems dealing with site-specific geologic frameworks, sources and sinks, and poorly understood boundary conditions (Neuman 2004; Renard 2007). Instead, most studies focus on general

insights and small-scale problems and applications (see, e.g., Li and McLaughlin 1991; Li et al. 2004; Alcolea et al. 2007).

Integrated Stochastic-Deterministic Approach. The initial approach was to utilize a deterministic framework for both the bedrock and glacial aquifers, given the relatively limited application of stochastic approaches for real-world, large scale sites. Because geophysical data and direct field measurements of K (e.g., from aquifer pump tests or slug tests) were lacking and collecting new data was not possible given the resources available for this study, significant time was spent studying water well boreholes and maps of large-scale glacial land systems (see Figure 3.2a) in an attempt to delineate zones consistent with geological understanding and raw borehole data. Yet, during model testing it became clear that this was a futile effort: the addition of a new zone or layer might improve the model locally, but other regions would then perform worse than before the zone/layer was added (often in ways not clear). For these reasons, the deterministic, layer-based approach was reserved for the bedrock aquifer, while the glacial aquifer geologic conceptualization utilized a conditional stochastic approach, transition probability (TP) geostatistics, for mapping heterogeneity and calibrating the flow model. After generating a continuous, stochastic ensemble representation of small-scale heterogeneity across the entire glacial aquifer, we delineated separate ‘TP zones’ for a few different areas defined by distinct geomorphologies. Each zone has its own set of hydraulic properties for different aquifer materials types (which are later calibrated), but retains the spatial structure determined from the aquifer-wide geostatistical analysis. In this way, a relatively few number of parameters describing the complex, non-stationary geologic structure needed to be estimated during model calibration. More details of geologic conceptualization are provided in the Stochastic-Deterministic Representation of Subsurface Geology subsection below.

3.3.2 Conceptualization of Long-term, Distributed Stress Dynamics

A Growing, Extensive Well Network. Figure 3.3 presents the spatiotemporal evolution of water wells within the study domain extracted from Wellogig, a statewide database with information from over 500,000 water wells, including private domestic wells, public supply wells, and wells used for agriculture and industry

(MDEQ 2014). The raw well dataset was filtered and geo-coded, and latitude and longitude and construction date information were extracted for wells within the study domain to generate Figure 3.3. Roughly 5% of the wells installed over the past 50 years are high-capacity wells, while the remaining are small-capacity, private-use wells. Note the significant increase in the number of wells from 2000 to 2015, which coincides with the significant population increase during the same time (US Census Bureau 2017). The absence of wells in the east-central portion of the study domain is where Grand Rapids is located, which uses water from Lake Michigan to meet its water demand.

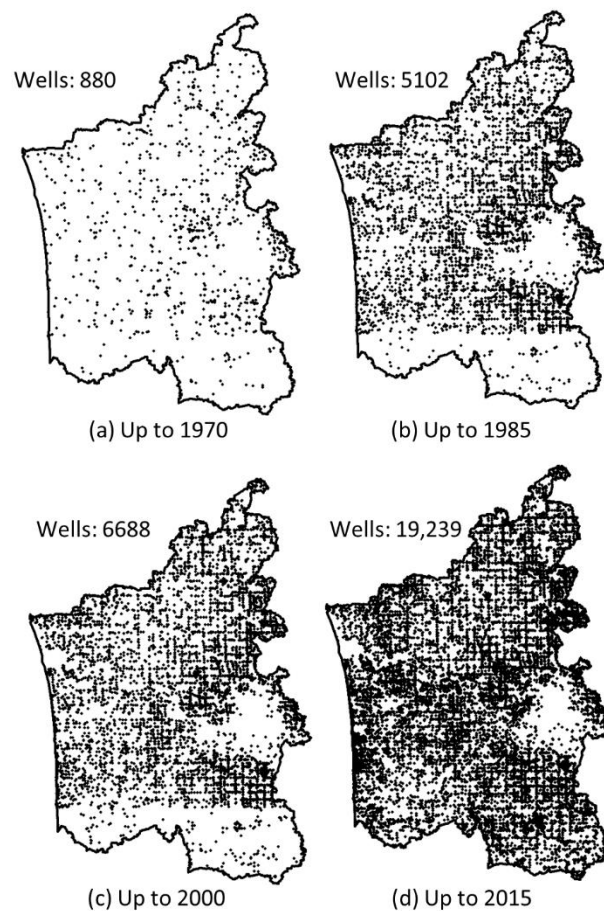


Figure 3.3: Evolution of water wells within the study domain. Data were extracted from Wellogic (MDEQ 2014).

Limitations of Space-Time Aquifer Stress Data. Groundwater pumping is a spatially-distributed process (Ruud et al. 2004), but may also have significant temporal variations (e.g., seasonal irrigation in northern latitude U.S. states or the growth of well networks across decades) that need to be quantified during model

development. In some of the most intensely used aquifer systems (e.g. the Ogallala Aquifer of the central United States), long-term pumping meter data from large-capacity wells are available, largely from the USGS water use website (USGS 2016), but also from long-standing state or provincial public databases developed for the purposes of permitting and water use regulation (see, e.g. Ontario' Permit to Take Water program [Kreutzwiser et al. 2004]) . However, the State of Michigan has historically lacked regulation requiring reporting of large-capacity commercial/industrial/agricultural wells; as a result, little historical data exists. During the time of model development, the only years of data made available from state agencies (Michigan Department of Environmental Quality – MDEQ and Department of Rural and Agricultural Development – MDARD) were 2012 and 2013. Clearly this temporal coverage was insufficient for a study of the past 50 years of groundwater conditions. We considered “extrapolating” the reported pumping rates backward in time, but it was not clear when to ‘turn on’ different wells as the datasets lacked information related to time of operation (e.g., well construction date). These datasets also lack well depth information. Because of the multi-layer, strongly 3D nature aquifer system, it was critical to know the depth of the well screen for accurately simulating groundwater conditions. Additionally, countywide aggregated groundwater use data are available from USGS for earlier years (e.g., 1985, 1990, etc.), but lack the temporal and (especially the) spatial resolution needed to accurately characterize groundwater dynamics relevant to the scale of this study. Thus, traditional pumping data with sufficient coverage and resolution were not available.

Also problematic is the treatment of domestic pumping in the aquifer system. Although this pumping uses relatively small amounts of groundwater and the drawdown cone around each well is commonly buffered by nearby surface water (Feinstein et al. 2016), ignoring domestic pumping in areas around high-density residential communities may lead to simulation errors. This is especially the case when simulating across periods of significant population growth and a corresponding increased dependence on groundwater pumping to meet new water demands – which was needed for this study. However, domestic pumping is often omitted, largely because simulating domestic well withdrawals requires many detailed data that are

typically not available, and even if such data were available, including (the potentially very large number of) domestic wells in models requires time and effort for pre-processing.

Sector-Based Water Use Parametrization. Given the lack of actual pumping data, an alternative water use parameterization scheme was developed – one that capitalized on the wealth of spatiotemporal information embedded in statewide water well datasets. Knowledge of the well type (domestic use, public supply, etc.) location, screen depth interval, and construction data – which are commonly available in such datasets – allows populating the groundwater model with extraction wells at the correct time and 3D location and assigning the pumping rate based on the well type. All wells are classified as part of a distinct water use sector (e.g., domestic, public supply, etc.), and pumping rates of different well types are adjusted during calibration and constrained by sector-specific water use data collected locally, as well as countywide estimates from USGS. Of course, it is possible that water use for a given sector will change across years or decades. Moreover, different wells within a given water use sector operate at their unique pumping rates and thus, the approach presented here is a simplification of the actual water use dynamics. However, we assumed that observed long-term trends (i.e., groundwater level declines) are driven by the extensive growth of wells across the entire system (see Figure 3.3) rather than year-by-year increases in pumping rates of existing/historical wells, and that seasonal or year-to-year variations (or variations within a water sector) are smaller than (and superimposed on) the long-term, overall groundwater level dynamics. As shown later, the calibration results support that this is a valid assumption (see Results and Discussion below). More details on model implementation are provided in the Water Use Model subsection below.

3.3.3 Characterization of System Dynamics

Limitations of Space-Time Aquifer Response Data. Ideally, numerous monitoring wells distributed relatively evenly throughout the aquifer would be used to collect time-series of groundwater levels for flow model calibration. Indeed, in many long-term studies of aquifer systems, e.g., regional investigations by the U.S. Geological Survey (USGS) (see Taylor and Alley 2001), monitoring well networks are established and operated for several/many years so that long-term groundwater level data are available for model

calibration (among other uses). However, for many areas with a growing (or emerging) dependence on groundwater, monitoring wells are not available (or do not span the appropriate times and/or locations). In addition, many groundwater management units face budget constraints and depend on modeling and analysis to be completed relatively quickly (i.e., within a few years), making it infeasible to establish a new monitoring network for the purposes of the groundwater management.

Alternative Source for Long-Term, Spatially-Distributed Head Data. It is for the above-mentioned reasons that thousands of Static Water Level (SWL) measurements – made at single points in time but distributed throughout the aquifer system – were used to identify long-term changes in water levels and calibrate the groundwater model. Static Water Level(s) are water levels measured in wells at the time of installation (prior to pumping) and almost universally available in water well records such as those contained in Wellogic. By aggregating many SWLs taken at different times within a relatively small area (e.g., for an entire township), it was possible to detect systematic changes in groundwater. This is because in many cases decreases in groundwater levels that have occurred over many years are larger than the SWL variability caused by spatial aggregation of observation data and noise in the measurements themselves (more details in the Model Calibration subsection below). Traditionally, detecting such groundwater dynamics would require a few monitoring wells at key locations, which would collect precise data. In the absence of such data, the proposed approach was the best available option.

3.4 Detailed Methodology and Model Development

A 3D unsteady groundwater flow model was developed for the last five decades (1966-2015), which represents the period over which a vast majority of the water wells were installed for groundwater use. The workflow integrating the datasets used for model inputs and calibration and the models needed to develop the numerical flow model is shown in Figure 3.4. Well information from *Wellogic* and local water well records compiled by the Ottawa County (Ottawa County, Michigan 2014) were used to 1) develop a water use model that provided yearly water use configurations, and 2) calibrate the groundwater model using Static Water Levels (SWLs) measured at the time of well installation. Lithologic information from

Wellogig borehole records was used to develop a Transition Probability (TP) geostatistical model to characterize the glacial aquifer heterogeneity. Spatially-explicit annual recharge distributions were simulated using *PRISM Climate Group* precipitation and temperature data and land surface data from USGS and the United State Department of Agriculture (USDA), e.g., soil type, root zone depth, etc. The number of cells and grid size for each model is shown in Table 3.1. *Interactive GroundWater (IGW)*, a modeling software introduced by Li and Liu (2006) but being periodically updated (see, e.g., Li et al 2006; Liao et al. 2015a;b), was used for simulating the saturated groundwater flow. Each of the components shown in Figure 3.4 are discussed in further detail in the following subsections.

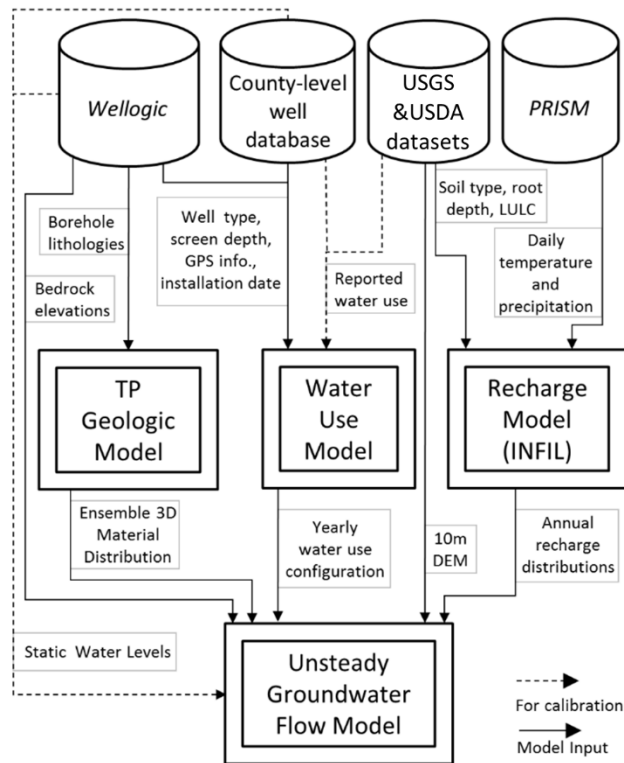


Figure 3.4: Workflow diagram of the models and data used for model input and calibration.

Table 3.1: Number of cells and grid size of the geologic TP model, recharge (ϵ) model, and groundwater flow model.

| Model | NX | NY | NZ | DX (m) |
|------------------|-----|-----|-----|-----------|
| TP model | 136 | 196 | 118 | 500 |
| ϵ model | 210 | 302 | -- | 300 |
| Flow model | 210 | 302 | 7 | 300 |

3.4.1 Stochastic-Deterministic Representation of Subsurface Geology

Zone-based Geostatistical Approach for the Glacial Aquifer. The Transition Probability Geo-statistical Software (T-PROGS) was used to apply the TP approach (Carle, 1999) for modeling the glacial aquifer heterogeneity. Transition Probability methods have been used in several studies attempting to model spatial distributions of aquifer heterogeneity (see, e.g., Weissmann and Fogg 1999; He et al. 2014), and have recently been integrated into flow and transport models of natural aquifer systems (see e.g., Traum et al. 2014; Sampath et al 2015; 2016). However, most previous flow modeling studies focused on providing general insights and understanding of flow systems and were not necessarily concerned with quantifying system dynamics for addressing long-term sustainability.

Roughly 19,000 Wellologic borehole records were available for TP analysis. First, lithologic descriptions for given depth intervals were classified into four different geologic material types following the approach described by Sampath et al (2015; 2016). ‘Sand’, ‘Gravel’, ‘Coarse stones’ or similar descriptions were classified as aquifer material (AQ); ‘Silt’, ‘Clay’, etc. were classified as confining material (CM); and descriptions that were a mix of AQ and CM materials, were classified as marginal aquifer (MAQ) or partially confining material (PCM), respectively. The boreholes with re-classified stratums were mapped (see step (1) of Figure 3.5), and each of the re-classified boreholes were analyzed to create a transition probability matrix of auto- and cross- correlations between the material types as a function of vertical lag spacing. Graphical depictions of the spatial correlations versus vertical lag distance were generated and geostatistical models were fit to the data using Markov chain analysis (see Carle and Fogg 1996; 1997 for more details on Transition Probability geostatistics). The vertical (‘Z-direction’) analysis was used to create

a 3D realization of glacial aquifer material distribution that extends from the 10m DEM top boundary to the top of the bedrock surface (500m resolution) interpolated from lithologic records in Wellogic. This was done by assuming a ratio of horizontal extent of a material to its vertical extent – or an anisotropy ratio – and applying the geostatistical models derived from Z-direction Markov chain analysis. The anisotropy ratios for AQ, MAQ, PCM and CM were chosen as 10, 10, 10, and 8.4, respectively, which are similar to the values chosen by Sampath et al (2016) when implementing the Transition Probability approach for a geologically similar region in south-central Lower Michigan. The geologic model cells had a vertical length of 4m and a horizontal length of 500m (see Table 1), and each cell was assigned as one of the four material types for each model realization. One thousand realizations were executed to produce an ensemble mean model by assigning the most frequently occurring material at each grid cell (see step (2) of Figure 3.5).

Provided in Figure 3.6 are cross-section views of the glacial aquifer material model and borehole lithologies along segments A-A', B-B' and C-C' from Figure 3.2. Note that the results from the TP simulation are generally consistent with the observed lithologies at the borehole locations. Also note that the TP results can capture the large-scale structures discussed above, namely, the thick aquifer material layer in the western portion of the study area, the thick confining layer underling the thin aquifer materials in the central portion; and the chaotic mixture of different aquifer materials in the western portion.

Using the large-scale glacial land system delineations presented in Figure 3.2 as a guide, three distinct zones were created to account for different geomorphologies that may alter the hydraulic properties for similar material types (see step (3) in Figure 3.5). In other words, this zonation allows for AQ to take on three different K values that are all orders of magnitude greater than those used for CM, but different enough to account for differences in large-scale depositional history across different areas of the model domain. The three zones created were: 1) the “River zone” (with materials AQ1, MAQ1, PCM1, CM1) – a narrow region following Grand River and its largest local tributaries with a relatively high hydraulic conductivity and a connection to the bedrock (see Appendix A at the end of this chapter); 2) the “Ice-marginal till zones” (with materials AQ2, MAQ2, PCM2, CM2) – areas of relatively high elevation, strong heterogeneity (especially in the vertical direction) and composed primarily of ice-marginal till zones; and 3) the “base

zone” (with materials AQ3, MAQ3, PCM3, CM3) – all remaining areas of the model domain with a relatively more ‘restrained’ depositional history and more continuity of geologic materials (e.g., a continuous clay layer across the west-central portion of the study domain).

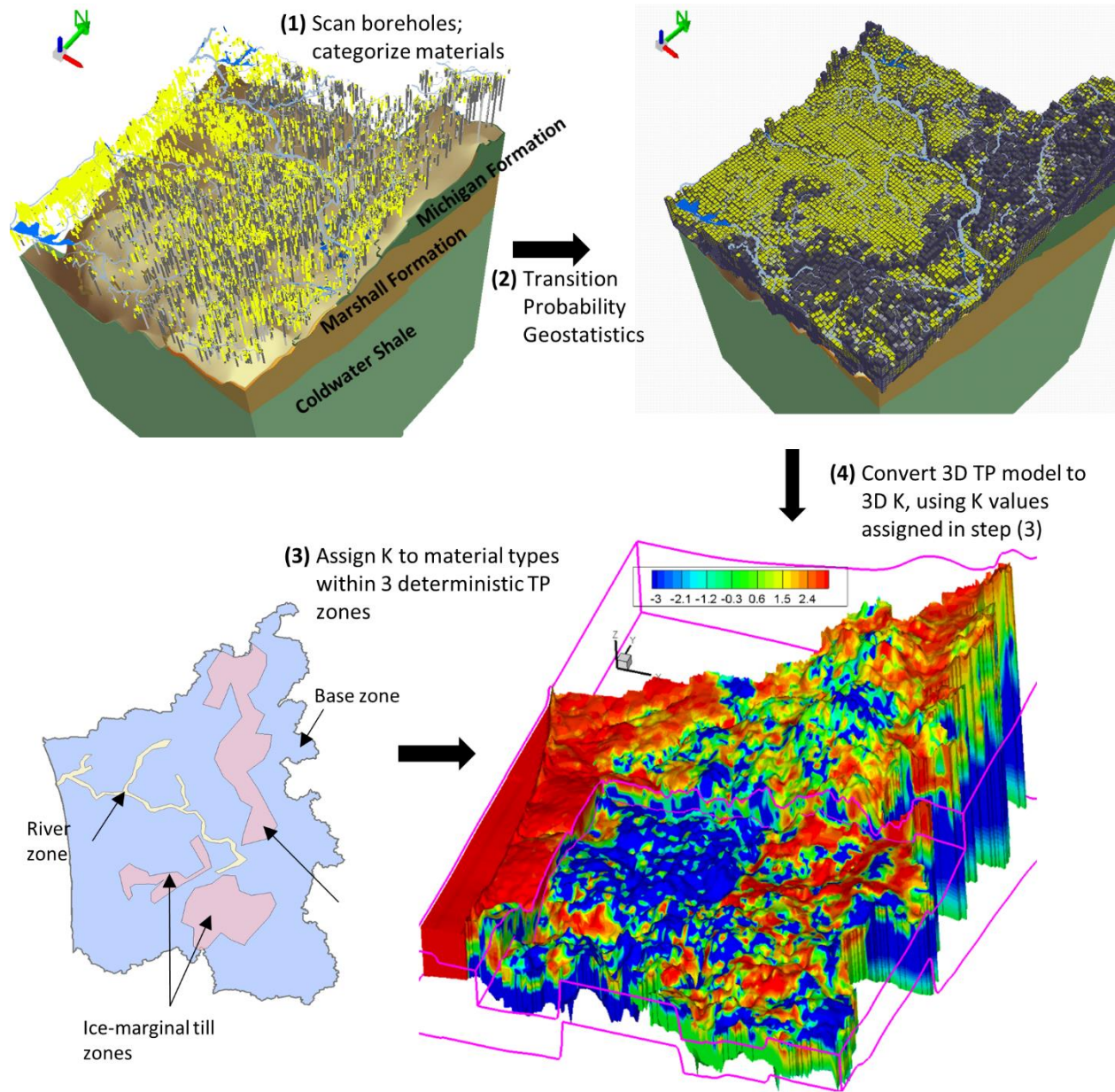


Figure 3.5: Workflow for developing a three-dimensional hydraulic conductivity (K) field using the zone-based transition probability approach. The K-field shown here represents $\ln(K)$ variations.

In the flow model, horizontal and vertical conductivities were used to calculate parallel flow (along a layer) and series flow (across a layer) flow according to Freeze and Cherry (1979). To incorporate the TP simulation results into the flow model, a horizontal conductivity (K_h) and horizontal to vertical anisotropy ratio (K_h/K_z , respectively) value for each material type was assigned (hereafter referred to as K_h^{TP} and K_h^{TP}/K_z^{TP}). Horizontal to vertical anisotropy ratios were interpreted to represent sub-cell layering/interbedding of different material types within a cell dominated by one material type. For all material types, and K_h^{TP} and K_h^{TP}/K_z^{TP} were assigned reasonable estimates based on typical aquifer and confining unit properties (Freeze and Cherry, 1979), which were then fine-tuned during calibration. These values were used to calculate the horizontal hydraulic conductivity K_h^{Model} and anisotropy ratio K_h^{Model}/K_z^{Model} in each model grid cell. For example, if one groundwater model cell contained two or more geologic model cells in the horizontal direction, the resulting K_h^{Model} of the groundwater cell was the arithmetic average of the K_h^{TP} values from the geologic model cells. If the groundwater cell contained two or more geologic model cells in the vertical direction, a harmonic average was utilized to calculate K_h^{Model} for the groundwater cell. The result is a complex 3D hydraulic conductivity field to be used in groundwater flow modeling, which is exemplified in step (4) of Figure 3.5. A single value of specific yield was applied to all glacial aquifer materials, the final value of which was determined during calibration.

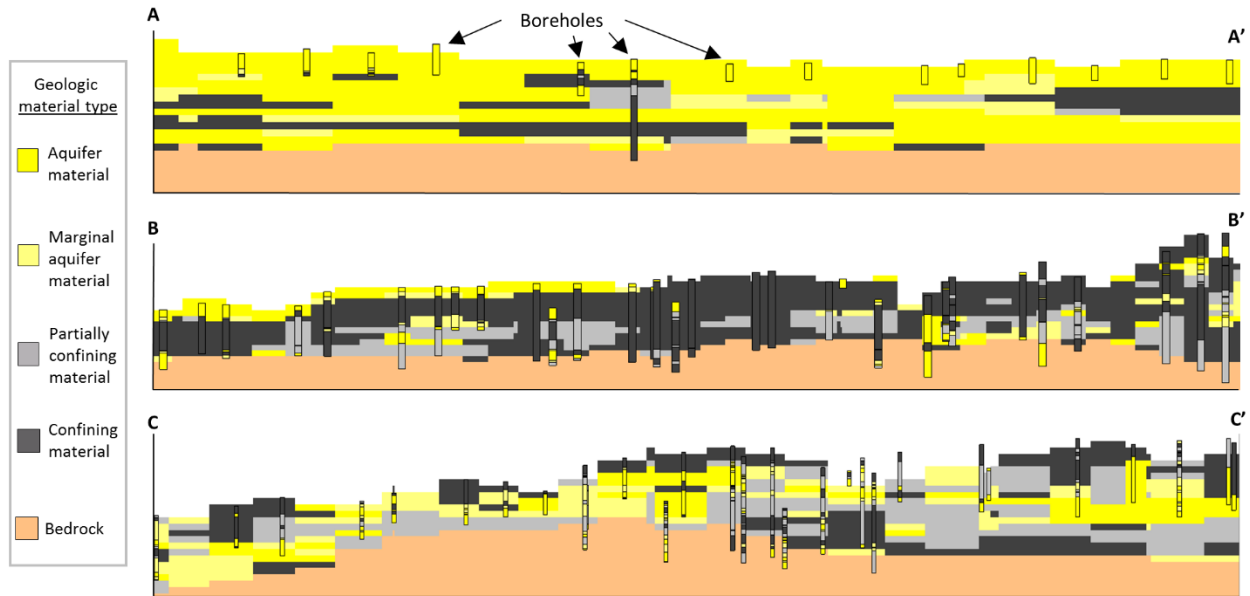


Figure 3.6: Cross-sections of the 3D glacial aquifer material model, overlaid with borehole lithologies from water wells. The approximate locations and horizontal/vertical extents of cross-sections A-A', B-B', and C-C' are shown in Figure 3.2.

Deterministic Representation of the Bedrock Aquifer. As shown in Figure 3.7, the Marshall Formation was represented using two layers: a shallow ‘fractured’ (weathered) portion extending 18.3 m (60 ft.) into the bedrock aquifer, and a deeper ‘unfractured’ portion that varied in thickness according to the geometry of the confining layers above and below (detailed rationale is presented in Appendix B of this chapter). The Marshall dips toward NE direction as the Michigan formation becomes the top interface to the Marshall in place of the glacial sediments, creating confining conditions. Directly beneath the Marshall is the Coldwater Shale, which also acts as a confining unit and was therefore assumed a ‘no-flow’ lower boundary condition for the model domain. All zones in both bedrock layers were assigned an effective hydraulic conductivity, which was later calibrated. The sloping interface between the different bedrock formations was conceptually simplified by having ‘transition zones’ (e.g. $K_{ave,1}$) to represent portions of a bedrock layer where Marshall or Michigan Formation are less than 60 ft. (~ 18.3 m) thick and include a different bedrock unit (Coldwater Shale or Marshall Formation, respectively) within the layer-based zone. A single storage coefficient was assigned to each layer (fractured and unfractured), which was also later calibrated.

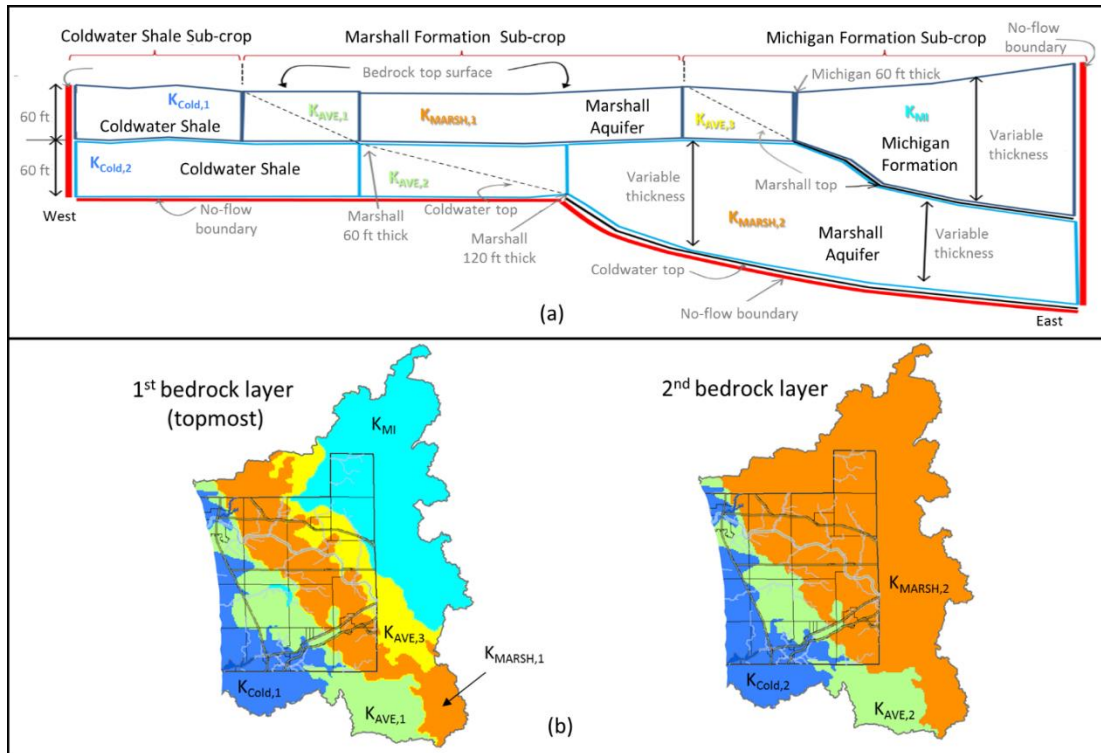


Figure 3.7: Conceptualization of the bedrock aquifer: (a) conceptual cross-section indicating the vertical extent of the different zones within the 1st (top-most) and 2nd bedrock layer; and (b) areal extent of the zones shown in (a) for the 1st and 2nd bedrock layer.

3.4.2 Water Use Model

Two sources of data were used for developing the water use model: *Wellogic* and the Ottawa County Department of Public Health (Environmental Health) – which maintains a system that organizes, on a property-by-property basis, borehole records and well logs from city or township government agencies (or even directly from the well drillers themselves). The choice to supplement the statewide dataset with local records was motivated by the fact that many wells installed during the 1990s have mostly not been added to *Wellogic* database. Approximately 2600 well data points were extracted from the local water well records to ‘fill in the gap’, including information of latitude and longitude, well depth, and date of well installation for the water use model, as well as SWLs for model calibration.

All compiled wells were classified as ‘domestic’, ‘irrigation’, ‘public supply’, or ‘industrial/commercial’ (based on information provided in driller logs), and the pumping rates of different well types were adjusted during calibration. In other words, all domestic wells pumped at the same rate, all irrigation wells pumped

at the same rate, etc. Because this study is concerned with long-term (multi-decadal) groundwater flow dynamics, seasonal fluctuations were ignored and wells were assumed to pump at a continuous rate throughout the remainder of the simulation once they were installed (note that this was problematic for a few relatively small areas where municipal surface water supply became available in recent years – see Appendix C at the end of this chapter for more details on the treatment applied here). As discussed above, the primary goal of the modeling exercise was to reproduce long-term trends over which seasonal or year-to-year variations in pumping rates of individual wells are superimposed.

Importantly, the approach used here was able to keep the number of parameters related to groundwater pumping relatively low, but the complex spatiotemporal structure of the well network (i.e., when and where the wells of a certain type should be operating) was well represented. This is somewhat similar to the zone-based TP approach used for parametrizing the glacial aquifer, where the spatial complexity of the hydraulic conductivity distribution was captured (i.e., the hydraulic conductivity varied in each groundwater model cell), by using a fairly small number of parameters. The results of model calibration indicate that capturing the spatiotemporal structure of many wells and the relative pumping rates between sectors is more important than prescribing the exact rates of all the different types of wells when attempting to simulate dominant, long-term trends in groundwater level declines (see Calibration Results subsection below).

3.4.3 Recharge Model

Estimating recharge to the aquifer system can be done using process-based simulations which integrate groundwater and surface water across the unsaturated zone (see, e.g., Shen and Phanikumar, 2010 or Davison et al. 2015) or empirical approaches (see Risser et al. 2008 or Reitz et al. 2017). Process-based models – although capable of producing detailed estimates of recharge in space and time and useful for probing impacts of potential changes in climate or abstracting of water – require time-steps on the order of minutes (or even seconds) to resolve the numerous surface processes impacting recharge. Such time-steps are impractical for the purposes of this long-term, large-scale groundwater study. On the other hand, most

empirical approaches provide long-term, average annual groundwater recharge estimates that lack temporal resolution. In this study, yearly recharge rates (as input to the flow model) was simulated following the procedure used in the USGS model INFIL 3.0 – a grid-based, distributed-parameter, semi-empirical/semi-process-based watershed model used to estimate net infiltration below the root zone (USGS, 2008). Drainage basin characteristics and daily climate records of precipitation and air temperature are used to estimate the daily near-surface water balance, including precipitation as either rain or snow; snowfall accumulation, sublimation, and snowmelt; infiltration into the root zone; evapotranspiration from the root zone; drainage and water-content redistribution within the root-zone profile; surface-water runoff from/to adjacent grid cells; and net infiltration across the bottom of the root zone.

Daily precipitation and minimum and maximum air temperature data were obtained from the *PRISM Climate Group*, which offers nationwide coverage at 4km spatial resolution for all years since 1981 (PRISM 2004). Surface topography was modeled using 10m DEM from USGS NED (2006), and land use and land cover (LULC) was represented using a modified version of the 16-class land cover classification scheme from the USGS National Land Cover 2006 Dataset (Fry et al. 2011). The modification was a greatly reduced hydraulic conductivity for ‘Developed’ LULC types due to the large extent of impervious surfaces present within such areas of the model domain (e.g., Grand Rapids in the eastern subregion). Soil type distribution and root zone depth across the model domain was obtained from the United States Department of Agriculture (USDA) Soil Survey Geographic (SSURGO) Database (SSS NRCS 2016). Soil type distribution was represented by applying the 12 classifications of USDA Soil Textural Triangle with percentages of sand, silt and clay obtained from the SSURGO Database.

Daily recharge to the aquifer system was computed from 1 Jan. 1981 to Dec. 31 2015. Annual averages were calculated at each grid cell location and used as input into the groundwater flow model at each time-step. Recharge from 1981 was applied for the 1966-1980 period of groundwater simulation, because the 4km *PRISM* climate data did not extend back beyond 1981. Figure 3.8 presents annual recharge distributions for selected time-steps. Although the magnitude of recharge at most of the grid cells varies from year to year (largely reflecting annual changes in precipitation and air temperature), the large-scale

patterns that are primarily controlled by the topography and surface lithology are consistent across the simulation period. In other words, the areas of relatively high and low recharge do not change significantly across the period of investigation.

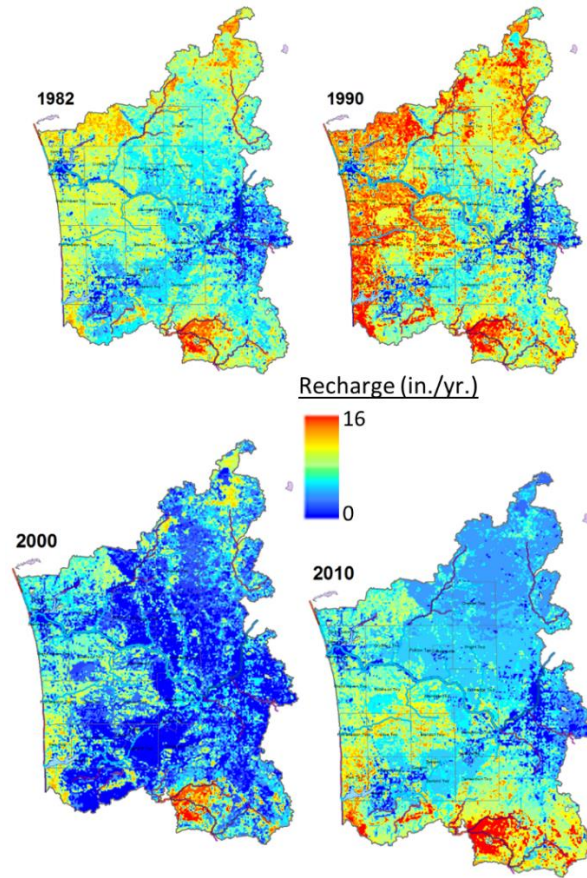


Figure 3.8: Simulated recharge distributions for select time-steps.

3.4.4 Groundwater Flow Model

Governing Flow Equations & Model Set-up. The groundwater flow model consisted of three ‘conceptual layers’ – the glacial drift aquifer and the fractured and unfractured bedrock aquifers. These were discretized using seven computational layers for solving the unsteady groundwater flow equation:

$$S_s \frac{\partial h}{\partial t} = \nabla(K \cdot \nabla H) + q \quad (4.1)$$

where S_s is the specific storage coefficient, h is the hydraulic head [L], t is time [T], K is the saturated hydraulic conductivity tensor [LT^{-1}], ∇ is the gradient mathematical operator, and q is the net source

(positive) or sink (negative) term, including pumping, recharge, and surface seepage [LT^{-1}] (see details below). The glacial layer, which needs to resolve the strong vertical structure of the aquifer material distribution derived from the TP geologic model, was subdivided into five computational layers of equal thickness. The fractured and unfractured bedrock conceptual layers were not subdivided, and thus flow was assumed to be predominantly horizontal within these units. *Interactive GroundWater* uses the finite difference approximation of the governing partial differential equation to solve confined and unconfined flow conditions (see Li and Liu 2006; Li et al 2006; Liao et al. 2015a;b for details on algorithms/schemes). *Model Boundary Conditions*. The northern, eastern, and southern lateral boundaries (see Figure 3.1) were constructed using 12-digit (small) watershed boundaries from USGS NHD (2010), and were assigned as no-flow boundaries conditions for all layers under the assumption that significant groundwater does not flow across local topographic divides. Of course, this may not reflect actual groundwater conditions, and for this reason calibration of the model to SWL temporal trends was done in areas far enough from the no flow boundaries to limit its influence. The western lateral boundary for all layers was a constant head that represented the long-term average lake level of 176.6m (579.3ft) obtained from Great Lakes Water Level Dashboard (Gronewold, et al. 2013).

DEM-Based Seepage Modeling. The land surface, modeled using the 10m DEM from USGS NED (2006), was treated as a one-way head dependent boundary condition (seepage) that allows groundwater to discharge to the surface where the groundwater level intercepts/exceeds the land surface:

$$q_{seepage} = \begin{cases} L(h - z) & \text{if } h > z \\ 0 & \text{otherwise} \end{cases} \quad (4.2)$$

where $q_{seepage}$ [LT^{-1}] is the flux per unit area leaving the aquifer through the land surface, h [L] is the head in the aquifer cell, and L [T^{-1}] is the leakance (hydraulic conductivity per unit thickness) of the land surface. Note that this technique ‘automatically’ accounts for the discharge of groundwater to surface water bodies such as streams, lakes, and wetlands, including the high-discharge Grand River. However, this process could be modeled in alternative ways, e.g., as prescribed head boundary conditions, two-way head dependent boundary conditions, or coupled surface water-groundwater modeling. The approach used here

was deemed most suitable for the purposes of the studying long-term groundwater sustainability because: 1) the other mentioned approaches require significantly more data as input and/or verification (e.g., stream or lake stages collected in space and time), without which significant errors in the groundwater balance may occur, especially as pumping lowers groundwater head in the underlying aquifer system; 2) the entire County of Ottawa is known to lie within a major groundwater discharge region (see Curtis et al. 2018), and therefore it is reasonable to assume that a vast majority of surface water bodies are gaining as opposed to losing;; and 3) the relatively high-resolution (10m) DEM from USGS NED effectively captures the long-term average surface water stages used as the z term in eq. (4.2).

The spatially-constant leakance term (1 day^{-1}) was calibrated and applied for the entire modeling domain, e.g., if the leakance is too low, the flooded area will be large, and vice versa. Surface seepage maps at different time-steps were compared to the surface water network features obtained from USGS NHD (2010) to ensure that this approach effectively captured the spatial patterns of groundwater discharge to lakes, streams and wetlands in the model.

Curvilinear Vertical Discretization Scheme & Time-Marching. The initial groundwater head distribution was generated by simulating steady-state groundwater flow for 1966 conditions, which incorporated all Wellogic wells completed prior to 1967 as pumping withdrawals. An iterative, curvilinear vertical discretization scheme was proposed to avoid the issue of “dry” cells when sub-dividing one layer into multiple sub-layers: first the glacial aquifer was discretized using one vertical layer to solve the head distribution, which was then used in the next iteration to subdivide the saturated thickness of the aquifer into multiple computational layers, say 2 or 3, which are solved. The process was repeated until a steady-state head distribution was solved for 5 glacial layers and 2 bedrock layers. The resulting layer configuration was used for the rest of the simulation computations.

With the initial head distribution obtained from the 1966 steady-state solution, the simulation was advanced in time by solving Eq. (4.1) with 2-year time-steps. Annual recharge distributions were included in the source/sink term at each time step. Withdrawals from wells constructed during the period over which the time-step extends contribute to the source/sink term of the groundwater model cells for that time-step. Once

added to the model, wells pumped ad infinitum at the calibrated pumping rate determined by its well type (see Water Use Model subsection and Appendix C at the end of this chapter). The approach to ignore sub-annual variabilities and model every 2-years reasonably is based on the assumptions described in the Conceptualization of Long-term Distributed Stress Dynamics subsection. (Note that a time-step of 1-year was tested and compared the results to those generated using a 2-year time-step. Resolving yearly details made no impact on being able to predict the observed drawdown ‘cloud’.)

Numerical Treatment of Well Discharge. It was possible that some of the well screen intervals spanned across multiple computational layers. Thus, it was necessary to apply a scheme for properly allocating withdrawals from a single well, Q , to different computational layers, Q_i (i.e., $Q = \sum Q_i$). In this study, the approach was to use ‘screen transmissivity’ as a weighting factor to divide one physical well into multiple computational wells depending on number of computational layers included within the screen interval:

$$Q_i = \frac{T_i}{\sum T_i} Q \quad (4.3)$$

where T_i is the transmissivity of the i^{th} layer through which the well’s screen goes (note that screen intervals were available in well logs used for this study). The hydraulic conductivity (K_i) and interval length thickness (B_i) at the cell location of each computational layer was used to compute the transmissivity for each layer ($T_i = B_i K_i$). Additionally, well withdrawals often needed to be mapped to multiple model nodes because of the proximity of multiple nodes to one physical well in the submodel. A similar scheme was also applied in the horizontal direction as was applied in the vertical direction, i.e., withdrawals from a single well were allocated to the nearest four nodes, where weightings were assigned based on the distance to the node and the hydraulic conductivity of the model cell.

3.4.5 Model Calibration

The key objective of model calibration was to capture the long-term water level trends (for different locations) in the aquifer system using a relatively small number of effective parameters. Because a network of established monitoring wells was lacking (i.e., there were no point-specific time-series data to use), thousands of SWL measurements from water well records in *Wellogic* and the local well files records

compiled by the Ottawa County (Ottawa County, Michigan 2014) were used to characterize the temporal dynamics across the aquifer system. More specifically, a comparison of SWL trends across time with model trends was made on a township-by-township basis to evaluate the model's ability to simulate long-term groundwater dynamics in different areas of the study area. Manual calibration was used to determine the final parameter values. In other words, trial-and-error was used to fit the 'cloud' of data about the line of best agreement in the case of the scatterplot comparing simulated head to observed SWLs or similarly, to fit the simulated model results through the center of the SWL data cloud for the SWL trend comparisons. Of course, SWL spatial variations within a township will create significant variability in SWL observations for a given time, and other sources of inaccuracy in SWL measurements contribute to variability – such as approximate wells location derived from geocoding or indirect information reported by the driller, measurement uncertainty introduced by inconsistencies from driller to driller (see Curtis et al. 2018 for more details), and inability of the model to resolve sub-grid or sub-time step (e.g., sub-annual) variabilities that are reflected in the observation data – albeit to a lesser degree. However, in some cases the decreases in groundwater levels that have occurred over the past 50 years are larger than the SWL variability caused by aggregation of observation data and noise in the measurements themselves (especially for the central portion of the model domain).

To summarize, the following parameters were calibrated to improve model performance: hydraulic conductivities of each glacial aquifer material set ('AQ_n', 'MAQ_n', 'PCM_n', 'CM_n') for three zones, including the horizontal conductivity (K_h) and the ratio of horizontal to vertical conductivity (K_h/K_z); the specific yield of the glacial aquifer materials; hydraulic conductivities of different bedrock zones and the specific storage for the fractured and unfractured layers; and sector-specific pumping rates for domestic, public supply, irrigation, industrial/commercial wells used in the water use model as inputs into the groundwater flow model. Note that this approach required a relatively low number of calibration parameters, but still was able to capture the complex spatiotemporal structure of the well network as well as the 3D spatial structure of the hydraulic conductivity distribution through the use of effective – or 'system' – parameters (e.g., sector-specific pumping rates, hydraulic conductivities of the aquifer material

sets). The results from model calibration indicate that such system parameters are effective for characterizing generalized flow systems dynamics if the complex geologic and stress configurations are captured with reasonable completeness.

3.5 Ch. 3 Results and Discussion

3.5.1 Calibration Results

Comparison of Observations and Simulated Outputs. The comparisons of all observed SWLs with simulated hydraulic head from the calibrated model is shown in Figure 3.9. SWL observations from 19,387 glacial wells and 1965 bedrock wells were used to calibrate the model. The solid line in each plot represents the 45° line of ‘perfect agreement’ (all points on this line have the same simulated and observed SWLs), and the dashed lines represent confidence intervals of one standard deviation. The results show that, for both the glacial and bedrock layers, the model performed reasonably well across both space and time, as indicated by strong correlation coefficients (R^2) of 0.969 and 0.937 and Nash-Sutcliffe model efficiency coefficients of 0.94 and 0.88 for the glacial and bedrock layers, respectively. And although there is a relatively large spread in the “data cloud”, the spread is centered about the line of perfect agreement (note the small mean error values of 0.06m, and 0.04m). This demonstrates that the model was able to capture the dominant spatial and temporal trends of the large groundwater system. The relatively large spread in the data (as indicated by the large standard deviation values of and 5.59m and 5.67m for the glacial and bedrock layers, respectively) primarily reflects the significant noise embedded in the SWL observations (Curtis et al., 2018). To a lesser degree, the RMSE values are impacted the inability of the model to resolve sub-grid or sub-time step (e.g., sub-annual) variabilities that are reflected in the observation data. Note that for both aquifers the RMSE values due to all sources of error are significantly smaller than the overall range of head variability in the aquifer.

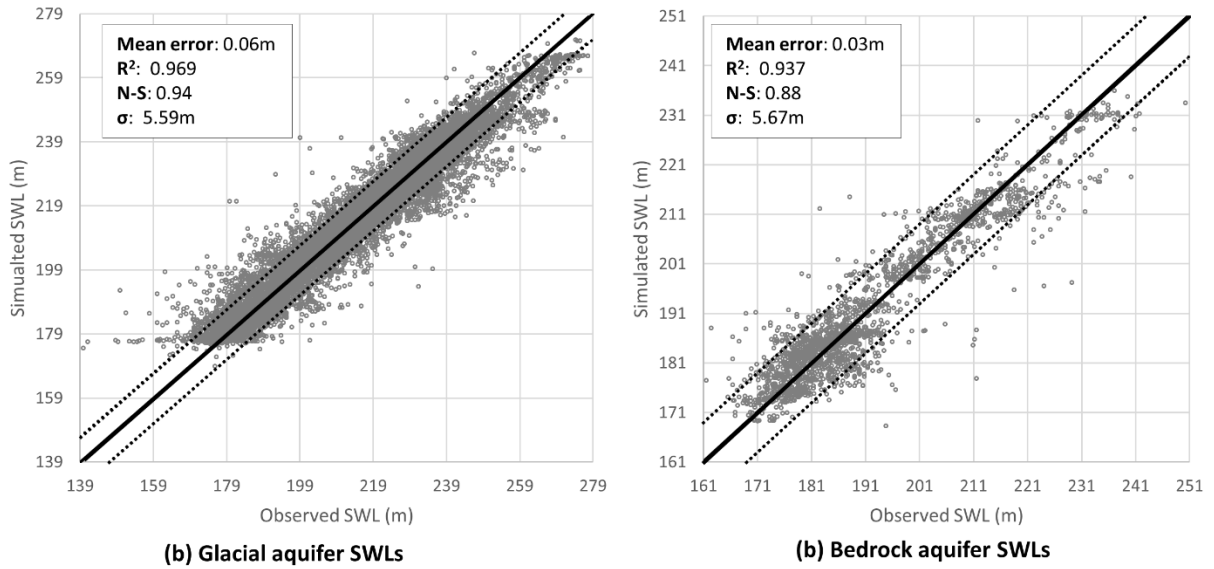


Figure 3.9: Comparison of simulated groundwater head with observation (SWL): (a) all glacial drift wells; and (b) all bedrock wells.

To calibrate the model to long-term changes in water levels, subsets of the SWL dataset were created by aggregating SWLs within each township of Ottawa County (for both the glacial and bedrock aquifer), which were then plotted against time. A few illustrative examples of areas with temporal trends stronger than the SWL spread is shown in Figure 3.10. Also shown in the simulated head for each measurement time and location. The model is able to reproduce the general downward trend observed in the SWL subsets from the bedrock aquifer in the central part of the model domain, although the spread in the simulated dataset is less because the values are exact, i.e., there are no sources of observation error, although the effects of spatial aggregation is apparent. For many of these charts created for the glacial aquifer (and for some for the bedrock aquifer), a temporal trend could not be detected, either because the noise was larger than the trend, or because a significant trend did not exist. Nonetheless, this township-by-township temporal analysis provided an additional constraint on the calibration that could not be discerned through inspection of Figure 3.9 alone.

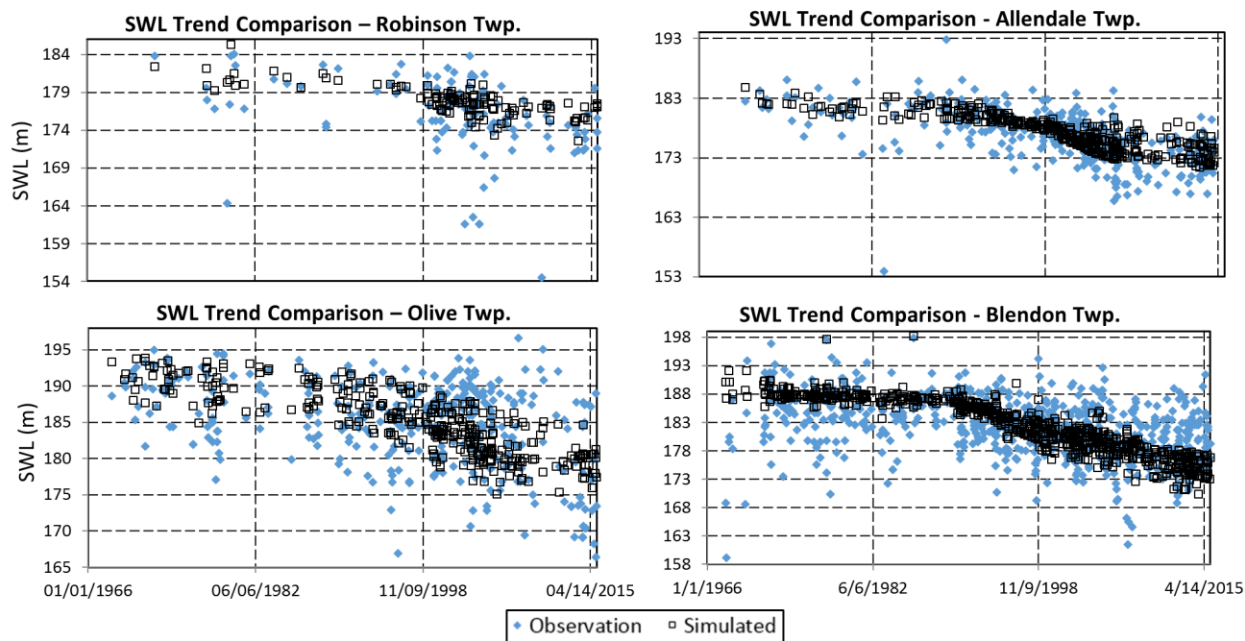


Figure 3.10: Static Water Level (SWL) trend comparison (observations vs. simulated head) for the bedrock aquifer of four central townships in Ottawa County, MI.

Calibrated Water Use. Table 3.2 presents the calibrated pumping rates of the different well types as well as average observed pumping rates as a comparison. The observed pumping rate for irrigation wells was derived from 2012-2013 self-reported agricultural withdrawals compiled by MDARD; the observed rate for public and industrial/commercial wells was calculated using 2012-2013 data made available by MDEQ; and the observed rate for domestic wells was based on an analysis of water meter data provided by Ottawa County Public Utilities Department. Calibrated and observed pumping rates are somewhat comparable, with a ratio of calibrated pumping rate to observed pumping rate of just over one for public supply, irrigation and industrial/commercial water use sector (1.03, 1.61, and 1.68, respectively). The overestimation may be because users are underreporting their water use, incentivized by strict laws recently passed regulating large-capacity groundwater withdrawals in Michigan, or it may be because some wells are missing in well dataset used to create the water use model and thus, a higher simulated pumping rate was needed to reach an equivalent total water use that could reproduce the observed drawdown exemplified in Figure 3.10 (this latter point is addressed in further detail in Appendix D at the end of this chapter).

Table 3.2: Calibrated and mean observed pumping rates for domestic, public supply, irrigation and industrial/commercial water use sectors.

| Well Type | Calibrated (GPM) | Observed (GPM) |
|-----------------------|------------------|----------------|
| Domestic | 0.65 | 0.19 |
| Public Supply | 8.00 | 7.76 |
| Irrigation | 13.50 | 8.36 |
| Industrial/commercial | 13.50 | 8.03 |

As a final constraint on the calibrated water use parameters, a comparison was made of aggregated simulated water use with reported countywide water use in Ottawa County (Figure 3.11). The solid lines represent the different simulated water use curves as well as the total water use (blue). The water use attributed to irrigation has significantly increased since 2000, consistent with recent report of expanded agricultural activity. Also note the importance of domestic well withdrawal increases (the 2nd largest user of groundwater since 2002). Overall, the total simulated water use is similar to the reported water use in recent years (2000-2013). Given the averaging of pumping rates required because of data limitations, it is encouraging that there is some level of agreement between the observations and simulated water use.

Examples of the final water use distribution for selected time-steps is shown in Figure 3.12.

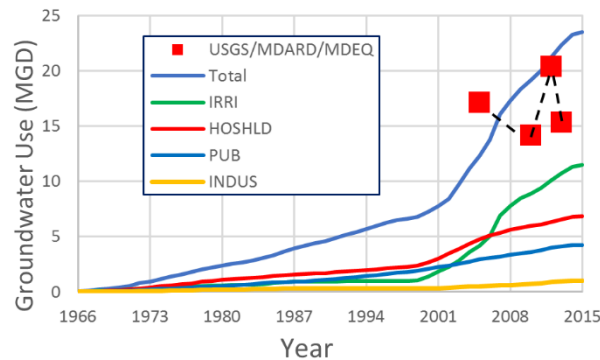


Figure 3.11: Calibrated water use curves and estimates of aggregated groundwater withdrawals for Ottawa County, Michigan from USGS (2005, and 2010) and MDARD/MDEQ (2012 and 2013). The red markers represents estimated water use, and the solid lines are simulated water use (IRRI = irrigation; HOSHLD=domestic; PUB = public supply; and INDUS = industry/commercial).

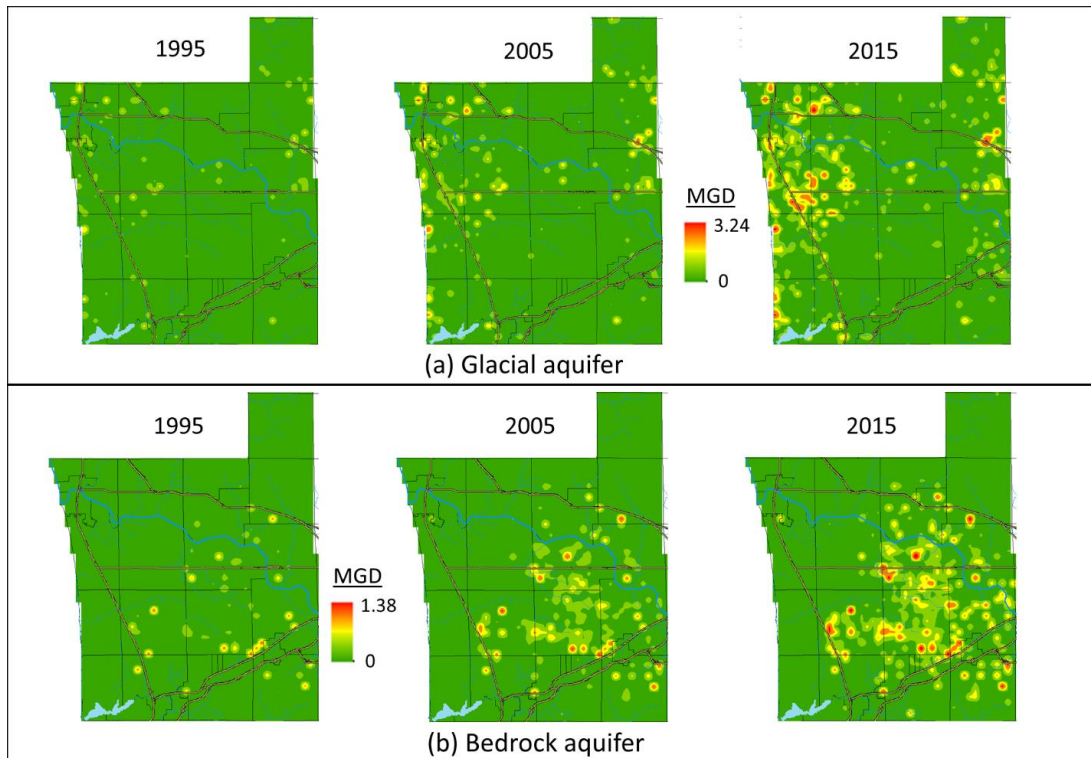


Figure 3.12: Simulated water use for 1995, 2005 and 2015, using the calibrated pumping rates presented in Table 2: (a) drift aquifer; and (b) bedrock aquifer.

Calibrated Hydraulic Parameters. The calibrated specific yield for all glacial materials was 0.1, and the final calibrated hydraulic conductivities for the glacial aquifer are presented in Table 3.3. The ‘River Zone’ (AQ1, MAQ1, etc.) has the largest horizontal conductivities and relatively small K_h^{TP}/K_z^{TP} , i.e., higher vertical hydraulic conductivities, which confirms that the underlying bedrock layer is connected to the Grand River. The ‘Ice-marginal till zones (AQ2, MAQ2, etc.) and ‘Base Zone’ (AQ3, MAQ3, etc.) have the same K_h and K_h^{TP}/K_z^{TP} values for aquifer materials (AQ and MAQ), but the confining materials for the ‘Base Zone’ are less transmissive than those of the ‘Ice-marginal till zones’. These patterns are consistent with the conceptual understanding of the three TP zones used to delineate areas of distinct geomorphologies.

The final horizontal hydraulic conductivity distributions for the five glacial layers is presented in Figure 3.13. There is a relatively continuous unit of low K_h^{Model} extending across multiple layers in the central

portion of the model domain, which has implications for groundwater recharge (or lack thereof) to the underlying bedrock. The eastern portion of the modeling domain is highly heterogeneous, while the western portion consists primarily of high K_h^{Model} material. Note that these large-scale patterns are consistent with the understanding of the large-scale geology. Also note that the spatial complexity of the K_h^{Model} distribution was achieved using a fairly small number of parameters. Moreover, this was done using an unbiased geostatistical representation of the aquifer material distribution rather than being done arbitrarily or subjectively, which, as mentioned, was time-consuming and impractical (if not impossible) to calibrate.

Table 3.3: Calibrated hydraulic conductivities (K_h^{TP}) of the aquifer material sets, including the ratio of horizontal conductivity to vertical conductivity (K_h^{TP}/K_z^{TP}).

| Material type | K_h^{TP} (ft/d) | $\frac{K_h^{TP}}{K_z^{TP}}$ |
|---------------|----------------------|-----------------------------|
| AQ1 | 160 | 4 |
| MAQ1 | 10 | 4 |
| PCM1 | 1 | 500 |
| CM1 | 1 | 500 |
| AQ2 | 80 | 20 |
| MAQ2 | 10 | 20 |
| PCM2 | 0.1 | 300 |
| CM2 | 0.1 | 300 |
| AQ3 | 80 | 20 |
| MAQ3 | 10 | 20 |
| PCM3 | 0.05 | 1500 |
| CM3 | 0.05 | 1500 |

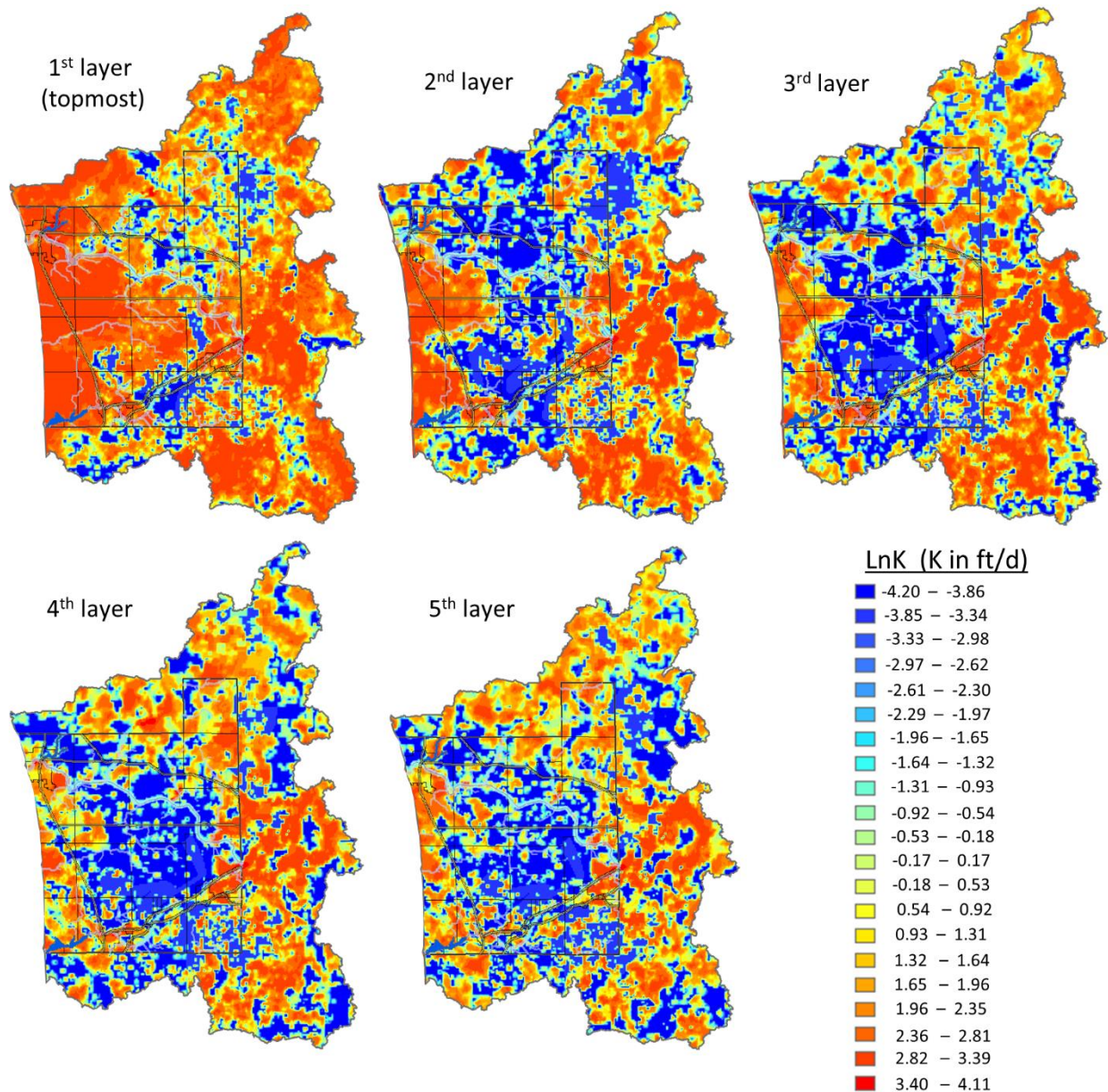


Figure 3.13: Hydraulic conductivity (K_x^{Model}) distribution in the six computational layers of the glacial aquifer.

The final calibrated horizontal hydraulic conductivities of the bedrock zones are presented in Table 3.4. The values are relatively consistent with previous studies. For example, the transmissivity for the Marshall Formation in western Lower Michigan was estimated at approximately $2.7 \times 10^{-3} \text{ m}^2/\text{s}$ ($2500 \text{ ft}^2/\text{d}$) by Feinstein et al. (2010), and given that the Marshall Formation is relatively thin ($<100 \text{ ft.}$) throughout a large portion of the study domain, the estimates of 7 ft/d and 2.5 ft/d for $K_{\text{marsh},1}$ and $K_{\text{marsh},2}$, respectively, appear to be realistic. The values for the confining units ($K_{\text{cold},1}$, $K_{\text{cold},2}$, K_{MI}) are at least two orders of magnitude

less than those of the aquifer units, consistent with the conceptual understanding of the local hydrogeology. The calibrated specific storage coefficient for the fractured and unfractured bedrock layers was $9.7 \times 10^{-5} \text{ m}^{-1}$ ($3 \times 10^{-5} \text{ ft}^{-1}$) and $9.7 \times 10^{-6} \text{ m}^{-1}$ ($3 \times 10^{-6} \text{ ft}^{-1}$), respectively.

Table 3.4: Calibrated hydraulic conductivities (K_x) of the bedrock zones.

| Zone | K_x (ft/d) |
|----------------------|--------------|
| $K_{\text{marsh},1}$ | 7 |
| $K_{\text{cold},1}$ | 0.005 |
| K_{MI} | 0.01 |
| $K_{\text{ave},1}$ | 2.5 |
| $K_{\text{ave},3}$ | 5 |
| $K_{\text{marsh},2}$ | 2.5 |
| $K_{\text{cold},1}$ | 0.001 |
| $K_{\text{ave},2}$ | 1.25 |

The process for calibration used here differed from the traditional approach in that SWL data were available everywhere in the aquifer system (consider that over 21,000 SWL measurements from wells were used in the calibration) but required spatial aggregation to detect temporal trends given the inconsistent temporal coverage across space (recall that each SWL represented one measurement made at one time). This, along with other sources of noise (see above) made it difficult to assess model performance at local scales (i.e., scales smaller than that used for spatial aggregation of SWLs). More importantly, although the “cloud” of data was fitted about the line of best agreement in the case of the scatterplot comparing simulated head to observed SWLs (Figure 3.9) or similarly, to fit the simulated model results through the center of the SWL data cloud for the SWL trend comparisons (Figure 3.10) – the set of final calibrated parameters is not unique in the sense that other sets with similar values (i.e., within an order of magnitude or less) could probably satisfy the criteria used for manual calibration. However rigorous testing of this is beyond the scope of the current study. Thus, we recommend two courses of future action to reduce uncertainty in final model parameters using the approaches described here:

- systematically test the geologic and water use parameterization schemes proposed here with numerical experiments, where the modeler control the quality and type of observation (e.g., regional head measurements, time-series monitoring well data, flux measurements along model boundaries, etc.) available for calibration - as well as the input data available for the calibrated model – and the complexity of the original model. This provides a flexible approach for probing impacts and uncertainties of model parameterization because the true model is entirely known (i.e., all components of the model are prescribed). Additionally, model output uncertainties associated with modeling structure (i.e., the geologic representation) of the present model may be evaluated a with Monte Carlo approach, in which head results are generated for each realization of the TP geostatistical model and estimates of mean head and head variance are calculated from the model output distribution and assessed spatially.
- Collect high quality data (i.e., data with less noise and time-series information) and perform systematic calibration and sensitivity analysis using the model developed for this study. An efficient way to approach this would be to focus data collection, modeling and analysis for an important subregion(s), using the current model to provide boundary conditions (at different times) that are consistent with the overall system dynamics. This would be of interest to local groundwater resource managers and larger sustainability investigations (see the Toward Sustainability: Next Steps subsection). The model could also be improved by constraining the geological model with additional sources of geophysical information (e.g., electric resistivity maps, seismic reflection profiles), geologic information (sediment-texture analysis, mineralogy, etc. from sedimentological studies), and/or geochemical information (e.g., major ion and isotope analyses). See Bajc et al. (2014), He et al. (2014) and Traum et al. (2014) as examples of studies utilizing these types of data for improving geologic models of the subsurface.

3.5.2 Groundwater Head Dynamics

The outputs from the transient groundwater model are the hydraulic head distributions and resulting velocity vectors for each computational layer from 1966-2015. Figure 3.14 presents the three-dimensional head distribution for the last time-step (2015). There is strong 3D variability in the head distribution,

especially near the local recharge nears of the glacial aquifer and where groundwater is converging to major streams and discharge areas. The central subregion with a portion of the head distribution made transparent is also shown to illustrate the area of relatively low hydraulic head in the deep (bedrock) aquifer south of Grand River.

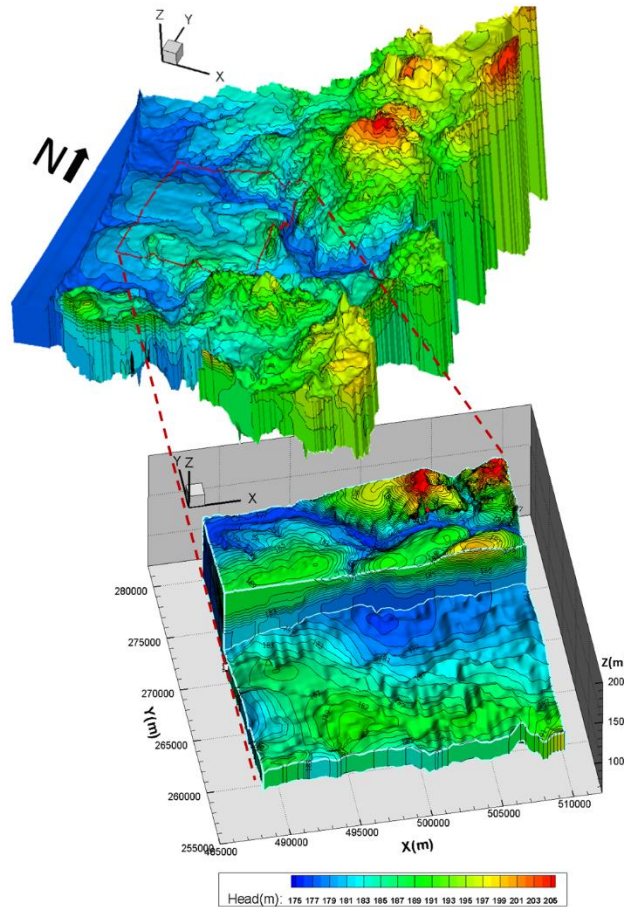


Figure 3.14: Three-dimensional head distribution for final time-step (2015). The magnified region is shown to highlight the significant depression in the central portion of the model domain due to significant increases in pumping.

Analysis of the simulated bedrock head distribution across time indicates that this ‘cone of depression’ has developed over time (see Figure 3.15), especially in the last 15 years. This part of the study area is where dramatic increases in water use have occurred over the same time period (see Figure 3.12), and where the relatively continuous, low K unit overlies the bedrock aquifer and effectively restricts recharge from the surface (see Figure 3.13). We interpret that this, coupled with the relatively low K_h of the bedrock aquifer, has caused the significant drawdown seen in the SWL dataset and the simulation results. Clearly, the

groundwater sustainability of the region is long-term water resource sustainability of this region is threatened because of unchecked increases in groundwater withdrawals being used to support rapid population growth and expanded agricultural activities.

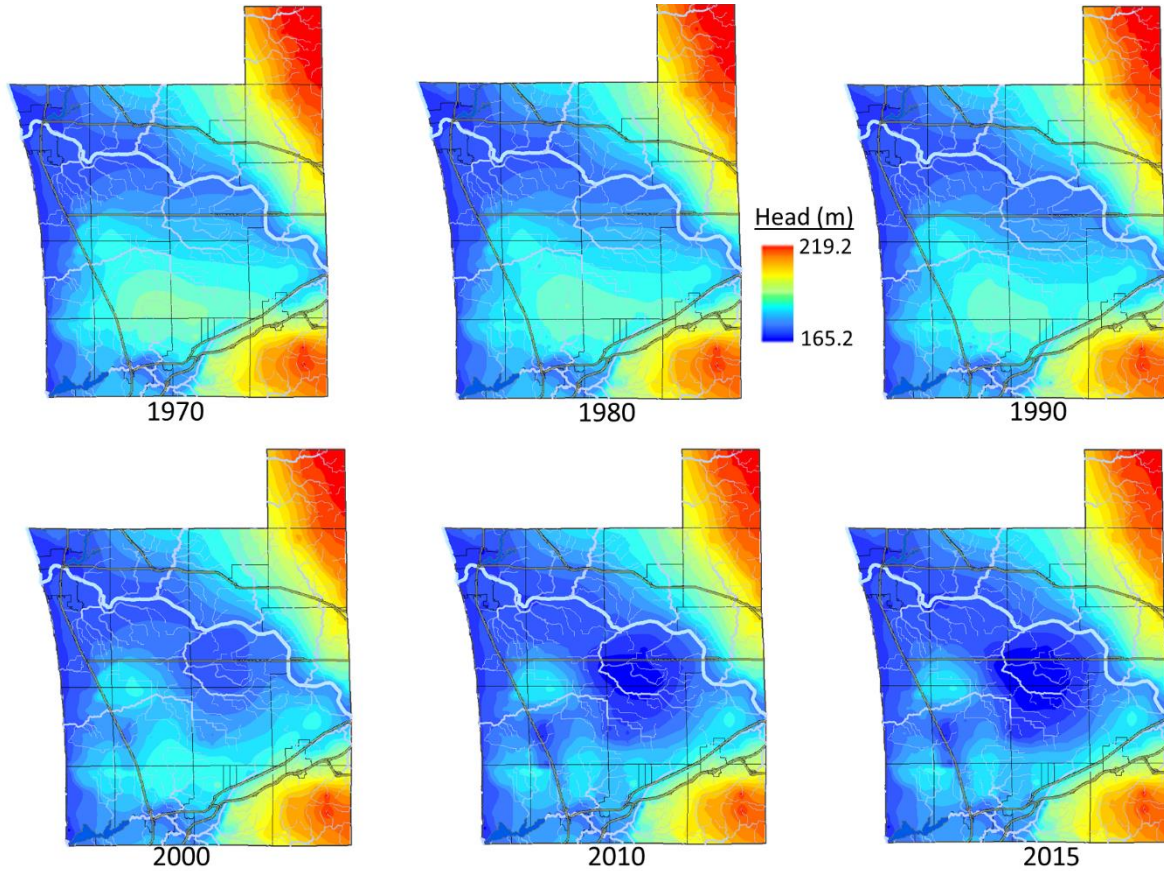


Figure 3.15: Simulated groundwater head distribution (bedrock aquifer) for representative time-steps.

A quantitative estimate of the impact of the long-term changes in the bedrock head distribution was obtained by performing bedrock aquifer water balance analyses for each township in Ottawa County over the past 50 years. Examples of transient bedrock aquifer flux balances for three townships over which most of the significant drawdown has occurred is shown in Figure 3.16. The values plotted represent net flux values (where positive fluxes represent water added to the township from the specified source and negative fluxes represent water removed). Recall that the bedrock aquifer was modeling using two computational layers, with the top-most layer representing the top 60 ft. of the fractured bedrock where most wells are screened,

hence the presence of bottom boundary fluxes (i.e., water moving vertically to/from the deeper bedrock aquifer).

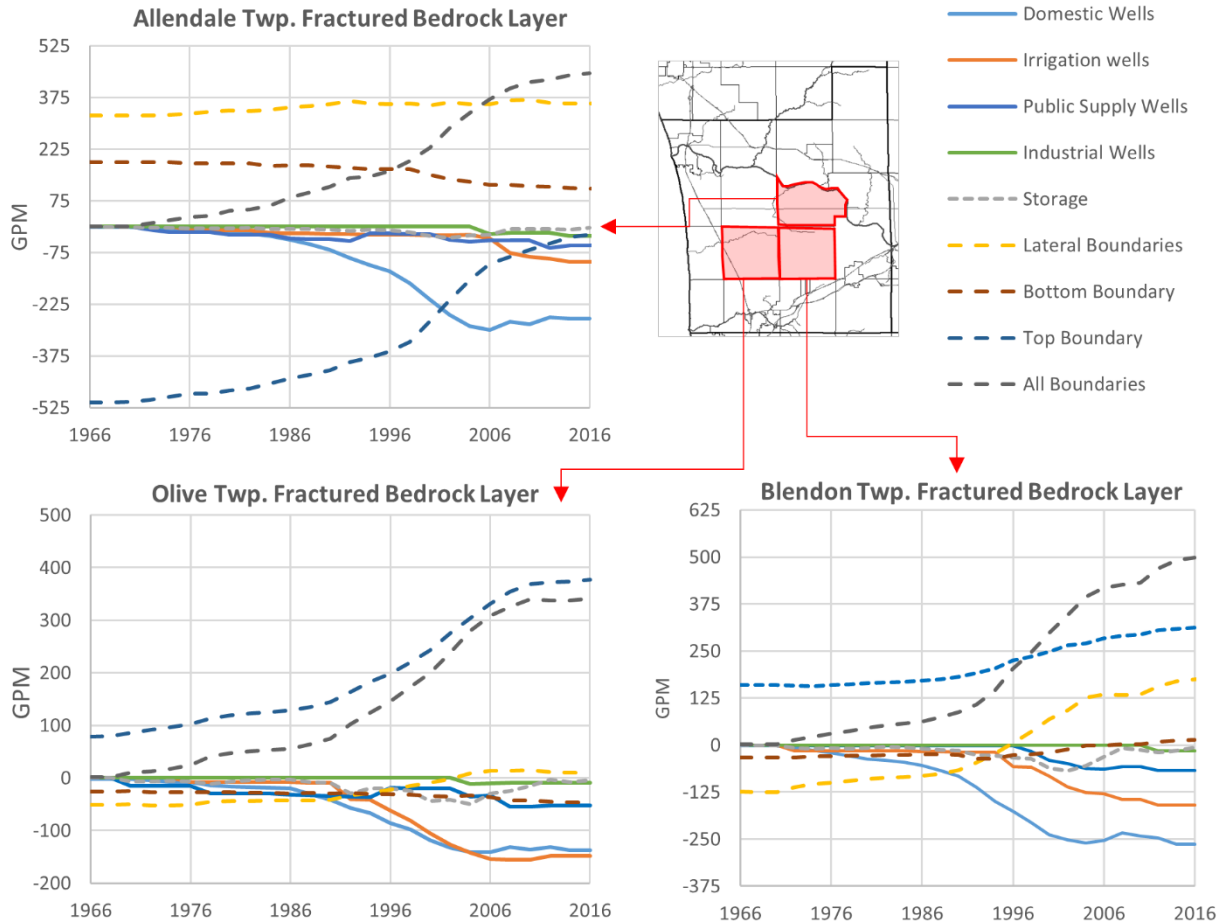


Figure 3.16: Graphical representation of flux dynamics in the three central townships exhibiting significant drawdown from 1966-2015.

For all three townships in Figure 3.16, the net flux out all of the boundaries of analysis was equal to zero during pre-development (i.e., inputs and outputs along boundaries were balanced). However, as the amount of groundwater being withdrawn from the bedrock has increased, particularly from domestic wells and irrigation wells, inputs from surrounding aquifer units have increased to balance the water budget, as evidenced by the growing, significant positive fluxes for ‘All Boundaries’. For Olive Twp. and Blendon Twp., net increases in flux through lateral boundaries is observed, particularly for Blendon Twp., whose lateral fluxes changes from -125 GPM in 1966 to over +125 GPM in 2015. Consequently, the bedrock

aquifer in Blendon Twp. has been converted from a local recharge area to a local discharge area. In Olive Twp. most of the increase in net boundary flux appears to have been satisfied with contributions from the glacial layer above. For Allendale Twp., whose northern boundary includes the Grand River (GR), net top boundary flux has increased from -520 GPM (water leaving the bedrock to the glacial layer above) to roughly zero as pumping withdrawals have significantly increased. Due to the connectivity between GR and the bedrock, and the relative isolation of other smaller streams from the bedrock due to the continuous clay layer, a majority of this change in top boundary flux can be considered a net loss in baseflow to the GR along the segment cutting through Allendale Twp. Overall, this loss in baseflow represents a small amount of the overall flow in the lower GR, although it is surprising that a portion of such a large, 6th-order stream located in a major regional discharge area could essentially lose its natural connection to the deeper aquifer system because of deep water well withdrawals.

3.5.3 Toward Sustainability: Next Steps

The simulation results are generally consistent with concerns raised by local policy makers and resource managers: cumulative impacts of gradual but steady increases in distributed groundwater pumping are lowering groundwater levels across large areas of the aquifer system. Although it is beyond the scope of study to develop a master resource plan for the region, we briefly review how the present model can be directly used for further analysis and what further steps are needed for reaching the overall goal of long-term sustainability of groundwater resources.

Subscale Data Collection, Modeling and Analysis. With a system-wide representation of the dominant driver of groundwater level decline (spatiotemporal well network growth and geologic variability), future efforts should focus on capturing finer spatial and temporal resolutions (e.g., seasonality in pumping and recharge, well-specific pumping rates, etc.) within key areas, especially for “limiting situations” that control sustainability (e.g., when recharge is lowest and pumping is most intense). The approach would prioritize resources for improving submodel structure (e.g., by integrating new field estimates of hydraulic conductivity from aquifer pump tests and/or seismic profiles into the geologic model, compiling well-specific pumping rates, etc.) and model calibration (e.g., strategically placed time-series groundwater level

data, streamflow measurements for constraining recharge, etc.), using the time-dependent boundary conditions of the parent model to effectively capture the ‘background’ effects of a dynamic pumping stress configuration propagating through the system over time. A better constrained submodel could then be utilized for scenario testing under a variety of future groundwater use scenarios, which could be idealized in nature or based on carefully planned well and land use build-outs complete by planners and resource managers. These simulations should be applied to quantify expected changes in flow patterns and water balances in the aquifer systems under different scenarios, and, in particular, to evaluate if future pumping may cause water levels in wells to fall below safe operating levels or cause unacceptable groundwater reductions to streams and other groundwater-dependent ecosystems (see Meyer et al. 2014 for an illustrative example). Continued monitoring would help verify and improve the submodel(s) simulations, which could then be used to improve the larger scale model for characterizing cumulative impacts to the system due to climate change, land use/cover change, etc.

Connections to Water Quality. In related work, it was demonstrated that a statistically significant number of wells in the Michigan Lowlands exhibit salinity levels well above expected natural levels, primarily because of mixing of deep, highly mineralized groundwater (brines) with fresh groundwater near the surface. Resulting concentrations in groundwater often make it unfit for drinking consumption or use in agricultural activities (Curtis et al., 2018). Thus, it is natural to ask whether deep pumping in this aquifer system is inducing migration of saline groundwater into parts of the aquifer system traditionally not impacted by the deep brines. In forthcoming work, we address this question by compiling groundwater quality (salinity) data across space and time and use integrated spatial (2D and 3D) overlays and statistical analyses to probe connections between water quality and simulated flow dynamics (Curtis et al. in review). This work also presents statewide and regional characterizations of groundwater salinity and more details on impacts of local geology and water quality.

Socio-political Considerations. In addition to a solid science-based understanding of the aquifer system, consideration of socio-political aspects of water governance is needed for developing a master water resource plan (Frind and Middleton, 2014; Wheatler and Gober, 2015). This includes but may not be limited

to: an accurate quantification of the current and future water demand for the region and exploration of water conservation options to reduce future demands; evaluation of costs for expanding alternative sources of water (a pipeline already exists that services Grand Rapids) now and in the future; complete inventory of important or protected surface features (e.g., groundwater-dependent ecosystems, potential contamination sites, etc.); master land use and build-out policy, including a means for protecting important groundwater recharge areas; and delineation and protection of capture zones of major well fields. Readers are referred to comprehensive investigations of sustainability of the Waterloo Moraine for an illustrative example of integrating socio-political aspects of water governance with a sound science-based understanding of a geologically similarly, complex groundwater system (see, e.g., Blackport and Dorfman, 2014; Frind and Middleton, 2014; Friend et al. 2014).

3.6 Ch. 3 Conclusions

A groundwater model of a complex and strongly heterogeneous aquifer system in west-central Lower Michigan was developed for the 50 last years. The ability to successfully simulate past conditions required a detailed characterization of the spatiotemporal evolution of water withdrawals and the strong 3D spatial structure of the subsurface. Parametrizing this model was challenging, given the lack of historical pumping and water level data and the multiple scales of geologic variability to consider (i.e., important large- and small-scale heterogeneities). To overcome these challenges we 1) implemented a ‘zone-based’ Transition-Probability (TP) geostatistical approach to conceptualize complex three-dimensional spatial variability using a relatively small set of geologic material types; 2) modeled the spatiotemporal evolution of water well withdrawals across several decades using a sector-based water use parameterization 3) used a large amount of noisy groundwater level data to capture long-term groundwater level declines in different parts of the aquifer system.

The ability of the model to reproduce long-term SWL trends across space and time suggests the proposed approaches are promising for the purposes of characterizing long term, groundwater system dynamics where data are limited and the subsurface is geologically complex. In particular, this study suggests that,

for the purposes of reproducing long-term groundwater level declines, it is less important to have quantitative data for ‘every’ well (i.e., specified pumping rates) or at many locations in the subsurface (e.g., hydraulic characteristics derive from aquifer pumping tests); what seems more important is having enough data to capture the space-time dynamics of the well network – or similarly, the complex spatial configurations of aquifer material types – which can be quantified using a limited number of system (effective) parameters. As shown here, detailed, high-density water well datasets, which have rarely been used for larger scientific groundwater analysis, are an excellent source of information for characterizing complex aquifer structures (geology and well network growth). Fortunately, these datasets are becoming increasingly available in different U.S. States and elsewhere (see, e.g., Illinois State Geological Survey repository (ISGS, 2015), Kansas’ WIZARD water well levels database (KGS, 2002), and the GeoSam Database for the State of Iowa (IGS, 2016), and thus, methods presented here have general applicability elsewhere.

With a proper representation of long-term dynamics based on existing data alone, limited resources and can be prioritized for 1) improving the model or subregions of the model through additional data collection, both for representation of the geology and pumping stresses as well as model verification (particularly at local/shorter scales important to sustainability); 2) performing risk and vulnerability assessment to groundwater resource supply and groundwater-dependent ecosystems and 3) quantifying uncertainties associated with all model applications and reconciling these with actionable policy decisions. This coupling of system-based flow modeling using massive space-time water well datasets with detailed local-scale monitoring and data collection represents an improved framework for sustainable management of regional groundwater resources in areas where historical monitoring and oversight has been lacking.

APPENDICES

APPENDIX A: Connection between the deep bedrock aquifer and the Grand River

The connection between the bedrock aquifer and the “River Zone” was an important but necessary conceptualization; temporal analysis of bedrock SWLs along the river and narrow bands north and south of the river confirms the natural hydraulic connection to the bedrock (see Figure 3.17). If the Grand River were not well connected to the bedrock, the trend along the Grand River would be similar to the trend south of the river (where significant pumping has occurred). However, a relatively flat trend is observed along the river and north of the river, which is consistent with the Grand River being connected to the bedrock aquifer (see the final vertical anisotropy values for the River Zone in Calibration Results). The conceptualization used here is supported by the known existence of relatively thin alluvium deposits (<40m) over the bedrock surface and localized occurrences of boulder-rich alluvial deposits along the Grand River throughout the study domain (Churches and Wampler 2013).

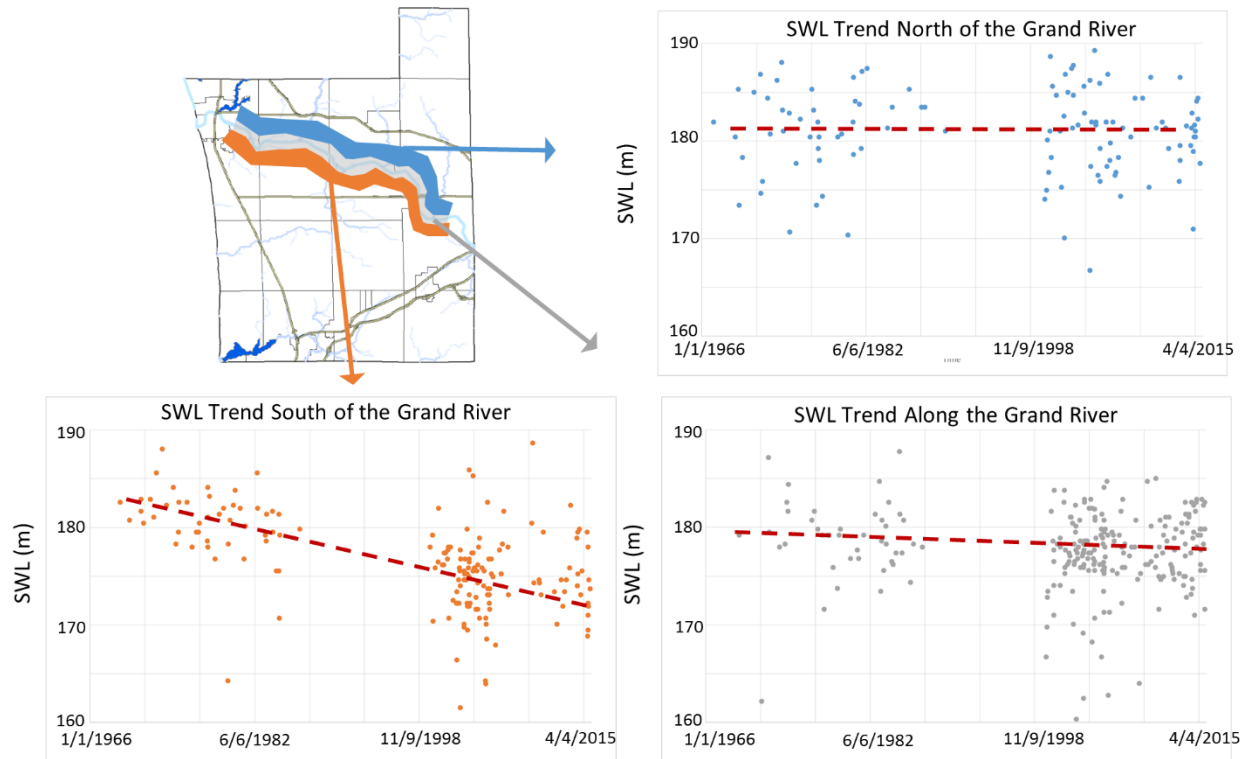


Figure 3.17: Comparison of SWL trends for bands north and south of the Grand River, and along it. Data are from Wellogic (MDEQ, 2014).

APPENDIX B: Justification for using two separate layers to represent the bedrock aquifer

The choice of using a separate layer to represent the ‘fractured zone’ of the Marshall Formation is based on the standard geologic rule that fracturing decreases with depth, so that the effective transmissivity of the aquifer changes by roughly an order of magnitude when going from fractured to non-fractured. The depth of the fractured zone was estimated by examining the penetration depth of water wells extracted from Wellogic into the bedrock, assuming that the wells would not be drilled into non-fractured (and thus, non-productive) depths of the Marshall. Many cross-sections were taken utilizing the IGW software to determine 18.3m (60 ft.) as a reasonable ‘fracture depth’. The Bayport Limestone and Saginaw Formation units shown in Figure 3.2 are relatively thin (<30m) in this part of the Michigan basin (Apple and Reeves 2007), and therefore were not explicitly modeled. Note that a minimum thickness of 60 ft. was assigned for both bedrock layers, even in eastern portions of the model domain where the only unit present is the Coldwater Shale, which is not an effective transmitter of water, and calibration data are lacking. This was done to alleviate issues related to numerical stability when trying to solve hydraulic head across a computational layer with significant variability in thickness.

APPENDIX C: Accounting for switches to municipal water supply

During model development it became clear that the assumption of all wells pumping ad infinitum once installed was problematic in some areas of the study domain where municipal surface water supply became available in recent years. In these areas, many older wells were abandoned as properties tapped into nearby public water distribution systems. Therefore, we carefully examined the evolution of the water distribution system for a key area in the central portion of the study area to terminate pumping at the appropriate times and locations (see Figure 3.18). Scanned drawings made available from the Ottawa County Public Utilities Department were converted into shapefiles, and wells constructed in polygons with installation dates prior to the year assigned to the polygons were terminated (i.e., turned off) in the year indicated by the polygon. If a well was installed within a polygon after the year assigned to polygon, it was assumed that the property was choosing to use groundwater over municipal surface water supply, and the pumping would continue throughout the groundwater simulation. In two areas of the study domain, detailed maps of the water system distribution were not available, but municipal water supply was first provided in 1995, and thus, the simplest treatment was to terminate wells installed prior to 1995 in these areas (see the smaller map in Figure 3.18) once the simulation proceeded through 1995.

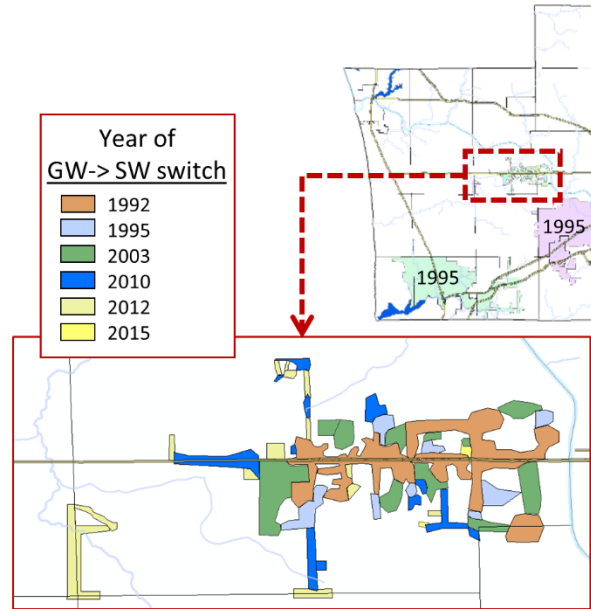


Figure 3.18: Polygons use to represent areas where municipal water supply became available at different times since 1992. “GW-> SW” is a shortened form of “groundwater to municipal water supply.”

APPENDIX D: Model well density vs. actual well density

There are roughly 1.3 million water wells in Michigan (MDEQ 2015), but thus far only about 550,000 wells have been incorporated into the Wellogic database. Although some areas of the state are more 'complete' than others, undoubtedly some domestic wells are missing from the model, and thus it is reasonable to have a simulated domestic pumping rate a few times higher than the observed pumping rate, assuming the relative spatial density distribution of the well dataset used for modeling represents the actual relative spatial density distribution. This assumption was checked for a portion of the model domain by completely exhausting information from local water well records compiled by the Ottawa County Environmental Health Department and 'visually' adding wells to the analysis: if properties did not have a well record and were not in proximity to a public water distribution line, a well was assumed to exist on the property (see Figure 3.19). Indeed, the relative spatial density distribution of the dataset used for modeling and that of the 'actual' well network is similar. Moreover, there are roughly 3 times as many wells in the latter dataset (most of which are domestic wells) as compared to the former dataset, suggesting that the ratio of 3.39 for simulated domestic pumping rate to observed pumping rate is accurate in terms of producing the overall impact of domestic well withdrawals.

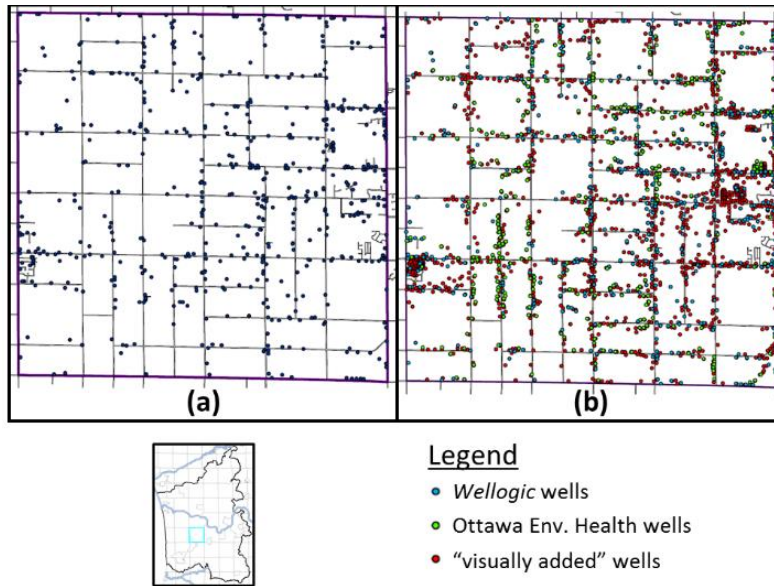


Figure 3.19: Comparison of well distribution in Blendon Township, Michigan (central portion of model domain): (a) from Wellogic only (834 wells); and (b) from Wellogic, Ottawa County Dept. of Environmental Health, and “visually added wells” (about 2500 wells).

REFERENCES

REFERENCES

- Alcolea, A., Castro, E., Barbieri, M., Carrera, J., & Bea, S. (2007). Inverse modeling of coastal aquifers using tidal response and hydraulic tests. *Groundwater*, 45(6), 711-722.
- Anderson, M. P., Woessner, W. W., & Hunt, R. J. (2015). *Applied groundwater modeling: simulation of flow and advective transport* (Second edition). London ; San Diego, CA: Academic Press.
- Bajc, A.F., Russell, H.A. and Sharpe, D.R., 2014. A three-dimensional hydrostratigraphic model of the Waterloo Moraine area, southern Ontario, Canada. *Canadian Water Resources Journal/Revue canadienne des ressources hydriques*, 39(2), pp.95-119.
- Best, L. C., & Lowry, C. S. (2014). Quantifying the potential effects of high-volume water extractions on water resources during natural gas development: Marcellus Shale, NY. *Journal of Hydrology: Regional Studies*, 1, 1-16.
- Blackport, R.J., Meyer, P.A. and Martin, P.J., 2014. Toward an understanding of the Waterloo Moraine hydrogeology. *Canadian Water Resources Journal/Revue canadienne des ressources hydriques*, 39(2), pp.120-135.
- Carle, S.F. (1999). T_PROGS: Transition probability geostatistical software. University of California, Davis, CA.
- Carle, S. F., & Fogg, G. E. (1996). Transition probability-based indicator geostatistics. *Mathematical geology*, 28(4), 453-476.
- Carle, S. F., & Fogg, G. E. (1997). Modeling spatial variability with one and multidimensional continuous-lag Markov chains. *Mathematical Geology*, 29(7), 891-918.
- Carrera, J., Alcolea, A., Medina, A., Hidalgo, J., & Slooten, L. J. (2005). Inverse problem in hydrogeology. *Hydrogeology journal*, 13(1), 206-222.
- Curtis, Z.K., Li, S.G., Liao, H.S. and Lusch, D., 2018. Data-Driven Approach for Analyzing Hydrogeology and Groundwater Quality Across Multiple Scales. *Groundwater*, 56(3), pp.377-398.
- Davison, J.H., Hwang, H.T., Sudicky, E.A. and Lin, J.C., 2015. Coupled atmospheric, land surface, and subsurface modeling: Exploring water and energy feedbacks in three-dimensions. *Advances in water resources*, 86, pp.73-85.
- Feinstein, D.T., Hunt, R.J. and Reeves, H.W. 2010. Regional groundwater-flow model of the Lake Michigan Basin in support of Great Lakes Basin water availability and use studies. U. S. Geological Survey Scientific Investigations Report 2010-5109. *Applied hydrogeology* (4th ed). Upper Saddle River, N.J: Prentice Hall.
- Feinstein, D.T., Fienen, M.N., Reeves, H.W. and Langevin, C.D., 2016. A Semi-Structured MODFLOW-USG Model to Evaluate Local Water Sources to Wells for Decision Support. *Groundwater*, 54(4), pp.532-544.
- Freeze, R. A., & Cherry, J. A.. 1979. *Groundwater*. Englewood Cliffs, New Jersey: Prentice-Hall, Inc.

- Frind, E.O. and Middleton, T.A., 2014. Toward water sustainability for Waterloo Region. *Canadian Water Resources Journal/Revue canadienne des ressources hydriques*, 39(2), pp.88-94.
- Frind, E.O., Molson, J.W., Sousa, M.R. and Martin, P.J., 2014. Insights from four decades of model development on the Waterloo Moraine: A review. *Canadian Water Resources Journal/Revue canadienne des ressources hydriques*, 39(2), pp.149-166.
- Fry, J., Xian, G., Jin, S., Dewitz, J., Homer, C., Yang, L., Barnes, C., Herold, N., and Wickham, J. 2011. Completion of the 2006 National Land Cover Database for the Conterminous United States, *PE&RS*, Vol. 77(9):858-864.
- Gronewold, A. D., Clites, A. H., Smith, J. P., & Hunter, T. S. (2013). A dynamic graphical interface for visualizing projected, measured, and reconstructed surface water elevations on the earth's largest lakes. *Environmental modelling & software*, 49, 34-39.
- GWIM. (2006). "Groundwater Inventory and Map Project", State of Michigan Public Act 148.
- He, X., Koch, J., Sonnenborg, T. O., Jørgensen, F., Schamper, C., & Christian Refsgaard, J. (2014). Transition probability-based stochastic geological modeling using airborne geophysical data and borehole data. *Water Resources Research*, 50(4), 3147-3169.
- ISGS (2015). Illinois State Geological Survey. ILWATER, Repository for records of wells drilled in the State of Illinois (periodically updated). Available at: <http://www.isgs.illinois.edu/ilwater>
- IGS (2016). Iowa Geological Survey, based at IIHR – Hydrosceience & Engineering, University of Iowa. Available at: <https://www.iihr.uiowa.edu/igs/geosam/home>
- Institute of Water Research (IWR), Department of Civil and Environmental Engineering. 2013. Ottawa County Water Resource Study Final Report. East Lansing, Michigan: Michigan State University.
- KGS (2002). Kansas Geological Survey. WIZARD, water well levels database (periodically updated). Available at: <http://www.kgs.ku.edu/Magellan/WaterLevels/index.html>
- Kreutzwiser, R.D., De Loë, R.C., Durley, J. and Priddle, C., 2004. Water allocation and the permit to take water program in Ontario: Challenges and opportunities. *Canadian Water Resources Journal*, 29(2), pp.135-146.
- Li, S.G. and McLaughlin, D. (1991). A nonstationary spectral method for solving stochastic groundwater problems: Unconditional analysis. *Water Resources Research*, 27(7), pp.1589-1605.
- Li, S.G., and Q. Liu. (2006). A Real-Time, Interactive Steering Environment for Integrated Ground Water Modeling." *Ground Water* 44(5), pg. 758-763.
- Li, S.G., Liu, Q., Afshari, S. (2006). An Object-oriented hierarchical patch dynamics paradigm (HPDP) for modeling complex groundwater systems across multiple scales. *Environmental Modeling and Software*, 21(5) 2006.
- Li, S.G., Liao, H.S. and Ni, C.F. (2004). Stochastic modeling of complex nonstationary groundwater systems. *Advances in water resources*, 27(11), pp.1087-1104.

- Liao, H.S. Sampath, P.V., Curtis, Z.K., Li, S.G. (2015a). Hierarchical modeling and parameter estimation for a coupled groundwater lake system. *Journal of Hydrologic Engineering*, 20(11), pg. 04015027. DOI: 10.1061/(ASCE)HE.1943-5584.0001219.
- Liao, H.S., Sampath, P.V., Curtis, Z.K. and Li, S.G. (2015b). Hierarchical modeling of a groundwater remediation capture system. *Journal of Hydrology*, 527, pp.196-211.
- Liu, X., & Kitanidis, P. K. (2011). Large-scale inverse modeling with an application in hydraulic tomography. *Water Resources Research*, 47(2).
- MDEQ. (2014). Michigan Department of Environmental Quality. *Wellogic System* (periodically updated). Available at: available at <https://secure1.state.mi.us/wellogic/>.
- MDEQ. (2018). Michigan Department of Environmental Quality, Drinking Water & Municipal Assistance Division. *MDEQ Groundwater Statistics* [Fact Sheet]. Retrieved from: http://www.michigan.gov/deq/0,4561,7-135-3313_3675_3694-81746--,00.html
- MSU. (2014). Michigan Groundwater Management Tool. East Lansing, Michigan: Department of Environmental Engineering, Michigan State University.
- National Ground Water Association (NGWA). 2016. National Ground Water Association. Groundwater Use in Michigan [Fact sheet]. <http://www.ngwa.org/Documents/States/Use/mi.pdf> (accessed December 20, 2016).
- NED USGS. (2006). National Elevation Dataset. US Department of Interior: United States Geological Survey, <http://ned.usgs.gov/Ned/about.asp>.
- NHD USGS. (2010). USGS: National Hydrography Dataset. US Department of Interior: United States Geological Survey, <http://nhd.usgs.gov/index.html>
- Neuman, S. P. (2004). Stochastic groundwater models in practice. *Stochastic Environmental Research and Risk Assessment*, 18(4), 268-270.
- Ottawa County, Michigan. 2014. Environmental Health—Scanned Well & Water Quality files (continuously updated). (accessed Nov. 2014–Sept. 2015).
- PRISM Climate Group, Oregon State University, <http://prism.oregonstate.edu>, created 4 Feb 2004.
- Reitz, M., Sanford, W.E., Senay, G.B. and Cazenias, J. (2017). Annual Estimates of Recharge, Quick-Flow Runoff, and Evapotranspiration for the Contiguous US Using Empirical Regression Equations. *JAWRA Journal of the American Water Resources Association*, 53(4), pp.961-983.
- Renard, F., & Jeannée, N. (2008). Estimating transmissivity fields and their influence on flow and transport: The case of Champagne mounts. *Water resources research*, 44(11).
- Ruud, N., Harter, T., & Naugle, A. (2004). Estimation of groundwater pumping as closure to the water balance of a semi-arid, irrigated agricultural basin. *Journal of hydrology*, 297(1), 51-73.
- Risser, D.W., Thompson, R.E. and Stuckey, M.H. (2008). Regression method for estimating long-term mean annual ground-water recharge rates from base flow in Pennsylvania (No. 2008-5185). US Geological Survey.

- Sampath, P.V., Liao, H.S., Curtis, Z.K., Doran, P.J., Herbert, M.E., May, C.A., and Li, S.G. 2015. Understanding the Groundwater Hydrology of a Geographically-Isolated Prairie Fen: Implications for Conservation. *PLOS ONE*, 10(10), pg. e0140430. DOI:10.1371/journal.pone.0140430.
- Sampath, P. V., Liao, H. S., Curtis, Z. K., Herbert, M. E., Doran, P. J., May, C. A., Landis, D.A., and Li, S. G. 2016. Understanding fen hydrology across multiple scales. *Hydrological Processes*, 30(19), pp. 3390-2407.
- Shen, C. and Phanikumar, M.S. (2010). A process-based, distributed hydrologic model based on a large-scale method for surface–subsurface coupling. *Advances in Water Resources*, 33(12), pp.1524-1541.
- Soil Survey Staff Natural Resources Conservation Service (SSS NRCS), United States Department of Agriculture. Soil Survey Geographic (SSURGO) Database for west-central southern Michigan. Available online at <https://gdg.sc.egov.usda.gov/>. Accessed October 10, 2016.
- Sun, N. Z., Yang, S. L., & Yeh, W. W. G. 1998. A proposed stepwise regression method for model structure identification. *Water Resources Research*, 34(10), 2561-2572.
- Taylor, C.J. and Alley, W.M. (2001). Ground-water-level monitoring and the importance of long-term water-level data (Vol. 1217). Geological Survey (USGS).
- Traum, J. A., Phillips, S. P., Bennett, G. L., Zamora, C., & Metzger, L. F. 2014. Documentation of a groundwater flow model (SJRRPGW) for the San Joaquin River Restoration Program study area, California (No. 2014-5148). US Geological Survey.
- United States (US) Census Bureau. 2017. Cumulative Estimates of Resident Population Change and Rankings: April 1, 2010 to July 1, 2016 [Data table]. <https://factfinder.census.gov/faces/tableservices/jsf/pages/productview.xhtml?src=bkmk> (accessed 08, 2017).
- U.S. Geological Survey (USGS). 2008. Documentation of computer program INFIL3.0-A distributed-parameter watershed model to estimate net infiltration below the root zone: U.S. Geological Survey Scientific Investigations Report 2008-5006, 98 p. (Online only)
- U.S. Geological Survey (USGS). 2016. National Water Information System data available on the World Wide Web (USGS Water Data for the Nation), accessed [July 23 2017], at URL [<http://waterdata.usgs.gov/nwis/>].
- Wheater, H.S. and Gober, P., 2015. Water security and the science agenda. *Water Resources Research*, 51(7), pp.5406-5424.
- Weissmann, G.S., Carle, S.F. and Fogg, G.E. (1999). Three-dimensional hydrofacies modeling based on soil surveys and transition probability geostatistics. *Water Resources Research*, 35(6), pp.1761-1770.
- Westjohn, D.B., T.L. Weaver, and K.F. Zacharias. 1994. Hydrogeology of Pleistocene glacial deposits and Jurassic red beds in the central lower peninsula of Michigan. Water-Resources Investigations Report.
- Zheng, C., & Gorelick, S. M. (2003). Analysis of solute transport in flow fields influenced by preferential flowpaths at the decimeter scale. *Groundwater*, 41(2), 142-155.

Zhou, H., Gómez-Hernández, J. J., & Li, L. (2014). Inverse methods in hydrogeology: Evolution and recent trends. *Advances in Water Resources*, 63, 22-37.

Zhu, J., & Yeh, T. C. J. (2006). Analysis of hydraulic tomography using temporal moments of drawdown recovery data. *Water Resources Research*, 42(2).

CHAPTER 4

A Multiscale Assessment of Shallow Groundwater Salinization in Southern Michigan

Contributing authors: Zachary Curtis, Hua-Sheng Liao, Shu-Guang Li, Prasanna Sampath, David Lusch

4.1 Executive Summary of Ch. 4

Managing non-point-source (NPS) pollution of groundwater systems is a significant challenge because of the heterogeneous nature of the subsurface, high costs of data collection, and the multitude of scales involved. In this study, we assessed a particularly complex NPS groundwater pollution problem in southern Michigan, namely, the salinization of shallow aquifer systems due to natural upwelling of deep brines. We applied a system-based approach to characterize, across multiple scales, the integrated groundwater quantity-quality dynamics associated with the brine upwelling process, assimilating a variety of modeling tools and data - including massive statewide water well datasets scarcely used for larger scientific analysis. Specifically, we combined 1) data-driven modeling of massive amounts of groundwater/geologic information across multiple spatial scales with 2) detailed analysis of groundwater salinity dynamics and process-based flow modeling at local scales. Statewide "hot-spots" were delineated and county-level severity rankings were developed based on dissolved chloride (Cl) concentration percentiles. Within local hot spots, the relative impact of upwelling was determined to be controlled by: i) streams - which act as 'natural pumps' that bring deeper (more mineralized) groundwater to the surface; ii) the occurrence of nearly impervious geologic material at the surface - which restricts freshwater dilution of deeper, saline groundwater; and iii) the space-time evolution of water well withdrawals – which appears to slowly induces migration of saline groundwater from its natural course. This multi-scale, data-intensive approach significantly improved our understanding of the brine upwelling processes in Michigan, and has applicability elsewhere given the growing availability of statewide water well databases.

4.2 Ch. 4 Introduction

In coastal and low-lying regions of the Lower Peninsula of Michigan (hereafter referred to as Lower Michigan), shallow, saline groundwater occurs, with total dissolved solids (TDS) concentrations

approaching and, in some cases, exceeding 1000 mg/L (Lane 1899; Long et al., 1988; Rheaume, 1991; Ging et al. 1996; Meissner et al. 1996; Westjohn and Weaver 1996b; Wahrer et al. 1996). More recently, the presence of a number of “salt springs” occurring on mineral soil saturated by sodium- and chloride-laden groundwater have been reported at isolated inland locations along major river valleys of central Lower Michigan (Albert 2001; Kost et al. 2007). Such saline groundwater is unfit for human consumption and many agricultural uses, and is detrimental to the environment (Ayers and Westcot, 1985).

In the absence of ocean influences and salt deposits, natural concentrations of dissolved Cl for most shallow aquifers in the mid-continent region of North America are typically less than 15 mg/L (Hem 1985). Of course, anthropogenic sources such as septic tanks, agricultural fertilizers (KCl) or roadway deicers – of which NaCl is the dominant type in Michigan (see Rustem et al. 1993) – may contribute to Cl contamination of groundwater. However, the resulting groundwater concentrations of dissolved Cl from such sources is expected to be well below the reported concentrations approaching (or exceeding) 1000 mg/L (Curtis et al. 2018). There is, however, mounting evidence from site-specific, geochemical studies that salinization in parts of Lower Michigan is due to the natural upward movement of deep brines, which are hypersaline pools of groundwater in the deep geologic formations of the Michigan Basin (TDS > 100,000 mg/L). Geochemical and isotopic analyses, geochemical modeling and an interpretation of groundwater flow was used to show that upwelling brine is the source for the high-salinity groundwater in the Saginaw Lowlands (Long et al. 1988; Kolak et al. 1999) (see Figure 1.2 in Chapter 1) – a major basin-scale groundwater discharge area (Westjohn et al. 1994; Hoaglund et al., 2002). Geochemical indicators of brine-influenced groundwater were also observed in the formation waters of the Antrim Shale bedrock unit in northern Lower Michigan (McIntosh et al. 2004) and from the shallower Marshall Formation in south-central Lower Michigan (Ma et al. 2005). In the Michigan Lowlands of west-central Lower Michigan (Figure 1.2) – also a major regional groundwater discharge area – chloride:sodium molar ratios derived from well water analyses suggest that brines are at least partially responsible for elevated groundwater salinity observed in this region (Long et al. 2015).

Westjohn and Weaver (1996b) suggested that the distribution of shallow, saline groundwater in the regional aquifer system is controlled largely by the broad-scale geology: discharge of saline water from bedrock aquifers into these regional lowlands coupled with the impedance of freshwater recharge by low K glacial deposits. Indeed, the findings of geochemical studies of the sources of shallow, saline groundwater in Lower Michigan suggests that the seemingly scattered occurrences are actual symptomatic of a larger, system-wide problem, namely, brines preferentially upwelling into coastal low-lying areas (*i.e.*, regional groundwater discharge areas). Curtis et al. (2017) probed this interpretation with a multi-scale, data-driven analysis of chloride (Cl) concentrations (as a proxy for salinity) and long-term Static Water Level (SWL) spatial dynamics across Lower Michigan, focusing on the Michigan and Saginaw Lowlands for subregional and local-scale analyses. The primary finding from this study was that, at each scale, chloride concentrations in discharge zones, where groundwater is expected to flow primarily upwards, are consistently and significantly higher than those in recharge zones (see Figure 4.1). A synoptic sampling campaign in the Michigan Lowlands showed Cl concentrations generally increase with depth (Curtis et al. 2018), a trend noted in previous studies of brine upwelling in the Saginaw Lowlands (Long et al., 1988). These consistent Cl distribution patterns across multiple spatial scales – along with the findings from previous geochemical studies – strongly suggest that natural upwelling of brines is the primary cause for the elevated chloride concentrations observed in discharge areas across the Lower Peninsula.

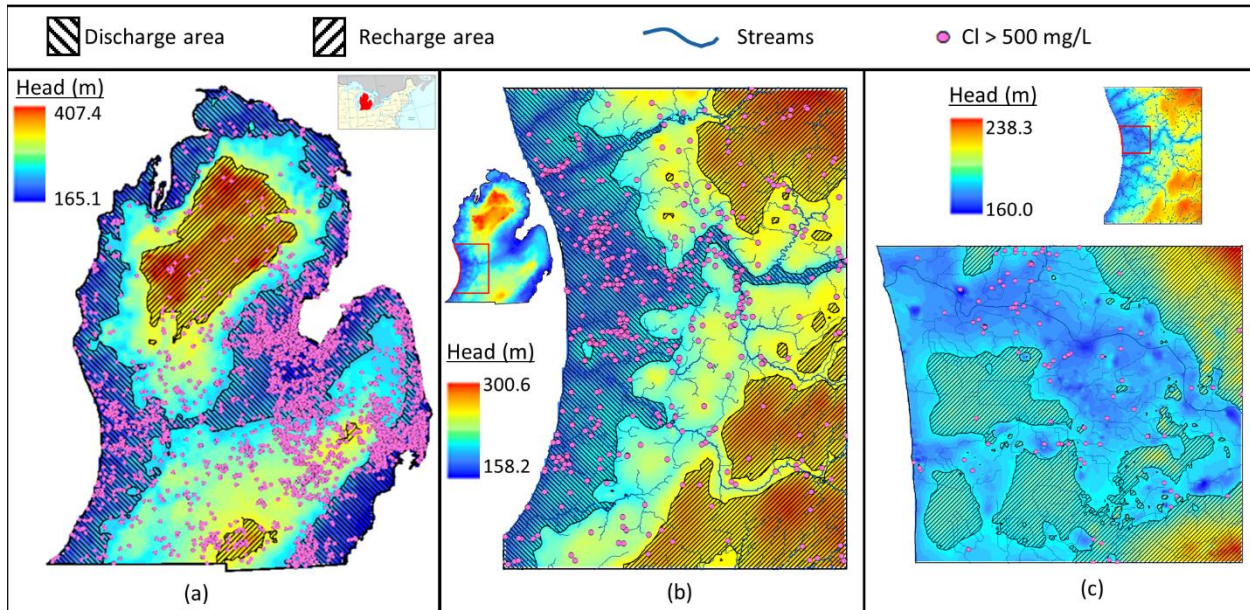


Figure 4.1: Occurrence of wells with elevated Cl concentrations (>500 mg/L) and static water level (SWL) distributions at the (a) basin-scale; (b) regional scale (Michigan Lowlands); and (c) local scale (central Michigan Lowlands). Adapted from Curtis et al. (2018).

The previously mentioned studies were critical for developing a conceptual understanding of the natural hydrogeologic process that largely controls the occurrence of shallow, saline groundwater in parts of Lower Michigan, namely, the upwelling of deep brines into low-lying discharge areas. However, translating these findings into ‘operational’ information for resource managers and planners proves challenging. Data, maps, and analyses from different studies related to the brine upwelling process in Lower Michigan have been completed at one particular scale and for one particular time, but an overarching investigation linking them as a unified body of work is lacking. As a result, a number of important management questions are left unanswered, including:

- Where is contamination is the worst? How can we prioritize resources for further study and sustainable management?
- To what degree does the local environment (geology, surface network, etc.) impact the 3D spatial characteristics of the pollution?

- Is human activity (e.g., pumping of groundwater) making the pollution worse, i.e., are we inducing the migration of brine-influenced groundwater into new areas?

In this chapter, these key management questions are addressed by performing a multi-scale, integrated analysis of groundwater flow and water quality dynamics associated with the brine upwelling process. Statewide characterization of groundwater salinity and hydrogeology is supplemented with a detailed modeling study of the shallow aquifer underling Ottawa County, Michigan – which sits squarely and almost entirely within the Michigan Lowlands (see Figure 1.2). The specific tasks are to: 1) characterize, at multiple spatial scales, groundwater salinity dynamics (and its controls) across the Lower Peninsula of Michigan, 2) delineate the three-dimensional (3D) spatial distribution (extent and severity) of the groundwater salinity in a county-wide aquifer system to better understand local sources and controls of the groundwater salinity; 3) evaluate long-term temporal trends of groundwater quality (salinity) and describe the impacts of pumping.

4.3 Overview of Ch. 4 Methods

To address the specific tasks of this study, it is necessary to account for the various mechanisms controlling the subsurface dynamics of brine-influenced groundwater, including aspects of geology (e.g., extent and distribution of geologic materials that control large- and small-scale flow patterns), hydrology (e.g., head distribution, pumping and the flow system response), and water quality (spatial and temporal dynamics of groundwater salinity). Because the current (and relatively recent) water quality and flow system observations reflect impacts of both humans and the natural upwelling processes, a characterization of past conditions is needed to determine if (and how) human activity affects the severity and extent of contamination. Yet, even for a regional or subregional analysis, data collected for scientific purposes typically lacks sufficient spatial and temporal coverage to characterize the system across years or decades because of the undocumented and strongly heterogeneous nature of the subsurface, the high costs of data collection, and the multitude of scales involved with the brine pollution process. This is problematic, as

changes in water quality due to migration of lower quality groundwater from adjacent/underlying geologic units may be slow (i.e., occurring across many years or decades).

This study capitalized on a vast storehouse of pre-existing groundwater/environmental data integrated into recently assembled federal and statewide databases, including two high-density water well datasets maintained by the State of Michigan. The *Wellogic* database contains massive amounts of physical groundwater data (e.g., static water levels in water wells and borehole lithology) (MDEQ 2015). The *WaterChem* database contains water quality information from over 1 million samples collected from water wells and analyzed at the State of Michigan's Drinking Water Analysis Laboratory (MDEQ 2010). These datasets contain many errors and sources of inaccuracy and have rarely been used for larger scientific investigations, but they can yield important hydrogeologic and geochemical insights when properly processed and critically evaluated (Sampath et al. 2015; Sampath et al. 2016; Curtis et al. 2018). Local-scale analyses requiring more detailed information were augmented with field-collected data and historical water well and water use information compiled by county-level planning departments and municipalities. These massive groundwater databases enabled two distinct yet complimentary approaches for understanding groundwater conditions across multiple scales: data-driven modeling and process-based simulation. Data-driven modeling provides an efficient method for identifying patterns, relationships, and key areas across different scales without the need for understanding the underlying processes. Process-based simulation – although requiring significant expertise and resources – allows you to test and refine your understanding of the processes that control the observed patterns and relationships discovered through data-driven modeling.

The datasets and workflow used for data-driven modeling in this study are shown in Figure 4.2. The primary steps were to : 1) map groundwater salinity levels at the statewide, regional and local (county-wide) to identify “hot-spots” at different spatial scales; 2) delineate long-term, average groundwater levels and aquifer material distributions and extents; 3) characterize temporal trends in groundwater levels and salinity; and 4) model water use to determine its impact on groundwater levels via process-based modeling (see below). TDS concentrations are used in most geochemical studies as a measure of groundwater

salinity. In our study, we used dissolved-chloride (Cl) concentrations as a proxy for salinity because Cl concentrations were available in the historical water quality records used for this study, while TDS concentrations were not. Also, it was possible to collect far more Cl field samples than TDS samples given the resources available for this study. Nonetheless, because the brines down-dip from the Marshall subcrop are composed primarily of calcium chloride (CaCl₂) and sodium chloride (NaCl) (Ging et al. 1996), Cl was considered an effective indicator of groundwater salinity for the purposes of this study. Groundwater levels were determined from analysis of Static Water Level (SWL) measurements on the well logs, which were made at the time of installation of a water well.

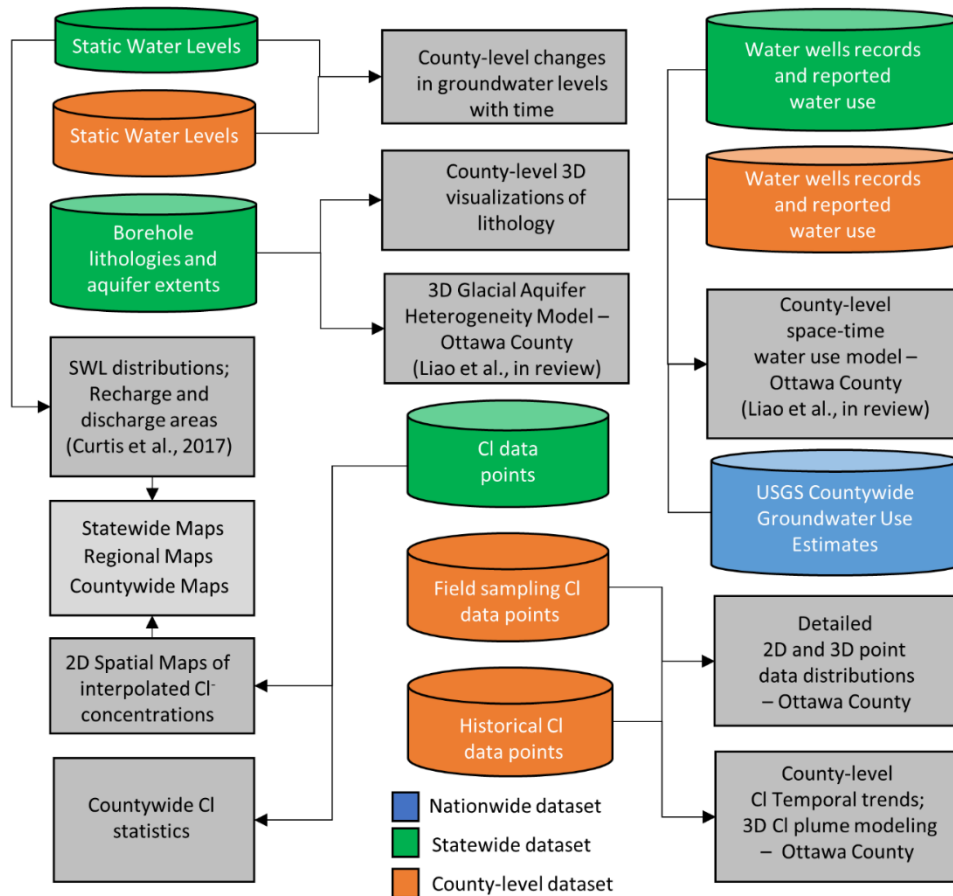


Figure 4.2: Multi-scale, data-driven modeling approach: datasets (cylinders), workflow (arrows), and resulting datasets/maps/analyses (rectangles).

The datasets and workflows associated with our process-based modeling are shown in Figure 4.3. The main goals were to: 1) evaluate the impact of long-term, distributed pumping on groundwater levels; 2) compare

Cl concentrations to groundwater level dynamics; and 3) visualize deep groundwater flow. Some of the results from the data-driven analysis were used as input for calibration of the process-based flow simulator (e.g., space-time water use model, changes in groundwater levels with time), while others (e.g., Cl point data) were used for comparative analysis with outputs of the process-based flow simulation. The details of the process-based flow model development are provided in Liao et al (in review). The model integrated a complex, fully three-dimensional (3D) glacial geologic material model, a sector-based dynamic water use model for the years 1966-2015, and a transient recharge model based on temperature and precipitation observations from the PRISM Climate Group and created using INFIL 3.0 (USGS, 2008). Water well records were used to develop a Transition Probability (TP) geostatistical model of the glacial aquifer system (Carle, 1999) and provided the necessary information to develop a sector-based water use model, including well type (domestic, public supply, irrigation, or industrial/commercial), well construction date, well screen interval, and well location (latitude and longitude). Thousands of SWLs from water well records across space and time were used to calibrate the model.

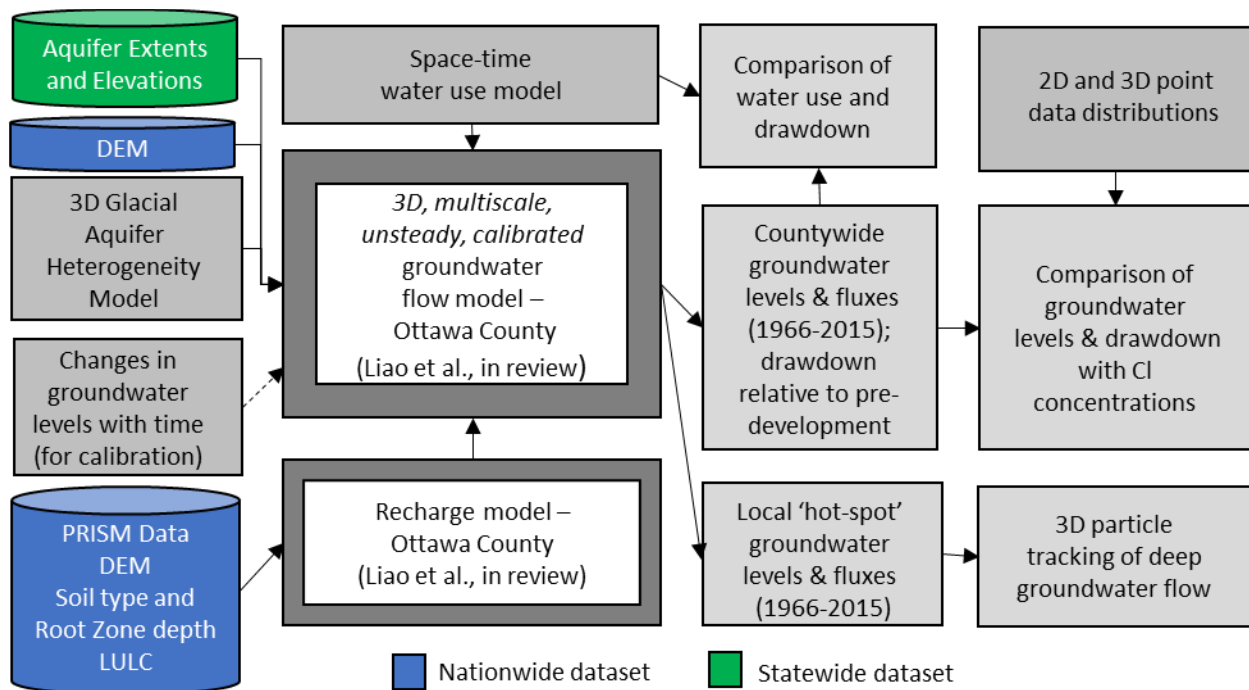


Figure 4.3: Multi-scale, process-based modeling approach and integrated analyses and spatial overlays.

The following sections provide more details on the different analyses, results and interpretations. The data-driven characterization of statewide groundwater conditions is presented first, followed by the detailed modeling, visualization, and analysis of groundwater in Ottawa County.

4.4 Statewide Data-Driven Characterization of Groundwater Conditions

To delineate statewide and regional salinity ‘hot-spots’, chloride concentrations were spatially interpolated from samples in the *WaterChem* database at both a 3x3 km and a 1x1 km cell size. Interpolation used a non-stationary kriging technique described in Curtis et al. (2018) that utilizes the nearest N points for modeling spatial variability and estimating values at node locations in a two-dimensional grid. No differentiation was made between samples collected from wells completed in shallow glacial deposits and deeper bedrock aquifers, as this information is not contained in the *WaterChem* records.

As shown in Figure 4.4, four regions stand out as statewide hot-spots with elevated (>20 mg/L) and severely elevated (>250 mg/L) Cl concentrations. These areas of elevated chloride concentrations are consistent with the spatial pattern of shallow mineralized groundwater that Rheume (1991) compiled. In Region 1, the nearly N-S trending hotspot occurs in Ottawa County, and the easternmost hotspot is within the Grand Rapids, high- and medium-density urban area, all of which is served by a water supply system that uses Lake Michigan as its source. Region 2 contains the largest, contiguous area of elevated and severely elevated Cl concentrations in groundwater in the State. Elevated chloride concentrations are pervasive throughout much of Bay and Saginaw counties, are common in coastal Tuscola and Arenac counties, and occur in central Midland and southern Iosco counties. As a result, most communities in this region rely on surface water from Saginaw Bay for their water-supply needs. The large area of elevated Cl concentrations in Region 3 occurs in southeastern Lenawee County. This phenomenon was studied by Caetta (1991), who concluded "... that deep bedrock brines are upwelling at specific locations and mixing with local meteoric waters, increasing total dissolved solids in unconsolidated aquifers." (Caetta, 1991, p. iii). In Region 4, the large areas of elevated chloride concentrations in southern St. Clair County, northeastern Sanilac County and eastern Huron County are all notable. The elevated chloride concentrations in southern St. Clair County

may be due, in part, to the legacy effects of poor well closure practices associated with early oil, gas and mineral wells (Curtis et al., 2017).

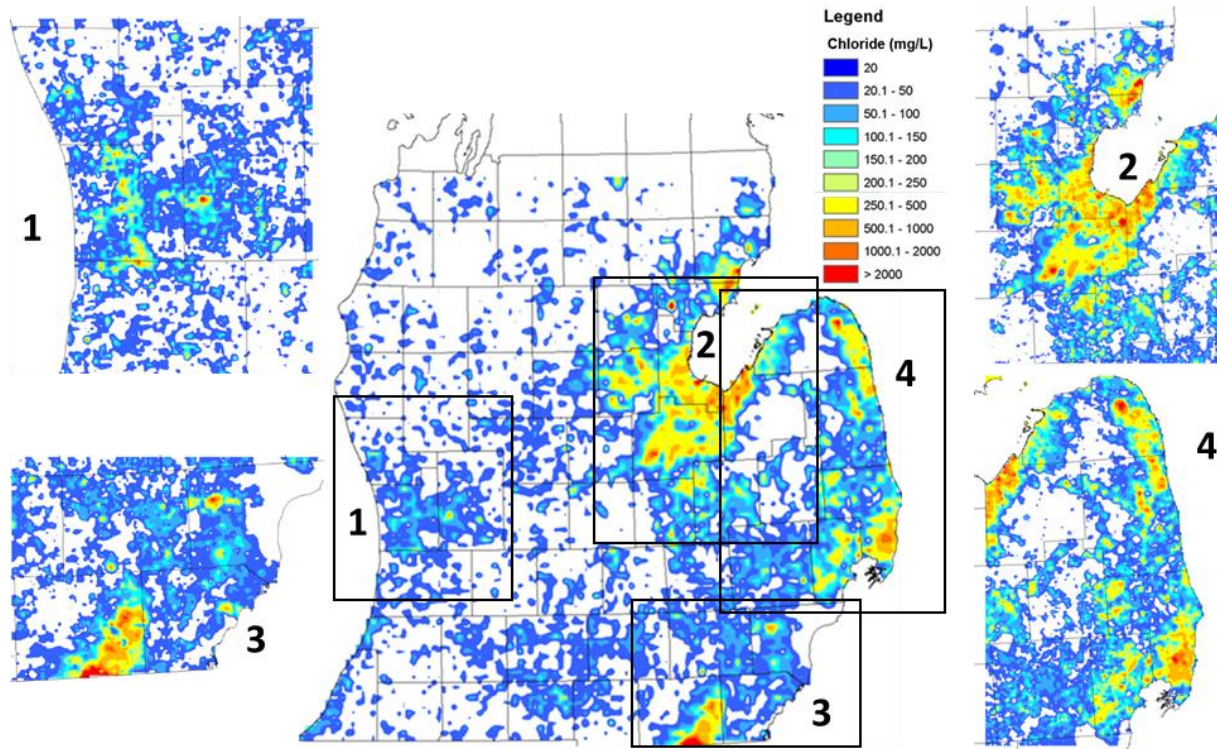


Figure 4.4: Chloride concentrations in groundwater, interpolated at the 3 km x 3 km cell size (center graphic) and at the 1 km x 1 km cell size (peripheral graphics).

The results from the statewide and regional mapping of Cl concentrations were used to identify 17 counties with notably elevated Cl concentrations. Groundwater quality ‘severity indicators’ were then developed based on countywide statistical analysis of Cl concentrations from samples in *WaterChem*. In particular, Cl concentrations were computed for 50th, 75th, and 95th percentile (e.g., the 75th Cl percentile represents the concentration that 75% of the Cl samples are less than and 25% are greater than). The 95th percentile analysis was included to give a sense of the concentrations of “extremely high” values in the datasets, while the 50th and 75th percentiles give a sense of the average and above-average concentrations, respectively. Percentiles were computed for two sets of analyses: i) using all Cl data points within an entire county; and ii) using only Cl data points existing within cropland (“cropland only” cases). The latter analysis is useful for groundwater irrigation planning, given the above-mentioned susceptibility of agricultural crops to

elevated levels of salinity. The number of data points available for analysis in each county is provided in Table 4.1. The areal extent of cropland within the seventeen counties is shown in Figure 4.5. Note that, for even the 95th percentile concentrations, a significant number of points were available for analysis (with exception to the cropland analysis of Wayne County). In other words, 95th percentile concentrations that are elevated or severely elevated represent a real problem in the aquifer system (i.e., 5% of thousands of data points are elevated or very elevated), and do not just represent outliers in the dataset.

Table 4.1: Total number of Cl scatter points available for countywide analysis and the number within cropland for each of the counties with notably elevated chloride concentrations in groundwater.

| County | Number of data points | Number of data points in cropland |
|-------------|-----------------------|-----------------------------------|
| Saginaw | 1113 | 436 |
| Macomb | 8485 | 1135 |
| Bay | 1663 | 665 |
| Saint Clair | 3597 | 781 |
| Midland | 5684 | 892 |
| Huron | 2516 | 1270 |
| Genesee | 6936 | 785 |
| Sanilac | 3488 | 1683 |
| Ottawa | 12179 | 2970 |
| Arenac | 1917 | 528 |
| Lenawee | 4170 | 1289 |
| Wayne | 752 | 20 |
| Gladwin | 4002 | 418 |
| Lapeer | 6802 | 1349 |
| Shiawassee | 5921 | 2123 |
| Iosco | 2437 | 225 |
| Tuscola | 5747 | 1919 |

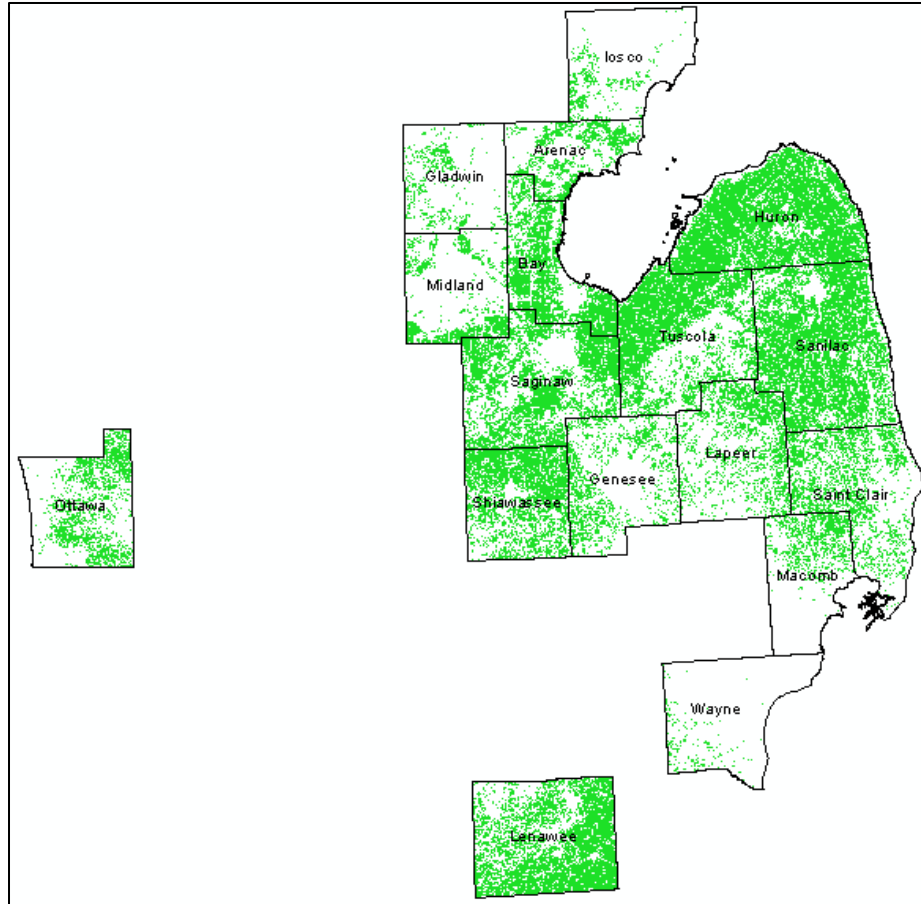


Figure 4.5: Cropland (green) within the seventeen counties analyzed for water quality severity. Source: USDA, NASS Cropland Data Layer (2014).

An illustrative example of the CI percentile results is shown in Figure 4.6, which presents spatial mapping of 95th percentile concentrations (cropland only) for each county in the Lower Peninsula of Michigan. The complete results for both the countywide and “cropland only” analyses are shown in graphical form in Figure 4.7. Regarding the countywide results, Saginaw County ranks first for the 50th and 75th percentiles, with concentrations of 78 mg/L and 314 mg/L, respectively. St. Clair County ranks first for the 95th percentile with a concentration of 811 mg/L. Five counties (Saginaw, Macomb, Bay, St. Clair and Midland) had 75th percentile CI concentrations above 200 mg/L, while 12 counties had 95th percentile CI concentrations above 250 mg/L. Regarding the “cropland only” results, three counties (Saginaw, Bay and Midland) had 75th percentile CI concentrations above 200 mg/L, while ten counties had 95th percentile CI

concentrations above 500 mg/L. The remaining seven counties had 95th percentile Cl concentrations above 250 mg/L.

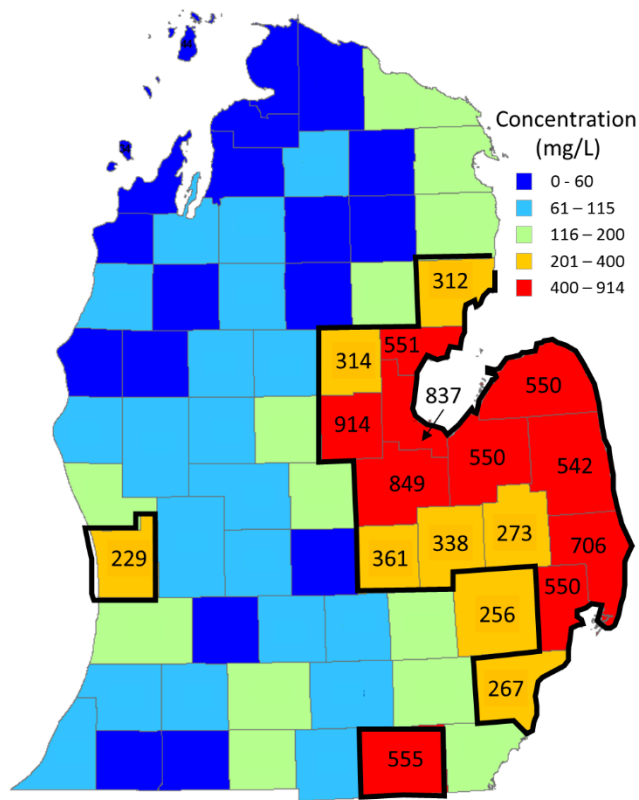


Figure 4.6: Spatial mapping of Cl concentrations for the 95th percentiles, using only scatter points existing within cropland for each county.

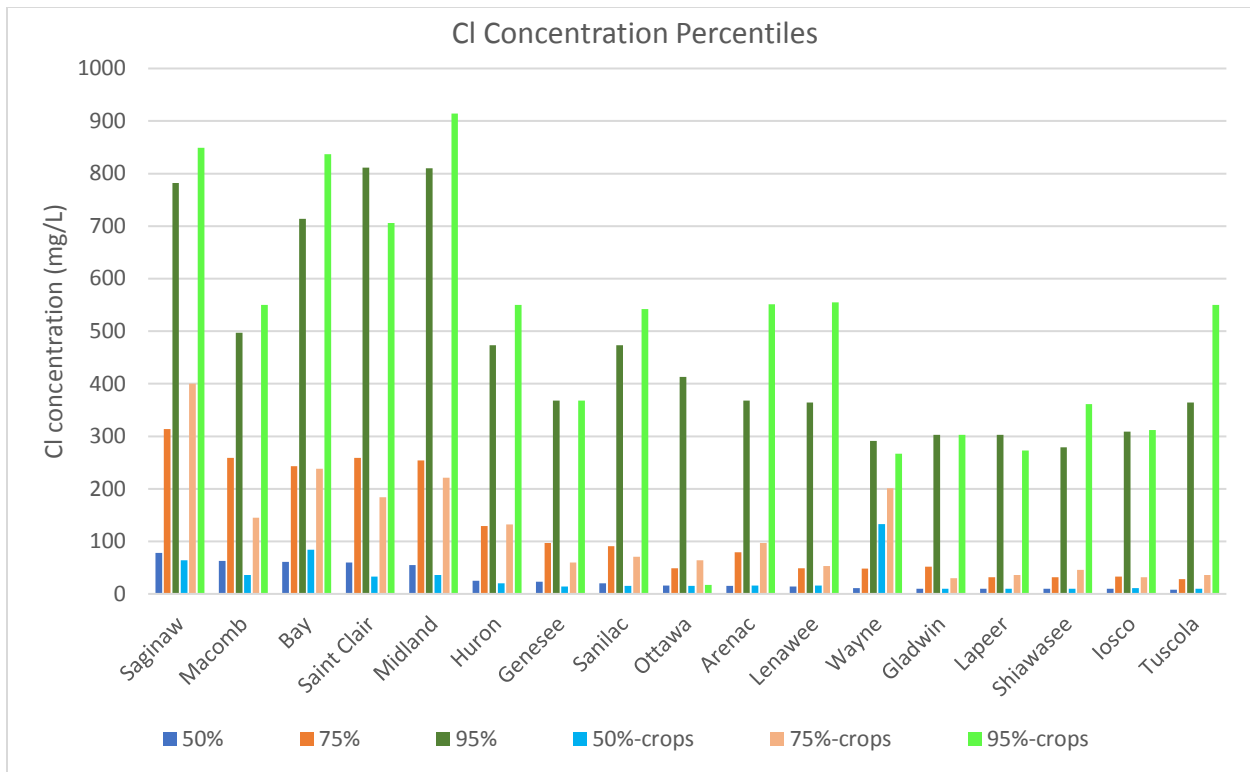


Figure 4.7: Graphical depiction of Cl concentration percentiles computed using all Cl data points available in each county (50%, 75%, 95%) and using only scatter points existing within cropland for each county (50%-crops, 75%-crops, 95%-crops).

The mapping of Cl concentrations and development of groundwater salinity severity indicators provides an improved characterization of the relative salinization of shallow groundwater supplies in different parts of Lower Michigan, which helps resource managers and decision-makers prioritize resources for future sustainability and management.

4.4.1 Screening-Level Evaluations of Local Conditions

The 17 counties used for developing countywide Cl concentration percentiles were also assessed using the data-driven approach to identify local-scale patterns and relationships between hydrogeology and groundwater salinity. For each county, we mapped: 1) Cl concentrations (point data); 2) Static Water Levels (shallow groundwater levels; 3) the 3D borehole lithology of unconsolidated sediments; and 4) bedrock formation subcrop extents. Cl concentrations were extracted from the *WaterChem* database. Long-term, average groundwater levels were mapped using spatial interpolation of SWL measurements from the *Wellogig* database. A non-stationary kriging technique using the nearest N=50 points modeled spatial

variability and estimated values at node locations (see Curtis et al. 2018 for more details). Borehole lithologic descriptions from Wellogig records are classified into four different geologic material types: aquifer ('AQ'); marginal aquifer ('MAQ'); partially confining material ('PCM'), and confining material ('CM'). Bedrock subcrop extents were obtained from the Groundwater Inventory and Map Project completed for the State of Michigan (GWIM 2006). Modeling and visualization was completed using the *Interactive Groundwater* modeling software (Li and Lui, 2006, 2008) and the Michigan Groundwater Management Tool developed for the Michigan Department of Environmental Quality (MDEQ) by Michigan State University (MSU, 2014).

The 17 counties used for developing countywide Cl concentration percentiles were also assessed using the data-driven approach to identify local-scale patterns and relationships between hydrogeology and groundwater salinity. For each county, we mapped: 1) Cl concentrations (point data); 2) Static Water Levels (shallow groundwater levels; 3) the 3D borehole lithology of unconsolidated sediments; and 4) bedrock formation subcrop extents. Cl concentrations were extracted from the *WaterChem* database. Long-term, average groundwater levels were mapped using spatial interpolation of SWL measurements from the *Wellogig* database. A non-stationary kriging technique using the nearest N=50 points modeled spatial variability and estimated values at node locations (see Curtis et al. 2017 for more details). Borehole lithologic descriptions from Wellogig records are classified into four different geologic material types: aquifer ('AQ'); marginal aquifer ('MAQ'); partially confining material ('PCM'), and confining material ('CM'). Bedrock subcrop extents were obtained from the Groundwater Inventory and Map Project completed for the State of Michigan (GWIM 2006). Modeling and visualization was completed using the *Interactive Groundwater* modeling software (Li and Lui, 2006, 2008) and the Michigan Groundwater Management Tool developed for the Michigan Department of Environmental Quality (MDEQ) by Michigan State University (MSU, 2014).

Four illustrative examples of the screening-level evaluations of Cl concentrations, groundwater levels, and subsurface geology are presented in Figure 4.8. Note that each county (Tuscola, Lenawee, Ottawa and St. Clair) is from one of the four Regions identified as a statewide Cl hotspot (and thus the selection of counties

is representative of conditions across Michigan's Lower Peninsula). In each example, Cl concentrations are highest in areas where groundwater levels are lowest (i.e., where groundwater flow is predominantly upward and discharging to the surface) along stream corridors and along freshwater coastlines. Conversely, the interfluves between major streams are mostly lacking elevated Cl concentrations. This is consistent with the multi-scale (statewide, regional, and countywide) ClSWL patterns revealed by Curtis et al. (2018) – which included local-scale analysis in Bay County (not shown here) – and supports the premise that the major source of salinity is deeper brines. Further examination of Figure 4.8 shows that the pollution is worst in areas typically associated with occurrence of low-permeability CM and PCM (e.g., clays and silts) at the surface and subcropping bedrock aquifers below. Together, these results provide further evidence that brines are preferentially impacting low-lying areas where groundwater is discharging and suggests that the relative severity and extent of groundwater salinization at local-scales is controlled in large-part by the distribution of geologic materials in the subsurface. Although these findings are not surprising or different from past studies of hydrogeology and groundwater salinity in Michigan (e.g., Long et al. 1988; Westjohn and Weaver 1996b, Curtis et al. 2018), the amount of data we used to provide detailed spatial information at these scales is unprecedented. Such detailed mapping may enable managers to prioritize resources and make management plans related to their water-supply needs.

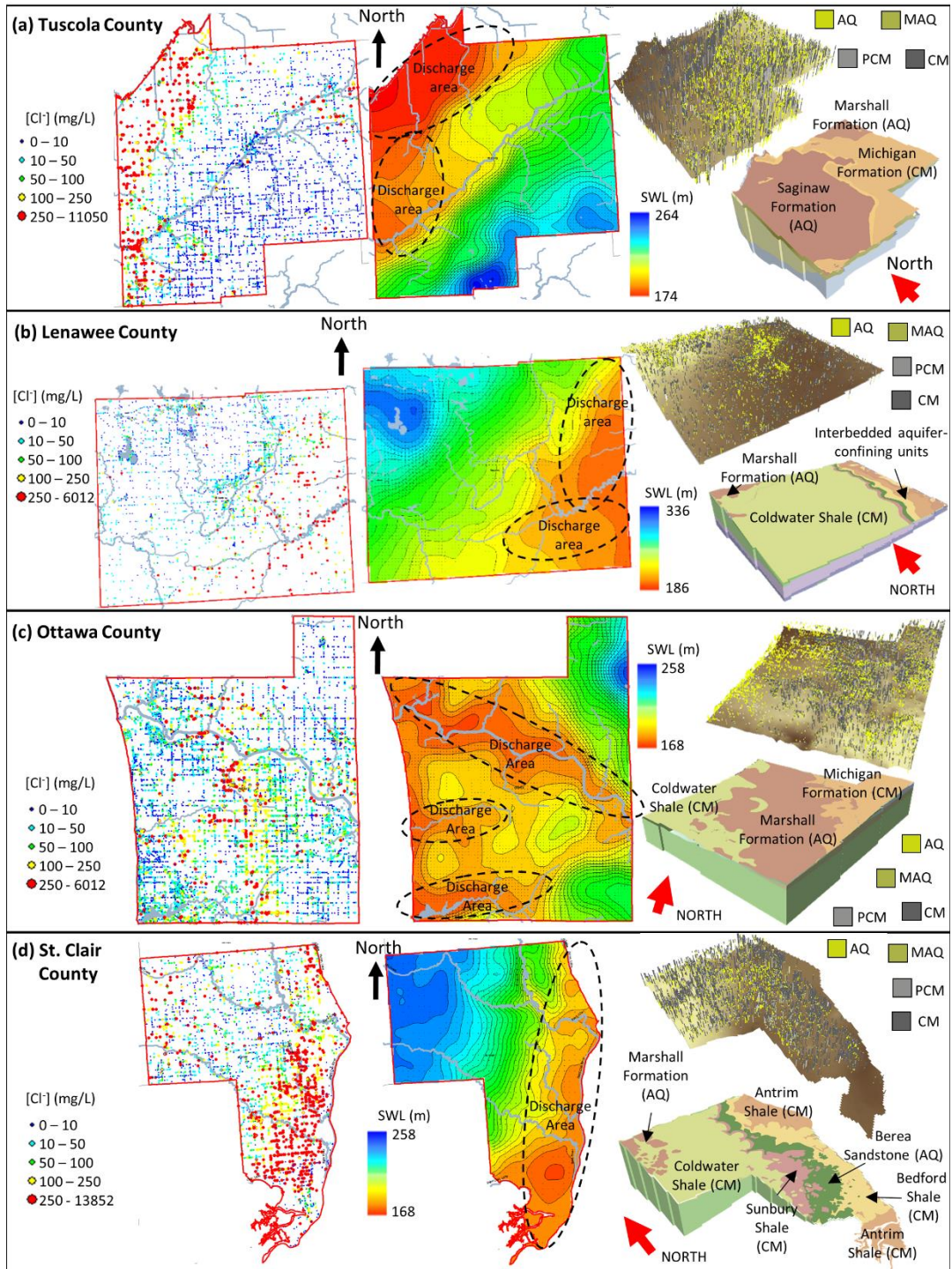


Figure 4.8: (from left to right) Screening-level mapping of chloride concentrations, SWL distributions and the stream network (gray-blue lines), glacial layer lithology, and bedrock formation subcrops: (a) Tuscola County (region 2 from Figure 4.4); (b) Lenawee County (region 3); (c) Ottawa County (region 1); and (d) St. Clair County (region 4). ‘AQ’ = aquifer, ‘MAQ’= marginal aquifer, ‘PCM’ = partially confining material, and ‘CM’ = confining material.

Temporal analysis of subsets of SWL data aggregated from selected townships were completed to identify potential impacts of pumping in these counties of concern. In many cases, it was difficult to identify a temporal trend because of the relatively large spread in SWLs due to variability introduced by spatial aggregation of observation data and noise in the measurements themselves (see Curtis et al. 2017 for more details). However, for some townships a trend was suggested for either wells screened in glacial deposits or wells completed in fractured bedrock. Figure 4.9 presents the results for the four counties analyzed in Figure 4.8. Although the estimates are approximate, and the trends were fit subjectively (by manually drawing a linear trend line that is centered about the cloud of data), as much as 9m (Tuscola County), 8m (Lenawee County), 7m (Ottawa County), and 11m (St. Clair County) of SWL decline is suggested by the analyses. In fact, water well records from 15 of the 17 counties analyzed presented evidence of SWL declines; 9 of these counties showed more than 5 meters of SWL decline. The complete results of the most compelling SWL declines are presented in Table 4.2: Compelling static water elevation declines observed within townships of the seventeen counties that were analyzed.. Clearly, in many of the seventeen counties where Cl concentrations in shallow groundwater are high (largely because of mixing with deeper brines), groundwater levels are declining. Therefore, it is possible that pumping-induced migration of brine-influenced groundwater is making the problem worse. This is explored in greater detail in the next section.

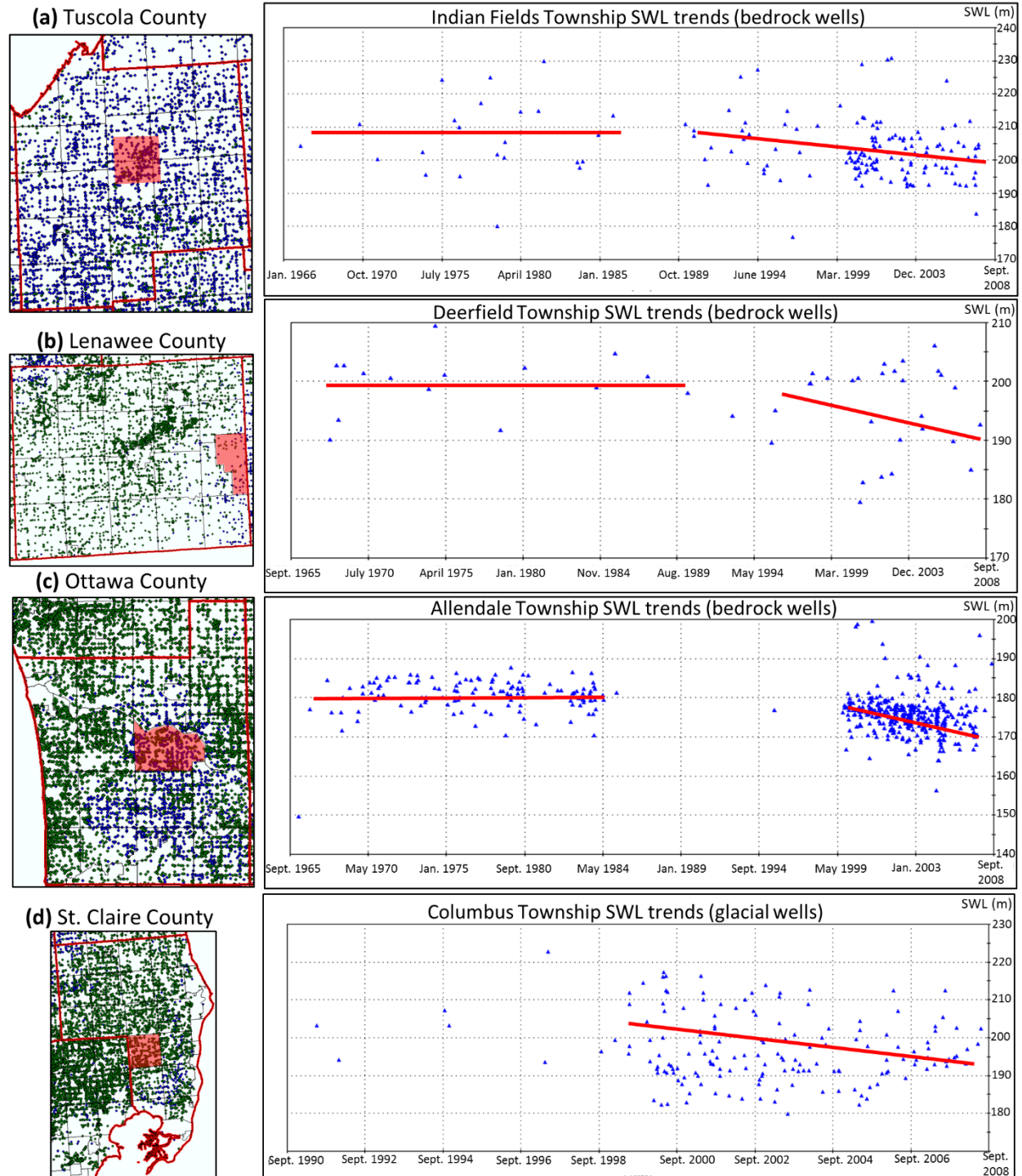


Figure 4.9: Static water level trends from selected townships in: (a) Tuscola County (b) Lenawee County; (c) Ottawa County; and (d) St. Clair County. The inset maps show the locations of wells extracted from Wellogic for the analysis. Green dots are glacial wells; blue dots are bedrock wells.

Table 4.2: Compelling static water elevation declines observed within townships of the seventeen counties that were analyzed.

| County | Glacial Aquifer | Time Period of Analysis | Bedrock Aquifer | Time Period of Analysis |
|------------|-----------------|-------------------------|-----------------|-------------------------|
| Ottawa | - 3 m | 1970-2009 | - 12 m | 1967-2009 |
| Saginaw | - 10 m | 1967-2009 | - 6 m | 1966-2012 |
| Iosco | - 6 m | 1972-2009 | - 6 m | 1975-2008 |
| Arenac | - 5 m | 1968-2009 | - 2 m | 1995-2009 |
| St. Clair | - 3 m | 1999-2009 | - 2 m | 1986-2008 |
| Macomb | --- | --- | - 10 m | 1969-2009 |
| Tuscola | --- | --- | - 9 m | 1976-2009 |
| Lenawee | --- | --- | - 7 m | 1966-2009 |
| Gladwin | --- | --- | - 6 m. | 1971-2009 |
| Genesee | --- | --- | - 4 m | 1965-2009 |
| Wayne | --- | --- | - 3 m | 1969-2009 |
| Sanilac | --- | --- | - 3 m | 1972-2009 |
| Bay | - 7 m | 1966-2009 | --- | --- |
| Shiawassee | --- | --- | - 2 m | 1965-2009 |
| Lapeer | --- | --- | - 2 m | 1998-2009 |

The findings of the statewide data-driven characterization of groundwater levels can be summarized as follows: 1) four hotspots of elevated or very elevated Cl concentrations exist in Lower Michigan, and a significant amount of cropland overlies groundwater of elevated or very elevated salinity; 2) across the Southern Peninsula, low-lying areas where groundwater is discharging systematically yield high Cl concentrations; 3) areas of continuous clay/silt glacial deposits overlying bedrock aquifers typically yield the highest Cl concentrations in groundwater; and 4) groundwater levels are declining, likely in response to pumping, and potentially aggravating the Cl problem. Note that all mapping and analyses were completed using entirely pre-existing data, most of which came from water well databases typically not utilized for multi-scale modeling. This was crucial, as many of the traditional sources for groundwater data (e.g., USGS monitoring wells) are not available in many of the counties in Michigan (and elsewhere). Therefore, the data-driven approach used here offers a significant ‘first step’ for efficiently and effectively characterize long-term, prevailing hydrogeologic and geochemical conditions. In this way, available (but

often limited) resources can be used to prioritize data collection and detailed analyses in key areas of concern identified from the system-based understanding of groundwater conditions.

4.5 Detailed Subregional Modeling, Visualization, and Analysis

Process-based flow modeling, coupled with field sampling, historical data mining, geostatistical analyses, and geospatial visualizations were used to better understand the underlying mechanisms controlling the patterns observed through data-driven modeling, and in particular, to characterize the impact of pumping. Ottawa County, Michigan was chosen for detailed local-scale analysis because: 1) groundwater in Ottawa County is clearly influenced by deeper brines, as demonstrated by the data-driven modeling presented here; 2) from a statewide perspective, it is an ‘emerging’ (and therefore relatively unknown) problem, as the Cl concentrations are generally lower than in areas along the Saginaw Bay and southeastern coastline of Lower Michigan; and 3) there is evidence from data-driven modeling of declining groundwater levels, likely due to pumping, as the area has experienced significant population growth in recent years whose water supply was mostly distributed groundwater withdrawals.

This reliance on groundwater to support a growing population has significantly increased the number of wells from 393 to 3247 to 9234 wells in the years 1970, 2000 and 2015, respectively (MDEQ 2015). The total volumetric pumping rates in Ottawa County, Michigan have almost doubled from 8 million gallons per day (MGD) in 1985 to about 15 MGD in 2010 (USGS 2012). As part of the transient flow modeling effort, we characterized and quantified the impact of the expanding well network in Ottawa County (for more details see Liao et al. in review). The simulated bedrock aquifer drawdown (difference between the 1966 head distribution and the distribution of the year indicated) and water use (which was used as input for the groundwater model) are shown in Figure 4.10. Clearly, the significant drawdown in the central portion of the bedrock aquifer has become systematically deeper and more extensive with time, especially since 1990 (Figure 4.10a). The evolution of water use for this area is fairly consistent with the drawdown evolution: during early periods of simulation (1970-1990), water use was relatively low and isolated to a few different areas, but since 1990, water use has increased in spatial extent and intensity, especially in the

central and eastern portions of the study area (Figure 4.10b). For temperate regions such as Ottawa County, recharge to shallow aquifer systems is typically assumed to be very large relative to the quantity pumped by wells and therefore drawdown can stabilize rather quickly due to significant diversions of baseflow from surface water to wells (Winter et al 1998; Alley and Leake 2004; Watson et al. 2013; Feinstein et al. 2016). The relatively continuous clay layer in central Ottawa County, however, precludes freshwater recharge from the glacial aquifer to the bedrock aquifer. Thus, the impact of deep bedrock pumping is localized within the deeper bedrock aquifer, at least in most of the central portion of the study area.

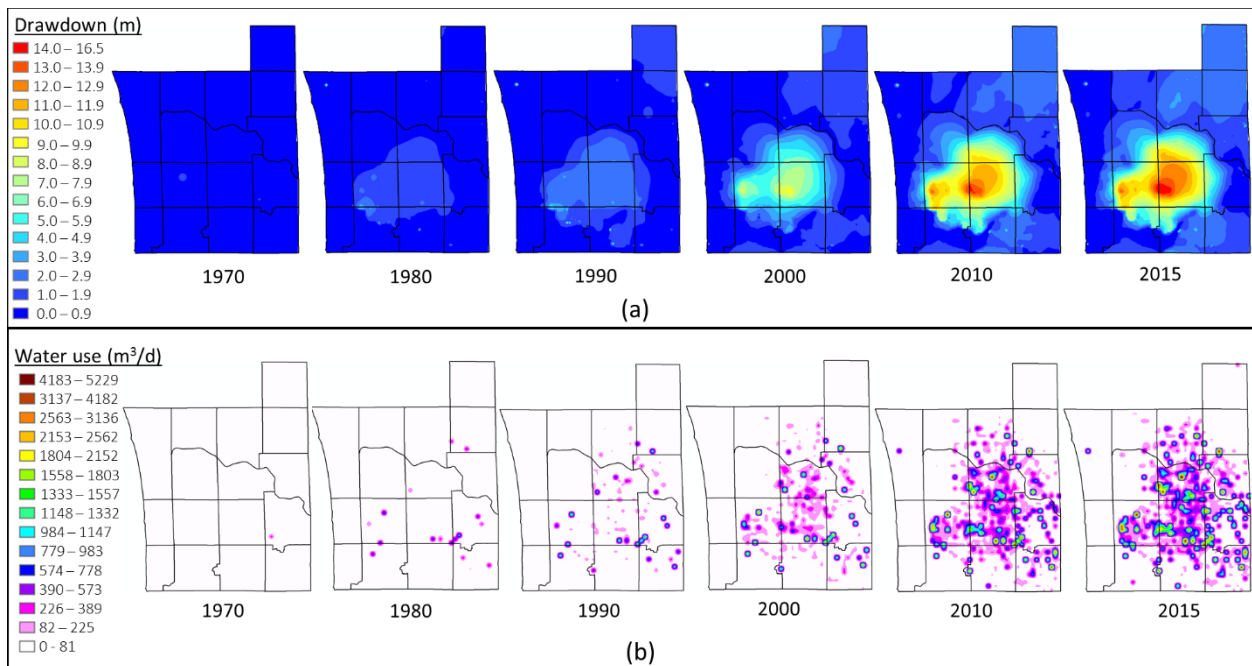


Figure 4.10: Key outputs from the modeling effort described in Liao et al. (in review) for the years 1970, 1980, 1990, 2000, 2010, and 2015. (a) Simulated drawdown in the bedrock aquifer and (b) simulated water use in the bedrock aquifer.

4.5.1 3D Spatial Characteristics of Cl Concentrations

A large dataset of Cl⁻ concentrations across space and time was compiled from field-collected water well samples and historical data mined from water well records in order to characterize current conditions and evaluate temporal dynamics. Over 545 groundwater samples from 467 locations during the fall of 2014 and the summer of 2015 were collected from both the glacial and bedrock aquifers. For each sampling

location, the latitude and longitude, well depth (i.e., aquifer sampling depth), and time of collection were recorded. See Curtis et al. (2018) for details on the collection protocols and analytical methods.

Historical Cl data and the associated latitude, longitude, well depth, and collection time were extracted from a file management system maintained by Ottawa County Department of Public Health. This parcel-based system organizes well logs with documentation from standard water quality testing (Fluoride, Chloride, Hardness, Nitrate, Nitrite, Sulfate, Sodium, and Iron). These so-called Partial Chemical tests are typically completed in Michigan at the time of well installation, following well or pump maintenance, at the time of property sale, or when property owners are experiencing water problems. Samples are analyzed by the State of Michigan Drinking Water Analysis Laboratory (MDEQ 2010) or by certified private testing labs. Well depth was extracted from the well log associated with each property. Well location (latitude, longitude) was often recorded on the well logs, but in some cases was estimated using the Ottawa County Interactive Mapping tool to obtain the coordinates of the centroid of the property (Ottawa County, 2016). This method introduced some locational uncertainty associated with the Cl data, but it was much less than the distance between most sampling locations used in the countywide analysis. In total, 2,832 Cl data points were extracted from roughly 1800 locations (some locations had more than one water quality test result). Records were extracted for the years 1966-2015, but most of the data are from 1990 or later. Contemporaneous geospatial analysis of Cl concentrations revealed that the highest concentrations and concentration gradients occurred in the bedrock aquifer and that Cl concentrations were generally low in the glacial aquifer. Therefore, the data mining effort was steered towards wells completed in the bedrock aquifer.

A plan-views and 3D side views of the results from the water-quality data mining and field sampling are shown in Figure 4.11. The bedrock surface (brown) and Coldwater Shale surface (light green) were delineated using lithologic information from water and oil/gas wells located in Ottawa County (MDEQ 2014). The areal distribution of the historical and field-collected Cl concentrations are consistent, with relatively high concentrations clustered primarily in the central and north-central portions of the County. The perspective views (Figure 4.11b and Figure 4.11c) of the combined dataset clearly demonstrate that

the majority of the samples with Cl concentrations above 250 mg/L – the US Environmental Protection Agency (EPA) secondary maximum contaminant level (SMCL) – occur within the bedrock aquifer or the basal glacial aquifer just above the bedrock surface. This distribution is consistent with a deep source, i.e., Michigan brines, as the primary cause of elevated groundwater salinity in the aquifer system, although anthropogenic sources may be responsible for the few isolated occurrences of Cl > 250 mg/L near the land surface.

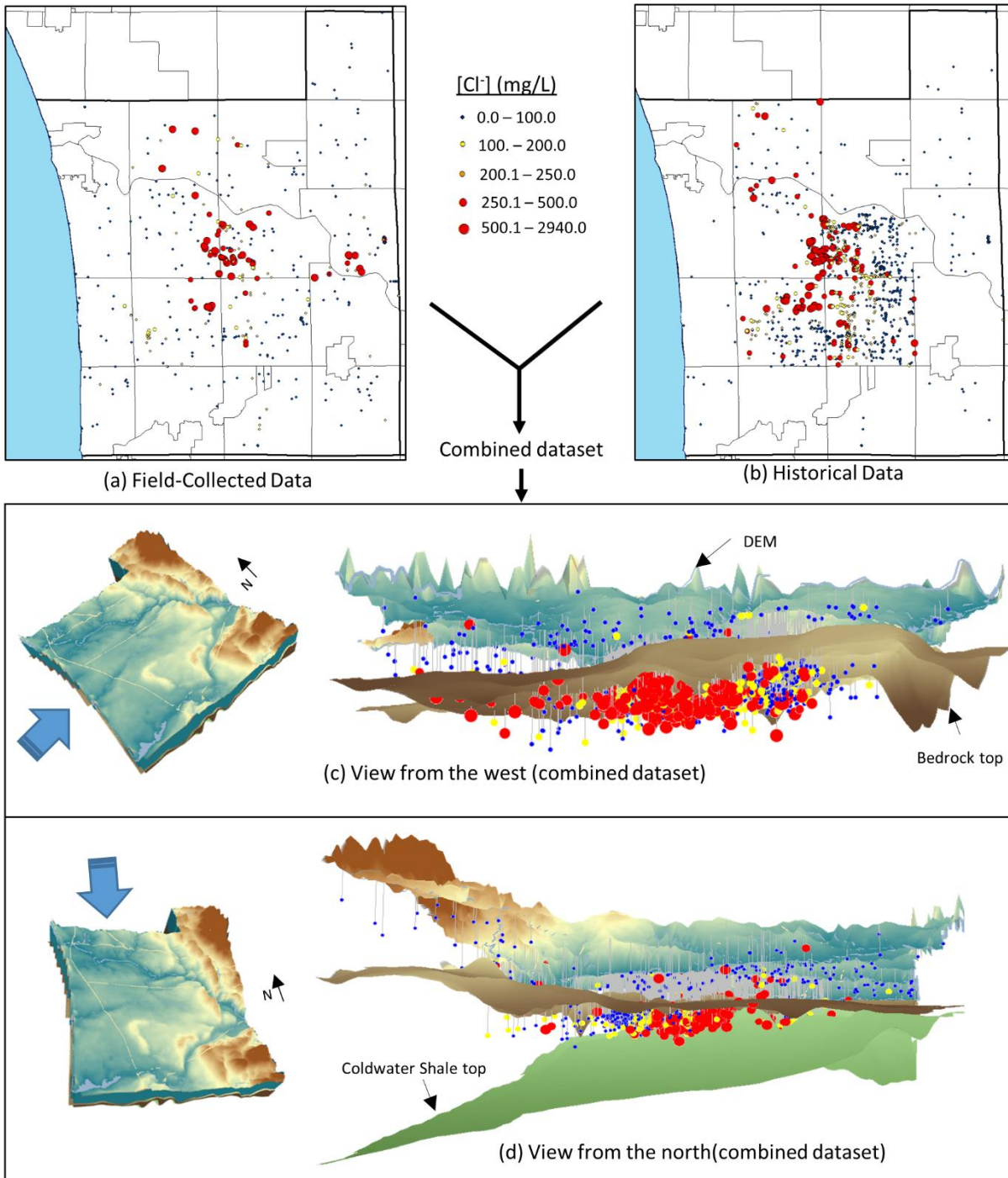


Figure 4.11: Chloride (Cl⁻) concentration point data for Ottawa County. (a) plan-view of Cl⁻ data collected in the field (adapted from Curtis et al. 2017); (b) plan-view of Cl⁻ mined from historical water quality records; (c) 3D visualization of Cl⁻ point data from the combined dataset, viewed from the west with the 10m DEM and bedrock surface (brown); and (d) 3D visualization of Cl⁻ point data viewed from the north, with the 10m DEM, bedrock surface, and the Coldwater Shale surface (green).

The stark contrast in Cl concentrations above and below the bedrock top as shown in Figure 4.11 suggests that very little mixing is occurring between the glacial and bedrock aquifers throughout much of the system. To further test this premise, the sodium (Na) concentration was measured in 248 samples from 175 of the locations checked during the data mining of historical Cl concentrations. This allowed for an analysis of Cl/Na ratios, which can be indicative of the controls on the environmental behaviors of Cl and Na (Neal and Kirchner, 2000; Long et al. 2015). At soil pH values typically encountered in the environment, Cl is usually considered conservative, i.e., non-reactive (Foth, 1999), but Na can be sequestered in soils and sediments by cation exchange or released from exchange sites depending on the salinity of the groundwater (Werner and DiPreto, 2006; Sun et al. 2012).

Figure 4.12 provides a graphical depiction of the molar ratio of Cl/Na versus Cl concentration, with the dataset was subdivided into samples from wells completed in the upper glacial aquifer and those completed in the bedrock aquifer or in the deep glacial aquifer just above the bedrock surface. The groundwater samples used in this analysis were only from systems that had been carefully checked to ensure that the well water did not pass through a water softener before discharge, as effluent from many softeners will contain artificially high levels of Na as a byproduct of the ion exchange process used to remove hardness ions, e.g., calcium. Most bedrock aquifer samples in Figure 4.12 plot below a Cl/Na ratio of one and show a clustering along a potential mixing curve between solutions containing low Cl concentrations and Cl/Na ratios approaching zero with solutions containing higher ratios (about 1) and high Cl concentrations. We interpret these relationships to suggest that, at higher salinity levels (i.e., deeper in the bedrock aquifer), cation exchange capacity of the solids is reached (or exceeded) such that little or no Na removal takes place, producing Cl/Na values approaching 1. At lower salinity levels (i.e., closer to the surface), Na is released from exchange sites and ratios of Cl/Na in groundwater decrease to levels below 1. The samples from the upper glacial aquifer, however, do not appear to be part of this mixing curve. Rather, all samples from the upper glacial aquifer have low Cl concentrations and a wide range of Cl/Na ratios ranging from just above zero to over 4. (Values of Cl/Na larger than 1 are interpreted to be a result from Na sequestration by soils and sediments by cation exchange). This shows that groundwater from the upper glacial aquifer is subject

to complex exchange processes with soils and sediments. Importantly, the pattern of the upper glacial aquifer samples suggests that the interaction (mixing) between groundwater in the upper glacial and bedrock aquifers is weak (or even negligible) due to the thick, relatively continuous aquitard separating them (especially in the center of the county).

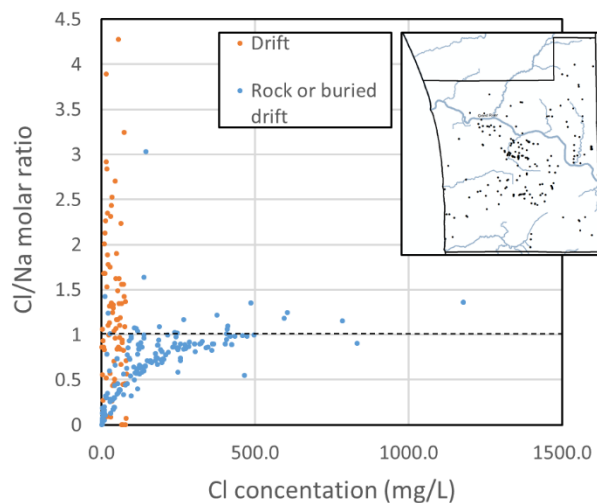


Figure 4.12: Graphical representation of Cl/Na molar ratio vs. Cl concentration for 248 locations yielding historical records of Na and Cl concentrations.

All field-collected data and the most recent historical Cl data were used to create a 3D spatial interpolation of the current Cl 'plume'. In most areas, data from 2010 or later were used for the 3D interpolation. In a few cases, earlier data were used although these represented only a small proportion of the 1,048 historical samples used. The total number of samples used was 1,593, 338 of which were from wells completed in the glacial aquifer and 1,255 from wells completed in the bedrock aquifer. Spatial interpolation was completed using 3D Inverse Distance Weighting (IDW). Weighting utilized a vertical exaggeration of 150, based on geometric anisotropy ratio between vertical thickness and lateral model/domain extent.

One key aspect of the 3D interpolation was the need to account for the thick, confining layer that occurs throughout the central portion of the study area (Apple and Reeves, 2007). This layer is expected to have relatively low Cl concentrations (i.e., close to zero) other than in locations directly adjacent to aquifer materials with high Cl concentrations, in which case diffusion may allow Cl to move a relatively short

distance into the clay layer. However, there are almost no water wells completed in this layer because of its impractical yield. Thus, Cl observations in this layer are unavailable. For this reason, we created ‘clay control points’ that were assigned a Cl concentration of zero and located systematically throughout the glacial aquitards and aquicludes in Ottawa County (see Figure 4.13). The 3D geologic model of the glacial sediments in the county was produced using the Transition Probability (TP) geostatistical method introduced by Carl and Fogg (1996; 1997). All lithologic descriptions in the *Wellogic* database are also classified into one of four material types: aquifer; marginal aquifer; partially confining material, and confining material. The vertical extents of these classified lithologies were used to develop a transition probability matrix of auto- and cross-correlations between material types and modeled using Markov Chain analysis. The original conditional 3D material distribution used 500 m by 500 m horizontal resolution and 4 m vertical resolution. Complete details of the TP modeling of the glacial aquifer in the study area are provided in Liao et al. (in review). (Also, see Chapter 3).

Clay control points were extracted from locations where the 3D geologic model predicted partially confining or confining material on a 1000 m by 1000 m grid (horizontal direction). We experimented with both 400 m by 400 m and 800 m by 800 m grids, but a graphical comparison of interpolated Cl concentrations versus observed Cl concentrations showed that the 1000 m by 1000 m grid was most appropriate, which also is close to the observed transverse (areal) Cl data density. The locations of the ‘clay control’ cells (Cl = 0 mg/L) are shown in Figure 4.13b. A comparison of the Cl ‘plume’ – defined as the spatial extent of Cl > 250 mg/L in the glacial deposits – with and without clay control points is shown in Figure 4.13c. Note that the Cl plumes generated without control cells are generally over-estimated in 3D extent and inconsistent with the point Cl data. When clay control cells were used, the Cl plume largely does not spread into the glacial deposits, which is what is suggested by the available point data.

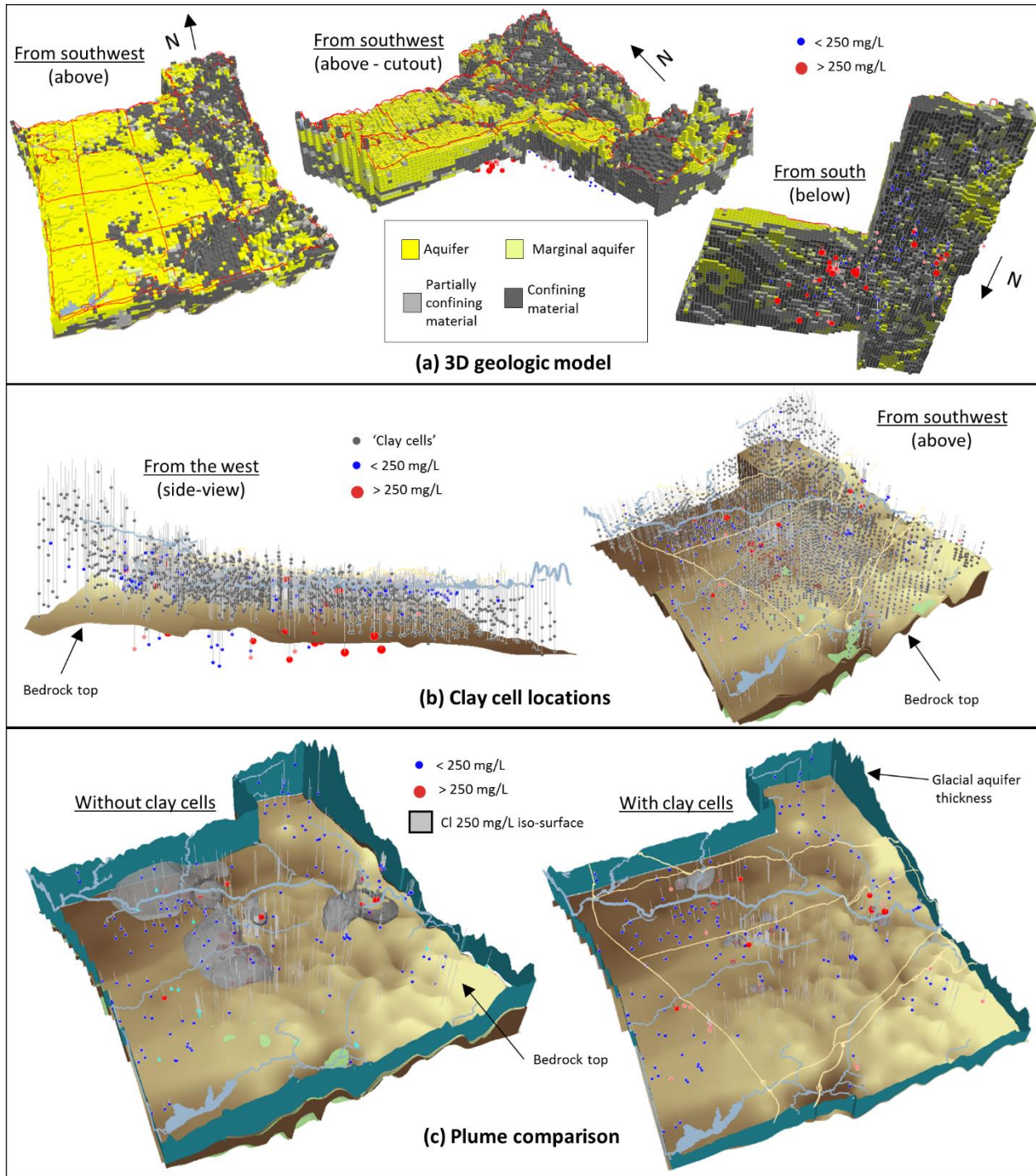


Figure 4.13: 'Clay control cells' used for 3D Cl interpolation. (a) 3D visualizations of the geologic material model characterizing the heterogeneity of the glacial deposits (from Liao et al., in review); (b) 3D depictions of control cell locations; and (c) Cl plume comparison.

The results from the 3D interpolation are shown in Figure 4.14. At each grid cell location, the aquifer system thickness (DEM surface elevation minus the Coldwater Shale top elevation) was computed and sub-divided

into 9 layers of equal thickness. The Cl concentration was extracted from the midpoint of each of these vertical layers (Figure 4.14b-g). The 2D distributions reveal that the extent and severity of the Cl contamination increases with depth into the aquifer system, e.g., in the northwest, central and east-central portions of the study domain. This 3D Cl spatial structure resembles “upconing” of saline water in the bedrock aquifer towards the surface, in which plumes of groundwater with relatively high Cl concentrations migrate from deeper saline regions of the regional groundwater system and mix with the overlying fresh groundwater. This phenomenon is discussed in several saltwater intrusion studies in which pumping induces a localized rise in the freshwater–saltwater interface underneath areas of groundwater withdrawals (Schmork and Mercado 1969; Paster and Dagan 2008; Werner et al. 2009; Jakovovic et al. 2011). While the extensive surface water network undoubtedly acts as ‘natural pumps’ to draw deeper, chloride-laden groundwater to the surface (Curtis et al. 2018), the following subsections explore the possibility of localized upconing of saline water toward pumping wells as the freshwater head is locally decreased due to pumping.

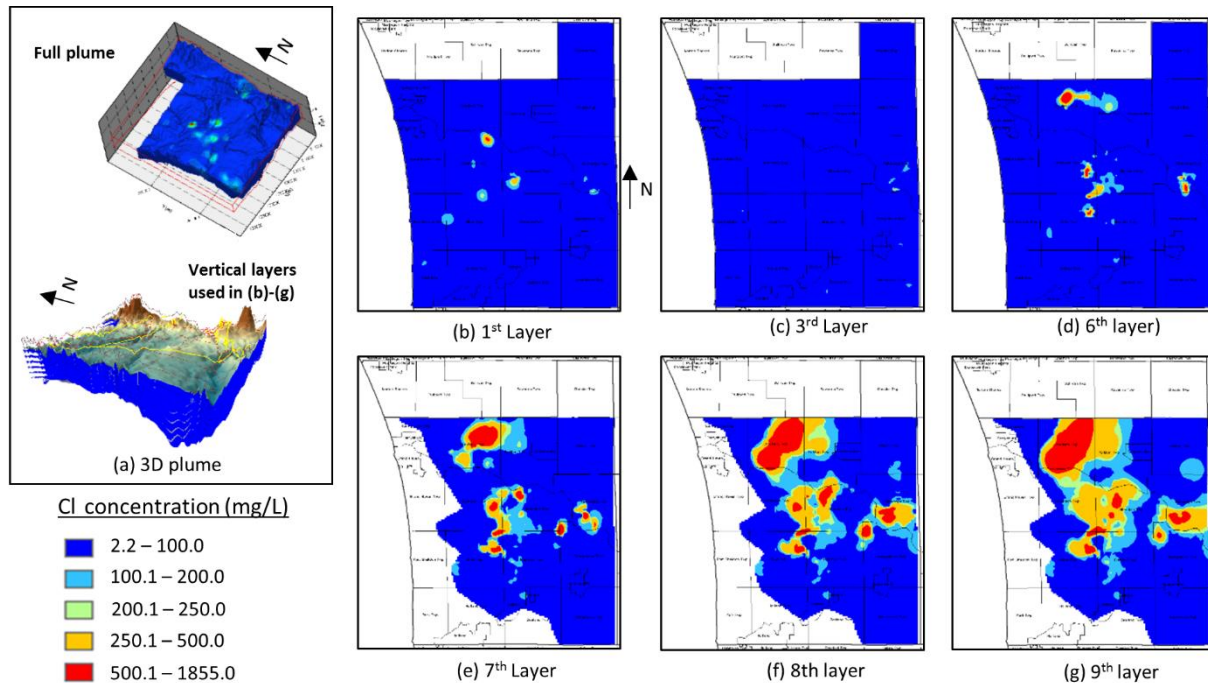


Figure 4.14: Results from the 3D interpolation of Cl concentrations, shown as 2D distributions at various depths from the land surface. (a) 3D plume and representative cross-sections through the domain used for interpolation (b)-(g) 2D distributions of Cl in the glacial deposits (top layer, 3rd layer and bottom layer, 7th, 8th, and 9th layers).

Figure 4.14 (cont'd)

respectively); and (d)-(f) 2D distributions from the bedrock aquifer (top layer, middle layer, and bottom layer, respectively).

4.5.2 Impacts of Pumping

With a characterization of the flow system dynamics and a compiled dataset of Cl concentrations across space and time, an analysis of the possible causal relationship between pumping and water quality was possible. One approach might have constructed a 3D interpolation of Cl concentrations for different time periods in an attempt to identify locations of significant changes. Although a significant amount of Cl concentration data were available for analysis, applying this approach with reasonable statistical confidence for different time periods was not possible given the large spatial scales involved. Alternatively, modeling Cl mass transport using the velocity vectors from the numerical flow modeling requires an accurate treatment of the boundary (source) conditions, which was an impractical (if not impossible) task given the scale and complexity of the problem. However, as shown next, by using 2D graphical overlays and aggregated statistical analyses, it becomes increasingly clear that pumping has exacerbated the brine upwelling in the region.

Overlays of all Cl concentration point data extracted from bedrock wells (field collected and historical) on the simulated drawdown (1966-2015) and the 2015 SWL distributions are presented in Figure 4.15. In general, many of the elevated samples (Cl > 250 mg/L) occur within the 'drawdown cone' (drawdown of 5 m or more) in central Ottawa County, although there are a number of samples with Cl < 125 mg/L also occurring within this area, especially along the eastern flank (Figure 4.15a). Moreover, there are a number of samples with very high concentrations occurring in areas with very little or no drawdown, e.g. northwest or east Ottawa County. There is a somewhat better spatial correlation between the occurrence of elevated Cl concentrations and groundwater 'valleys' or areas of low SWLs (Figure 4.15b) where groundwater is expected to have a relatively greater upward flow component. All of the elevated Cl samples occur in groundwater valleys, including those samples from the northwest and east portions of the study domain. As demonstrated from the simulated drawdown results (see Figure 4.10), some of the areas in the bedrock

aquifer have historically contained naturally low SWLs, for example, along the Grand River and in northwest Ottawa County, whereas some areas are “artificially low” of because increased groundwater withdrawals, e.g. south of the Grand River in central Ottawa County.

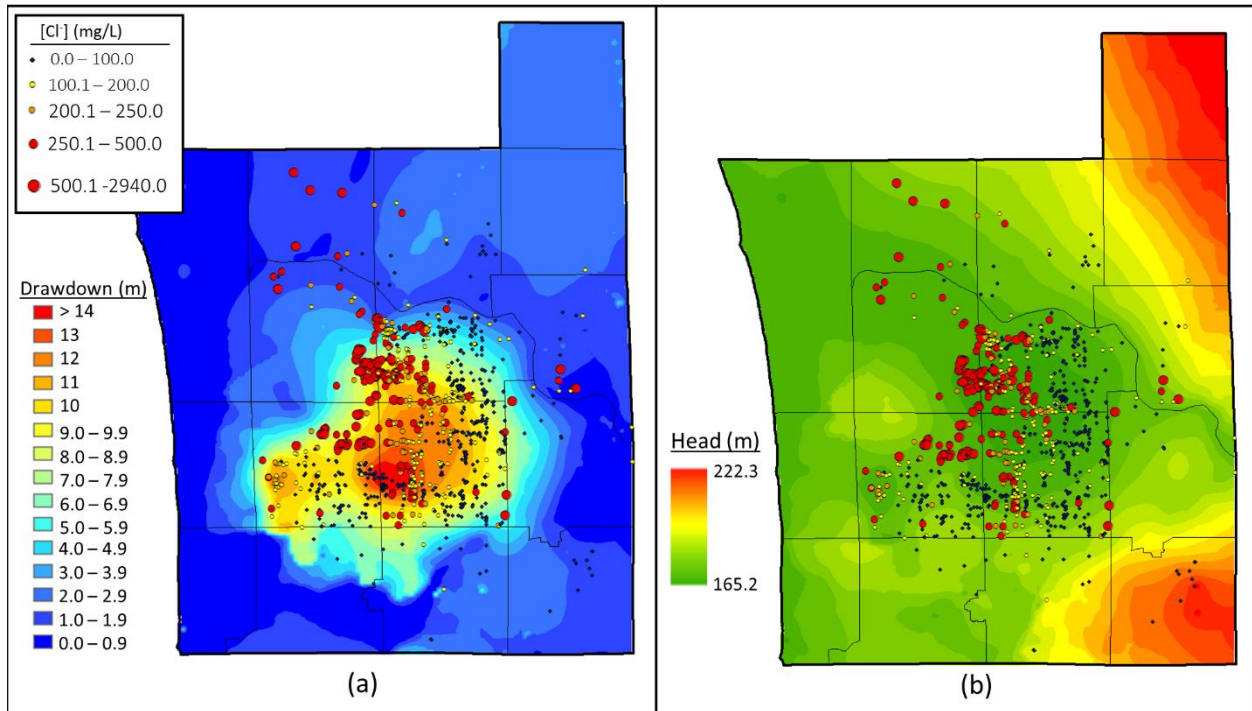


Figure 4.15: Spatial relationship between Cl concentration and groundwater flow dynamics. (a) simulated drawdown (1966-2015) in the bedrock aquifer and all Cl point data collected from the bedrock aquifer (field sampling and data mining); and (b) 2015 head distribution in the bedrock aquifer and all Cl point data collected from the bedrock aquifer.

The large concentration gradients within the groundwater valleys indicate preferential upwelling to discrete points or sub-regions rather than a widespread salinization of the near-surface environment. This is consistent with the upconing structure revealed in the 3D spatial interpolation of Cl concentrations. Consideration of subsurface geology suggests that aquifer geometry plays an important role as well. Denser, more saline groundwater will occupy the bottom portion of the aquifer system (i.e., along the Coldwater Shale-Marshall aquifer interface). However, the top surface of the Coldwater Shale unit is highly irregular, and thus, wells completed at a similar elevation (but at different locations) may yield significantly different Cl concentrations. In other words, in areas where the Marshall aquifer is relatively thick,

concentrations may be lower because the underlying ‘plume’ is occupying the basal portion of the aquifer further away from the well bottom than in the case of wells completed in areas where the Marshall aquifer is thin.

From the preceding analysis, it appears that the spatial distribution of Cl concentrations are controlled primarily by two mechanisms: 1) natural discharge of high-Cl groundwater into the bedrock aquifer beneath the County; and 2) pumping-induced migration of high-Cl groundwater into areas of significant drawdown. For areas impacted by the latter mechanism, increases in Cl concentrations with time are expected. Using the entire historical Cl dataset (glacial (drift) and bedrock wells), concentrations were plotted as a function of time (Figure 4.16). This analysis shows that the number of samples yielding very high Cl concentrations increased with time and that, on average, the Cl concentrations in bedrock wells also increased with time. Conversely, the drift wells do not exhibit a trend of increasing Cl concentrations, although there are more drift wells with high concentrations in recent times.

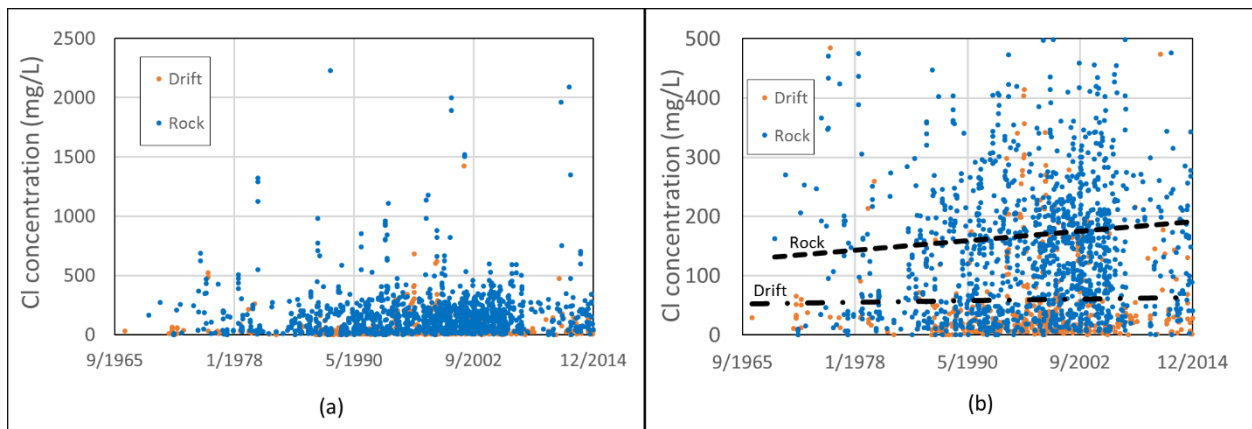


Figure 4.16: Graphical comparison of Cl concentrations vs. time. (a) dataset consisting of mined data from historical water well records; and (b) dataset from (a) shown with a reduced Cl concentration scale and linear regression trendlines.

Although pumping-induced migration of brines toward the land surface may be responsible for the general upward trend in Cl concentrations in groundwater from bedrock wells, it is possible that some newer wells are drilled deeper than older wells thus penetrating into the deeper saline groundwater. To investigate this possibility, an analysis was completed using samples taken at different times from the *same* wells (i.e.

historical water quality data and field-collected data). Comparing the field-collected Cl concentrations versus the historical Cl concentrations for 248 wells (Figure 4.17a) shows a general increase in Cl concentrations (i.e., most of the data points fall above the 45 degree line of perfect agreement). This is especially the case for wells with a field-collected Cl concentration of 250 mg/L or more, with 62 of the 75 (83%) such locations showing an increasing Cl concentration with time. Most of these locations occur in central Ottawa County, and analysis of Cl concentration residuals (field-collected Cl concentration minus the historical Cl concentration) and well bottom elevations shows that most of the significant increases in Cl concentrations are occurring in deeper portions of the aquifer system (Figure 4.17b). Of the 59 wells with Cl residuals of 50 mg/L or more, 40 of them (68%) were completed at bottom elevations of 160 m or lower, which is a reasonable approximation of the average bedrock top surface in Ottawa County (Churches and Wampler 2013).

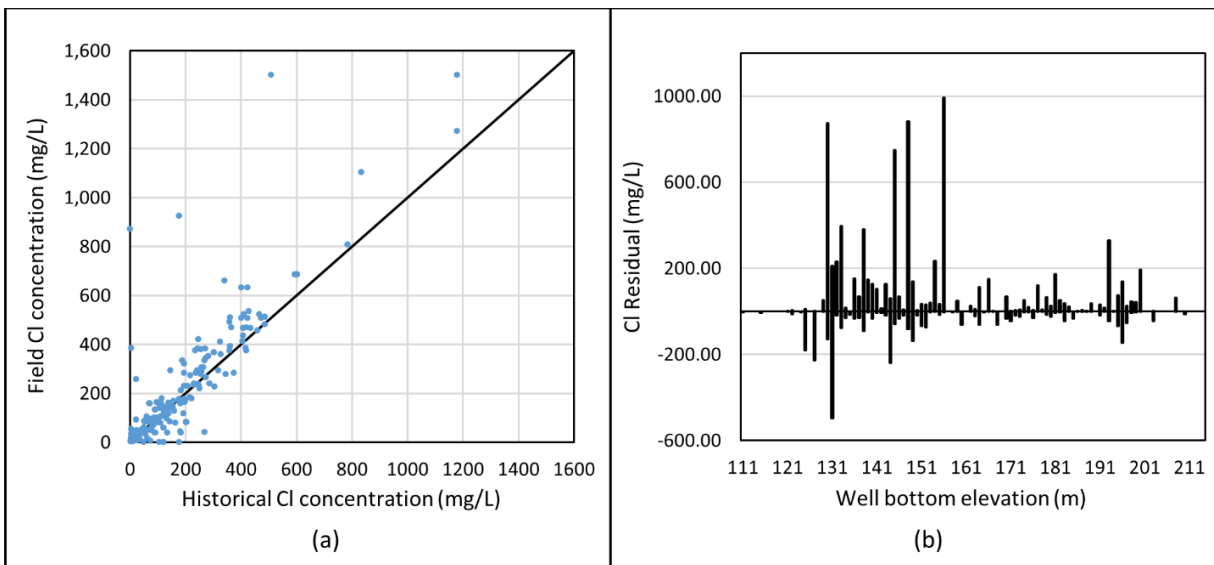


Figure 4.17: Temporal analysis at wells with both historical and field-collected Cl concentration data. (a) comparison of Cl concentrations from field-collected data and historical water quality records at 248 locations (see inset map in Figure 4.11 for map of locations used in analysis); and (b) graphical comparison of Cl residual (field-collected mg/L – historical mg/L) as a function of well bottom elevation (amsl).

The interpretation of the results shown in Figure 4.17 is that deep groundwater pumping is causing an upward movement of deeper, more saline water into the upper portions of the bedrock aquifer system. Over time, this water mixes with and/or displaces the fresh groundwater originally occupying the region around

the well, thereby significantly increasing the Cl concentration. Modest (< 50 mg/L) increases or decreases in Cl concentration that are seen at predominantly lower concentrations may be due to short-term fluctuations caused by surface processes (e.g., infiltration of dissolved road salts, periodic water withdrawals, etc.). To test this interpretation, the simulated flow in the deep part of the bedrock aquifer system was visualized using a forward 3D particle tracking technique. Particles were placed on a surface interpolated from scatter points created 10 m directly below all bedrock well bottoms, and moved based on the velocity vector results of the transient simulation. The particle path represents the flow direction in that part of the groundwater system.

To provide greater vertical details, a submodel was developed from the countywide flow model for just the central portion of the County where significant changes in groundwater levels and fluxes were observed and where the highest Cl concentrations generally occur. The submodel consisted of 15 computational layers (as compared to 7 in the parent model) and derived its boundary and initial conditions (in the form of head values) from the 2015 simulation results (see Liao et al. 2015 for more details about this multi-scale modeling approach). The 2015 pumping configuration and recharge distribution was applied *ad infinitum* and the simulation was run for 20 consecutive years with one year time-steps.

As shown in Figure 4.18, deep upwelling can be observed toward 1) the Grand River (GR) in the western and eastern portions of the submodel; 2) local capture zones around high-capacity wells where deep groundwater is upwelling towards well bottoms; and 3) major capture zones created by clusters of many small-capacity wells (not shown here for aesthetic reasons) and high-capacity wells (e.g., in the western portion of the submodel). These patterns are consistent with the idea that slow upwelling of deeper, more saline groundwater is responsible for the significant increases in Cl concentrations, especially in the deeper bedrock wells.

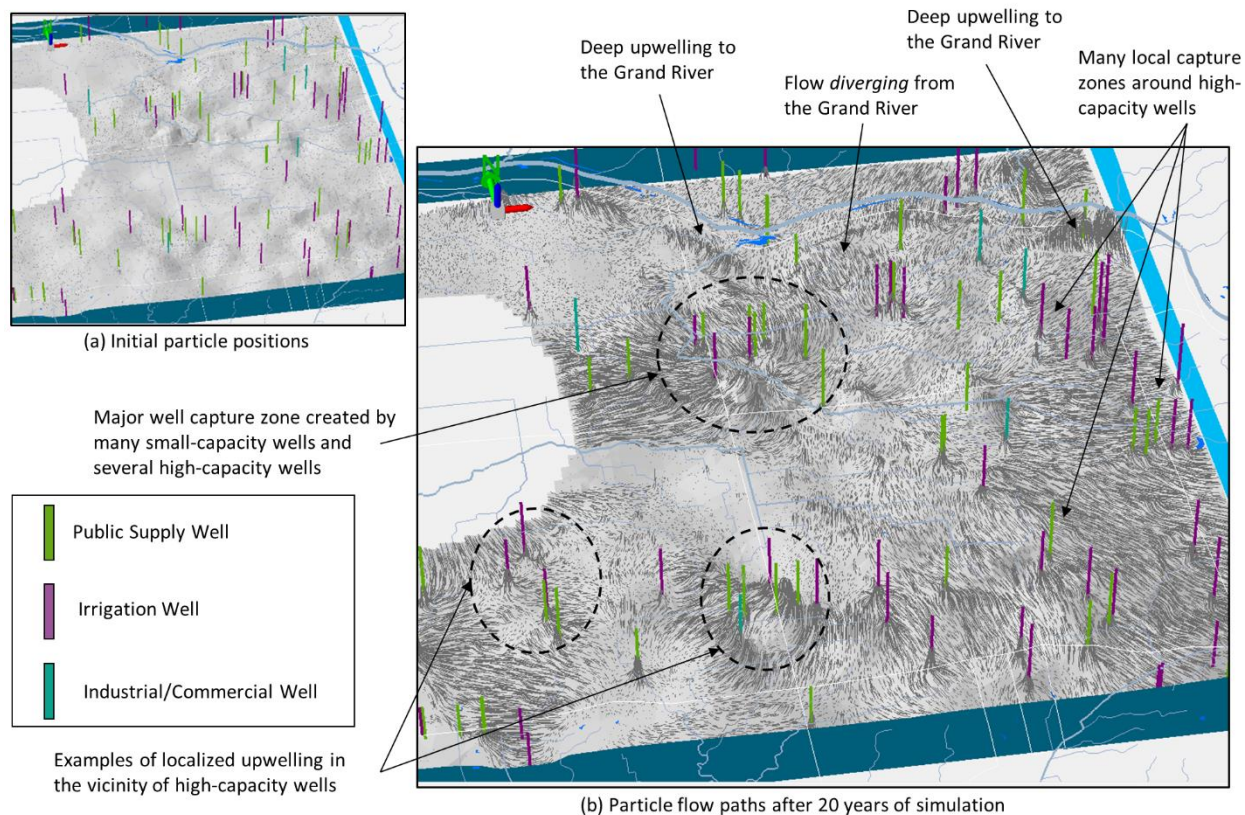


Figure 4.18: Results from 3D particle tracking. (a) initial particle positions and the position of high-capacity wells existing in 2015; and (b) particle flow paths after 20 years of steady-state simulation (2015 pumping and recharge simulated *ad infinitum*).

A final step in evaluating the impacts of pumping was to determine if the 3D spatial extent of elevated Cl concentrations is increasing in response to pumping. As previously mentioned, constructing and visualizing countywide 3D interpolations of Cl concentrations for different time periods was not possible. However, there was enough data in the key area in central Ottawa County to perform separate 3D interpolations for the past three decades. The spatial interpolations shown in Figure 4.19 present the transverse (areal) data density for Allendale Twp. for the time periods: up to 1995; 1996-2005, and 2006-2015 (note the relatively even distribution of Cl data across space and time). Also shown are the 250 mg/L and 400 mg/L Cl iso-surfaces for the three specified time periods. Clearly, the extent and severity of Cl contamination is becoming worse, especially in the western portion of the aquifer where it is relatively thin and drawdown is significant. This is additional evidence for the pumping-induced migration of brine-influenced groundwater over the recent-past years of development.

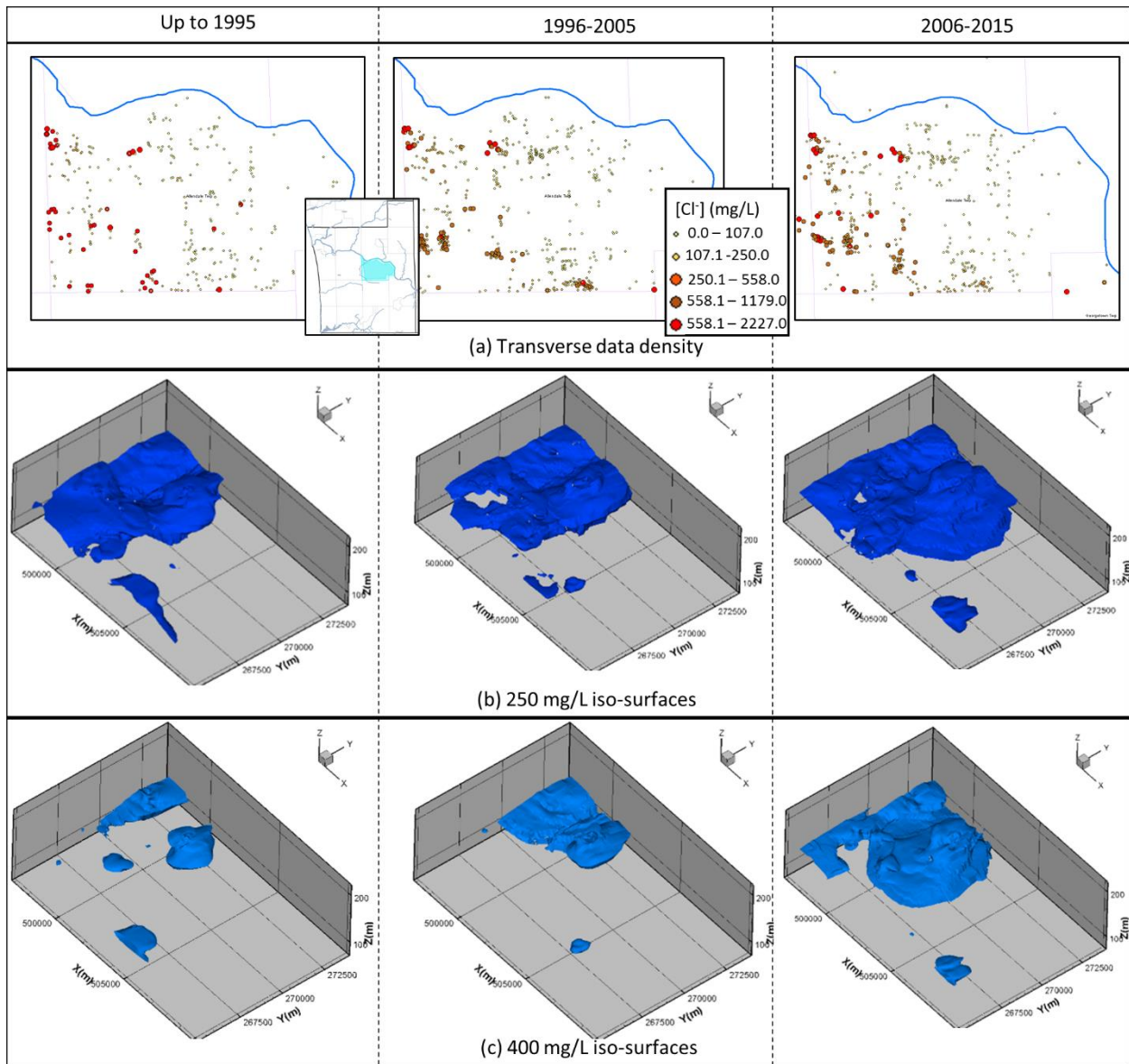


Figure 4.19: Cl plume modeling in Allendale Township (central Ottawa County) for three time periods: up to 1995 (left column), 1996-2005 (center column), and 2006-2015 (right column). (a) transverse data density across the three time periods; (b) 250 mg/L iso-surfaces for the three time periods; and (c) 400 mg/L iso-surfaces for the three time periods.

While the analysis of many Cl measurements from water wells distributed across the county and from past decades provided compelling evidence that, in general, concentrations are increasing with time, the quantification of Cl changes across time proved difficult to address. There was no consistent interval of analysis available (*i.e., each comparison had its own unique set of sampling dates that may be very close

or very far apart in time), and at lower concentrations, there appeared to be no clear decreasing or increasing trend – likely the result of the complex interplay between natural variability, anthropogenic sources, and the complex, dynamic structures of the Cl ‘plume’. These aspects related to water quality dynamics and data availability made it difficult to quantify the rate of salinization in the aquifer system at a given location or across a specific time period; and ii) the coupling between pumping rates and changes in Cl concentrations. Such characterization requires a network of strategically-placed water quality sensors delivering long-term measurements of groundwater salinity.

4.6 Ch. 4 Conclusions

In this study, we investigated the widespread salinization of shallow groundwater in the Lower Peninsula of Michigan due to natural upwelling of deep brines. We performed a holistic, system-based evaluation of the groundwater conditions across the southern two-thirds of the peninsula, unifying data-driven modeling of massive amounts of hydrogeologic information across multiple spatial scales with detailed analysis of groundwater salinity dynamics and process-based groundwater flow modeling for an emerging area of concern (Ottawa County, Michigan). The key findings are as follows:

- Brines are systematically impacting low-lying areas where groundwater is discharging (moving upwards) in different regions and subregions across the Lower Peninsula.
- Within local hot spots, the relative impact of upwelling was determined to be controlled by: i) streams acting as ‘natural pumps’ that bring deeper (more mineralized) groundwater to the surface; ii) the occurrence of nearly impervious geologic material at or near the surface which restricts freshwater flushing of deeper groundwater; and iii) the space-time evolution of water well withdrawals which slowly induces migration of saline groundwater from its natural course.
- Four regions were identified as statewide hot spots: west-central Lower Michigan, the Saginaw Bay region of east-central Lower Michigan; southeastern Lower Michigan; and the coastal plain of southeastern Michigan and the ‘Thumb region’.

- The salinization is most severe in the Saginaw Bay region and along the southeastern coastline of Lower Michigan. In west-central Michigan, the pollution is less severe, but increased groundwater use threatens the long-term sustainability of the region because of pumping-induced migration of saline groundwater from its natural course.

Although some of these findings are not surprising or different from past studies of groundwater salinity in Michigan, especially those related to the natural sources and hydrogeologic controls of the pollution (e.g., Long et al. 1988; Westjohn and Weaver 1996b, Curtis et al. 2017), the amount of data used in this study to provide detailed information at and across different scales is unprecedented. Detailed mapping and characterizations of groundwater conditions across space and time is what enables managers to prioritize resources and make management plans for water-supply needs. As demonstrated here, a new opportunity is afforded by the recent assimilation of water well datasets by state and local agencies that contain massive amounts of physical groundwater data, geological information, and in some cases, water quality information (e.g., the Illinois State Geological Survey repository (ISGS 2015), the Kansas WIZARD water well levels database (KGS 2002), the Geosam Database for the State of Iowa (IGS 2015), the Water Data Library for the State of California (WDL 2017), and the Virginia Department of Environmental Quality well database). Combined and integrated with process-based models, field-sampling, and geospatial or geochemical analyses, these data support the detailed aquifer system characterizations required to manage NPS groundwater pollution.

REFERENCES

REFERENCES

- Albert, D. A. 2001. Natural community abstract for Inland salt marsh Michigan Natural Features Inventory (pp. 4). Lansing, Michigan.
- Alley, W.M., T.E. Reilly, and O.L. Franke. 1999. Sustainability of Ground-Water Resources. United States Geological Survey Circular 1186.
- Alley, W.M., and S.A. Leake. 2004. The journey from safe yield to sustainability. *Ground Water* 48, no. 1: 12–16.
- Apple, B.A. and Reeves, H.W. 2007. Summary of Hydrogeologic Conditions by County for the State of Michigan—U.S. Geological Survey Open-File Report 2007-1236, 87 pp.
- Ayers, R.S. and Westcot, D.W. 1985. Water quality for agriculture (Vol. 29). Rome: Food and Agriculture Organization of the United Nations.
- Caetta, M. 1991. An Investigation of Possible Subsurface Brine Springs in Southeastern Lenawee County, Michigan. Unpublished M.S. Thesis, Akron, Ohio: University of Akron. 107 p.
- Curtis, Z.K., Li, S.G., Liao, H.S. and Lusch, D., 2018. Data-Driven Approach for Analyzing Hydrogeology and Groundwater Quality Across Multiple Scales. *Groundwater*, 56(3), pp.377-398.
- DOGRR. 2017. State of California Department of Conservation, Division of Oil, Gas, and Geothermal Resources (DOGRR). *Well Finder*, Repository for records of wells drilled in the State of Illinois (periodically updated). Available at: <http://www.isgs.illinois.edu/ilwater>
- Feinstein, D. T., Fienen, M. N., Reeves, H. W., & Langevin, C. D. (2016). A Semi-Structured MODFLOW-USG Model to Evaluate Local Water Sources to Wells for Decision Support. *Groundwater*, 54(4), 532-544.
- Ging, P. B., Long, D. T., & Lee, R. W. 1996. Selected Geochemical Characteristics of Ground Water from the Marshall Aquifer in the Central Lower Peninsula of Michigan U.S. Geological Survey Water-Resources Investigations Report 94-4220.
- GWIM. (2006). "Groundwater Inventory and Map Project", State of Michigan Public Act 148.
- Hem, J.D. 1985. Study and Interpretation of the Chemical Characteristics of Natural Water, U.S. Geological Survey Water-Supply Paper 2254, 2nd ed. Reston, Virginia: USGS.
- Hoaglund, J. R., Kolak, J. J., Long, D. T., & Larson, G. J. 2004. Analysis of modern and Pleistocene hydrologic exchange between Saginaw Bay (Lake Huron) and the Saginaw Lowlands area. *Geological Society of America Bulletin*, 116(1-2), 3-15.
- ISGS. 2015. Illinois State Geological Survey. *ILWATER*, Repository for records of wells drilled in the State of Illinois (periodically updated). Available at: <http://www.isgs.illinois.edu/ilwater>
- IGS. 2016. Iowa Geological Survey, based at IIHR – Hydrosceience & Engineering, University of Iowa. Available at: <https://www.iihr.uiowa.edu/igs/geosam/home>

- Jakovovic, D., Werner, A. D., & Simmons, C. T. (2011). Numerical modelling of saltwater up-coning: Comparison with experimental laboratory observations. *Journal of hydrology*, 402(3), 261-273.
- KGS. 2002. Kansas Geological Survey. *WIZARD*, water well levels database (periodically updated). Available at: <http://www.kgs.ku.edu/Magellan/WaterLevels/index.html>
- Kost, M. A., Albert, D. A., Cohen, J. G., Slaughter, B. S., Shillo, R. K., Weber, C. R., & Chapman, K. A. 2007. Natural Communities of Michigan; Classification and Description. Michigan Natural Features Inventory Report Number 20007-21 (pp. 314). Lansing, MI.
- Lane, A.C. 1899. Lower Michigan mineral waters U.S. *Geological Survey Water Supply Paper* 30.
- Li, S.G., Liu, Q. (2006). "A Real-Time, Interactive Steering Environment for Integrated Ground Water Modeling." *Journal of Groundwater*, 44, 758-763.
- Li, S. G., & Liu, Q. (2008). "A new paradigm for groundwater modeling." *Quantitative Information Fusion for Hydrological Sciences*, Springer Berlin Heidelberg, 19-41.
- Long, D. T., Wilson, T. P., Takacs, M. J., & Rezabeck, D. H. 1988. Stable-isotope geochemistry of saline near-surface ground water; east-central Michigan Basin. *Geological Society of America Bulletin*, 100(10), 1568-1577.
- Long, D. T., Voice, T. C., Chen, A., Xing, F., & Li, S. G. 2015. Temporal and spatial patterns of Cl⁻ Na⁺ concentrations and Cl/Na ratios in salted urban watersheds. *Elementa: Science of the Anthropocene*, 3(1), 000049.
- Ma, L., Castro, M. C., Hall, C. M., and L.M. Walter. 2005. Cross-Formational Flow and Salinity Sources Inferred from a Combined Study of Helium Concentrations, Isotopic Ratios, and Major Elements in the Marshall Aquifer, Southern Michigan: AQUIFER FLOW AND SALINITY SOURCES." *Geochemistry, Geophysics, Geosystems* 6, no. 10.
- McIntosh, J. C., L. M. Walter, and A. M. Martini. 2004. Extensive microbial modification of formation water geochemistry: Case study from a midcontinent sedimentary basin, United States, *Geol. Soc. Am. Bull.*, 116(5-6),743-759.
- MDEQ (Michigan Department of Environmental Quality). 2014. Michigan Department of Environmental Quality. Wellogic System (periodically updated). <https://secure1.state.mi.us/wellogic/> (accessed August 2017).
- MDEQ (Michigan Department of Environmental Quality). 2015. Groundwater Statistics [Fact sheet]. Retrieved from http://www.michigan.gov/deq/0,4561,7-135-3313_3675_3694-81746--,00.html (Accessed 8/14/2017).
- Meissner, B. D., Long, D. T., & Lee, R. W. 1996. Selected Geochemical Characteristics of Ground Water from the Saginaw Aquifer in the Central Lower Peninsula of Michigan U.S. Geological Survey Water-Resources Investigations Report 93-4200.
- MSU. 2014. Michigan Ground Water Management Tool. East Lansing, Michigan: Department of Environmental Engineering, Michigan State University.

- Neal C, Kirchner JW. 2000. Na⁺ and Cl levels in rainfall, mist, streamwater and groundwater at the Plynlimon catchments, mid-Wales: inferences on hydrological and chemical controls. *Hydrol Earth Syst Sci* 4: 295–310.
- Ottawa County, Michigan. 2016. GIS Property Mapping web application. Available at <https://gis.miottawa.org/ottawa/geocortex/propertymapping/> (Accessed 9/7/2017)
- Ottawa County, Michigan. Environmental Health – Scanned Well & Water Quality files (continuously updated). Accessed 2014-2015.
- Paster, A., & Dagan, G. (2008). Mixing at the interface between fresh and salt waters in 3D steady flow with application to a pumping well in a coastal aquifer. *Advances in water resources*, 31(12), 1565-1577.
- Polizzotto, M. L., Kocar, B. D., Benner, S. G., Sampson, M., & Fendorf, S. (2008). Near-surface wetland sediments as a source of arsenic release to ground water in Asia. *Nature*, 454(7203), 505.
- Rheaume, S. (1991). Hydrologic provinces of Michigan. USGS Water-Resources Investigations Report 91-4120. 73 p.
- Rustem WR, Long DT, Cooper WE, Armoudlian A. 1993. The Use of Selected Deicing Materials on Michigan Roads: Environmental and Economic Impacts [Online]. Prepared by Public Sector Consultants for the Michigan Department of Transportation. <http://cdm16110.contentdm.oclc.org/cdm/ref/collection/p9006coll4/id/97524>. (Accessed 8/16/2017).
- Sampath, P.V., Liao, H.S., Curtis, Z.K., Doran, P.J., Herbert, M.E., May, C.A. and Li, S.G. (2015). Understanding the groundwater hydrology of a geographically-isolated prairie fen: implications for conservation. *PloS one*, 10(10), p.e0140430.
- Sampath, P.V., Liao, H.S., Curtis, Z.K., Herbert, M.E., Doran, P.J., May, C.A., Landis, D.A. and Li, S.G. (2016). Understanding fen hydrology across multiple scales. *Hydrological Processes*, 30(19), pp.3390-3407.
- Schmork, S., & Mercado, A. (1969). Upconing of fresh water—sea water interface below pumping wells, field study. *Water Resources Research*, 5(6), 1290-1311.
- Sun H, Huffine M, Husch J, Sinpatanasakul L. 2012. Na/Cl molar ratio changes during a salting cycle and its application to the estimation of Na⁺ retention in salted watersheds. *J Contam Hydrol* 136: 96–105.
- Toth, J. 2009. *Gravitational Systems of Groundwater Flow: Theory, Evaluation, Utilization*. Cambridge: Cambridge University Press.
- Watson, K. A., Mayer, A. S., & Reeves, H. W. 2014. Groundwater availability as constrained by hydrogeology and environmental flows. *Groundwater*, 52(2), 225-238.
- WDL 2018. State of California Department of Water Resources, Division of Statewide Integrated Water Management. Water Data Library (periodically updated). Available at: <http://wdl.water.ca.gov/waterdatalibrary/index.cfm>
- Werner, A. D., Jakovic, D., & Simmons, C. T. 2009. Experimental observations of saltwater up-coning. *Journal of Hydrology*, 373(1), 230-241.

Westjohn, D. B., Weaver, T. L., & Zacharias, K. F. 1994. Hydrogeology of Pleistocene glacial deposits and Jurassic red beds in the central lower peninsula of Michigan. Water-resources investigations report (USA).

Westjohn, D. B., & Weaver, T. L. 1996a. Hydrogeologic framework of Mississippian rocks in the central Lower Peninsula of Michigan U.S. Geological Survey Water-Resources Investigations Report 94-4246.

Westjohn, D. B., & Weaver, T. L. 1996b. Configuration of Freshwater/Saline-Water Interface and Geologic Controls on Distribution of freshwater in a regional aquifer system, central Lower Peninsula of Michigan U.S. Geological Survey Water-Resources Investigations Report 94-4242.

Winter, T.C., J.W. Harvey, O.L. Franke, and W.M. Alley. 1998. Ground water and surface water—A single resource. U.S. Geological Survey Circular No. 1139. Reston, Virginia: USGS.544

CHAPTER 5

Well-scale Predictions of Groundwater Sustainability that Account for Human-environment System Dynamics

5.1 Executive Summary of Ch. 5

This chapter presents the application of the calibrated groundwater flow model discussed in Chapter 3 to estimate future groundwater sustainability in Ottawa County, Michigan. A systematic process is developed and applied for providing operational, well-scale estimates of current and future groundwater availability at key locations of concern, utilizing the future model results to account for detailed human-environment system dynamics. Specifically, it augments (1) long-term (2016-2036) simulated changes of groundwater levels due to and human activity (e.g., expected countywide groundwater use and land development.) and climate change (recharge dynamics); with (2) well-scale analyses of groundwater levels to estimate sustainable yield (pumping rates) at different locations during ‘limiting situations’ – when groundwater pumping will be at its largest and recharge is lowest. The modeling framework enables calculation of available drawdown and sustainable groundwater yield (pumping) under different management criteria (water availability and acceptable water quality). The approach is applied at 10 locations of interest. The results suggest that future groundwater availability is largely controlled by acceptable water quality of the intended user, although large-capacity water wells used to support agriculture or industry may face challenges producing required yields without utilizing an unacceptable portion of the local saturated aquifer thickness. The results from the future modeling effort will be provided to Ottawa County to guide future data collection and augment policy and community planning based on evaluation of likely future conditions.

5.2 Ch. 5 Introduction

The calibrated groundwater flow model of the subregional aquifer system underlying Ottawa County, Michigan (and immediate surrounding areas) described in Chapter 3 was applied to estimate countywide groundwater flow conditions 20 years into the future (2016-2036). The future simulations were informed by best estimates of projected land use/land cover (LULC) and future groundwater use developed by

county-level planning and utilities departments. Analysis of long-term temperature and precipitation observations from the National Climate Data Center was used to estimate temperature and precipitation patterns needed to project future recharge conditions. A framework using future model results and different management criteria (water availability and acceptable water quality) was developed and applied for well-scale analyses of available drawdown and sustainable yield at 10 different locations of interest during ‘limiting situations’ – when groundwater pumping will be at its largest and recharge is lowest during the summer months of Michigan (July, August and September). In this way, the local analysis considers larger human-environment interactions by considering ‘background’ groundwater level dynamics controlled by expected groundwater use, land development, and recharge.

5.3 Countywide Estimates of Future Groundwater Conditions

Figure 5.1 presents the work-flow relating different components of the countywide future modeling effort. The following subsection discusses i) how future groundwater use and land development was estimated, and ii) preparing flow model inputs (water use and recharge).

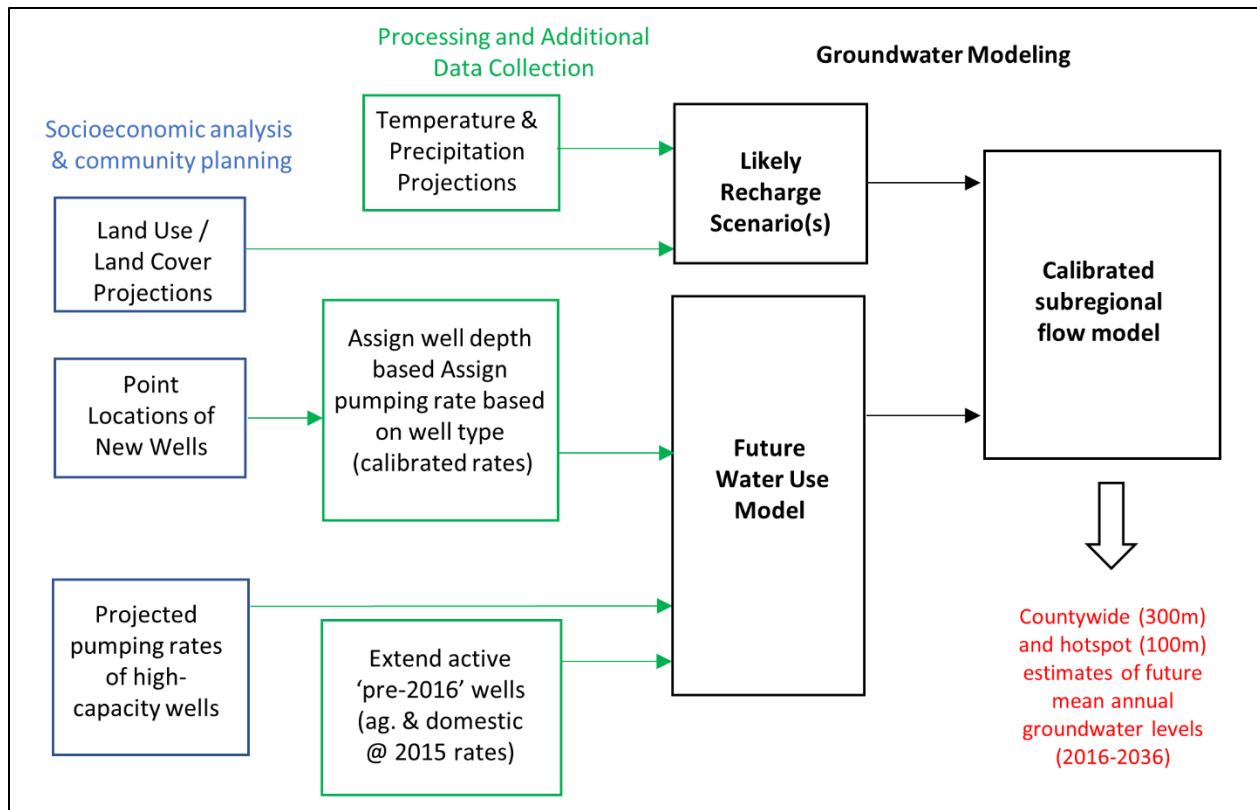


Figure 5.1: Work-flow of preparing projections provided by Ottawa County into future recharge and water use models needed for application of calibrated flow model.

5.3.1 Planning and Projections

Land use projections. Ottawa County Planning and Performance Improvement Department (PPID) and Public Utilities Department (PUD) worked with township-level officials and decision-makers to carefully plan land development (zoning build-out) and translate this information into county-wide spatial maps of LULC for every five years for the 2015-2035 period. These maps were converted into input for the future recharge modeling. The projected LULC is not expected to undergo significant large-scale changes during the next 20 years, although small-scale changes may have important impacts on water use (see details about projecting well-dependent land parcels below). Chapter 3 provides more details of land use/land cover in Ottawa County and its use in recharge modeling completed for this integrated study.

Projecting Future Water Use. Ottawa County PPID provided two important sets of information required for modeling future groundwater use: 1) projected pumping rates of specific industrial, commercial and

public supply wells based on adjustments to calibrated pumping rates (see Chapter 3); and 2) locations of new water wells based on detailed zoning and infrastructure planning completed at the township levels.

Estimated pumping rates of currently existing wells. Expected changes in water use for industrial/commercial wells were calculated by Ottawa County PPID and PUD based on Gross Domestic Product (GDP) growth projections for different industrial/commercial categories from the UpJohn Institute for Employment Research of southwest Michigan. For example, if a 16% increase in the GDP was expected for the period 2015-2020 for a well supporting a particular type of industry, the pumping rate was increased by 16% from the calibrated rates (see Table 5.1). In a similar way, expected changes in public supply wells (e.g., those serving schools, small residential communities, etc.) were based on predicted changes in student enrollment, expansions/constrictions in residential development, etc. In most cases, significant changes in expected water use were not expected for existing public supply wells (rather, increases in water use are expected to come primarily from installation of new wells on converted land parcels – see below). A simple treatment of high-capacity irrigation wells was applied: existing wells were allowed to continue pumping ad infinitum at their calibrated rates determined from model development (see Chapter 3), and no new wells were added to the model nor were any wells removed (‘turned off’) during future simulation. The approach applied here was considered pragmatic and reasonable considering that: 1) the large number of socio-economic and biophysical factors controlling crop production and related water demand makes projecting irrigation patterns difficult and time-consuming; 2) the extent and spatial distribution of agricultural lands is not expected to change significantly in coming decades; and 3) based on discussions with several authorities on local agriculture, it is predicted that the number of agricultural wells will actually decrease over time due to the movement from small-scale to large operation farming in Ottawa County (internal communications – Ottawa County PPID). However, it is not clear when and where this will occur. Thus, the analysis provided was considered a conservative analysis in the context of sustainability – a ‘worst case scenario’ which is ultimately for what management hopes to prepare. For those existing irrigation wells that continue to operate, long-term monitored and/or site-specific problem solving is recommended (see

Well-Scale Analysis of Sustainability). Existing private wells also continued pumping with rates determined through model calibration.

Table 5.1: Projected percent change in GDP and estimated groundwater pumping rates for large-use industrial/commercial wells in Ottawa County. Source: Ottawa County Planning and Performance Improvement Department (Ottawa County 2017).

| Company | % Change in GDP (2015- 2020) | % Change in GDP (2021- 2025) | % Change in GDP (2026- 2035) | Number of wells | 2015 Water Use (GPM) | Projected water use (GPM) (2015- 2020) | Projected water use (GPM) (2015- 2020) | Projected water use (GPM) (2015- 2020) |
|-------------------------------------|--|--|--|--------------------|-------------------------------|---|---|---|
| Applied Mechanics Corporation | -2% | 16% | 59% | 1 | 13.5 | 13.2 | 15.6 | 21.4 |
| Autumn Hills Landfill | -7% | -9% | -2% | 1 | 13.5 | 12.6 | 12.3 | 13.2 |
| Blink Lumber Company | 13% | 22% | 57% | 1 | 13.5 | 15.2 | 16.5 | 21.2 |
| Consumers Energy | 8% | 12% | 21% | 9 | 121.5 | 131.4 | 136 | 146.6 |
| Dewitt Barrels Incorporated | 8% | 14% | 26% | 1 | 13.5 | 14.6 | 15.4 | 17 |
| DeWys Manufacturing | -2% | 16% | 59% | 2 | 27 | 26.4 | 31.2 | 42.8 |
| Grassmid Transport | 4% | 11% | 40% | 2 | 27 | 28 | 30 | 37.8 |
| Holland Pallet Repair | 6% | 13% | 34% | 1 | 13.5 | 14.3 | 15.2 | 18.1 |
| Hudsonville Truck and Trailer | 4% | 11% | 40% | 1 | 13.5 | 14 | 15 | 18.9 |
| J&R Automation | 22% | 40% | 68% | 2 | 27 | 32.8 | 37.8 | 45.4 |
| Landscape Design | 4% | 3% | 10% | 1 | 13.5 | 14 | 13.9 | 14.9 |
| Leprino Foods | 19% | 19% | 21% | 3 | 40.5 | 48.1 | 48.2 | 49.1 |
| Superior Steel Components | -2% | 16% | 59% | 1 | 13.5 | 13.2 | 15.6 | 21.4 |
| Trailpoint Brewing | 7% | 14% | 37% | 1 | 13.5 | 14.4 | 15.4 | 18.5 |

Future well-dependent parcels. Ottawa County PPID used an ArcGis add-on called CommunityViz (ESRI 2011) and compiled and translated township data and regulations into a format that could be used by the program to predict occurrence (in space and time) of future parcels requiring new wells. The overall process consisted of, on a countywide basis: identifying developable land; defining structure density for differently zoned land; prescribing layout patterns of development; determining growth rates of development; and excluding parcels that will likely connect to municipal water supply (water mains from urban centers, e.g., Grand Rapids, Holland or Grand Haven).

The process of identifying developable land consisted of eliminating land that would be unsuitable for development: park land, cemeteries, bodies of water, wetlands, 100-year floodplains, and roads and existing structures. Structure density was calculated by considering floor area ratios (FAR), allowable building height, open space requirements, and setbacks from roadways. The analysis also included an efficiency factor as a percent of developable land that will actually be developed. Factors, such as future roads, development patterns, typical lot size, or other barriers to development reduce the efficiency rating for each zoning district. Each zoning type was carefully assigned a layout pattern based on current development trends. For instance, mobile home parks are generally laid out in a grid pattern, while commercial properties tend to develop along roads. Growth rates were calculated by analyzing population projections and historical building permit data and reaching out to local organizations for input regarding growth rates (e.g., Lakeshore Advantage, Michigan Department of Environmental Quality, and the Upjohn Institute). In order to determine which parcels would likely connect to surface water, it was assumed that any development that occurs within 250 ft. of an existing water main would connect to that source. (Water main extensions planned for the future were also considered as part of the master build-out completed by Ottawa County PPID and PUD). Large, dense groupings of development within 1000 ft. of water mains were also excluded, as these larger developments would likely opt to extend the main to their location for cost effectiveness. Local input was also collected by speaking with township officials to identify proposed developments, locate future utility connections, and to verify the overall buildout process for that specific township. The

output from analysis was a map of future well-dependent parcels with 3800 new wells. Parcel attributes included: expected well type, development period (2015-2020, 2021-2025, or 2026-2035), and number of wells expected. A vast majority of these parcels will support private domestic wells, but a handful are associated with commercial/industrial development. All new wells were assigned pumping rates derived in the development of the calibrated flow model (see Chapter 3).

Conversion of wells into model inputs. The aquifer from (and depth at) which new wells extract groundwater is important and must be provided as input the 3D groundwater flow model. The subsurface geology, mapped during the county-wide geologic modeling (see Chapter 3) was used as a guide for determining depth to each well provided by Ottawa County PPID. The first step was to determine where the glacial aquifer likely not productive (because of extensive fine-grained material, e.g., clay) and the Marshall aquifer is accessible below. The wells that satisfied these criteria were added to the fractured bedrock layer (see Figure 5.2). Of course, in some of the locations (e.g., southeast Ottawa County) is it possible that productive “pockets” of the glacial aquifer will be encountered. But as previously mentioned, the goal was to provide a conservative analysis of long-term sustainability, which is consistent with the approach used here.

After assigning wells to the bedrock aquifer, the remaining wells were assigned to one of the five glacial layers utilized in the countywide flow model. The hydraulic conductivity distributions from the five glacial layers were used to determine which layer was most appropriate for well screen location. First – considering that wells will go deep enough to avoid surface contamination and/or water table fluctuations/drawdown but no deeper (to save costs) – wells were overlaid to the K map of the 4th deepest glacial layer. Wells that fell in places of high expected yield (high K values) were assigned to the 4th glacial layer. The remaining wells were then overlaid to the 5th deepest layer, and the process was repeated. Any wells that were in locations of low K in the 4th and 5th deepest glacial layers were forced to go to a shallower glacial layer (layer 3 or layer 2, depending on the K distribution). The wells assigned to each glacial layer are shown in Figure 5.2.

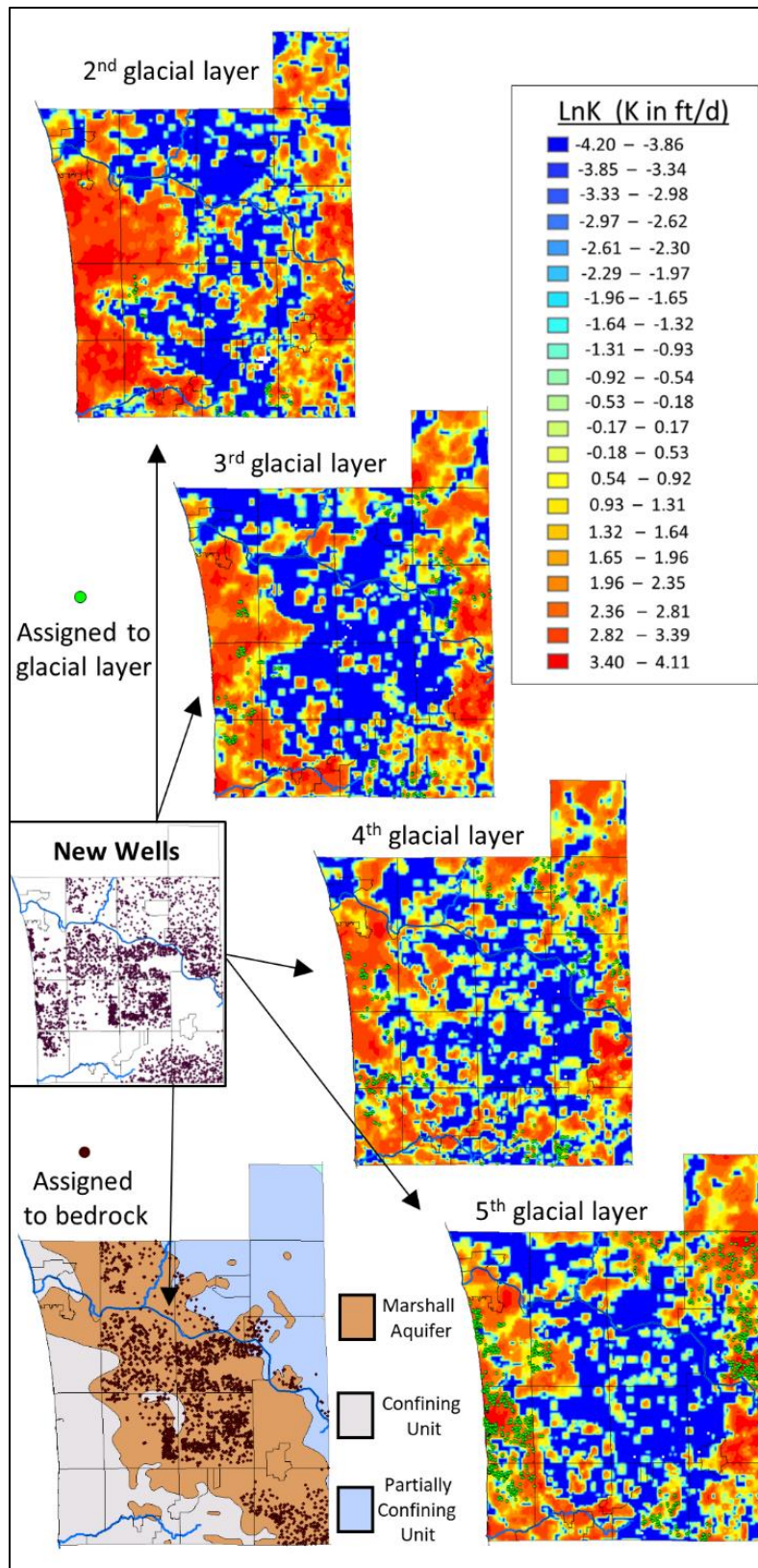


Figure 5.2: Assigning new future wells to different vertical layers in the calibrated flow model. The ‘5th glacial layer’ is the deepest of the layers representing the unconsolidated glacial deposits.

It was also necessary to convert the estimated time period of installation (e.g., 2015-2020) to a specific installation date for input to the flow model. A reasonable assumption is that the well installation dates are distributed evenly across the estimated time period of installation (i.e., the percentage of wells added to the model during the time period follows a linear trend). Without additional information, however, it is difficult to determine which wells (in which locations) to ‘turn on’ at the appropriate date. A mathematically similar approach was used which added all wells at the half-way point of a time period of. This approach was deemed sufficient given that the key objective of the future modeling was to determine the long-term impact of additional water use relative to 2015 conditions.

Temperature and precipitation trends for recharge modeling. The National Climatic Data Center operates 351 temperature stations and 857 precipitation throughout the Lower Peninsula of Michigan. In recent work by Zhang (2014), 10-year annual averages for southwest Michigan were calculated using data from 1972-2012. Linear regression was applied to the 10-year averages to provide an estimate of long-term temporal trends. The analysis revealed a warming trend of 0.228° C per decade and 0.190° per decade for maximum and minimum air temperature, respectively. No clear trend was detected for long-term precipitation. The air temperature trends were used to estimate future air temperatures via the Delta-method. In this approach, short-term (e.g., day-by-day) temperature or precipitation variations are repeated in future extrapolations, but each temperature is offset using the trend from the analysis of historical data, the magnitude of the offset depending on how far into the future one wishes to estimate (see, e.g., Gago Da Silva et al. 2012). Daily, 4km estimates of maximum and minimum temperature from the PRISM Climate Group (PRISM 2004) from the past decade (2006-2016) were ‘recycled’ two times to generate daily temperature data for 2016-2036 (with the appropriate offset applied via the Delta method). Because there was clear long-term trend, precipitation patterns from the last decade (2006-2016) were simply recycled without using an offset.

5.3.2 Estimates of Future Groundwater Flow Patterns

The future recharge scenario and water use model were used as input to the calibrated flow model to estimate mean annual flow patterns across Ottawa County from 2016-2036. The results suggest that future

wells withdrawals and expected recharge are not expected to significantly impact shallow groundwater levels in unconsolidated glacial deposits, at least at the scales modeled in this study (300m x 300m). However, noticeable change is expected for the deeper bedrock aquifer in response to the addition of new wells. In particular, decreases in groundwater levels are predicted for the central region of the county in response to the addition of new wells (see bottom portion of Figure 5.3). To quantify the impact of adding new wells to the aquifer system over the next 20 years, a 'baseline' simulation was executed and compared to the future simulation. In the baseline model, new wells were not added for the 2016-2036 time period (i.e., the 2015 pumping configuration was applied 'as is' throughout the simulation). Both simulations used as input the future recharge estimates based on changes in LULC and projected temperature, and thus, differences in their results can be attributed to additional groundwater withdrawals. A spatial differencing of simulated head distributions was computed by subtracting the baseline simulation head results from the future simulation head results for each year of simulation. Figure 5.3 (upper portion) shows results for select years to demonstrate how water level decline is expected to evolve over time. The most significant decline (3-5 m) due to pumping is likely to occur in south-central Ottawa County, while modest pumping-induced decline (1-3 m) is expected for the rest of central Ottawa County.

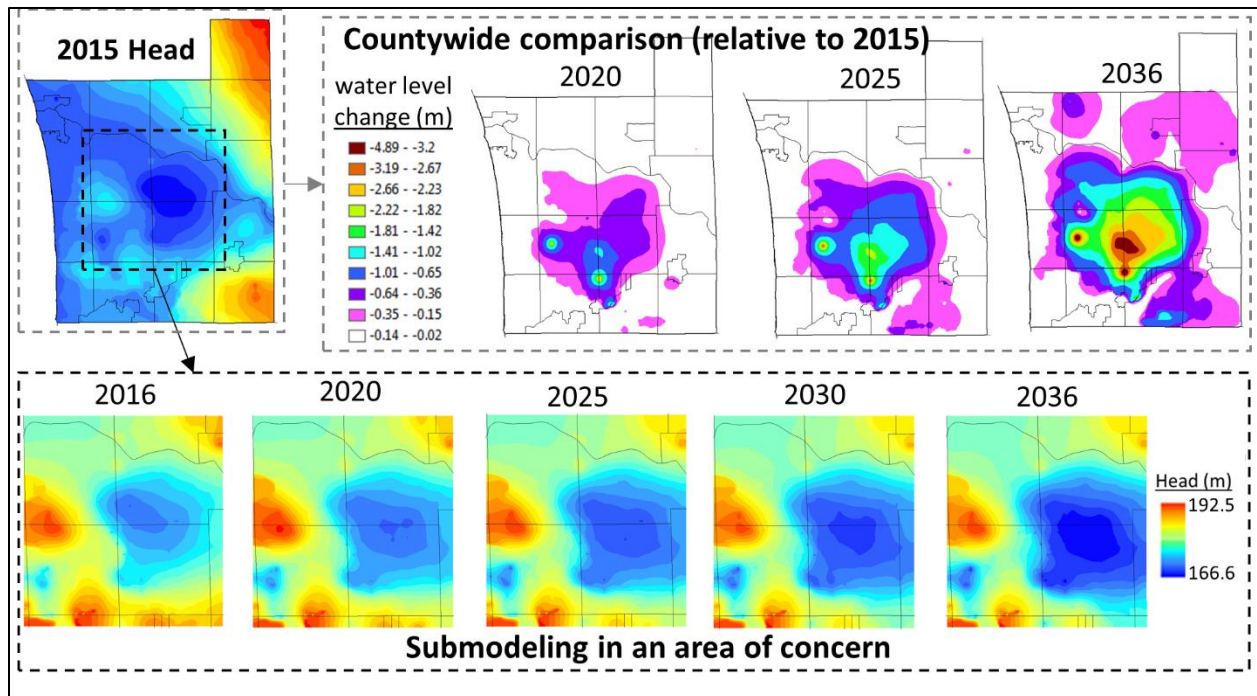


Figure 5.3: Estimates of future groundwater levels based on application of the calibrated flow model: (top-right) countywide spatial mapping of additional groundwater decline expected over next 20 years; (bottom) detailed head dynamics in an area of concern.

While the projected increases in groundwater withdrawals are expected to result in groundwater level decline in parts of the bedrock aquifer, it is insightful to consider the impact relative to historical trends. Figure 5.4 show the bedrock aquifer head output from each simulation (‘baseline’ and future) for two-point locations in central Ottawa County from 1966-2036. Clearly, these plots suggest that SWL decline experienced over the previous 50 years (1966-2015) is much more than the SWL decline expected to occur over the next 20 years (2016-2036) based on projections of well buildouts provided by Ottawa County PPID. (Also note that the SWL variability due to recharge – as expressed in the baseline simulation curves – is significantly less than the SWL decline caused by pumping in the bedrock aquifer). The graphics in the bottom-half of Figure 5.4 shows simulated drawdown (groundwater level decline) at all locations in the bedrock layer of the groundwater model. The left-most graphic provides a spatial map of the drawdown occurring during the 1966-2015 time period, while the right-most graphic shows the expected drawdown

over the next 20 years (relative to 2015 conditions). Clearly, the changes during the past 50 years are greater in magnitude and extent.

In short, increases in groundwater use in the deep aquifer will cause additional water level decline, although the rate of decline will diminish in response to checks on groundwater increases in parts of the system. However, groundwater will still be significantly less than “natural” (1966) SWLs in many parts of the bedrock aquifer. This has important implications for water quality: the low SWLs may continue to induce migration of C-laden water away from its natural path of discharge to the Grand River and its tributaries (see Chapter 4).

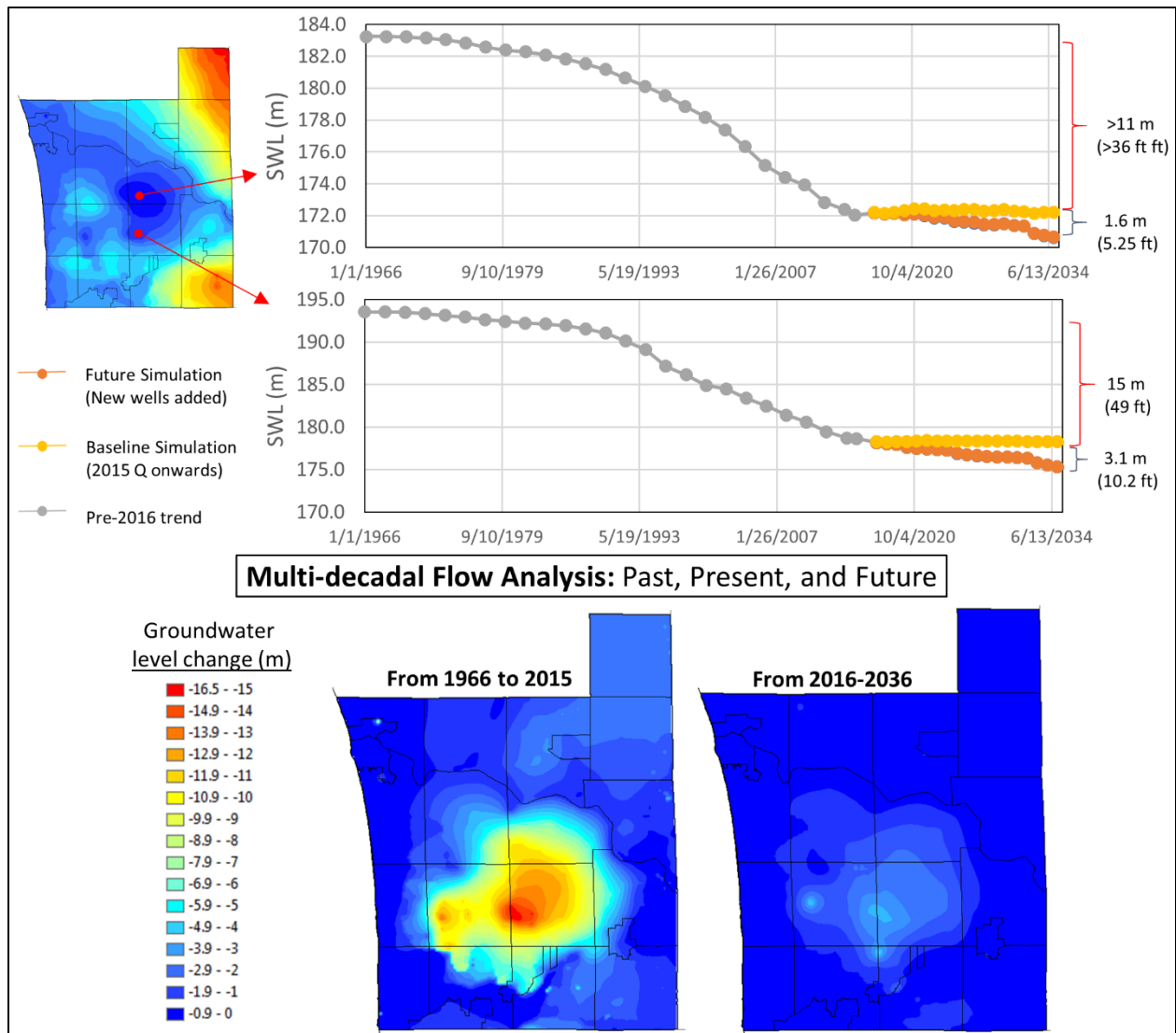


Figure 5.4: Groundwater level dynamics for 70 year of analysis (1966-2036): (top): Time-series of simulated heads at two different areas undergoing significant temporal change; (bottom): countywide spatial analysis of simulated groundwater level change for 1966-2015 (left) and 2016-2036 (right).

5.4 Well-Scale Analysis of Future Groundwater Availability

The results of the future simulations helped illustrate the expected cumulative impacts of projected water use and land development on groundwater levels in Ottawa County, which is predicted to be less significant than changes in previous decades. A natural question raised by this analysis is: given the understanding of the subregional groundwater system, what is the available drawdown at a particular location, and what is maximum sustainable yield (pumping)? Although the applied groundwater model is expected to reproduce

systematic decline (or drawdown) in groundwater levels, drawdown at a single well is larger than what was simulated. This is because: a) the model used representative cells for contiguous areas, which tends to smooth out the sharp changes in water levels near a well, despite correct predictions of head further from the well (Anderson and Woessner, 1992); and b) wells in our model used long-term “effective rates” (as if the pumping was spread out over an entire year). In reality, water wells pump at rates higher than the effective rates for discrete amounts of time (see Chapter 3), during which drawdown will be larger than the “background” decline characterized by the groundwater model. In light of the foregoing, a well-scale analysis was applied to provide guidance on “limiting situations” – when groundwater pumping will be at its largest and recharge is lowest during the summer months of Michigan (July, August and September). Specifically, local analytical corrections were applied to 2036 simulated bedrock head at key locations in order to assess available drawdown and maximum sustainable yield. In this way, systematic long-term decline of ‘background’ groundwater levels over 20 years was captured with the subregional future simulation, while location-specific limits on pumping are provided through straight-forward analytical groundwater analysis. (Note that this analysis could be done for any future time of interest simulated by the calibrated model).

5.4.1 Analytical Approach

The analytical solution used here was the Cooper and Jacob (1946) approximation of the Theis (1935) solution for radial groundwater flow to a well in confined aquifers:

$$s = \frac{2.3Q}{4\pi T} \log \frac{2.25Tt}{r^2S} \quad (5.1)$$

where s is the drawdown (or decline in water level relative to pre-pumping levels) (m), Q is the applied pumping rate (m³/day), T is the local aquifer transmissivity (m²/day), t is the duration of pumping (days), r is the radial distance (m) from the well center at which the analysis is being made, and S is the local aquifer storage coefficient (dimensionless). Use of this equation for estimating well-specific drawdown in the bedrock aquifer is justified because negligible local recharge to the aquifer system is expected for the analysis of interest, due to the combined effect of the thick continuous layer of confining material in the

overlying sediments and low recharge expected during summertime months in Michigan. Further, it is known that the Jacob-Cooper approximation provides good estimates of drawdown when input to the Theis well function, u , is small:

$$u = \frac{r^2 S}{4Tt} \quad (5.2)$$

This condition was satisfied at all locations, as drawdown at the well location was of the analysis of interest (i.e., values of r were very small).

The process of estimating available drawdown and its maximum sustainable yield (pumping) at a particular location is presented in Figure 5.5. First specific capacity, Q/s , was calculated by re-arranging equation (5.1):

$$\frac{Q}{s} = \frac{4\pi T}{2.3} \left(\log \frac{2.25Tt}{r^2 S} \right)^{-1} \quad (5.3)$$

Local bedrock aquifer properties (T and S) were derived from the calibrated groundwater flow model (see Table 5.2 in next subsection), a value of 0.0508 m (2 in.) was used as the well radius (although this could change based on well type), and 90 days (≈ 3 months) was used for pumping duration. (Note that, in this analysis, it is assumed that pumping would operate continuously for 3 months; in reality, pumping would be intermittent and more intense than the 3-month continuous values reported here. However, using smaller values of t would yield larger values of maximum sustainable yield, and thus, the approach used here is conservative in the context of sustainability evaluation, consistent with the approach used for countywide estimates of future groundwater conditions (see above). Well losses due to turbulent flow through the well screen and inside the borehole were applied through the use of a well efficiency factor, E , to calculate the effective specific capacity, $(Q/s)_{eff}$, as Q/s multiplied by E . Well efficiency was assumed to be 0.75, but again, this this could change based on well type and could be fine-tuned based on further information. Next, available drawdown was calculated by considering the 2036 local bedrock head and management criteria for acceptable use of available drawdown, s_{avail} . Four management scenarios were considered:

- *Scenario 1*: well water level drops to elevation at a distance of 5% of total depth from the bedrock top surface (i.e., just when the local bedrock aquifer switches from confined to unconfined conditions).
- *Scenario 2*: well water level drops to elevation at a distance of 50% of total depth from the bedrock top surface, representing an aggressive use of the saturated aquifer thickness. (Note that, in this case, the bedrock aquifer transmissivity changes during unconfined conditions. An average transmissivity calculated with a saturated thickness of $0.75B$ was used, where B is the local aquifer thickness. See Appendix at the end of this chapter.)
- *Scenario 3*: water level drops to elevation where present-day dissolved chloride concentrations are 100 mg/L
- *Scenario 4*: water level drops to elevation where present-day dissolved chloride concentrations are 250 mg/L

The results from 3D interpolation of Cl concentrations (see Chapter 4) were used to determine appropriate elevations for scenarios 3 and 4. Finally, a maximum sustainable yield, Q_{max} , was calculated for each management scenario by multiplying effective specific capacity by available drawdown.

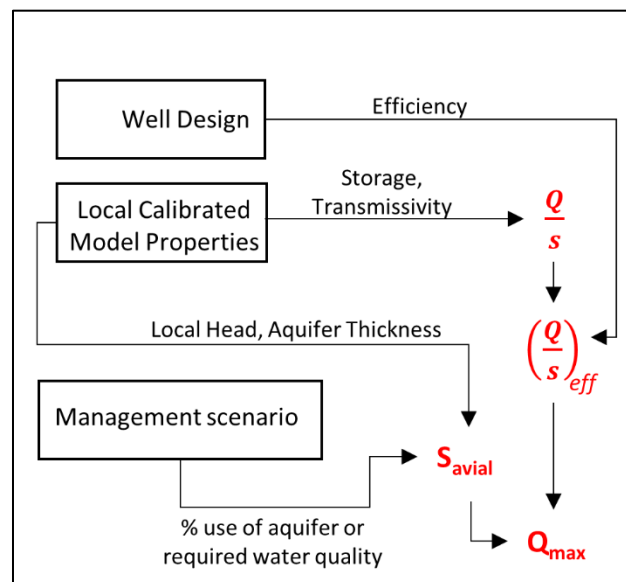


Figure 5.5: Work-flow for estimating available drawdown and maximum sustainable yield (pumping) at a specific location using results from the future simulations.

5.4.2 Illustrative Application to Several Key Areas

The well-scale analysis was applied at 10 locations across Ottawa County which exhibited problems related to groundwater decline and/or high Cl concentrations bedrock aquifer in the central portion of Ottawa County (see section 4.5 of Chapter 4). Figure 5.6 shows the locations used in the analysis with an example conceptual schematic of available drawdown and maximum allowed pumping under different management scenarios. The local values for local bedrock aquifer properties (T and S) are shown in Table 5.2, and analysis results for all 10 locations are provided in Table 5.3. There is significant variability between different locations and management scenarios. Specific capacity varies from 8.2 m²/day to 39.0 m²/day, available drawdown from 10.5 m to 183.8 m, and maximum sustainable yield from 21.4 GPM (gallons per minute) to 387.6 GPM. Locations 2, 6, 7 and 8 are predicted to have the lowest maximum sustainable yields (25-35 GPM). Some locations are water quantity-limited (smaller s_{avail} and Q_{max} for scenarios 1 and 2 than those for scenarios 3 and 4), e.g., Locations 4, 7 8 – while others are water quality-limited, e.g., Locations 9 and 10. In all cases, Q_{max} is expected to be well above rates typical of private domestic pumping, although supporting large-capacity irrigation or industrial wells may be problematic, especially Locations 2, 6, 7 and 8.

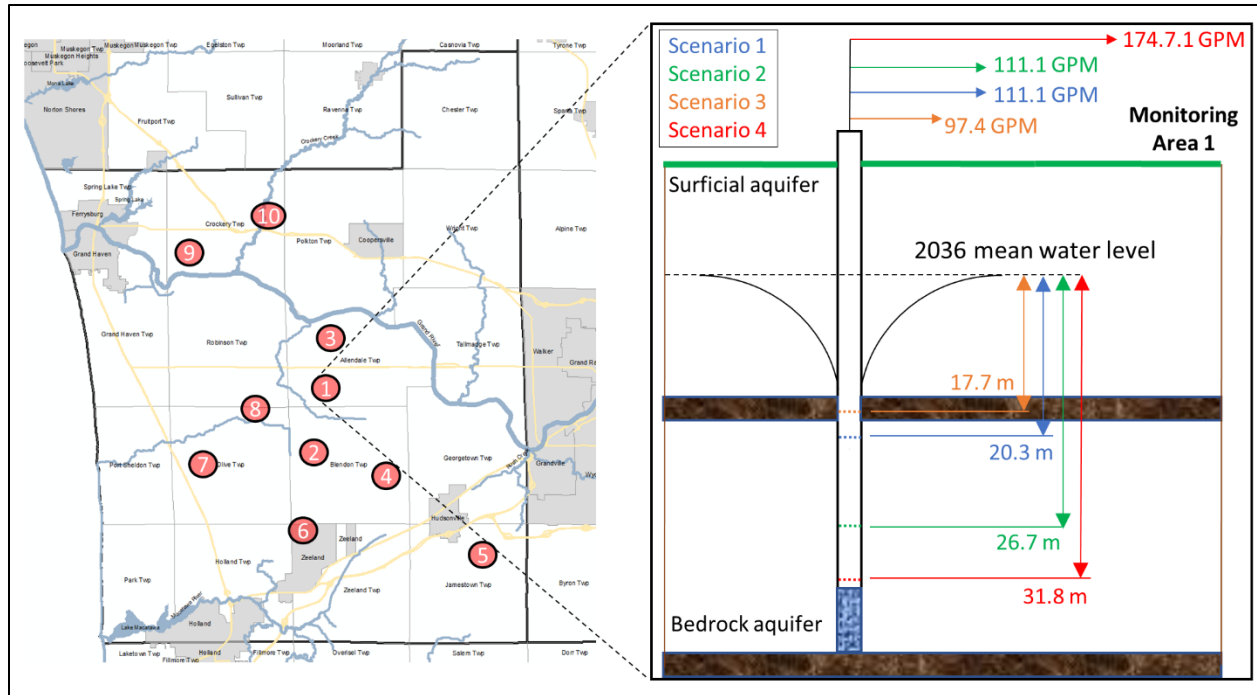


Figure 5.6: Locations used for well-scale analysis (left) and an example conceptual schematic of available drawdown and maximum allowed pumping under different management scenarios (right).

Table 5.2: local transmissivity (T) and local effective specific capacity $(Q/s)_{\text{eff}}$ utilized for well-scale analysis.

| Monitoring Area | Local T (m ² /day) | Local $(Q/s)_{\text{eff}}$ (m ² /day) | Local thickness (m) | Bedrock top Z (m) | 2036 Head (m) |
|-----------------|-------------------------------|--|---------------------|-------------------|---------------|
| MA-1 | 80.8 | 29.9 | 14.3 | 148.2 | 167.7 |
| MA-2 | 20.9 | 8.2 | 12.9 | 146.7 | 168.6 |
| MA-3 | 97.1 | 35.2 | 57.9 | 144.1 | 174.1 |
| MA-4 | 80.8 | 29.9 | 27.2 | 161.3 | 170.4 |
| MA-5 | 88.0 | 32.2 | 46.0 | 172.1 | 211.0 |
| MA-6 | 20.9 | 8.2 | 1.9 | 158.0 | 177.3 |
| MA-7 | 20.9 | 8.2 | 6.9 | 153.5 | 173.0 |
| MA-8 | 20.9 | 8.2 | 6.2 | 154.6 | 176.5 |
| MA-9 | 90.8 | 33.1 | 49.7 | 132.5 | 177.1 |
| MA-10 | 109.3 | 39.2 | 74.0 | 133.3 | 183.8 |

Table 5.3: Results from the well-scale analysis. Sc.1 = Scenario 1, Sc.2 = Scenario 2, etc. Empty entries for Sc.3 and Sc.4 indicate that concentrations of Cl^- were not measured at or above 100 mg/L or 250 mg/L during the analysis of subregional water quality.

| Location | Specific capacity (m ² /day) | S _{avail} (m) Sc.1 | S _{avail} (m) Sc.2 | S _{avail} (m) Sc.3 | S _{avail} (m) Sc.4 | Q _{max} (GPM) Sc. 1 | Q _{max} (GPM) Sc. 2 | Q _{max} (GPM) Sc. 3 | Q _{max} (GPM) Sc. 4 |
|----------|---|-----------------------------|-----------------------------|-----------------------------|-----------------------------|------------------------------|------------------------------|------------------------------|------------------------------|
| 1 | 29.9 | 20.3 | 26.7 | 17.7 | 31.8 | 111.2 | 111.2 | 97.4 | 174.7 |
| 2 | 8.2 | 22.5 | 28.3 | 14.3 | 18.7 | 33.7 | 32.2 | 21.4 | 28.0 |
| 3 | 35.2 | 32.9 | 59.0 | 19.5 | 21.9 | 212.3 | 288.5 | 125.8 | 141.6 |
| 4 | 29.9 | 10.5 | 22.7 | 29.5 | -- | 57.4 | 94.5 | 128.8 | -- |
| 5 | 32.2 | 41.2 | 56.9 | -- | -- | 243.5 | 255.1 | -- | -- |
| 6 | 8.2 | 19.4 | 61.9 | -- | -- | 29.1 | 70.4 | -- | -- |
| 7 | 8.2 | 19.9 | 23.0 | 21.1 | -- | 29.8 | 26.1 | 31.6 | -- |
| 8 | 8.2 | 22.2 | 25.1 | 23.9 | -- | 33.3 | 28.5 | 35.8 | -- |
| 9 | 33.1 | 47.1 | 69.5 | 44.8 | 127.0 | 286.3 | 320.3 | 271.7 | 288.5 |
| 10 | 39.2 | 47.5 | 183.8 | 48.1 | 127.8 | 341.0 | 476.3 | 345.5 | 387.6 |

The final Q_{max} values reported above are meant to be indicators of sustainable use at different locations rather than absolute, strictly-enforceable values. This is because the inputs used for calculating specific capacities and available drawdowns are derived from relatively coarse model parameters/outputs, that tend smooth out (or fail to capture) important local variabilities. For example, aquifer thickness was based on 500 m resolution data layer representing the bedrock top surface raster, 2036 bedrock groundwater levels were captured at 300 m and 90m resolution (parent model and submodel, respectively), and transmissivity was calculated using representative hydraulic conductivity values for large regions of the bedrock aquifer (see Chapter 3). And as mentioned before, well efficiency may vary significantly, which leads to a wide range of calculated effective specific capacities. For more accurate calculations of Q/s , S_{avail} , and Q_{max} (especially in areas with low values for S_{avail} and Q_{max}), long-term monitoring of groundwater levels and field measurements and should be implemented to improve accuracy of calculations inputs (e.g., estimates of hydraulic conductivity and aquifer thickness from aquifer pump tests and/or seismic profiles into the geologic model).

Nonetheless, the work-flow developed and applied here is an effective use of the calibrated flow model results, most directly by providing necessary inputs for well-scale calculations of available drawdown and

sustainable pumping rates, but also by ensuring the local analysis considers larger human-environment interactions by considering ‘background’ groundwater level decline caused by expected future pumping dynamics.

5.5 Ch. 5 Conclusions

The calibrated flow model described in Chapter 3 was applied to generate future groundwater simulations informed by best estimates of projected groundwater use, land development and recharge dynamics. The results suggest that the rate of groundwater level decline will slow down as future developments/structures make careful use of existing and planned water infrastructure (water mains). However, groundwater will still be significantly less than “natural” (1966) SWLs in many parts of the bedrock aquifer. This has important implications for water quality: the low SWLs may continue to induce migration of Cl-laden water away from its natural path of discharge to the Grand River and its tributaries.

A framework using calibrated model results and different management criteria (water availability and acceptable water quality) was developed and applied for well-scale analyses of available drawdown and sustainable yield at 10 different locations of interest. Future groundwater sustainability is largely controlled by acceptable water quality of the intended user, although large-capacity water wells used to support agriculture or industry may face challenges producing required yields without utilizing an unacceptable portion of the local saturated aquifer thickness.

Results from the analysis done here are being used to guide long-term monitoring and influence policy and continued community planning in Ottawa County, Michigan. Key socioeconomic factors will be considered, including but may not be limited to: an exploration of water conservation options to reduce future demands; evaluation of costs for expanding municipal water supply beyond its currently planned build-out; complete inventory of important or protected surface features (e.g., groundwater-dependent ecosystems, potential contamination sites, etc.); master land use and build-out policy, including a means for protecting important groundwater recharge areas; and delineation and protection of capture zones of

major well fields. This work will be integrated into a research paper to be submitted to a policy-oriented environmental journal in the near future.

APPENDIX

Table 5.4: Average local transmissivity (T) and local effective specific capacity (Q/s)_{eff} utilized for evaluation of management scenario 2.

| Monitoring Area | Local T (m ² /day) | Local (Q/s) _{eff} (m ² /day) |
|-----------------|-------------------------------|--|
| MA-1 | 60.6 | 22.7 |
| MA-2 | 15.7 | 6.2 |
| MA-3 | 72.8 | 26.7 |
| MA-4 | 60.6 | 22.7 |
| MA-5 | 66.0 | 24.4 |
| MA-6 | 15.7 | 6.2 |
| MA-7 | 15.7 | 6.2 |
| MA-8 | 15.7 | 6.2 |
| MA-9 | 68.1 | 25.1 |
| MA-10 | 82.0 | 29.7 |

REFERENCES

REFERENCES

- Anderson, M.P., Woessner, W.W., 1992. Applied Groundwater Modeling. Academic Press, San Diego.
- Cooper, H.H. and Jacob, C.E., 1946. A generalized graphical method for evaluating formation constants and summarizing well-field history. Eos, Transactions American Geophysical Union, 27(4), pp.526-534.
- ESRI. 2011. ArcGIS Desktop: Release 10. Redlands, California:Environmental Systems Research Institute.
- Gago Da Silva, A., Gunderson, I., Goyette, S. and Lehmann, A., 2012. Delta-method applied to the temperature and precipitation time series-An example.
- Ottawa County, Michigan. Performance and Planning Department — Industrial Data and Projections. (provided July 2017).
- Theis, C.V., 1935. The relation between the lowering of the piezometric surface and the rate and duration of discharge of a well using ground-water storage. Eos, Transactions American Geophysical Union, 16(2), pp.519-524.
- Zhang, J. 2014. Research on Data-driven Model of Infiltration Groundwater Recharge Based on Big Data, Ph.D Dissertation, Michigan State University.